THE DEVELOPMENT OF ADSORPTION/THERMAL DESORPTION FOR THE DETERMINATION OF TRACE LEVELS OF VOLATILE ORGANIC COMPOUNDS IN GROUNDWATER

Michael Elliott Rosen
B.A., Harpur College, State University of New York at Binghamton, 1981

A dissertation submitted to the faculty
of the Oregon Graduate Center
in partial fulfillment of the
requirements for the degree
Doctor of Philosophy
in
Environmental Science and Engineering

January 1988

The dissertation "The Development of Adsorption/Thermal Desorption for the Determination of Trace Levels of Volatile Organic Compounds in Groundwater" by Michael E. Rosen has been examined and approved by the following examination committee:

James F. Pankow, Thesis Advisor
Professor

William Fish
Assistant Professor

James J. Huntzicker
Professor

William L. Pengelly
Associate Professor

Dedication

This dissertation is dedicated to my grandmother, Etta B. Rosen whose tireless commitment to the needs of her family and community has inspired me and many others.

Acknowledgements

While the work in this dissertation has been attributed to a single author, it was by no means a solitary effort and I am greatly indebted to the following people for all their support. First, I would like to thank my thesis advisor, James F. Pankow who provided me with financial support and gave me a great deal of encouragement throughout my tenure as a graduate student. I also gratefully acknowledge the financial support provided to this project by the U.S. Geological Survey (Intergovernmental Personnel Agreement of June 10, 1985). In addition, I am grateful to Tom Imbrigiotta and Jack Gibs of the U.S. Geological Survey for their assistance during the field portion of this work, and many helpful discussions concerning all aspects of this study.

I greatly appreciate the help of Lorne Isabelle whose technical expertise in analytical troubleshooting, data reduction and evaluation, sampling equipment design, and auto repair proved to be invaluable.

The technical support staff at the Oregon Graduate Center is incredible and was always eager to help. Many thanks to Jerry Boehme and Gordon Frost in the electronics shop, Allan Ryall in the glass shop, Barbara Ryall in the graphics shop, and Fred Thone in the machine shop. I would also like to thank Dennis Tuuri in purchasing, and Chris Lightcap and Maureen Sloan of the library. In addition, I

have always been thankful for the assistance of the Environmental Science Department secretaries, Dorothy Malek, Edie Taylor, and Judi Irvine.

I am also indebted to my thesis committee, James F. Pankow, William Fish, James J. Huntzicker, and William L. Pengelly for their careful evaluation of my work, their helpful comments, and their signatures. In particular, I would like to thank James J. Huntzicker for his constant encouragement of my work, motivations, and aspirations.

I would like to thank all the faculty, staff and students (past and present) of the Environmental Science and Engineering Department for their support and interest in my work. I am especially grateful to Mike Anderson and Bill Asher for critiquing my work, patiently guiding me through the pitfalls of computer programming, providing me with insight into the application of engineering principles to my work, and for many intriguing discussions concerning life and the pursuit of happiness. Thanks to Ken Hart and Mike Schlender for everything from tolerating my moods, to packing my suitcase and providing airport shuttle service. I also appreciated the unique perspective and friendship of Christian Leuenberger. I would also like to extend my thanks to Nancy Christie for secretly editing a lot of my work, teaching me to write good, and raising my consciousness.

Finally, I would like to acknowledge the assistance of my family and closest friends. I am deeply grateful for the love and support provided throughout my studies by my parents, George and Mercedes Rosen, my grandmother, Etta Rosen, my mother, Anne Hunter, and my aunt and uncle, Sara and Linwood Baird. To my dearest friends, Stanley Alpert, Julia Rabinowitz, and Paul Weinstein (each born and raised in Brooklyn, N.Y.), thank you for being my dearest friends. And to the truest love I have ever known, Teresa Mae Hoos, without whose love, patience, and generosity this work surely would not have been completed, I am deeply indebted.

Table of Contents

ABBREVIATIONS

ACB	Adsorbent cartridge breakthrough
ATD	Adsorption/thermal desorption
CAS	Concentrated analyte solution injected into the mixing vessel
DS	Data system
EIC	Extracted ion chromatogram
EPA	United States Environmental Protection Agency
FBAS	Fixed bed adsorption system
GC	Gas chromatograph
HPLC	High performance liquid chromatograph
IBT	Instantaneous percent breakthrough value
MS	Mass spectrometer
OGC	Oregon Graduate Center
P&T	Purge and Trap
P&T/WCC	Purge and trap with whole column cryotrapping
ppb	Part-per-billion (μg/L water or ng/g)
ppm	Part-per-million (mg/L of water)
PPP	Purgeable priority pollutant
ppt	Part-per-trillion (ng/L of water)
PTFE	Poly(tetrafluoroethylene)
P/WCC	Purging with whole column cryotrapping
RIC	Reconstructed ion chromatogram
RW	Reagent water
UP-He	Ultra-pure Helium

US	United States
USGS	United States Geological Survey
USGS-D	United States Geological Survey, Denver, CO Central Laboratory
USGS-NJ	United States Geological Survey, New Jersey District of the Water Resources Division
VOC	Volatile organic compound
WCC	Whole column cryotrapping

SYMBOLS

A	Area below mass spectra extracted ion profile (area counts)
A_{ac}	Area above an adsorbent cartridge breakthrough curve (area counts)
A_b	Cross-sectional area of a sorbent bed (cm^2)
A_{bc}	Area below an adsorbent cartridge breakthrough curve (area counts)
A_r	Area below mass spectra, extracted ion profile for cartridge redesorption (area counts)
A_t	Area surrounding an adsorbent cartridge breakthrough curve (area counts)
$\bar{B}$	Mean blank level (ng)
$\bar{C}$	Mean analyte concentration ($\mu g/L$)
C_{as}	Concentration of concentrated analyte solution ($\mu g/L$)
C_e	Cartridge effluent analyte concentration ($\mu g/L$)
C_i	Cartridge influent analyte concentration ($\mu g/L$)
C_{max}	Maximum analyte output concentration achieved by the mixing vessel ($\mu g/L$), defined by eqn. 4.5
C_s	Analyte concentration in the sorbent bed (ng/g)
$C(t)$	Analyte output concentration (ng/g) of the mixing vessel at time (t), defined by eqn. 4.3
C_w	Analyte concentration (ng/g) in influent reagent water of the mixing vessel
CV	Coefficient of variation (%), *s* expressed as a percentage of the mean
D	Diffusion coefficient in the liquid phase (cm^2/s)
$\bar{D}$	Diffusion coefficient in the solid phase (cm^2/s)
E	Adsorbent cartridge sampling efficiency (%)
f	Fraction ($= 0 < f \leq 1$)

H Henry's law constant (atm-m^3/mole)

H_o Null hypothesis

H_1 Alternative hypothesis

i One of 100 arbitrary volume or distance units of an adsorbent cartridge

K Constant of differentiation in eqn. 4.2

K_w Analyte sorbent/water equilibrium partition coefficient (defined as C_s/C_i) (unitless)

$\bar{K}_w$ Mean of four individual K_w measurements (unitless)

$K_{w\text{-}ow}$ Value of K_w predicted from K_{ow} with eqn. 4.10 (unitless)

$K_{w\text{-}s}$ Value of K_w predicted from S with eqn. 4.9 (unitless)

M Mass contained in a deignated sample volume (= C_i x V) (ng)

M_s Mass retained by the sorbent bed (ng), defined by equations 4.6 and 4.7

N Number of theoretical plates of an elution chromatography column, defined by equations 5.1 and 5.7

P Vapor pressure (torr)

P Statistical probability

p_a Intrabead bed porosity (unitless)

p_e Interbead bed porosity (unitless)

PD Difference between two numbers (%), defined by eqn. 3.1

p_t Total bed porosity (= p_e + p_a) (unitless)

Q Sample volume flow rate (cm^3/s)

r Radius of a sorbent particle (cm)

r^2 linear correlation coefficient resulting from the linear regression analysis performed on two variables

$\bar{R}$ Average analyte recovery (%)

R_m Flow rate into and out of mixing vessel (mL/min)

R_s Syringe pump flow rate (mL/min)

s unit of standard deviation

t elapsed time (s or min)

T Analyte transmission through ATD-glass bead drier system (%), defined by eqn. 2.3

V Volume of sample passed through a sorbent bed (mL)

V_m Volume of mixing vessel (mL)

V_R Analyte retention volume (mL/g sorbent)

v_s "Superficial" linear velocity ($= Q/p_e A_b$) (cm/s)

W Elution chromatography analyte peak width ($= 4\sigma$) (mL)

z Length of sorbent bed (cm)

α Level of significance for a statistical test

δ Thickness of a stagnant film surrounding a sorbent particle in a flowing system ($= 0.2r/(1.0 + 70rv_s)$) (cm)

ϑ Contact time parameter ($= (2\bar{D}/r^2)(t - (z/v_s))$) (dimensionless)

μ_n Sample mean

ξ Film resistance parameter ($= K_w\delta\bar{D}/rD$) (dimensionless)

σ A measure of the breadth of an elution chromatography analyte peak which may be approximated by a Gaussian curve ($= V_R/\sqrt{N}$) (mL)

σ_{i+1} Breadth of Gaussian impulse peak i (mL), defined by eqn. 5.4

Φ Fraction of analyte mass not retained by the sorbent (%), defined by equations 5.2 and 5.3

χ Bed length parameter ($= (3\bar{D}K_w z/v_s r^2)((1 - p_t)/p_t)$) (dimensionless)

ω Dispersion in an adsorbent cartridge breakthrough curve (mL/g)

List of Figures

List of Tables

ABSTRACT

The Development of Adsorption/Thermal Desorption for the Determination of Trace Levels of Volatile Organic Compounds in Groundwater

Michael E. Rosen Ph.D.
Oregon Graduate Center 1988

Supervising Professor: James F. Pankow

In this study aqueous adsorption/thermal desorption (ATD) with the porous polymer sorbent Tenax has been investigated as a sampling and analysis methodology for the determination of sub-μg/L levels of volatile organic compounds (VOC) in groundwater. During the sampling step, water is passed through a glass cartridge containing Tenax and organic compounds are concentrated by the sorbent (adsorption). During the analysis step, the cartridge is heated while an inert gas is passed through the sorbent (thermal desorption). This step recovers trapped compounds and transfers them to a gas chromatograph-mass spectrometer where they are separated and analyzed. Relative to other sampling and analysis procedures frequently used, ATD minimizes sample handling, allows an investigator to obtain samples from small diameter groundwater monitoring wells, and offers increased method sensitivity.

Four aspects concerning the use of ATD have been studied. First, a new ATD cartridge analysis technique was developed and tested. Second, a field evaluation of ATD was performed. In this portion of the study ATD was compared with a traditional sampling and analysis

technique at three sampling sites at which groundwater was known to be contaminated with a variety of VOCs. For the third portion of the study, laboratory experiments were conducted to determine the capacity of the sorption system as a function of sample matrix and individual compound concentration. In addition, these experiments were used to estimate the method sensitivity of ATD for a group of VOCs with a range of physical properties. The final aspect of this thesis involved the determination of the ability of two models to accurately predict the adsorption efficiency of this sampling system under a variety of sampling conditions. Model parameters determined from laboratory experiments were used with each model, and model predictions were directly compared with experimental results in order to determine the accuracy of each model.

ATD was determined to be sensitive, accurate relative to more commonly used techniques, and precise. In addition, experimental information now exists for a group of VOCs which will allow a priori predictions concerning adsorption efficiency to be made for similar compounds under a variety of sampling conditions.

CHAPTER 1 INTRODUCTION

1.1 Occurrence of Organic Chemicals in Groundwater Supplies of the United States

Few would dispute the value of groundwater as a national resource. Groundwater is the major source of the drinking water for 50% of the population of the United States (US) and supplies 36% of all municipal drinking water. Seventy five percent of the major cities in the US rely on groundwater for their drinking water supplies (1). For the most part, the groundwater supply of the nation is relatively clean. It is estimated that less than one percent is contaminated. However, this contamination is unevenly distributed and the most densely populated parts of the country are suffering the most (2).

Over the past 10 years the increase in the incidence of groundwater contamination by organic compounds has been dramatic. The widespread use of these compounds, particularly chlorinated organic compounds, has made their frequent detection in groundwater understandable. Chlorinated organic compounds have been used for many years as industrial degreasers (3), septic tank cleaners (4) and in the drycleaning industry (5). One area of the country where this type of contamination is particularly acute is the Atlantic coastal plain of New Jersey, where the majority of the water is supplied from groundwater sources. In 60% of 315 wells sampled in the Potomac-Raritan-Magothy aquifer system in southwestern New Jersey and an

adjacent area of Pennsylvania, detectable levels of organic compounds were found (6). In some wells concentrations exceeded 100 μg/L. Trichloroethene, tetrachloroethene and benzene were the most frequently detected compounds.

Since 1975 the United States Environmental Protection Agency (EPA) has conducted six national surveys to determine the occurrence of organic compounds in drinking water (7). In the 1982 Groundwater Supply Survey, 21% of 100 drinking water supplies which used groundwater as a source, were found to be contaminated with one or more organic chemicals (primarily in the low μg/L range) (7). With evidence from studies such as these pointing to the increasing occurrence of these contaminants in our nation's drinking water supplies, the EPA has been forced to take regulatory action.

In accordance with the June 1985 ammendments to the Safe Drinking Water Act, the EPA has set Maximum Contaminant Levels for eight volatile organic chemicals which occur most frequently in drinking water, see Table 1.1. These standards go into effect Dec. 31, 1988 (8). Each of these compounds is considered by the EPA to be a probable human carcinogen or to cause adverse health effects in humans (7). The EPA has also published a list of 45 chemicals that are possible candidates for health protective regulations by 1991 (8). The majority of these 53 chemicals are volatile, chlorinated organic compounds. The Maximum Contaminant Levels set by the EPA are essentially the lower limits of analytical detection in water for the specific compounds regulated (9). The EPA proposed Recommended

Table 1.1. EPA Final Maximum Contaminant Levels (MCL) for the Eight Volatile Organic Chemicals Most Commonly Found in Drinking Water[a].

Compound	MCL (μg/L)
Benzene	5.0
Tetrachloromethane	5.0
para-Dichlorobenzene	75
1,2-Dichloroethane	5.0
1,1,1-Trichloroethane	200
1,1-Dichloroethene	7.0
Trichloroethene	5.0
Chloroethene	2.0

[a]Ref. 8.

Maximum Contaminant Levels for most of these compounds are zero. These are the levels for these compounds which EPA has determined would result in no known or anticipated adverse health effects in humans, with an adequate margin of safety (7). Therefore, there is a need for sensitive sampling and analysis methodologies capable of detecting sub-μg/L levels of volatile organic compounds in groundwater.

1.2 Analytical Procedures for the Determination of Volatile Organic Compounds in Water

Levels of volatile organic compounds in water traditionally have been determined by purge and trap (P&T) type analysis techniques. Because these compounds are often present at μg/L levels, a concentration step is required for their analysis. The volatile nature of these compounds allows them to be easily separated from the water matrix by stripping with an inert gas. During the purge step an inert gas is bubbled through a sample of water. As the gas exits the sample it is passed through a trap which retains and concentrates the compounds purged from the sample (the trapping step). The trap, which is a bed of sorbent material, is then heated and flushed with an inert gas (thermal desorption) and the compounds originally stripped from the water are transferred to a gas chromatograph for separation and analysis. The P&T method has been adopted by the EPA for the determination of a group of 30 volatile organic compounds, termed the purgeable priority pollutants (PPP), in water (10). Table 1.2 is a

list of the PPPs. All eight of the EPA regulated volatile organic compounds and 20 of the volatile organic compounds proposed for regulation are designated as PPPs.

Several drawbacks may exist when P&T is used for the determination of PPPs in groundwater. Due to the volatility of these compounds, care must be taken to prevent their loss from the sample during sample collection and storage. A 40 mL sample of water is usually collected for P&T analysis (10). Of this volume anywhere from 5 to 25 mL is usually analyzed. Samples may be retrieved from a well by a variety of bailing or pumping procedures (12). However, changes in sample pressure (13) and the exposure of a sample to air (14,15) during sampling may cause compound-volatilization losses from the sample to occur. Samples are also exposed to air as they are transferred to containers for storage and from storage containers to the analysis system. Each sample transfer may contribute to compound-volatilization losses prior to analysis (16-19). Sampling apparatus can cause sample contamination by the leaching of organic compounds from polymer materials used for pumping mechanisms and associated tubing, or bailers (14,20-23). In addition, compounds can also be lost from the sample by adsorption onto sampling materials, particularly the tubing associated with the pump (24). Therefore, the reuse of a pump or a bailer on separate wells can cause sample cross-contamination by the leaching of these previously adsorbed compounds (15,23,24). Thus, the traditional sampling and sample-handling

Table 1.2. EPA Purgeable Priority Pollutants: Solubilities and Octanol-Water Partition Coefficients at 25°C.

Compound	S^a(mg/L)	$K_{ow}{}^a$(unitless)
p-Dichlorobenzene	79	3600
o-Dichlorobenzene	100	3600
m-Dichlorobenzene	123	3600
Ethylbenzene	152	2200
Tetrachloroethene*	200	759
1,1-Dichloroethene	400	135
Chlorobenzene*	488	690
Toluene	535	620
trans-1,2-Dichloroethene	600	123
1,1,1-Trichloroethane	720	320
Tetrachloromethane	785	912
Bromomethane	900	12.3
Trichloroethene*	1100	263
Trichlorofluoromethane	1100	331
Benzene*	1780	135
trans-1,3-Dichloropropene	2700	100
Chloroethene	2700	17
1,2-Dichloropropane*	2700	105
1,1,2,2-Tetrachloroethane*	2900	245

Table 1.2 (cont'd). EPA Purgeable Priority Pollutants: Solubilities and Octanol-Water Partition Coefficients at 25°C.

Compound	S[a](mg/L)	K_{ow}[a](unitless)
Tribromomethane*	3010	240
cis-1,2-Dichloroethene*[b]	3500	NA[c]
Dibromochloromethane	4000	174
Bromodichloromethane*	4500	126
1,1,2-Trichloroethane*	4500	117
1,1-Dichloroethane*	5500	63
Chloroethane	5740	30.9
Chloromethane	6450	8.9
Trichloromethane*	8200	91
1,2-Dichloroethane*	8690	30
2-Chloroethylvinylether	15000	13.8
Dichloromethane	20000	18.2

[a]Ref. 11
[b]Only the trans isomer is listed as a purgeable priority pollutant.
[c]Not available.
*Compound used in at least one adsorbent cartridge breakthrough experiment (see Section 4.2.2).

procedures associated with the P&T analysis methodology may lead to an innaccurate measurment of PPP levels in groundwater.

The practical limitation on the method sensitivity of P&T is another drawback which may be associated with its use for the determination of PPPs in groundwater. As mentioned above, the standard analysis volume ranges from 5 to 25 mL of sample. These analysis volumes, however, will not always be sufficient to detect sub-μg/L levels of many of the PPPs. P&T type procedures have been developed, such as the one by Bertsch et al. (25) and Grob et al. (26), which significantly increase the analysis volume (on the order of 1 L of sample). However, the complexity of the analysis and the time required for its completion also increases dramatically. Therefore, these procedures are often impractical for large scale groundwater quality investigations.

Aqueous adsorption/thermal desorption (ATD) with the porous polymer sorbent Tenax (27-30) is an alternative sampling and analysis methodology which may be used for the determination of PPPs in groundwater. This procedure involves the passage of a specific volume of water at a controlled flow rate through a glass cartridge filled with the sorbent material (the adsorption/sampling step). As the water passes through the bed, organic compounds are quantitatively retained and concentrated by the sorbent. The cartridge is later heated while an inert gas is passed through the sorbent bed (thermal desorption/cartridge analysis step). This step recovers trapped compounds and transfers them to a gas chromatograph/mass spectrometer

where they are separated and analyzed. This procedure has been used successfully by Pankow et al. (31,32) for the determination of some PPPs in groundwater.

The primary advantages of ATD are its potential for increased method sensitivity and decreased sample handling. While the volume of sample which can be concentrated by P&T has practical limitations, ATD may be used to concentrate relatively large volumes of water provided that the compound adsorption step is quantitative. In other words, it must be shown that the PPPs are completely removed from the volume of water passed through the sorbent bed. As the percent removal from water of the targeted compounds increases so too does the sampling efficiency and the accuracy of the method.

The ATD sampling step may be designed (31,32) so that the groundwater sampled contacts only the glass cartridge and the sorbent material. Therefore, there is little chance of contaminating samples through their contact with sampling materials or of losing compounds by adsorption onto these materials. Because each cartridge is a dedicated sampler cross-contamination problems are also eliminated. Samples may also be concentrated at their in-situ pressure in the well (31,32). Cartridges may be lowered to any point in a well and the desired volume of groundwater passed through them. Therefore, the ATD sampling step performed in this manner, involves no changes in sample pressure or exposure of the sample to air during sampling. Because a volume of water is not recovered from the well and returned to the laboratory for analysis, compound losses due to the transfer of

a sample to and from a storage container are also eliminated. The development of ATD for the determination of PPPs in groundwater may therefore provide a more sensitive and accurate method than P&T for the detection and quantitation of trace levels of these compounds.

1.3 Objectives

The primary objective of this research project was the development of ATD for the determination of sub-μg/L levels of PPPs in groundwater. For this purpose, four aspects concerning the use of ATD have been investigated. In Chapter 2 the general ATD cartridge analysis procedure is reviewed and the modifications required for the determination of volatile organic compounds are discussed. Two new cartridge analysis techniques were developed and tested for this purpose. In Chapter 3 the results of a field evaluation of ATD are discussed. The intention was to determine the precision and accuracy of ATD for the determination of a variety of PPPs in groundwater relative to that of a more traditional sampling and analysis method. Two ATD sample acquisition techniques, each incorporating significantly different degrees of sample handling, were tested. The ATD sampling and analysis method was compared with a traditional sampling and P&T analysis technique.

In Chapter 4 the design and results of experiments conducted to determine the capacity of the sorption system under various sampling conditions are discussed. The capacity of the sorption system as a function of sample matrix and individual compound concentration was

investigated. The results of these experiments were used to determine the method sensitivity of ATD for a group of PPPs with a range of physical properties. Finally, Chapter 5 discusses the use of two models for the prediction of adsorbent cartridge sampling efficiency for a variety of sampling conditions. Modeling parameters obtained from the data generated in Chapter 4 are used with each model to predict the efficiency of the sampling system for a group of PPPs over a range of sample volumes. The modeling results are compared with the experimental results of Chapter 4 to determine the accuracy and general utility of each model.

CHAPTER 2 ADSORPTION/THERMAL DESORPTION - METHOD DEVELOPMENT

2.1 Introduction

2.1.1 General Description of Adsorption/Thermal Desorption

Adsorption/thermal desorption is both a sampling and analysis technique for the determination of trace quantities of organic compounds in air and water. This study concerns the use of ATD for the sampling and analysis of groundwater contaminated with volatile organic compounds at concentrations ranging from 1 ng/L to 20 μg/L (ng/L = part-per-trillion (ppt) and μg/L = part-per-billion (ppb)). During the adsorption (sampling) step a specific volume of water is passed at a controlled flow rate through a glass cartridge containing a sorbent. Organic compounds in the water partition to the sorbent and are adsorbed; thus, compounds in the water are concentrated on the sorbent bed. If the adsorption step operated efficiently, the cartridge effluent should be essentially free of the compounds which the cartridge was designed to retain. Prior to analysis, residual water trapped in the pore spaces of the sorbent bed is removed by a two step drying procedure.

The thermal desorption (cartridge analysis) step involves the heating of the cartridge while a stream of inert (carrier) gas flows through it. During this procedure compounds (analytes) which are trapped on the sorbent are transferred to a gas chromatograph/mass spectrometer analysis system which separates, identifies, and quantifies them. By knowing the total volume of water passed through

each cartridge and the mass of each analyte determined by the analysis system, the concentration of each analyte in the water is determined. The first part of this study focussed on the improvement of the ATD methodology for the determination of the PPPs, see Table 1.2.

2.1.2 Cartridge Preparation

The following is a brief description of ATD cartridge preparation. This procedure has been described in detail previously by Pankow et al. (31). Each sorbent cartridge was constructed of borosilicate glass. A 2.5-cm length of 0.64 cm O.D. and 0.20 cm I.D. tubing was fused to the inlet end of the cartridge body and a 1.5-cm length of the same tubing was fused to the outlet end. The body of the cartridge was a 5.4-cm length of 0.64 cm O.D. and 0.40 cm I.D. tubing. The total length of the cartridge was 9.4 cm. The length of the sorbent bed, its cross-sectional area and volume were 5.4 cm, 0.13 cm^2 and 0.68 cm^3, respectively. Each cartridge was identified by a three digit number fired onto its outer surface.

Each cartridge was packed with ~0.13 g of 60/80 mesh Tenax-TA (obtained from Alltech Assoc. Inc., Deerfield, IL) a porous polymer adsorbent. In some work described here Tenax-GC has been used. The term "Tenax", however, will be used to refer collectively to Tenax-GC and Tenax-TA. Tenax-TA is formed by a process that leads to lower blank levels and therefore has been the sorbent of choice in recent work. The Tenax was held in place with small plugs of silanized glass

wool. A solvent extraction/thermal conditioning procedure was used to clean each cartridge. One liter of 60:40 acetone:hexane was pumped at a flow rate of 2 mL/min through six cartridges connected in series. All solvents used throughout this work were of reagent grade quality and obtained from Burdick and Jackson (Muskegon, MI).

Following solvent extraction, each cartridge was then heated for for 3 hours at 300°C while passing ultra-pure helium (UP-He, guaranteed minimum purity 99.995% He, obtained from Air Products Inc., Portland, OR) at a flow rate of ~60 mL/min, through each bed. All cartridges were sealed with Swagelok (Crawford Fitting Co., Solon, OH) 0.64 cm brass endcaps equipped with poly(tetrafluoroethylene) (PTFE) ferrules. Prior to use, all PTFE ferrules and Swagelok fittings were washed in hot soapy deionized water, air dried, sonicated in 60:40 acetone:hexane, air dried, and then heated for 1 hour at 110°C under vacuum. The sealed cartridges were stored and transported in clean borosilicate glass culture tubes with PTFE lined caps.

2.1.3 Analysis Procedure

The following is a general description of the ATD analysis procedure which has been described previously by Pankow et al. (30). Following sampling, each ATD cartridge was resealed, transported on ice and stored in the laboratory under refrigeration at 4°C until analysis. Prior to analysis, residual water trapped in the pore spaces of the sorbent bed was removed from the cartridge by a two step centrifugation/vacuum desiccation procedure. Each cartridge was first

centrifuged at 3500 rpm for 10 min. Following this, ~30 μL of water remained in each cartridge. Each cartridge was then desiccated under vacuum for 20 min in a multi-port vacuum chamber. At the end of this procedure, ~2 μL of water remained in each cartridge.

The thermal desorber used for the desorption of each cartridge is depicted in Figure 2.1. The construction and operation of the thermal desorber is also described in detail elsewhere by Pankow et al. (30). The desorber was mounted horizontally onto the front of a Hewlett-Packard 5790 gas chromatograph (GC) (Palo Alto, CA). The outlet of the thermal desorber was connected to a fused-silica capillary gas chromatography column. In turn, the outlet of the column was connected to a Finnigan 4000 mass spectrometer/data system (MS/DS) (Sunnyvale, CA) according to the procedure developed by Pankow and Isabelle (29).

The cartridge analysis procedure involved three steps: 1) an O_2/solvent purge; 2) a thermal desorption; and 3) a gas chromatography run. After 2 μL of an internal standard or standard solution in methanol was injected into a cartridge bed (see Section 2.1.5), the cartridge was inserted into the thermal desorber. The unit was then sealed and UP-He was passed through the cartridge at a flow rate of ~15 mL/min for 5 min. The cartridge effluent was vented to the outside. This step was designed to purge the cartridge of O_2, which causes the degradation of Tenax at high temperatures. This step also aided in the removal of a portion of methanol (the standard solvent) from the sorbent bed prior to the desorption. For the thermal

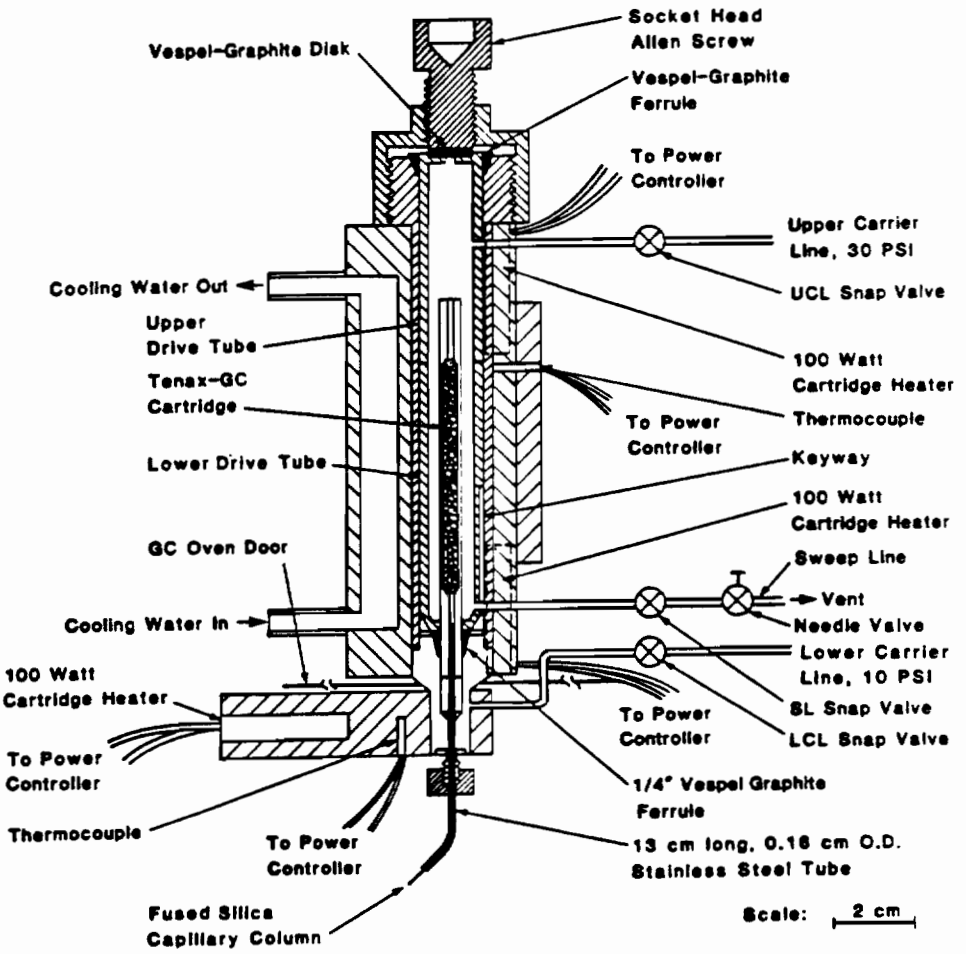

Figure 2.1. Device for thermally desorbing ATD cartridges. Reprinted from Pankow et al. (30).

desorption step the desorber was heated to 250°C for 5 min while UP-He was passed through the cartridge at a flow rate of ~10 mL/min. It took ~2 min for the desorber to reach a temperature of 250°C. Therefore the total desorption time was ~7 min.

The cartridge effluent was transferred to the fused-silica capillary gas chromatography column. The column was maintained at -80°C, with liquid-N_2, in order to focus the desorbed analytes in the beginning portion of the column. This procedure, developed by Pankow (33) and termed whole column cryotrapping (WCC), requires that each cartridge contain no more than 2 μL of residual water. If > 2 μL of water is desorbed from a cartridge the water (which freezes) plugs the capillary column (for columns with an I.D. of 0.32 mm or less). Thus, an incomplete cartridge desorption results and the analysis is ruined.

When the desorption was completed the GC oven temperature was raised to 0°C ballistically. An oven temperature program of 5 to 10°C/min, for 10 to 20 min, was then started. A carrier gas (UP-He) flow rate of ~2 to 3 mL/min was utilized. The gas chromatographic run was used to separate the mixture of target analytes. As each target analyte exited the capillary column it entered the MS/DS where a mass spectral analysis was performed. This enabled the identification and quantitation of each compound present.

The desorber was cooled during the gas chromatographic analysis by circulating cold water through an aluminum jacket which surrounded

the brass body of the desorber. The total time required for the cartridge analysis was 22 to 32 min, depending on the length of the gas chromatographic analysis.

The importance of WCC during thermal desorption cannot be over emphasized. This procedure prevents a loss of analyte resolution which would be otherwise unavoidable. The thermal desorption step required ~7 min to complete, with a carrier gas flow rate of ~10 mL/min. Therefore, ~70 mL of carrier gas passed through the sorbent bed and the capillary column during the analyte desorption procedure. This volume of carrier gas is very large in comparison to the 20 to 60 mL of carrier gas which is required for the gas chromatographic analyte separation. Without the WCC procedure the mixture of analytes would spread out in a broad band through the column prior to the gas chromatographic separation and very poor analyte resolution would result. Therefore, WCC is used to focus all the analytes at the head of the capillary column during thermal desorption. Thus, WCC allows the benefits (increased sensitivity and analyte separation) of the excellent resolution provided by capillary column gas chromatographic analysis to be utilized.

2.1.4 Target Analyte Identification and Quantitation

Target analytes were identified and quantified according to procedures that were analogous to those outlined for the PPPs in EPA Test Method 624 (10). Before samples were analyzed, the ATD-GC/MS/DS was calibrated with a series of multi-level standards spanning the

analyte concentration range of interest. The data system of the mass spectrometer produced and stored a reconstructed ion chromatogram (RIC) for each sample analyzed. The mass spectrometer is simply a mass-selective detector for the GC. As each compound eluted from the chromatography column it entered the ion source of the mass spectrometer where it was ionized and its mass spectra was obtained. The RIC is a total mass chromatogram, a representation of the mass spectrometer (detector) response over time. The data system was used to search the RIC of each sample for the characteristic mass ions, extracted ion chromatograms (EIC), of the target analytes.

A target analyte was considered to be identified when three characteristic ions with appropriate relative responses maximized at the correct retention time. The response equaled the integrated area under the peak of a characteristic ion and the retention time was the chromatographic elution time of the peak. The EICs of a standard, analyzed according to the ATD analysis procedure, were used to establish the preceding criteria. Figure 2.2 displays the RIC of a standard containing the PPPs which was analyzed using ATD, and Figure 2.3 displays the ion profiles for three of the characteristic ions of benzene from the same standard.

An internal standard calibration procedure was used in order to determine the amount of each target analyte in an ATD sample cartridge. Each sample cartridge was injected with a solution containing three internal standard compounds. These compounds were also present, at the same level, in each ATD standard analyzed. The

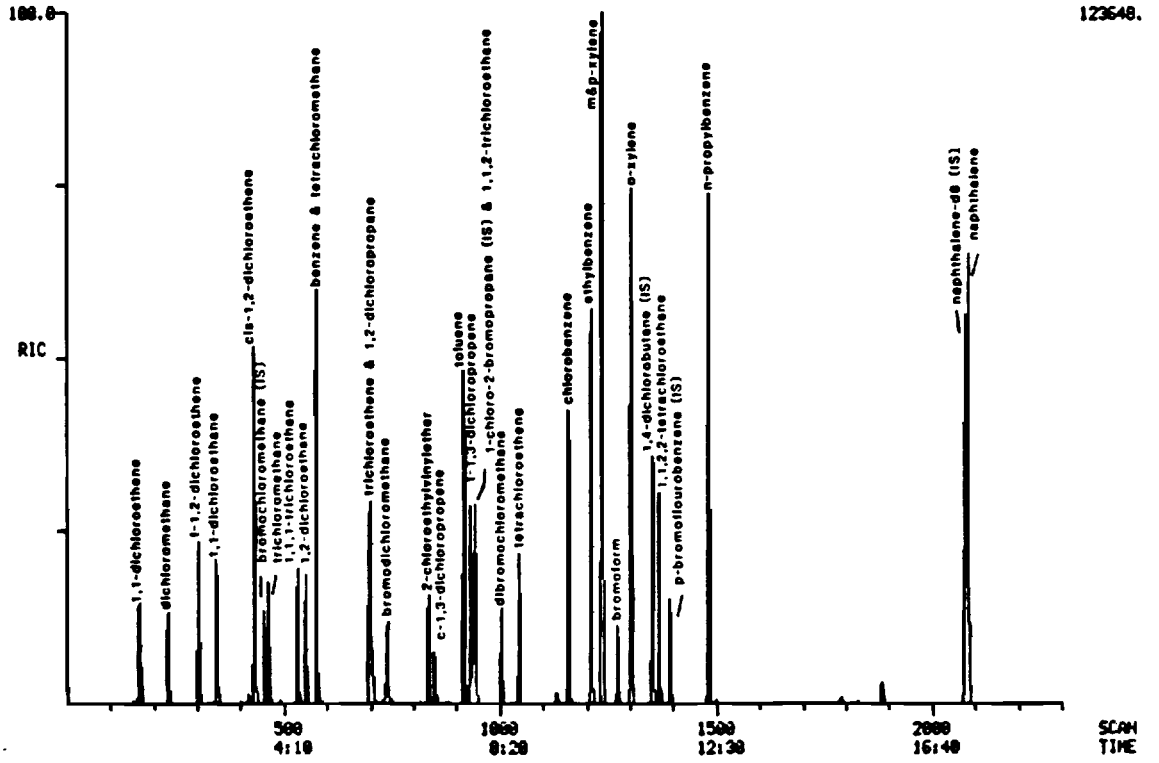

Figure 2.2. RIC (total mass chromatogram) of a 100 ng/component standard of 34 compounds including 23 PPPs analyzed using ATD with GC/MS.

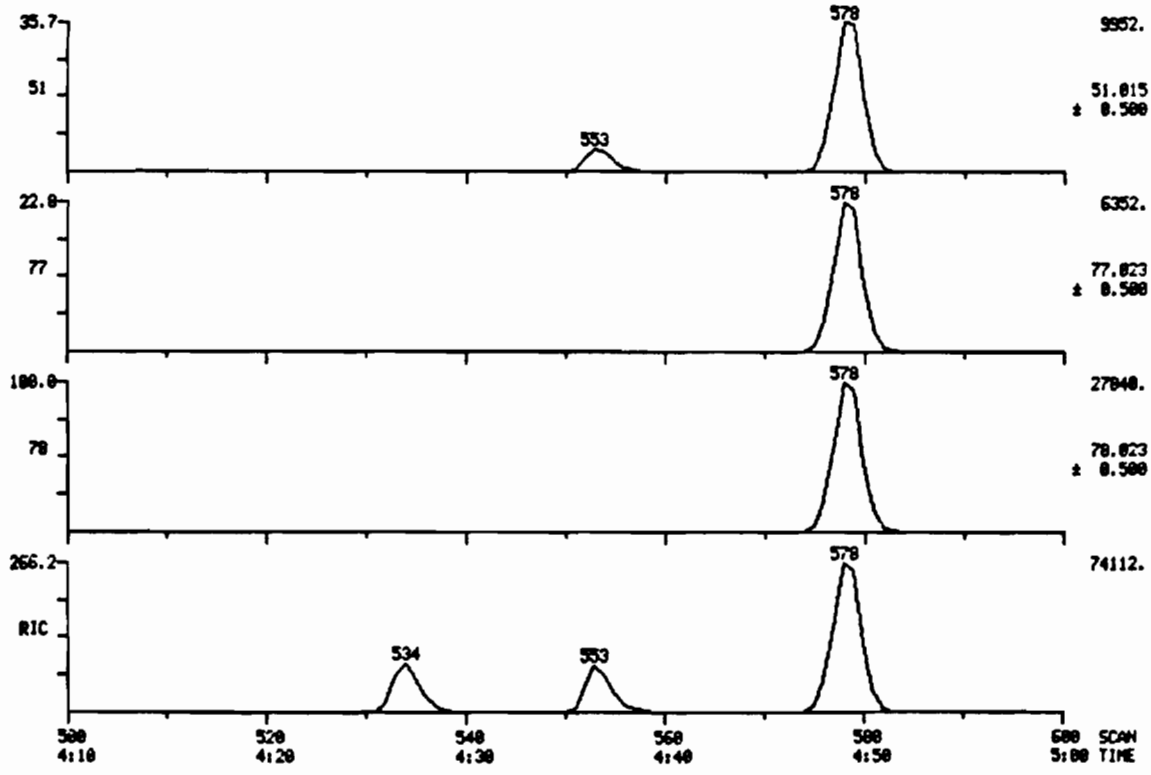

Figure 2.3. Extracted ion profiles for three characteristic ions of benzene, from a 100 ng/component standard analyzed using ATD with GC/MS.

three internal standard compounds used most often were bromochloromethane, 1-chloro-2-bromopropane and 1,4-dichlorobutane. Each of these compounds eluted in a distinct region of the chromatogram. The internal standards were used to calculate response factors for the target analytes that eluted in their respective retention regions, according to the following equation:

$$\text{response factor} = \frac{(\text{area})(\text{internal standard amount})}{(\text{internal standard area})(\text{amount})} \qquad 2.1$$

The data system software enabled the use of response factors which were a function of target analyte amount. Once the target analyte response factor was determined the following equation was used to calculate the target analyte amount in a sample:

$$\text{amount} = \frac{(\text{area})(\text{internal standard amount})}{(\text{internal standard area})(\text{response factor})} \qquad 2.2$$

Multi-level standards were run throughout each day of the sample analysis period in order to verify the system calibration. The advantage of using internal standard calibration was that it increased the analysis precision by allowing the the analyst to correct for the fluctuation in system response during an analysis period.

2.1.5 Standard Preparation

Standards were prepared by making successive dilutions of analytes purchased as mixtures in methanol (Purgeable A,B and internal

standards, obtained from Supelco, Bellefonte, PA). As purchased, the purgeable internal standard solution contained bromochloromethane, 1-chloro-2-bromopropane and 1,4-dichlorobutane at 2000 μg/mL. Purgeable A and B each contained approximately half the PPPs at 200 μg/mL. All successive dilutions of these standards were made with reagent grade methanol. Each final dilution (standard) was stored in a freezer in a 1 mL amber mini-vial sealed with an open topped screw cap and PTFE-faced septum. Two types of standards were prepared, one containing the internal standards only, and the other containing the PPPs and the internal standards. Both types were prepared at concentrations which allowed 2 μL injections into an ATD cartridge. Each standard contained the internal standard components at ~75 ng/μL. For samples where it was necessary to quantify additional compounds not contained in the Supelco mixtures, separate dilutions in methanol were prepared. For these standards, compounds were obtained from Chem Service Inc. (Westchester, PA) in neat form. Final standards were prepared by combining the Supelco dilutions with these. A Hamilton (Reno, Nevada) 10 μL syringe was used to withdraw a standard from its container (by piercing the septum of the vial), and inject it into an ATD cartridge. Standard analyses were performed with clean ATD cartridges prepared for this purpose.

2.2 Cartridge Vacuum-Desiccation

2.2.1 Preliminary Considerations

Once compounds have been concentrated on a sorbent bed, the most efficient method of their removal, for the purpose of analysis, is thermal desorption (25,27,34,35). Tenax, unlike other porous polymers, exhibits thermal stability at temperatures in excess of 300°C (27,36). This makes Tenax ideal for the thermal desorption of trapped analytes. There are several advantages to the thermal desorption technique. In a single, quick, efficient, and simple step, the entire amount of adsorbed material may be transferred from the bed to the GC column.

Solvents have also been utilized for analyte desorption (37-39) however, increased sample handling, decreased sensitivity, and solvent interference during analysis are the major drawbacks of this technique (34). Typical solvent elution volumes (for cartridge extraction) range from one to tens of milliliters (34,37-39). Therefore, only a small amount of the total analyte concentrated by the sorbent is usually analyzed because a typical gas chromatographic analysis is limited to 1 to 2 μL of sample. In order to increase sensitivity the solvent eluent may be concentrated by partial evaporation (37,38). However, such a concentration procedure can cause losses for volatile analytes (34). Finally, a large solvent peak (the solvent is present in great excess) will often partially overlap or elute over target analyte peaks and therefore detract from the gas chromatographic analysis. Thus, thermal desorption which is

less time consuming, involves less sample handling and is inherently more sensitive will often be the analyte desorption technique of choice for volatile organic compounds.

The presence of residual water in the Tenax bed after sampling, has caused some difficulties in the use of ATD for the determination of volatile low molecular weight organic compounds in water. Indeed, if allowed to enter the analysis system, residual water may interfere with GC detector performance (27,35). In cases where subambient cooling of a capillary gas chromatography column is used to help focus the desorbing analytes, the column may plug due to ice formation, resulting in incomplete sample desorption (27). In recognition of these problems Ryan (35) developed an elaborate and complicated technique allowing the thermal desorption of a wet ATD cartridge. Bertsch et al. (25) attempted to dry the Tenax bed prior to analysis but found sample losses to be high and non-reproducible. Versino et al. (40) developed a pre-analysis drying technique, in which samples were placed overnight in a desiccator maintained at reduced pressure. They noted, however, that analyte volatilization losses for compounds more volatile than benzene were likely to occur during this long desiccation procedure.

A two-step centrifugation/vacuum-desiccation cartridge drying method was developed by Pankow and Isabelle (27). This technique showed promise because it required relatively little time to complete (30 min total, see Section 2.1.3), removed enough residual water from the cartridge to allow WCC, and provided excellent percent recoveries

for several semi-volatile organic compounds tested. However, it seemed likely that the vacuum-desiccation step might cause losses for the lighter more volatile PPPs.

2.2.2 Review of Previous Vacuum-Desiccation Percent Recovery Studies

As discussed above, the initial testing of the two-step cartridge drying technique by Pankow and Isabelle (27) determined that very high percent recoveries could be obtained for several classes of organic compounds including aromatics, alkanes, chlorinated hydrocarbons and methyl esters of fatty acids. For a total drying time of 30 min (10 min centrifuge- and 20 min vacuum-desiccation) close to 100% of the residual water could be removed from each cartridge. It should be noted that these experiments were conducted with large bed ATD cartridges of the following dimensions: 7.0, 0.90, and 1.3 cm for the bed length, I.D. and O.D., respectively and 4.5 cm^3 for the bed volume. Each cartridge was packed with ~0.75 g of Tenax.

Percent recovery studies of the full ATD method were conducted by Pankow et al. (30,41) for the small bed ATD cartridges for a variety of volatile (41) and semi-volatile (30) compounds. Because the use of ATD for the determination of volatile compounds is of particular interest here, only the preliminary results from those studies will be discussed.

Analyte volatilization losses during the centrifuge-desiccation step were determined to be negligible (41). Vacuum-desiccation related losses were first investigated (41) in the following manner.

Three dry Tenax cartridges were each injected with 2 μL of a 50 ng/μL per component standard in methanol containing most of the PPPs. Each cartridge was then subjected to the 20 min vacuum-desiccation step and analyzed. Analyte peak areas from these analyses were compared with those obtained from three analyses of 2 μL of the same standard also injected onto dry Tenax cartridges, which were immediately analyzed (without vacuum-desiccation). Average analyte percent recoveries, $\bar{R}$, were determined ($\bar{R}$ = 100 x (average analyte response with vacuum-desiccation ÷ average analyte response without vacuum desiccation)). These results were very positive. For most compounds tested, the values of $\bar{R}$ ranged from 90 to 100%.

With the above results of Pankow et al. (41) in mind, ATD samples obtained during two separate groundwater sampling trips (see Section 3.7.1) were analyzed according to the ATD procedure outlined thus far (i.e., including the vacuum-desiccation step). The results of these analyses indicated that a systematic loss of some analytes was in fact occurring during the vacuum-desiccation step, with the most volatile analytes affected to a significant degree. This caused the results of the vacuum-desiccation percent recovery study, described above, to be considered suspect.

Pankow et al. (41) felt that had the percent recovery study been performed by injecting a standard onto a pre-wetted, pre-centrifuged cartridge which was then vacuum-desiccated, lower analyte percent recoveries would have been obtained. Therefore, the vacuum-desiccation percent recovery study was repeated by Pankow et al. (41)

in the following manner. Three pre-wetted, pre-centrifuged Tenax cartridges were each injected with 2 μL of a 50 ng/μL per component standard in methanol containing most of the PPPs. Each cartridge was then subjected to the 20 min vacuum-desiccation step and analyzed. In a manner similar to that described above, analyte peak areas from these analyses were compared with those obtained by three analyses of 2 μL of the same standard injected onto pre-wetted, pre-centrifuged, pre-vacuum-desiccated Tenax cartridges. Average analyte percent recoveries, $\bar{R}$, were determined ($\bar{R}$ = 100 x (average analyte response with vacuum-desiccation ÷ average analyte response without vacuum-desiccation)). Table 2.1 presents $\bar{R}$ values $\pm$ one standard deviation unit, *s*, for the vacuum-desiccated cartridges. In addition, the vapor pressure, P, and the Henry's law constant, H, of each analyte is also presented.

The results in Table 2.1 indicate that the vacuum-desiccation step worked well for only a small fraction of the PPPs tested. Only five of the 23 compounds tested experienced mean recoveries of 85% or greater. It appears that as $\bar{R}$ decreases H increases. In fact, it seems that only compounds with an H value in the vicinity of 2×10^{-3} atm-m^3/mole or lower, experience reasonable values of $\bar{R}$. The results from two ATD field investigations (see Section 3.7.1) tend to support this conclusion. This information indicated that an alternative to the vacuum-desiccation technique had to be developed if ATD was to be used for the determination of a broad range of PPPs in water.

Table 2.1. Average Recoveries[a] ($\bar{R}$) of Purgeable Priority Pollutants from a Pre-wetted, Pre-centrifuged ATD Cartridge after the Vacuum-Desiccation Procedure[b], and Henry's Law Constants and Vapor Pressures at 25°C.

Compound	$\bar{R}$[c] (%)	H[d] (atm-m^3/mole)	P[d](torr)
1,1-Dichloroethene	1.6 ± 0.60	1.6 E-1	591
trans-1,2-Dichloroethene	9.0 ± 2.0	4.2 E-2	326
1,1,1-Trichloroethane	27 ± 4.0	3.5 E-2	123
Tetrachloromethane	18 ± 3.0	2.3 E-2	90
Tetrachloroethene	26 ± 3.0	2.0 E-2	14
Trichloroethene	54 ± 8.0	9.1 E-3	58
Toluene	58 ± 16	6.6 E-3	29
Ethylbenzene	50 ± 8.0	6.4 E-3	7
Benzene	43 ± 12	5.5 E-3	95
1,1-Dichloroethene	30 ± 6.0	4.3 E-3	180
Chlorobenzene	72 ± 12	3.8 E-3	12
Trichloromethane	46 ± 9.0	2.9 E-3	151
Dichloromethane	1.4 ± 2.1	2.7 E-3	362
Bromodichloromethane	76 ± 14	2.4 E-3	50
1,2-Dichloropropane	76 ± 12	2.3 E-3	42
trans-1,2-Dichloropropene	90 ± 10	1.3 E-3	25
Tribromomethane	105 ± 19	1.0 E-3	5

Table 2.1 (cont'd). Average Recoveries[a] ($\bar{R}$) Purgeable Priority Pollutants from a Pre-wetted, Pre-centrifuged ATD Cartridge after the Vacuum-Desiccation Procedure[b], and Henry's Law Constants and Vapor Pressures at 25°C.

Compound	$\bar{R}$[c] (%)	H[d] (atm-m^3/mole)	P[d](torr)
Dibromochloromethane	99 ± 14	9.9 E-4	76
1,2-Dichloroethane	79 ± 15	9.1 E-4	61
1,1,2-Trichloroethane	98 ± 14	7.4 E-4	19
1,1,2,2-Tetrachloroethane	88 ± 13	3.8 E-4	5
cis-1,3-Dichloropropene	57 ± 8.0	NA[e]	NA
2-Chloroethylvinylether	16 ± 13	NA	27

[a]Pankow et al. (41).
[b]± 1 *s* are based on three replicate analyses.
[c]Average recoveries are based on the average analyte response for three replicate analyses of a ~100 ng/component standard desorbed from a dry ATD cartridge.
[c]Ref. 11.
[d]Not available.

2.2.3 Alternatives to Cartridge Vacuum-Desiccation

Two new types of cartridge drying systems were constructed and tested. Both were designed so that cartridges which had only been centrifuged (~30 μL of water remains on a cartridge after this procedure) could be analyzed. Each drier was constructed so that it could be connected between the desorber and the GC/MS/DS analysis system and operated during the thermal desorption step. The first system to be tested consisted of a polymer tubing (Nafion) which acted as a semi-permeable membrane. During the thermal desorption step, water diffused through the tubing walls while the target analytes were largely transmitted to the analysis system. This system, however, was found to significantly detract from the high quality capillary gas chromatographic analysis usually obtained with ATD.

The second system tested, and ultimately used, employed a glass bead trap. During the thermal desorption step, water vapor condensed on glass beads contained inside a stainless steel tube. The target analytes were quantitatively transferred to the analysis system. A high quality GC/MS separation and analysis could then follow. The development and testing of both systems is described in the following two sections.

2.3 Nafion Drier System

2.3.1 Introduction

Nafion tubing has been used by many researchers for the purpose of carrier gas drying. Foulger and Simmonds (42) used Nafion tubing

to dry ambient air prior to its analysis for trace halocarbons. Trichloroflouromethane, tetrachloromethane and 1,1,1-trichloroethane were reported to have been completely transmitted to the analysis system while water vapor was selectively removed. In a direct aqueous injection technique developed by Simmonds and Kerns (43), Nafion tubing was used to dry carrier gas containing a 1 to 20 μL sample of vaporized water. It was claimed that trichloroethene, bromodichloromethane, dibromochloromethane and bromoform, in addition to the compounds listed above, were quantitatively transferred to a gas chromatographic column for analysis. More recently, Simmonds (44) has developed a modified purge and trap methodology which uses Nafion tubing to dry the nitrogen effluent stream resulting from the 10 min purging of a 5 mL sample of water. A cryofocussing step was used to enhance resolution of the volatile target analytes. The Nafion tubing was necessary in order to prevent the plugging with ice of a 30 μL capillary loop immersed in liquid-N_2. Simmonds (44) also claimed to be able to almost completely transmit a broad range of volatile organic compounds through the tubing.

Palmer et al. (45) used Nafion tubing for the drying of effluent from the thermal desorption of Tenax cartridges used in ambient air sampling. In their study cryofocussing was also used prior to gas chromatographic analysis. Therefore, moisture from the air which accumulated in the sorbent bed during sampling, had to be removed from the analysis stream to prevent plugging of the cryofocussing unit. While Palmer et al. (45) noted that the Nafion effectively transmitted

a variety of organic compounds to the analysis system, they recommended against the use of Nafion with polar compounds, which they felt the material was likely to adsorb. This hypothesis was supported by Cox and Earp (46) who reported that Nafion tubing was capable of completely transmitting specific analytes from many classes of organic compounds however, relatively polar compounds such as alcohols and ketones were found to be poorly transmitted through the tubing. Therefore, excluding the most polar of the PPPs, it appeared that Nafion tubing could be used to remove water vapor from the cartridge effluent stream resulting from the thermal desorption while transmitting the analytes of interest to the column.

2.3.2 Experimental

As discussed in Section 2.2.3, the reason for investigating the utility of a Nafion drier system was to allow the desorption and analysis of a cartridge after only the standard centrifuge-desiccation step. During the thermal desorption procedure the cartridge effluent is first passed through a heated drying chamber containing Nafion tubing. Nafion tubing (developed by E.I. DuPont de Nemours, and obtained from Perma-Pure Products, Inc., Toms River, NJ) is formed from a perflourinated aliphatic ether polymer with pendent sulfonic acid groups. This material acts as a semi-permeable membrane. During thermal desorption a portion of the water vapor diffuses through the walls of the tubing. Thus, the water may be removed from the analysis

system while target analytes are either partially or completely transmitted through the tubing and into the analysis system.

Figure 2.4 is a diagram of the ATD-Nafion drier system. A box to contain the Nafion tubing was constructed of aluminum. The width, length and depth of the box were 6.4, 15.2 and 6.4 cm, respectively. The floor of the box was constructed from a 1.9 cm thick piece of aluminum. Two holes were drilled through the side of this portion of the box to accommodate two 150 watt cartridge type heaters. The heaters, held in place by set screws, were used to heat the box to the desired temperature. A thermocouple, inserted through a hole in the floor of the box and fastened with a set screw, was connected to a feedback temperature control unit that powered the cartridge heaters. The front and rear plates of the box were constructed of stainless steel (SS) in order to impede the conduction of heat from either the desorber or the GC oven to the box. Six evenly spaced 0.64 cm holes were drilled through the floor of the box. A removeable lid, with two 0.64 cm holes and sliding flaps, was also constructed. The lid, in conjunction with the holes in the floor of the box, allowed the box to be ventilated while in use. This removed water vapor from the system by inducing its diffusion through the wall of the Nafion tubing.

The heater was removed from the front end of the desorber (see Figure 2.1) which was set inside the aluminum box and connected by four screws passing through the front plate of the box and into the desorber. The lower carrier gas line, which enters the desorber at

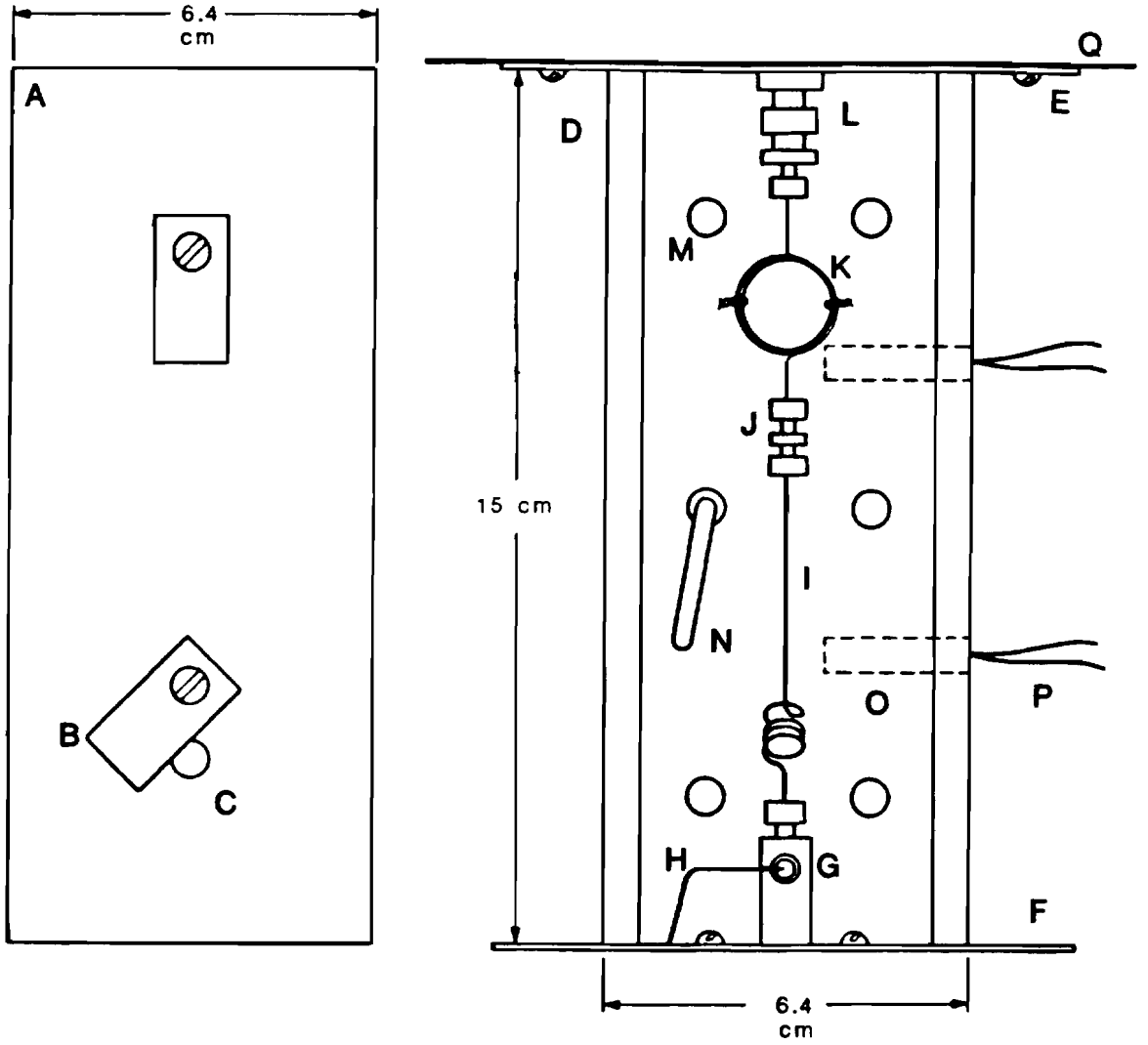

Figure 2.4. Diagram of the ATD-Nafion drier system. This is an overhead view of the device which is mounted to the GC oven door. **A** aluminum lid. **B** moveable flap. **C** 0.64 cm in diameter ventilation hole. **D** aluminum box; 6.4 cm in width and depth, and 15 cm in length. **E** SS rear plate of the box. **F** SS front plate of the box. **G** outlet of the thermal desorber. **H** lower carrier gas line of the desorber; 0.16 cm O.D. SS tubing. **I** 18-cm length of 0.16 cm O.D. SS tubing. **J** Swagelok 0.16 cm brass union, utilizes a 5 mm Vespel/graphite ferrule on the Nafion side. **K** 2 ft of 815X Nafion tubing, 1.0 mm I.D. and 1.3 mm O.D. **L** Swagelok 0.32 to 0.16 cm brass reducer connected to a Swagelok 0.32 cm brass bulkhead union. **M** 0.64 cm in diameter ventilation hole in the floor of the box. **N** thermocouple, leads to power controller. **O** 150 watt cartridge heater. **P** cartridge heater leads to power controller. **Q** GC oven door.

this point (see Figure 2.1), was inserted through a hole in the front plate of the box. The rear plate of the box was mounted to the front of the GC oven with three screws.

Two feet of type 815X Nafion tubing, 1.0 mm I.D. by 1.25 mm O.D., were coiled and bound with two small strips of wire. It was determined (see Section 2.3.3) that this length of tubing was capable of removing ~28 of 30 μL of water, in each cartridge, from the analysis system. The coil of Nafion tubing was supported on a frame constructed of SS tubing (not depicted in Figure 2.4). This frame prevented the tubing from coming in contact with the hot floor of the box and thus decreased the likelihood that the tubing would melt. The thin wall of the tubing had to be supported in order to allow Swagelok fittings to be used with it. Therefore, a 2.5-cm length of small O.D. SS tubing was inserted into each end of the Nafion tubing. The ferrules used were 0.16 cm I.D. by 5 mm Vespel/graphite, and were drilled out to accomodate the Nafion tubing.

During desorption, the desorber body reaches temperatures in excess of 250^{o}C and the Nafion tubing is only stable to ~200^{o}C (47). Therefore, a "heat barrier" was needed to prevent the conduction of heat from the desorber to the Nafion tubing. The desired heat barrier was provided by a coiled 18-cm length of 0.16 cm O.D. SS tubing connected to the outlet end of the desorber. The opposite end of this tubing was connected to the inlet end of the Nafion coil with a Swagelok 0.16 cm brass union. The outlet end of the Nafion tubing was connected to a Swagelok 0.32 to 0.16 cm brass reducer (fractional tube

to fractional tube stub). This fitting was in turn connected to a Swagelok 0.32 cm bulkhead union which was fastened to a hole in the rear plate of the box. The portion of the bulkhead fitting on the backside of the plate (i.e., inside the GC oven) was also connected to a Swagelok 0.32 to 0.16 cm brass reducer through which, a 0.16 cm O.D. SS tube was inserted. This connection is displayed in Figure 2.5. The SS tube travelled through the bulkhead fitting and the other reducer connected to the opposite end (i.e., inside the Nafion drier). The SS tubing ended ~2 mm from the outlet end of the Nafion tubing. This configuration was designed to reduce the dead volume inside the bulkhead union. The other end of this SS tubing (also depicted in Figure 2.5) was connected to a Swagelok 0.64 to 0.16 cm SS reducing union, with a Vespel/graphite ferrule, and in turn connected to the inlet end of a packed gas chromatography column. The outlet end of the packed column was connected to the inlet end of the MS jet separator with a Swagelok 0.64 cm SS union, using Vespel/graphite ferrules.

Work with the Nafion drier was originally performed with packed column GC/MS analyses. It was felt that it would be easier to first investigate the potential of the Nafion drier in this manner because a packed column would be better able than a capillary column to tolerate small amounts of water entering the analysis system. Until this drying system was optimized it was likely that some water would enter the analysis system. Therefore, if capillary column GC/MS with WCC was first utilized the analysis system may have plugged with ice.

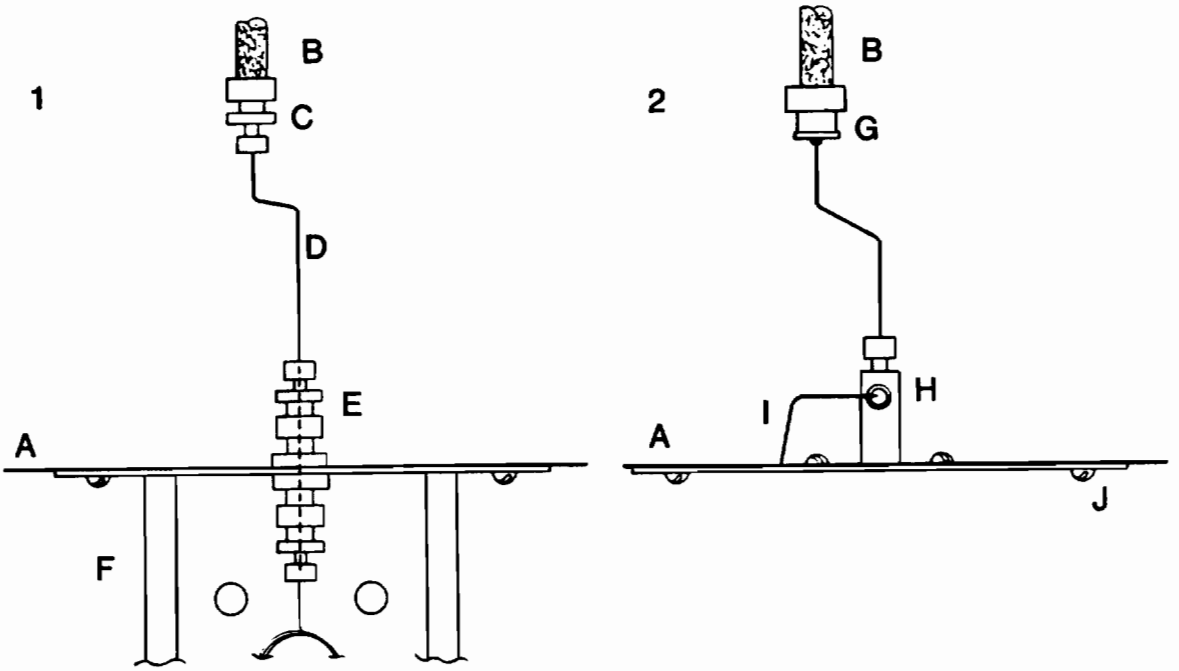

Figure 2.5. Packed column GC connections to Nafion drier and thermal desorber.
1 Nafion drier to packed column GC.
A GC oven door. **B** packed GC column. **C** Swagelok 0.64 to 0.16 cm reducing union with a Vespel/graphite ferrule. **D** 0.16 cm O.D. SS tube. **E** Swagelok 0.32 to 0.16 cm brass reducer connected to a Swagelok 0.32 cm brass bulkhead union. The SS tubing travelled through this fitting into the Nafion drier and ended ~1 mm from the Nafion tubing. **F** Aluminum box with Nafion drier system.
2 Thermal desorber to packed column GC.
A GC oven door. **B** packed GC column. **G** 15-cm length of 0.16 cm SS tubing silver soldered to one half of a Swagelok 0.64 cm SS union. **H** outlet of the thermal desorber. **I** lower carrier gas line of the desorber; 0.16 cm O.D. SS tubing. **J** SS mounting plate of the thermal desorber, which attachs to the GC oven door.

However, the packed column could be maintained at ambient temperature during thermal desorption without a loss of analyte resolution. Therefore, by performing preliminary analyses in this manner Nafion tubing could first be tested to determine its ability to quantitatively transmit the PPPs. The packed column utilized was constructed of 1.8 m of 0.64 cm O.D. and 2.0 mm I.D. borosilicate glass. It was filled with Carbopack B (60/80 mesh) graphitized carbon coated with 1% SP-1000 that was obtained from Supelco. The carrier gas flow rate was set at ~30 mL/min, and the column was conditioned overnight at 210°C with UP-He.

As discussed previously, the ultimate intent of this portion of the study was to interface the ATD-Nafion drier system with capillary column GC/MS analysis. This would allow significantly enhanced compound resolution relative to that available with packed column GC. Recently, wide-bore (0.53 mm I.D.) capillary columns have been developed, such as the VOCOL column by Supelco (48) and the DB-624 Megabore column from J&W Scientific (49), which are capable of completely separating most of the PPPs. In addition to providing good resolution, these columns also provide short GC run times. The stationary phase coatings in these columns are also unique in that small amounts of water present during analysis do not adversely affect the chromatography (49). The phase coatings of these columns are on the order of 3 μm thick. The wider bore of these columns

(0.53 mm I.D. vs. 0.32 mm I.D. of a standard capillary column) may also help to prevent their plugging with ice, should small amounts of water pass through the Nafion drier system.

A J&W Scientific (Folsom, CA) DB-624 Megabore capillary column (30 m x 0.53 mm I.D., 3 um film) was utilized for the ATD-Nafion drier capillary column GC/MS analyses. This work required slightly different interfaces between the column and the drier, and the column and the MS jet separator. The inlet end of the capillary column was connected to the outlet end of the Nafion tubing with a Swagelok 0.16 cm SS union that was mounted through the hole in the rear plate of the aluminum heater box. The following fitting was constructed for the connection of the capillary column outlet to the MS jet separator inlet. One half of a Swagelok 0.16 cm brass union was brazed onto the inlet end of a 5-cm length of 0.64 cm O.D. tubing with an I.D. just slightly larger than the O.D. of the capillary column. The outlet end of the capillary column was inserted through the inlet end of the tube (outlet end of the column flush with the outlet end of the tube) and sealed inside the tube with a Swagelok 0.16 cm brass nut and an 8 mm Vespel/graphite ferrule. Once the capillary column was connected to the tube, the outlet end of the tube was inserted into the inlet end of the MS jet separator and sealed with a Swagelok 0.64 cm SS nut and Vespel/graphite ferrule.

For the desorption of standards directly to the packed column (i.e., minus the Nafion drier), the outlet of the desorber was connected to the inlet of the packed column by use of the fitting

depicted in Figure 2.5. A 15-cm length of 0.16 cm O.D. SS tubing was silver soldered to one half of a Swagelok 0.64 cm SS union. The free end of the SS tubing extended ~3.8 cm into the desorber and was secured with a Vespel/graphite ferrule and a Swagelok 0.16 cm brass nut. The opposite end of the fitting was connected to the inlet end of the packed column by means of a Swagelok 0.64 cm brass nut and a Vespel/graphite ferrule. For the capillary column GC/MS analyses the inlet end of the capillary column was connected to the outlet of the desorber according to the configuration of Pankow et al. (30). This connection is depicted in Figure 2.1.

The following procedure was adopted for sample analysis when the thermal desorber was connected to the Nafion drier. An ATD cartridge that had been injected with 30 μL of water was inserted into the desorber. With the GC oven maintained at 25°C and all carrier gas flow off, the lid (with windows open) was placed on the Nafion box which was then heated to ~100°C. If carrier gas had been allowed to flow through the system as the Nafion was heated, carrier gas heated by contact with the Nafion tubing could have caused the premature desorption of the ATD cartridge. The Nafion tubing was heated to induce the diffusion of water through the walls of the tubing and to prevent the adsorption of target analytes onto the tubing. When the box reached ~100°C the upper carrier supply of UP-He was switched on (flow rate = ~9 ml/min), the desorber was heated to 250°C and maintained at this temperature for 5 min. The O_2 purge step (see Section 2.1.3) was eliminated from these analyses. While the

degradation of Tenax at high temperatures in the presence of O_2 was still a concern, it was believed that in the two minutes required for the desorber to reach 250°C the majority of O_2 would be flushed from the cartridge. In fact, no significant increase in the Tenax background was noted with the omission of the cartridge purging procedure.

When the desorption was complete, the desorber was cooled, carrier gas flow was switched from upper to lower, and the GC temperature program and the MS acquisition were started simultaneously. The GC oven temperature was raised to 45°C and held there for 3 min, the oven temperature then increased from 45 to 220°C at 8°C/min and held at 220°C for 15 min. During the GC/MS analysis the sweep line for the desorber was opened. This enabled carrier gas to backflush the Nafion tubing and prepare it for the next analysis (i.e., remove any water retained by the tubing). For this purpose, the Nafion box was maintained at 100°C for 5 min beyond the completion of the thermal desorption and then allowed to cool.

The above procedure remained essentially the same when the Nafion drier was utilized with capillary column GC/MS analysis, except that the capillary column was maintained at 10°C during the desorption step, and the MS acquisition was initiated at the beginning of the thermal desorption step. A temperature program of 10 to 120°C at 5°C/min, and a carrier gas flow rate of ~9 mL/min was utilized.

Since the possibility existed that some compounds might be adsorbed by the Nafion tubing or diffuse through it (45,46), the

least amount of Nafion tubing used in the drier system should be the minimum amount required. It was first investigated whether 0.60 m of tubing would be able to remove 30 μL of water from the analysis system. The inlet end of a 0.60-m length of Nafion tubing was connected to the outlet of the thermal desorber, while the outlet end of the tubing was connected to one end of a glass cartridge filled with 40 mesh anhydrous $CaCl_2$. This system was used to measure what fraction of the 30 μL of water spiked onto an ATD cartridge would be removed by the Nafion tubing during the thermal desorption procedure. The $CaCl_2$ cartidge was used to trap water which was transmitted through the tubing. The pre- and post-thermal desorption weights of the $CaCl_2$ were compared to determine the amount of water not removed by the Nafion.

In order to evaluate the performance of the ATD-Nafion drier system (i.e., determine the percent transmissions of target analytes through the system) the following experiment was conducted. To start, 2 μL of a standard in methanol containing most of the PPPs at 50 ng/μL, was desorbed from dry ATD cartridges directly to the packed column GC/MS analysis system. Individual compound responses (analyte peak areas) were compared with those obtained when 2 μL of the same standard was analyzed using the ATD-Nafion drier system (also with packed column GC/MS analysis), with ATD cartridges which were either dry or spiked with 30 μL of water. Three dry and four wet cartridge analyses were performed and compared with two analyses of the type first described (i.e., minus the drier). Average analyte percent

recoveries, $\bar{R}$, were determined ($\bar{R}$ = 100 x (average analyte response with the Nafion drier system)÷(average analyte response without the drier system)).

2.3.3 Results and Discussion

With a thermal desorption flow rate of ~9 mL/min, the 0.60-m length of Nafion tubing removed all but ~2 μL of the 30 μL of water injected onto the ATD cartridge. As the thermal desorption flow rate was increased, however, the Nafion tubing was less efficient. At a flow rate of ~30 mL/min, only ~23 μL of the 30 μL of water was removed by the tubing. Therefore, it was concluded that with a thermal desorption flow rate of < 10 mL/min, 0.60 m of Nafion tubing would be sufficient for the removal of enough water (28 of 30 μL) from the analysis system.

Table 2.2 presents the results of the target analyte percent recovery experiment performed with the Nafion drier system. For most compounds, at least 70% of the total analyte mass was transmitted through the Nafion tubing to the analysis system. The exception was 2-chloro-ethyl-vinylether whose value for $\bar{R}$ was less than 2%, as might be expected (45,46) for this relatively polar compound. Considering its polarity, it's possible that 2-chloro-ethyl-vinylether diffused through the Nafion tubing along with the water. In general, there was little difference in analyte recoveries whether they were desorbed from dry cartridges or from cartridges containing 30 μL of water. For some compounds the percent recoveries in the presence of water were

Table 2.2. Average Recoveries ($\bar{R}$) of Purgeable Priority Pollutants from a Wet or Dry ATD Cartridge Analyzed using the ATD-Nafion Drier System and Packed Column GC/MS[a].

Compound	$\bar{R}$[b] (%) wet[c] cartridge	$\bar{R}$[b] (%) dry cartidge
Dichloromethane	78 ± 0.90	74 ± 3.0
1,1-Dichloroethene	99 ± 3.8	110 ± 6.8
Bromochloromethane	85 ± 2.3	95 ± 6.5
1,1-Dichloroethane	97 ± 5.4	96 ± 4.5
trans-1,2-Dichloroethene	100 ± 3.0	93 ± 6.2
Trichloromethane	91 ± 2.7	89 ± 4.0
1,2-Dichloroethane	96 ± 2.9	90 ± 5.8
1,1,1-Trichloroethane	97 ± 4.5	100 ± 4.9
Tetrachloromethane	92 ± 2.3	98 ± 7.4
Bromodichloromethane	84 ± 6.1	87 ± 5.5
1,2-Dichloropropane	85 ± 5.9	87 ± 4.4
cis-1,3-Dichloropropene	80 ± 3.2	75 ± 3.4
Trichloroethene	92 ± 4.7	93 ± 5.8
Benzene	89 ± 5.2	89 ± 3.7
1,1,2-Trichloroethane	89 ± 2.4	80 ± 3.4
trans-1,3-Dichloropropene	85 ± 3.2	83 ± 5.5
Dibromochloromethane	86 ± 1.2	80 ± 3.0
Chlorobromopropane	86 ± 5.4	82 ± 3.2

Table 2.2 (cont'd). Average Recoveries ($\bar{R}$) of Purgeable Priority Pollutants from a Wet or Dry ATD Cartridge Analyzed using the ATD-Nafion Drier System and Packed Column GC/MS[a].

Compound	$\bar{R}$[b] (%) wet[c] cartridge	$\bar{R}$[b] (%) dry cartidge
2-Chloroethylvinylether	1.8 ± 0.11	1.7 ± 0.05
Bromoform	86 ± 3.1	69 ± 3.2
Tetrachloroethene	83 ± 3.6	81 ± 3.8
1,1,2,2-Tetrachloroethane	81 ± 4.2	77 ± 3.6
1,4-Dichlorobutane	83 ± 1.3	81 ± 3.2
Toluene	85 ± 2.5	82 ± 2.9
Chlorobenzene	92 ± 8.9	89 ± 9.5
Ethylbenzene	78 ± 5.2	80 ± 4.9

[a] ± 1 *s* values are based on four replicate analyses for the wet cartridges and three replicate analyses for the dry cartridges.
[b] Average recoveries are based on the average analyte response for two replicate analyses of a ~100 ng/component standard desorbed from a dry ATD cartridge directly to a packed column GC/MS system.
[c] Dry cartridges were spiked with 30 μl of water.

slightly lower. The presence of a large amount of water vapor may slightly enhance the ability of some compounds to diffuse through the walls of the Nafion tubing. In the case of bromochloromethane, however, the response was higher for standards analyzed in the presence of water. It therefore appears that the presence of the water vapor may have diminished the ability of this compound to diffuse into the Nafion. The most extreme difference occurred for bromoform where the recoveries were 86% and 69%, from a dry cartridge and a wet cartridge, respectively.

The coefficients of variation (*s* expressed as a percentage of the mean) of the average percent recoveries ranged from 4 to 13%. The average percent recovery for the 25 compounds analyzed (excluding 2-chloro-ethylvinylether) in the presence of 30 μL of water was 86 $\pm$ 9%. Therefore the percent recoveries were both reasonable and reproducible. Based on this, it would be reasonable to account for the differences in analyte percent transmissions through the Nafion between wet and dry cartridges, by analyzing standards on cartridges spiked with 30 μL of water. Normally, the analysis system is calibrated with standards desorbed from dry ATD cartridges, see Section 2.1.4. However, because the presence of water affects the percent transmission of target analytes through the Nafion tubing, standards should be analyzed on wet ATD cartridges to account for the resulting changes in analyte response.

Figure 2.6 displays two chromatograms of the standard used above. One was obtained when the standard was analyzed on a dry cartridge

using ATD and packed column GC/MS. The other resulted from the analysis of the standard on a wet cartidge with the ATD-Nafion drier system interfaced with packed column GC/MS. It is seen that the peak widths (width at the base of the peak) are equivalent for most compounds with both analysis methods. Therefore, the transfer of analytes through the Nafion drier system (and in the presence of 30 μL of water) did not detract from the compound resolution obtained by the ATD packed column GC/MS analysis.

When a J&W DB-624 Megabore column was used analyte percent recoveries from the Nafion drier were the same as with the packed column. Compound resolution for the early eluting compounds, however, was very poor. Figure 2.7 displays the chromatogram obtained for a standard desorbed in the presence of 30 μL of water. The column was maintained at 10^{o}C during the thermal desorption step. In general, the chromatography was found to be very poor. Most of the early eluting compounds were only partially resolved (separated), and all the peaks were very broad and tailed significantly. In fact, the chromatography was generally much worse (in terms of individual compound resolution) than that of the packed column analysis, see Figure 2.6.

Due to these unsatisfactory results, the capillary column was cooled to -25^{o}C, during the desorption step. Figure 2.8 displays the chromatogram obtained using this procedure. It is seen that the quality of the chromatogram improved dramatically. All peaks were baseline resolved, only a small amount of tailing was experienced with

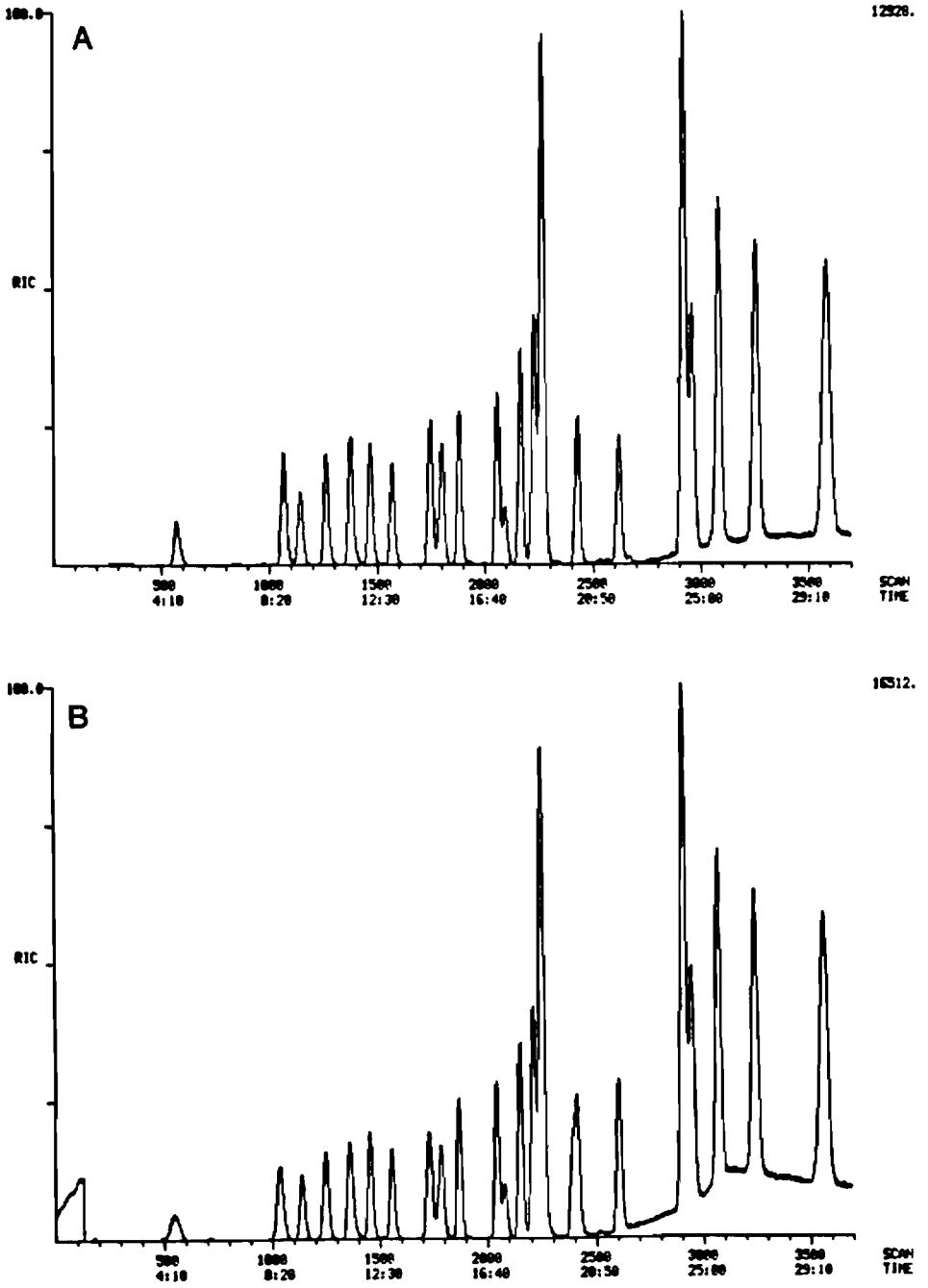

Figure 2.6. Comparison of chromatograms resulting from an ATD packed column GC/MS analysis.
A RIC of a 100 ng/component standard of 23 PPPs desorbed from an ATD cartridge spiked with 30 μL of water and analyzed with the ATD-Nafion drier packed column GC/MS system.
B RIC of the same standard desorbed from a dry cartridge and analyzed with the ATD-packed column GC/MS system.

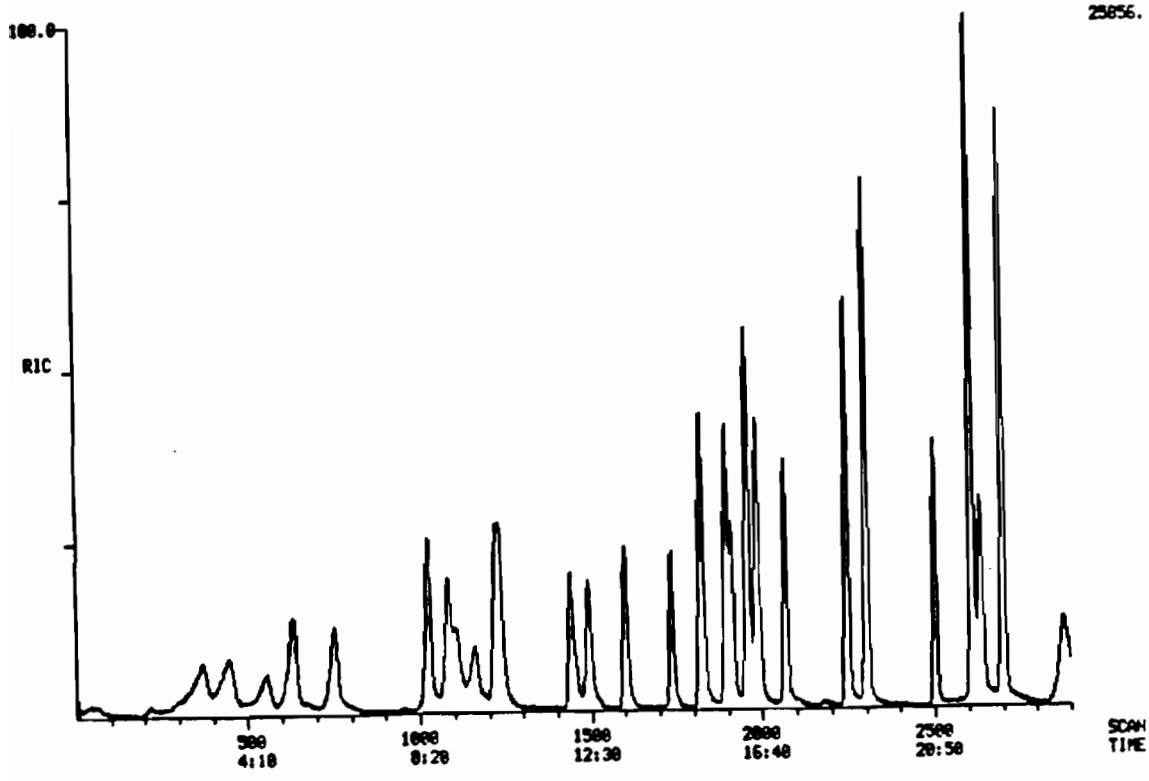

Figure 2.7. RIC of a 100 ng/component standard of 23 PPPs desorbed from an ATD cartridge spiked with 30 μL of water and analyzed with the ATD-Nafion drier-capillary column GC/MS system. The J&W D-624 megabore column was maintained at 10^{o}C during the thermal desorption step.

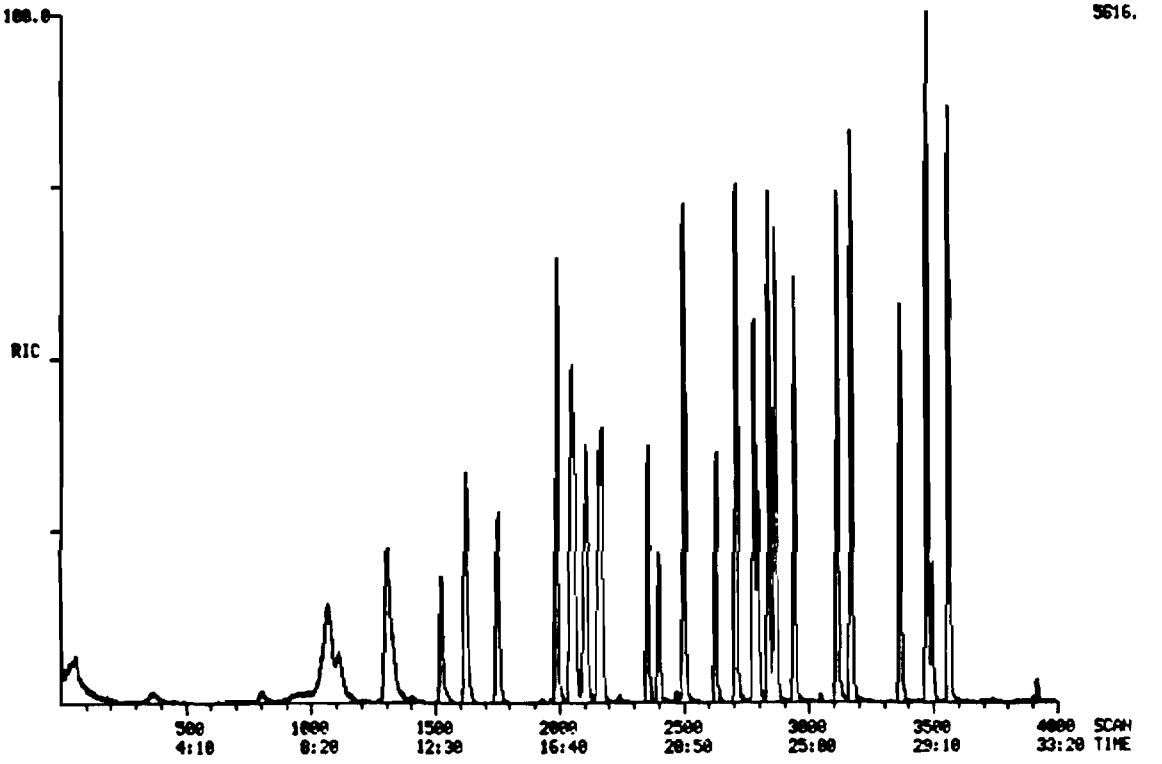

Figure 2.8. RIC of a 100 ng/component standard of 23 PPPs desorbed from an ATD cartridge spiked with 30 μL of water and analyzed with the ATD-Nafion drier-capillary column GC/MS system. The J&W D-624 megabore column was maintained at -25^{o}C during the thermal desorption step.

the early eluting compounds, and all of the individual peak widths decreased significantly. In all cases, the analyte peak widths for the analysis performed at -25°C were narrower by a factor of 2 to 3 than those obtained with the 10°C analysis (see Figure 2.7). The same is true when these peak widths (-25°C) are compared with those obtained during the packed column analysis (see Figure 2.6).

If the individual compound responses obtained by the two capillary column analyses (above) at different trapping temperatures are compared, the results are disturbing. In particular, individual compound responses for the analysis with the capillary column maintained at -25°C during the thermal desorption step dropped by a factor of 4 relative to those obtained at 10°C. The drop in analyte response was not considered to be due to a loss in MS sensitivity because the sensitivity of the system had remained constant for six previous standard analyses performed with the column maintained at 10°C during thermal desorption. In addition, further analyses with thermal desorption and subambient cooling (< 0°C) of the capillary column indicated that the column was becoming either partially or completely plugged during the desorption of the wet cartridges. It is therefore likely that the compound responses were reduced due to incomplete cartridge desorption.

It was determined that the column would plug even when completely dry ATD cartridges were desorbed. It appeared that after only a few analyses with wet ATD cartridges, the Nafion tubing became saturated with water. Thus, when the drier was at 100°C during the thermal

desorption step, traces of water were being transmitted from the Nafion tubing to the capillary column. It appeared that the heating and backflushing of the Nafion tubing, during the acquisition of the chromatogram, was incapable of sufficiently drying the tubing in order to prevent the capillary column from plugging during the next analysis. Based on these results it was felt that continued work on the development of the ATD-Nafion drier system for use with capillary column GC/MS analysis would not be worthwhile. It was also decided that the ATD-Nafion drier system connected to the packed column GC/MS analysis system would only be used as a "last resort". In other words, it was hoped that a suitable drying system could be developed which was capable of utilizing capillary column GC/MS analysis. The above results led to the decision to pursue the development of the ATD-glass bead drier system.

2.4 Glass Bead Drier System

2.4.1 Introduction

The development of a suitable drying system for the analysis of wet ATD cartridges was being developed on an "immediate need" basis. It was intended to use the system on ATD samples that had already been collected (see Section 3.7.1). Because of the uninspiring performance of the ATD-Nafion drier system with capillary column GC/MS analysis (see Section 2.3.3), an additional drying system was constructed and tested in a relatively short period of time.

An ATD-glass bead drier system was designed which "trapped" water during the thermal desorption step and prevented it from reaching the capillary gas chromatography column. The method was designed to handle a wet ATD cartridge after the centrifugation step. A stainless steel tube containing glass beads was connected between the desorber and the capillary column. During thermal desorption water vapor condensed inside the glass bead trap. Most of the target analytes however, as they are much more volatile than water, were quantitatively transmitted to the capillary column. Thus, the enhanced resolution of WCC and capillary column GC/MS analysis may be taken advantage of, provided the trap retains enough water to prevent the capillary column from plugging.

2.4.2 Experimental

Figure 2.9 is a diagram of the ATD-glass bead drier system. An 8-cm length of 0.32 cm O.D and 0.22 cm I.D. SS tubing was filled with 0.5 mm diameter glass beads, held in place at each end by a small glass wool plug. An aluminum block was constructed to house the tube, a 150 W cartridge type heater, and a thermocouple. The tube was inserted through the block and sealed on each end with a Swagelok 0.32 to 0.16 cm brass reducing union. The aluminum box designed for the Nafion drier system was used to contain the glass bead drier and was connected to the thermal desorber and GC oven as previously described (see Section 2.3.2). The desorber outlet was connected to the glass bead water trap by means of a short section of 0.16 cm O.D. SS tubing

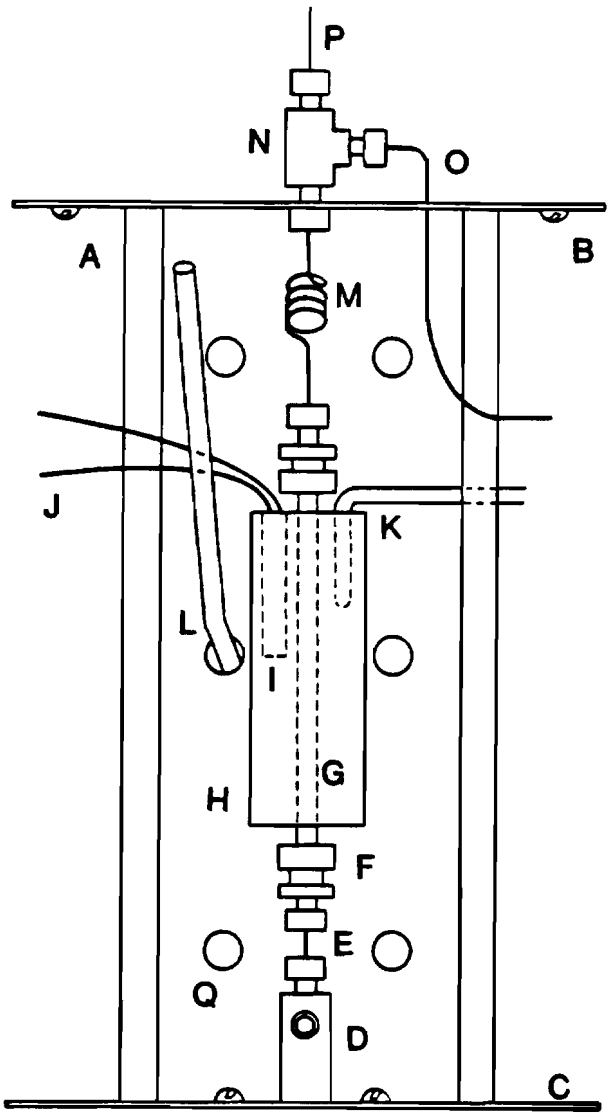

Figure 2.9. Diagram of the ATD-glass bead drier system. This is an overhead view of the device which is mounted to the door of the GC oven. **A** aluminum box; 6.4 cm in width and depth and 15 cm in length. **B** SS rear plate of the box which attachs to the GC oven door. **C** SS front plate of the box. **D** outlet of the thermal desorber. **E** short section of 0.16 cm O.D. SS tubing. **F** Swagelok 0.32 to 0.16 cm brass reducing union. **G** 8-cm length of 0.32 O.D and 0.22 cm I.D. SS tubing filled with 0.5 mm in diameter glass beads, held in place at each end by glass wool plugs. **H** aluminum heater block. **I** 150 watt cartridge heater. **J** cartridge heater leads to power controller. **K** thermocouple, leads to power controller. **L** 0.64 cm O.D. SS tube connected to compressed air pump. **M** 8-cm length of 0.16 cm O.D. SS tubing. **N** Swagelok 0.16 cm SS union-tee. **O** 0.16 cm O.D. SS tubing connected to lower carrier gas line (0.16 cm O.O. SS tubing) of the thermal desorber carrier gas flow controller unit. **P** wide bore capillary GC column inserted halfway through the three-way union (**N**) and connected with a 0.80 mm Vespel/graphite ferrule. **Q** 0.64 cm in diameter hole in the floor of the box.

with a Swagelok 0.16 cm brass nut on each end. The outlet of the trap was connected to an 8-cm length of coiled 0.16 cm O.D. SS tubing. This tubing was in turn connected to a Swagelok 0.16 cm SS union tee (three way union). One end of this union was connected to the SS tubing through a hole in the rear plate of the aluminum box. The 8-cm coiled length of SS tubing was utilized to prevent a cold spot from forming at the outlet of the trap, when the GC oven was at subambient temperature during the thermal desorption procedure. A 0.64 cm O.D. SS tube connected to a compressed air pump, and inserted through one of the holes in the floor of the box, was directed toward the rear wall of the box. Compressed air was also blown on the rear wall of the box to aid in preventing a cold spot from forming inside the box.

A J&W DB-624 Megabore capillary column was inserted through the end of the SS union tee at 180^{o} to the coiled SS tubing. The column was inserted half-way through the union and connected with a 0.80 mm Vespel/graphite ferrule and a Swagelok 0.16 cm brass nut. The middle arm of the SS union tee was connected to the 0.16 cm O.D. SS lower carrier gas line emanating from the ATD carrier gas flow control unit. The lower carrier gas entry port into the desorber was capped with a Swagelok 0.16 cm brass plug. The upper and sweep carrier gas lines were connected to the desorber in their normal configurations.

The carrier gas flow rates were set as follows. The upper carrier gas (used during thermal desorption) was set at ~9 mL/min. The lower carrier gas (used for the chromatographic analysis) was set at ~9 mL/min, with the sweep line open. With the lower carrier and

sweep gas lines open, carrier gas was supplied to the column and the glass bead water trap, causing the trap to be backflushed. Therefore, if during the GC analysis the trap was heated, condensed water could be driven from it.

The ATD-glass bead drier system was operated in the following manner for sample analysis. The GC oven was cooled to and maintained at -30°C using liquid-N_2. A wet cartridge was loaded into the thermal desorber and the compressed air blower was turned on. The cartridge was desorbed for 5 min at 250°C using UP-He from the upper carrier gas line. During desorption the trap remained at ambient temperature. When the desorption was complete, the carrier gas supply was switched to the lower line, the sweep line was opened and the blower was turned off. The GC oven was ballistically brought to 10°C and the MS acquisition was started. The oven was then programmed up to 120°C at 5°C/min. During the GC/MS analysis the glass bead water trap was backflushed and heated to 150°C for 5 min. Following this, the desorber was cooled with water and the trap was cooled with compressed air.

Theoretically, analyte losses could occur in two ways: 1) by analyte adsorption or degradation on glass and stainless steel surfaces inside the trap; or 2) by analytes dissolving in water vapor which has condensed inside the trap. Both glass and stainless steel are very inert materials with respect to the PPPs (which are relatively non-polar), and therefore it is unlikely that adsorption onto these materials would be a significant source of error. Analytes

may dissolve in the ~30 μL of water trapped in the unit however, ~70 mL of carrier gas will also pass through the trap. This means that the ratio of gas volume passing through the trap to the water volume in the trap will be ~2000:1. Therefore, based on equations presented by Pankow (13), even the PPPs with relatively low Henry's law constants should be effectively purged from the trap. Thus, this potential source of analyte loss should also be insignificant.

2.4.3 Results and Discussion

Six analyses were performed in order to test the reproducibility of the ATD-glass bead drier system for use with capillary column GC. Three dry ATD cartridges injected with 2 μL of a standard in methanol (containing ~50 ng/μL of most of the PPPs) were first analyzed. Three more ATD analyses of the same amount of standard were then performed on cartridges loaded with 30 μL of water. Table 2.3 presents the average compound response ± one standard deviation unit, for the wet and dry cartridge analyses, for eight of the compounds in the standard. Individual compound responses fluctuated very little between analyses. The compound response reproducibility for both types of cartridges (wet or dry) was very good. In some cases, the responses from compounds analyzed on wet cartridges were slightly higher or lower than the responses obtained from dry cartridges. The absolute differences in response, however, were small. In either case these differences in response could be compensated for by analyzing standards on cartridges spiked with 30 μL of water. As discussed in

Table 2.3. Average Response (Area Counts) for Selected Compounds Desorbed from a Wet or Dry ATD Cartridge Analyzed Using the ATD-Glass Bead Drier System.

Compound	Average Response[a] (area counts) dry cartridge	Average Response[a] (area counts) wet cartridge[b]
1,1-Dichloroethane	7.33 E4 ± 692	6.09 E4 ± 9320
Bromochloromethane	3.53 E4 ± 607	3.18 E4 ± 479
Trichloromethane	5.50 E4 ± 894	5.29 E4 ± 269
Benzene	1.62 E5 ± 3160	1.48 E5 ± 1200
Trichloroethene	3.80 E4 ± 809	3.01 E4 ± 255
1-Chloro-2-bromopropane	4.16 E4 ± 137	3.93 E4 ± 548
Tetrachloroethene	2.12 E4 ± 184	1.91 E4 ± 275
1,4-Dichlorobutane	1.92 E5 ± 1910	2.13 E5 ± 6340
1,1,2,2-Tetrachloroethane	6.82 E4 ± 2440	8.73 E4 ± 2830

[a]Compound response in area counts ± 1 *s* value for three replicate analyses of a 100 ng/component standard.
[b]Each cartridge was spiked with 30 μL of water.

Section 2.3.3, the analysis system is normally calibrated by the analysis of standards desorbed from dry ATD cartridges. However, as was also noted with the Nafion drier system, the presence of water affects the percent transmission of target analytes through the glass bead drier system. Therefore, standards should be analyzed on wet ATD cartridges to account for the resulting changes in analyte response.

The results of the wet cartridge analyses showed that the glass bead water trap was capable of removing enough water from the analysis stream (cartridge effluent) in order to keep the capillary column from plugging during the thermal desorption/WCC procedure. Several additional analyses of ATD cartridges injected with 2 μL of standard and spiked with 30 μL of water provided the same results. In fact, during the subsequent analysis of some 60 samples (see Section 3.7.4) the capillary column never plugged. Further testing showed that even 70 μL of water could be desorbed from the cartridge without plugging the capillary column. While the tendency of the column to plug is determined only by the volume of water contained in the trap and the volume of dry gas which passes through it (i.e., not the total volume of water desorbed from the wet cartridge), the ability of the trap to condense this relatively large volume of water is an indication of the resiliency of the drying method.

Figure 2.10 presents a typical chromatogram obtained from the analysis of a standard desorbed from a cartridge spiked with 30 μL of water. The chromatography was found to be excellent, with most analyte peaks being baseline resolved and very sharp. The first two

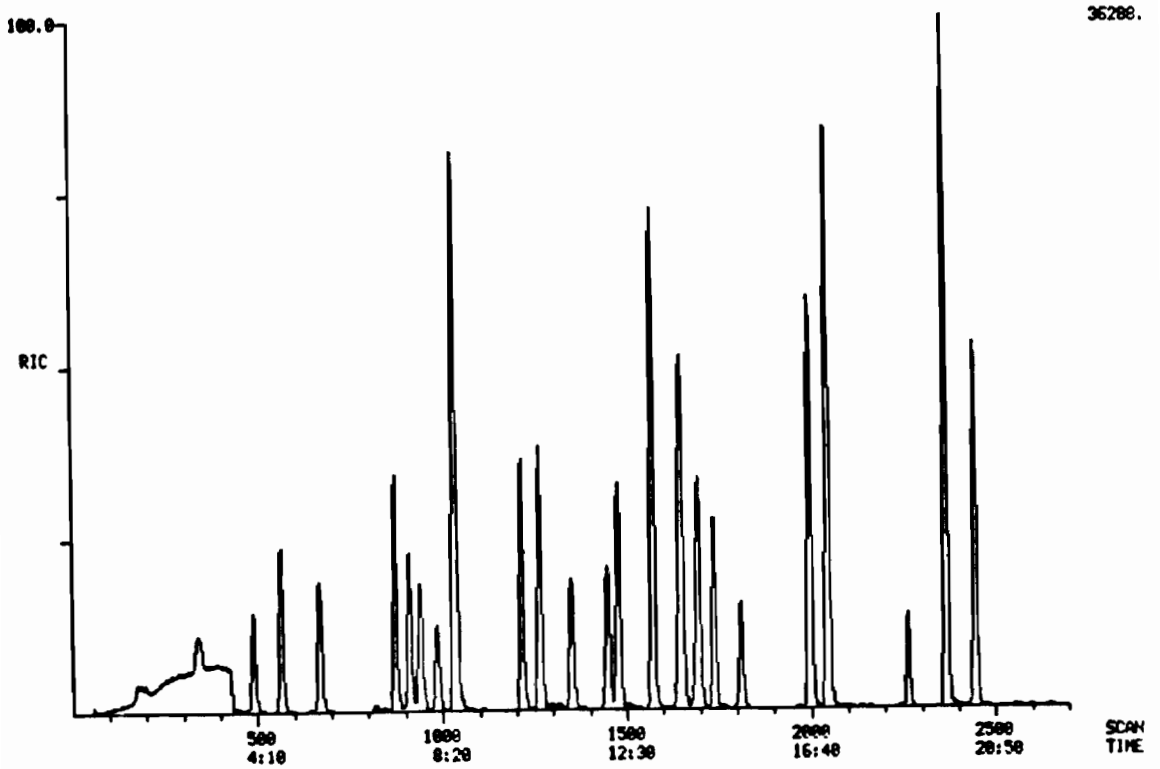

Figure 2.10. RIC of a 100 ng/component standard of 23 PPPs desorbed from an ATD cartridge spiked with 30 μL of water and analyzed with the ATD-glass bead drier-capillary column GC/MS system. The J&W D-624 megabore column was maintained at -30^{o}C during the thermal desorption step.

peaks appear distorted in this figure due to background contamination eluting from the trap. The extracted ion chromatograms for the ions were well shaped. Figures 2.11-2.15 display individual peaks for some of the compounds in the chromatogram. Generally, the peaks were 20 scans (10 s) wide (at the base) throughout the chromatogram. This is an increase in resolution of a factor of 2 to 4 over what was achieved with packed column ATD.

Figure 2.16 presents the chromatogram for the redesorption of the sample whose chromatogram was presented in Figure 2.10. For this analysis the trap was not backflushed during the GC/MS analysis. This enabled the determination of the amount of each analyte retained in the trap (i.e., dissolved in the condensed water, see Section 2.4.2). In general, the chromatogram from the sample redesorption was found to be relatively clean, and although several individual peaks were detected their areas were relatively small. By comparing the areas of some of these individual peaks with their areas obtained from the original desorption, an estimate of the percent transmission of these compounds through the trap may be determined.

Peak areas were determined for chlorobenzene, ethylbenzene, 1,4-dichlorobutane and 1,1,2,2-tetrachloroethane, for both Figure 2.10 and 2.16. The percent analyte transmission, T, was estimated for each of these compounds with the following equation:

$$T = 100 \left[1 - \left(\frac{A_r}{A + A_r}\right)\right] \qquad 2.3$$

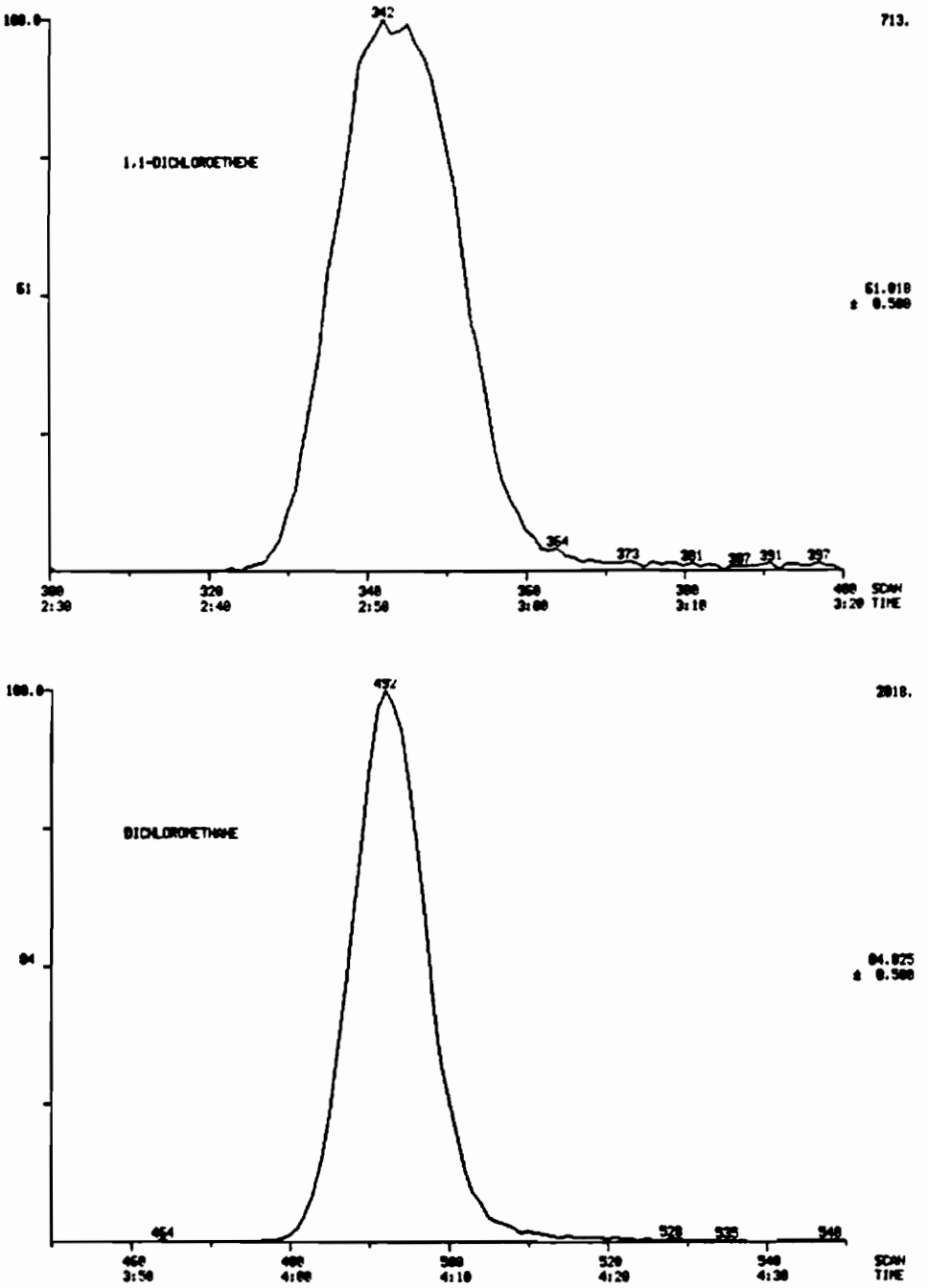

Figure 2.11. Extracted ion profiles for 1,1-dichloroethene and dichloromethane resulting from the analysis of a 100 ng/component standard (in the presence of 30 μL of water) using the ATD-glass bead drier-capillary column GC/MS system.

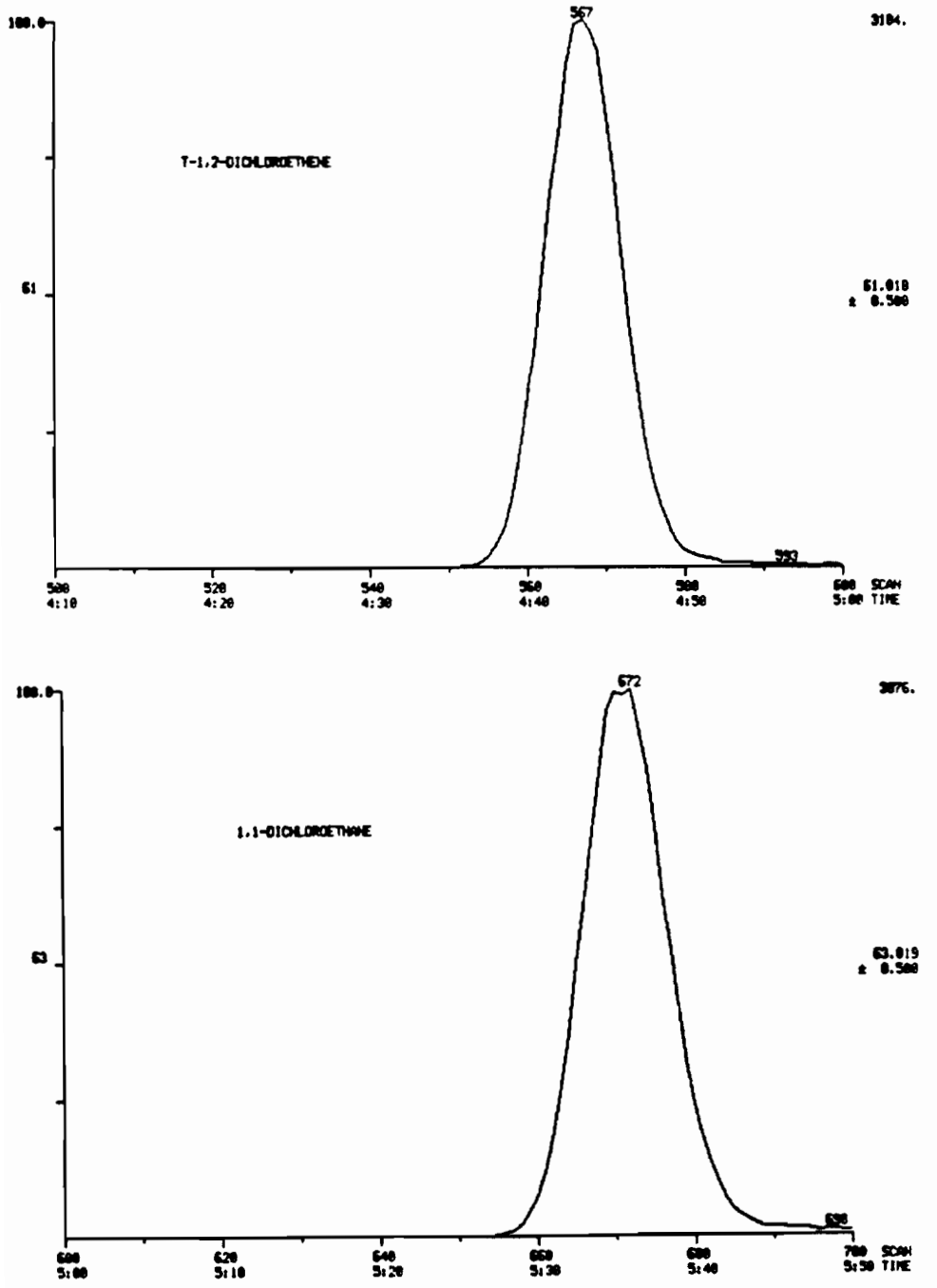

Figure 2.12. Extracted ion profiles for t-1,2-dichloroethene and 1,1-dichloroethane resulting from the analysis of a 100 ng/component standard (in the presence of 30 μL of water) using the ATD-glass bead drier-capillary column GC/MS system.

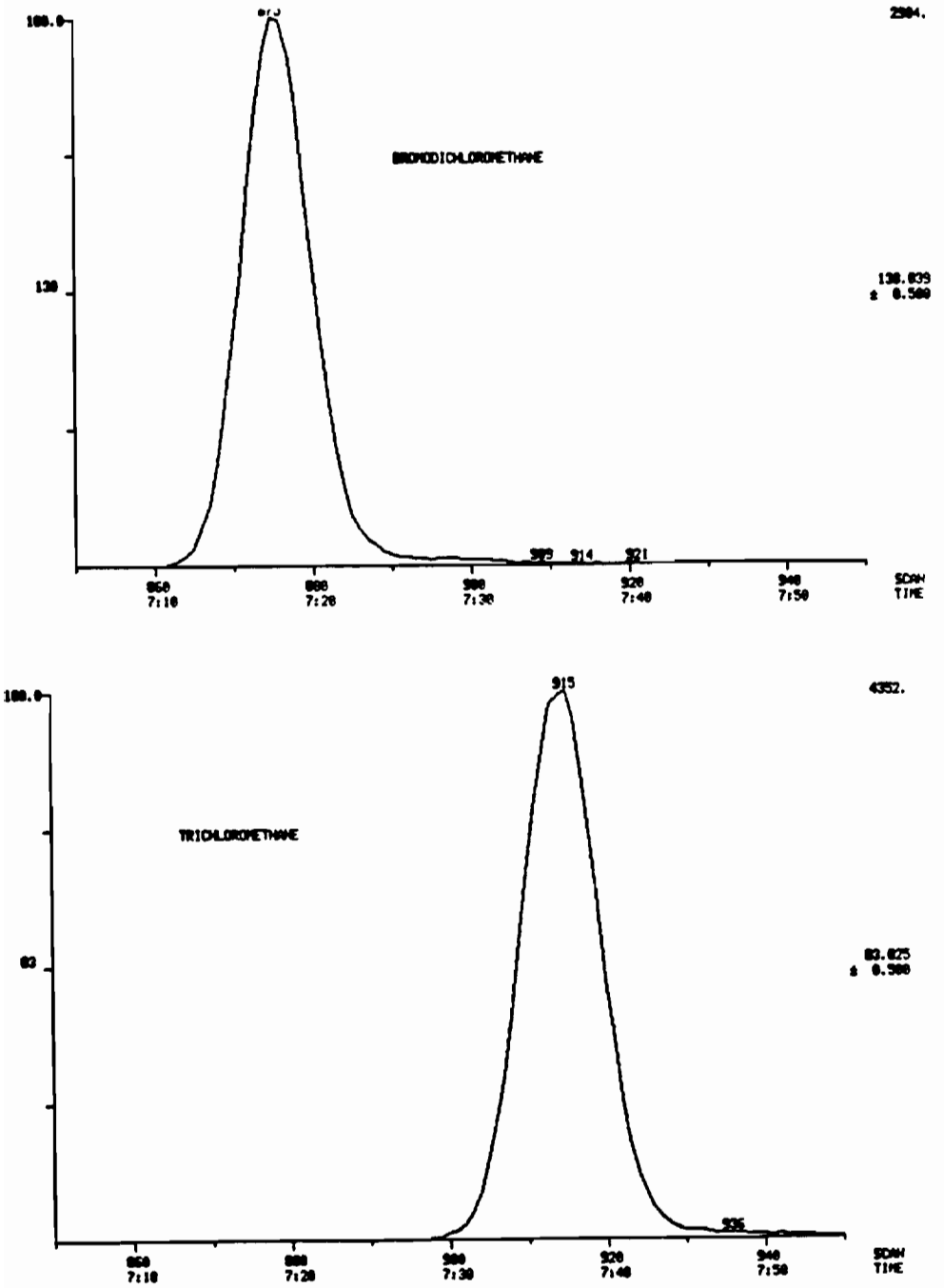

Figure 2.13. Extracted ion profiles for bromodichloromethane and trichloromethane resulting from the analysis of a 100 ng/component standard (in the presence of 30 μL of water) using the ATD-glass bead drier-capillary column GC/MS system.

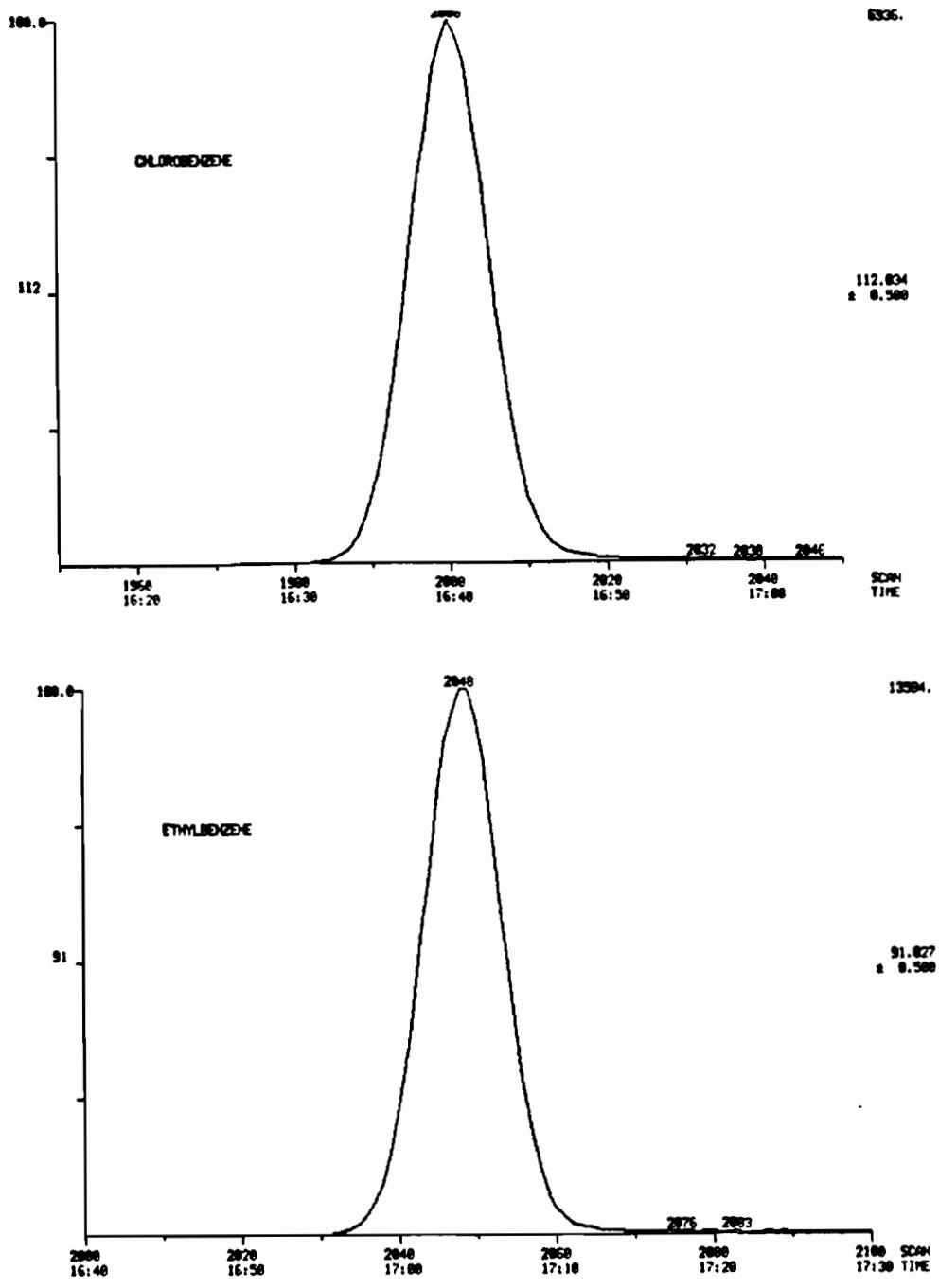

Figure 2.14. Extracted ion profiles for chlorobenzene and ethylbenzene resulting from the analysis of a 100 ng/component standard (in the presence of 30 μL of water) using the ATD-glass bead drier-capillary column GC/MS system.

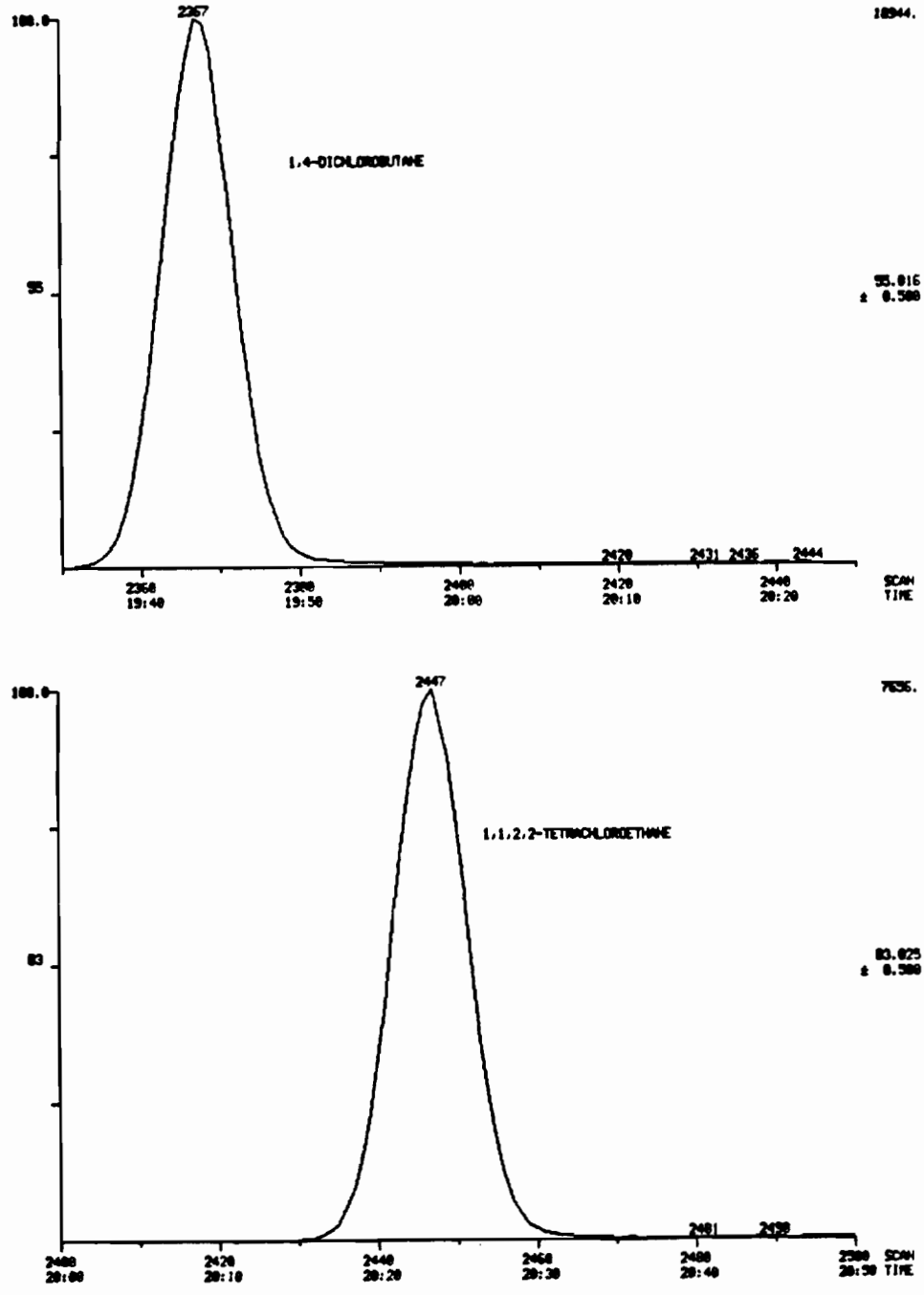

Figure 2.15. Extracted ion profiles for 1,4-dichlorobutane and 1,1,2,2-tetrachloroethane resulting from the analysis of a 100 ng/component standard (in the presence of 30 μL of water) using the ATD-glass bead drier-capillary column GC/MS system.

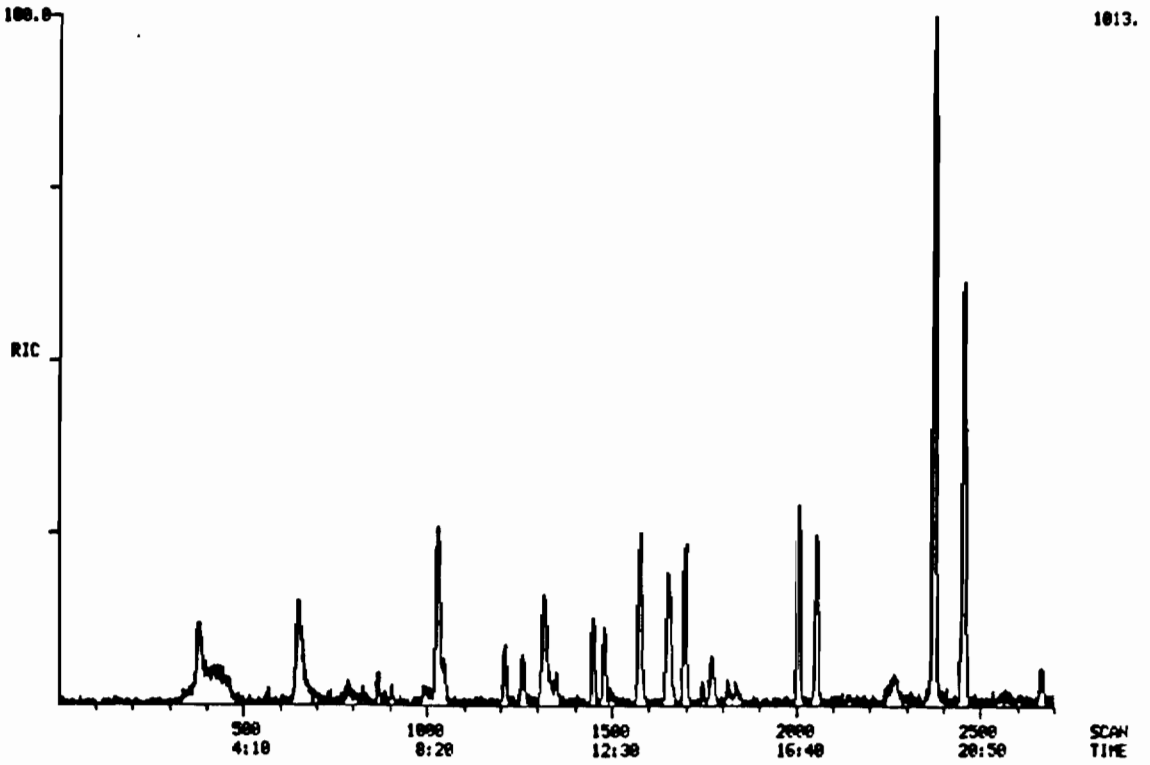

Figure 2.16. Chromatogram resulting from the redesorption of a 100 ng/component standard of 23 PPPs originally desorbed from an ATD cartridge spiked with 30 μL of water and analyzed with the ATD-glass bead drier-capillary column GC/MS system. During the original analysis (see Figure 2.10) the glass bead trap was not backflushed and heated. Therefore, the 30 μL of water remaining in the trap was repurged with carrier gas for this analysis.

where:

A = analyte area from the original desorption, and

A_r = analyte area from the redesorption.

Equation 2.3 will be accurate provided that $A >> A_r$. For this situation the analyte area provided by the third desorption would be very small relative to A. Because the percent transmissions determined by eqn. 2.3 ranged from 96 to 99% for the four compounds, this is likely to be the case. Based on equations presented by Pankow (13), it may be predicted that the PPP with the lowest Henry's law constant (1,1,2,2-tetrachloroethane) should experience the lowest percent transmission through the glass bead water trap. However, even for 1,1,2,2-tetrachloroethane the percent transmission (~96%) was found to be excellent.

Due to time constraints, only this preliminary investigation of the ATD-glass bead drier system could be conducted. The overall results were favorable enough however, to warrant its use for the analysis of ATD samples already collected (see Sections 3.7.1 and 3.7.4).

2.5 Conclusions

Two modifications of the standard ATD analysis method were developed. For both, an ATD cartridge could be analyzed after only the standard centrifugation-desiccation step, i.e., with ~30 μL of water remaining on the cartridge. The ATD-Nafion drier system could only be utilized with packed column GC. The Nafion drier also caused

analyte losses during analysis. These losses were probably due to the diffusion of analytes into the tubing along with the water during desorption.

The ATD-glass bead drier system was easily connected to a capillary column GC/MS analysis system. The system was easily constructed, durable and simple to operate. The system was also very robust. Relatively large amounts of water (at least 70 μL) could be desorbed from an ATD cartridge, without the capillary column plugging with ice during the thermal desorption/WCC procedure. The drier system did not detract from the chromatographic efficiency that would be expected from a capillary column of the type used. Finally, the glass bead drier system was able to transmit > 95% of the total mass of individual PPPs. Therefore, while both the Nafion and glass bead drier systems were found to be capable of permitting the analysis of wet ATD cartridges containing PPPs, the glass bead drier system was found to be superior in terms of overall efficiency, sensitivity and operating simplicity.

CHAPTER 3 ADSORPTION/THERMAL DESORPTION - FIELD EVALUATION

3.1 Background and Introduction

Several field investigations utilizing ATD for the analysis of groundwater have been conducted by our laboratory. These investigations have determined that ATD performed well in terms of sampling and analysis precision and sensitivity for the determination of a variety of organic compounds in groundwater.

In 1982 samples from several groundwater wells in Camden, NJ were collected and analyzed by Pankow and Isabelle (50) utilizing both surface-ATD and surface-P&T sampling and analysis methods. The term surface sampling may be taken to mean any method by which groundwater samples are obtained at ground level at the well head. A sample is retrieved with either a pump or a grab sampler from a desired depth in the well. At the surface the sample is either transferred to a storage container (P&T) or passed through a Tenax bed and concentrated (ATD). Therefore, the term surface-P&T is used to refer to a sampling and analysis procedure by which a groundwater sample is obtained at the well head and analyzed by a P&T technique. Similarly, the term surface-ATD is used to refer to a sampling and analysis procedure by which a groundwater sample is obtained at the well head where it is concentrated on a sorbent bed, and the sorbent is later analyzed by the thermal desorption technique. At Camden, samples were pumped to the surface through PTFE tubing with a hand vacuum pump. A comparison of the results of both methodologies, from seven wells sampled,

indicated the following. The surface-ATD method was more sensitive than surface-P&T. Several compounds were detected with surface-ATD that were not detected by surface-P&T. The reproducibility of replicate surface-ATD samples was very good. However, the trichloroethene concentrations determined by surface-ATD were a factor of 3 to 10 times lower than those determined by surface-P&T.

In Camden, surface-ATD samples were only collected with single cartridges. Therefore, it was not possible to determine whether the low surface-ATD trichloroethene concentrations were due to poor ATD sampling efficiency. An estimate of the ATD sampling efficiency can be made by sampling with two cartridges connected in series. The backup cartridge (the secondary cartridge) traps material which has passed through the primary cartridge (the lead cartridge) during sampling. The determination of the mass of an analyte on the backup cartridge is used to estimate the percent analyte breakthrough during sampling. Percent analyte breakthrough is the percent ratio of the analyte mass on the backup cartridge to the total analyte mass (sum of the analyte mass on the primary and secondary cartridge) (51). Although Pankow and Isabelle (50) showed that surface-ATD generally performed well, trichloroethene was the only compound which occurred at high enough concentrations so as to be detected by both methods. Therefore, it was not possible to adequately compare the relative accuracy of the surface-ATD and surface-P&T sampling and analysis methods.

In 1983 two downhole-ATD sampling devices were developed and used by Pankow et al. (31,32) to sample monitoring wells at the Bayview Park Landfill in Burlington, Ontario, Canada. The term downhole sampling may be taken to mean any method by which groundwater samples are collected and isolated at the sampling point inside a well. Therefore, the term downhole-ATD is used to refer to a sampling and analysis procedure by which a groundwater sample is concentrated on a sorbent bed at the sampling point inside a well, and the sorbent is later analyzed by the thermal desorption procedure. Both the syringe and cartridge (31) and the tube and cartridge (32) downhole-ATD sampling devices operated well, and good precision and sensitivity was obtained for several chlorinated and aromatic hydrocarbons. Concentration limits of detection were found to range from 1.5 to 140 ppt for the compounds detected. Finally, these studies also demonstrated that ATD cartridges can be incorporated into downhole sampling methods that can obtain samples from narrow bore piezometers (0.65 to 3.8 cm I.D.) and at any depth.

In 1983 Pankow and Rosen (52) collected and analyzed both downhole-ATD and surface-P&T samples from several wells at Stovepipe Wells National Monument, Death Valley, CA. The P&T samples were collected from the surface of the water table with a galvanized steel, open top bailer. The bailer collected ~800 mL of water at a time. Downhole-ATD samples were collected by the syringe and cartridge device developed by Pankow et al. (31). The groundwater at this site became contaminated, during an unknown period of time prior to 1979,

with gasoline from a leaking underground storage tank. The purpose of the sampling event was to compare the relative accuracy of the two sampling and analysis methods. Unfortunately, the contaminant levels in many of the wells sampled were so high (in the mg/L range for some compounds), that analyte mass loadings on the Tenax cartridges prevented accurate ATD analyses from being performed. Thus, it was not possible to compare the results of downhole-ATD and surface-P&T for many of the compounds detected. For a few wells that were situated in regions of low contamination (at the leading edge of the gasoline plume), a few compounds were detected at higher levels by downhole-ATD than surface-P&T. Also, in some of these low level samples, there was reasonable agreement between some of the analyte concentrations determined by both methods. However, most of these compounds were C_3- and C_4-benzenes, not PPPs. Thus, the extent of the comparison of the two methods was very limited.

Each of the above studies clarified some of the advantages of ATD for the determination of organic compounds in groundwater. However, prior to this study, a definitive study had yet to be completed which determined the relative accuracy of ATD, when compared with other sampling and analysis methods more frequently used for the determination of the PPPs in groundwater.

In an effort to better define the ability of ATD to determine trace quantities of PPPs in groundwater, downhole and surface sampling and analysis techniques were field tested jointly by personnel of the Oregon Graduate Center (OGC) and the New Jersey District of the Water

Resources Division of the United States Geological Survey (USGS-NJ). Downhole- and surface-ATD samples were collected and analyzed by OGC, while downhole-P&T samples (collected using a sampler designed by James Ficken of the USGS (53)), were collected and analyzed by USGS-NJ. In addition, surface-P&T samples were collected for analysis by both laboratories. All OGC sampling and analysis procedures are described in Sections 3.4 through 3.6. Three wells, one at each of three different sampling sites in the northeastern United States, were selected for sampling. A separate sampling trip was devoted to each well.

3.2 Selection of Sampling Sites

The three wells sampled all satisfied a set of general physical well characteristics and water quality criteria agreed upon by USGS-NJ and OGC personnel. It was desired to test the operation of the downhole samplers under a considerable pressure head. Therefore, wells were sought in which samples could be collected under at least a 15 m column of water. It was also desired to test the feasibility of operating these samplers at as much as 30 m below land surface. Thus, wells were also sought where the total depth (below land surface) to the sampling point would be as much as 30 m. Also, by obtaining downhole and surface samples from wells with the latter characteristic it was hoped to determine whether the contact of a sample with a pump and ~30 m of associated tubing, could significantly alter compound concentrations during the acquisition of a surface sample. A more

detailed discussion of this potential sampling artifact is presented in Sections 1.2 and 3.7.6. There was no preference as to whether monitoring or production wells were selected, as long as the I.D. of each well sampled was at least 8 cm. This enabled the use of the downhole-ATD samplers, as designed (see Section 3.4).

It was intended to sample groundwater containing a variety of PPPs at concentrations ranging from 0.01 to 100 ppb. The physical properties of the PPP compounds relevant to analyte volatilization and analyte Tenax sorption efficiency span a wide range. It was desired to select wells contaminated with compounds that spanned as much of these ranges in physical properties as possible. Since it was desired that each well be developed twice during the day it was sampled (see Section 3.3), the source of contamination had to be well defined. This was necessary so that the level of contamination measured did not change, over time, due to well development and sampling (i.e., pumping) activities.

An abundance of information concerning the physical and water quality characteristics of many wells in the northeastern United States was available to USGS-NJ due to their extensive sampling of aquifers throughout this region of the country (6). This information, combined with data obtained by the preliminary sampling and analysis (by USGS-NJ and OGC personnel) of groundwater from several candidate wells, led to the selection of the three wells that were ultimately sampled. Table 3.1 contains some pertinent information concerning these three wells.

Table 3.1. Information on Wells Selected for Sampling.

Location	--	Camden, NJ	Syosset, NY	Repauno, NJ
Date Sampled	--	9/5/85	10/9/85	6/20/86
Well I.D. (cm)	--	25	10	15
Depth to Water (m)	--	17	10	4.0
Depth to Sampling Point (m)	--	34	23	20
Height of Water Column Above Sampler (m)	--	16	12	16
No. of Compounds Detected	--	14	16	12
Concent'n. Range (μg/L)	--	0.024-170	0.057-130	0.11-370

3.3 Sampling Protocol

There were two separate sampling rounds completed during the one day sampling was conducted at each site. Prior to each sampling round, each well was developed according to the following procedure developed by Imbrigiotta et al. (54), in order to provide fresh formation water for sampling. This procedure was performed by USGS-NJ personnel. A 10 cm O.D. submersible pump, placed ~3 m below the surface of the water, was used to flush standing water from the well casing. Samples from the pump output were collected at each 5- or 10-min interval and monitored for changes in temperature, pH, specific conductance, chloride concentration, and dissolved O_2 concentration, using standard procedures (54), in order to determine the inorganic stability of the water pumped from the well. The ultraviolet absorbance, at 254 nm, of each sample was also measured in the field, using a Hitachi model 100-20 single-beam ultraviolet-visible spectrophotometer. Absorbance at this wavelength is characteristic of unsaturated aliphatic and aromatic compounds and thus, this measurement was used as an indication of the organic stability of the water pumped from the well. Chemical stability was assumed to have been achieved when measurements varied within 5% for three successive readings. All chemical stability measurements were performed by USGS-NJ personnel. The volume removed from each well in order to reach chemical stability, always far exceeded the minimum four to six casing volumes usually recommended to flush a well prior to sampling (55).

During each sampling round four replicate downhole-ATD and four replicate surface-ATD samples were collected by OGC personnel. In addition, four replicate downhole-P&T and 10-12 replicate surface-P&T samples were collected by USGS-NJ personnel. Four of the surface-P&T samples collected during each sampling round were analyzed by OGC, four were analyzed by USGS-NJ and the remaining samples were analyzed by the USGS Central Laboratory (USGS-D) in Denver, CO.

Four of the replicate downhole- and surface-ATD samples were collected with backup Tenax cartridges in order to estimate the sampling efficiency of the Tenax bed. Five ATD and five P&T travel blanks were transported to and from each sampling site and were subjected to the same sample handling and analysis methods as the field samples. Each P&T travel blank consisted of 40 mL of reagent water stored in a standard P&T sample container (10). The ATD travel blanks consisted of clean Tenax cartridges which were exposed (i.e., the fittings were removed) at the sampling site at the completion of the first round of sampling. The results of the travel blank analyses were used to estimate the concentration limits of detection for the sampling and analysis procedures (see Appendix 1). All samples collected were stored on ice for transport back to the laboratories and then stored under refrigeration at $4^{o}C$, until analysis.

Sample acquisition usually proceeded in the following manner. Two USGS-NJ downhole-P&T samples were collected, followed by four downhole-ATD samples and then the remaining two USGS-NJ downhole-P&T samples. Four surface-ATD samples were then collected simultaneously

with the 10 to 12 surface-P&T samples. During the first round of sampling each ATD sample was collected with a backup cartridge. After the first round of sampling was complete, the well was redeveloped, as described above. Following this the second round of sampling was completed, with the same sampling order utilized in round one. Each round, including the well development, required an average of 4 to 6 hours to complete.

As discussed in Section 3.1, downhole- and surface-ATD have never been compared directly with surface-P&T, the more commonly used method for the determination of PPPs in water. Therefore, in order to determine the relative precision and accuracy of the ATD sampling and analysis methods surface-P&T samples were collected at each site. Thus, the surface-P&T samples were collected to provide reference concentrations. While the accuracy of these concentrations were not known, their use provided a reasonable way to determine the relative performance of the ATD sampling and analysis methods tested.

3.4 Downhole Adsorption/Thermal Desorption Samples - Collection Procedures

3.4.1 Modified Syringe and Cartridge Sampler

The two types of downhole-ATD samplers used in this study were modified versions of the syringe and cartridge sampler designed by Pankow et al. (31) and the tube and cartridge sampler also designed by

Pankow et al. (32), which were used in a previous field investigation (see also Section 3.1). In general, both samplers had the following characteristics in common:

(1) Prior to and during sampling, water contacted only stainless steel, glass or Tenax.

(2) Four samples could be obtained simultaneously from any depth up to 46 m in a well with an I.D. of 8 cm or greater.

(3) The initiation and termination of sampling, the sampling flow rate and the amount of sample passed through each cartridge could be controlled from the surface.

(4) The water that passed through each cartridge was retained by the sampler so that it could be measured when the sampler was returned to the surface.

The first downhole sampler to be discussed is a modification of the syringe and cartridge design of Pankow et al. (31), and was used only at the Camden, NJ sampling site. Prior to the sampling, it was believed that the groundwater at this site contained relatively high levels of several compounds (> 200 ppb). Therefore, in order to prevent the type of cartidge overloading that was experienced at Death Valley (52) (see also Section 3.1), it was decided to utilize large bed ATD cartridges and sample small volumes of water.

The bed volumes of the ATD cartidges used were 5.7 mL. This is approximately eight times the bed volume of the ATD cartidge described in Section 2.1.2. It was intended to pass ~10 mL of water through each cartridge. Assuming a total bed porosity of ~0.8 (see Section

5.3.2), the void volume of each cartridge is ~4.6 mL. Because samples were to be collected under a column of water ~15 m in height, the air trapped in each cartridge would compress as it was lowered to the sampling point. Thus if simply lowered down a well, a cartridge would fill with ~3 mL of water. This water would be obtained throughout the length of the water column. The acquisition of such a large fraction of the total volume of water to be sampled from a location above the designated sampling point was considered to be undesirable. One of the basic advantages of downhole sampling is the ability to control the location in the well of sample acquisition. This downhole sampler was therefore modified to prevent large ATD cartridges from filling with water prior to the initiation of sampling at the desired depth.

A manifold with four arms, which separated into a top and bottom portion, was constructed of 0.64 cm O.D. SS tubing. The manifold was capable of supporting four separate, single ATD cartridges, or four sets of two cartridges connected in series with a Swagelok 0.64 cm SS union. The manifold is depicted in Figure 3.1. A one-way check valve and syringe assembly was included on each arm of the manifold. The total diameter of the this apparatus was between 6.4 and 7.0 cm. Two 0.95 cm O.D. polyethylene tubes (~46 m in length) were connected to the sampler. One tube connected to a 0.95 cm SS Swagelok fitting welded to the center of the top portion of the cartridge manifold. The other tube connected to another one-way check valve with a 0.95 to 0.64 cm SS Swagelok reducer (fractional tube to fractional tube stub). The check valve in turn connected to a 61-cm length of 0.64 cm

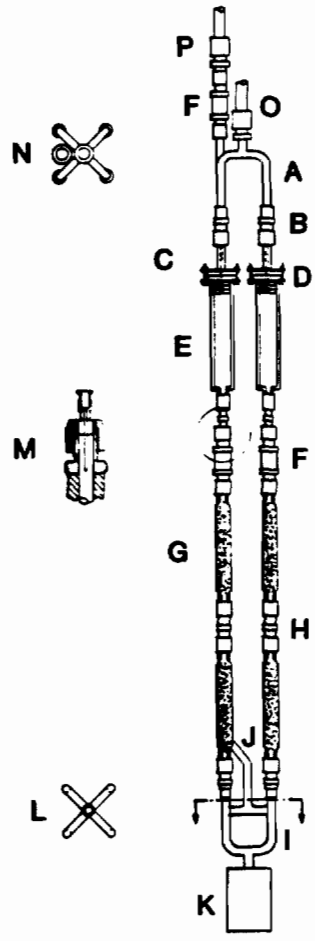

Figure 3.1. Diagram of the modified syringe and cartridge downhole-ATD sampler. The diameter of this apparatus at its widest point is ~7 cm. Its total length ranges from 0.60 to 0.69 m. **A** top portion of the manifold (two of the four arms are shown) constructed of 0.64 cm O.D. SS tubing. **B** Swagelok 0.64 cm SS fitting welded to the manifold, used with PTFE ferrules. **C** PTFE syringe barrel insert used to couple the barrel to the upper portion of the manifold. **D** aluminum bracket. **E** 10 mL glass syringe barrel with luer-lok hub. **F** Nupro one-way SS check valve. **G** Large bed Tenax cartridge ~5.7 mL in volume. **H** Swagelok 0.64 cm SS union with PTFE ferrules. **I** Lower portion of the manifold (two of the four arms shown) constructed of 0.64 cm O.D. SS tubing. **J** center arm of the lower portion of the manifold, constructed of 61 cm of 0.64 cm O.D. SS tubing and welded to the center of two cross tubes constructed of the same material. **K** 53 mL SS cylinder welded to the bottom of the lower portion of the manifold. **L** overhead view of the center arm and cross tubes. **M** enlarged view of the 2.5 cm, 27 gauge syringe needle silver soldered into a Swagelok 0.64 cm SS plug. **N** overhead view of the top portion of the manifold and the center tube. **O** Swagelok 0.95 cm SS fitting welded to the top portion of the manifold and connected to ~46 m of 0.95 cm O.D. polyethylene tubing. **P** Swagelok 0.95 cm to 0.64 cm SS reducing union connected to ~46 m of 0.95 cm O.D. polyethylene tubing.

SS tubing with a 0.64 cm SS Swagelok nut and ferrule. This length of tubing, with the check valve, is the center arm of the bottom portion of the manifold.

A total of five Nupro (Cleveland, OH) one-way check valves were used. Each was constructed of stainless steel with inlet and outlet ends designed for 0.64 cm Swagelok tubing connections. The "cracking pressure" of each valve was 0.33 psi. Therefore, if a 0.33 psi pressure gradient was placed across the valve (higher pressure at the inlet end) the valve would open and allow fluid to flow through it. The hub of a 2.5 cm 27 gauge (0.020 cm I.D.) SS syringe needle was silver soldered into the 0.64 cm SS Swagelok plug placed on the outlet end of each check valve. Therefore, when the nut was fastened to the check valve, the syringe needle extended through the inside of the check valve. The syringe needle was used as a flow restrictor. When a pressure gradient of 5 psi was set across a Tenax cartridge with a check valve/syringe needle connection at the outlet, a flow rate of ~1.5 to 3.0 mL/min resulted. Using an equation developed by Pankow et al. (56), it was predicted that a sampling efficiency of > 99% would result with sampling flow rates on the order of 6 mL/min. In other words, > 99% of the mass contained in the volume of water passed through the cartridge would be retained by the sorbent. It was desired, however, to sample at even lower flow rates due to the expected high concentrations of individual contaminants (> 200 ppb).

It was felt that lower flow rates would help maintain a high sampling efficiency if the sorbent bed tended to become overloaded due to the high concentrations of some individual compounds.

The outlet end of each Tenax cartridge was connected to the inlet end of a check valve with a 0.64 cm SS Swagelok nut with a PTFE ferrule. The syringe needle hub, connected to the outlet end of the check valve, was fastened to the luer-lok tip of a 10 mL glass syringe barrel (obtained from Popper and Sons, New Hyde Park, NY). The plunger from each syringe barrel was replaced with a PTFE insert that allowed coupling to the upper portion of the manifold. O-ring grooves were placed in the insert in order to ensure a water-tight seal with the glass syringe barrel. Conventional Buna-N O-rings were used. The stem of the insert had a 0.64 cm O.D. and could therefore be connected to the 0.64 cm SS Swagelok fitting welded to each arm of the top portion of the manifold. A 0.032 cm I.D. of the stem of the insert allowed the syringe barrel and check valve connected to it to be pressurized. An aluminum bracket was fastened around the PTFE insert and the lip of the syringe barrel in order to hold the insert in place during sampling. The syringe barrel served as a reservoir for the volume of water that passed through the Tenax cartridge. This enabled the measurement of the volume of water passed through each cartridge after sampling.

A 0.64 cm Swagelok fitting was also welded to each arm of the bottom portion of the manifold. Therefore, the inlet end of each Tenax cartridge was connected to the lower portion of the SS sampler

manifold with a 0.64 cm SS Swagelok nut and PTFE ferrule. A stainless steel cylinder with an I.D., length and volume of 3.5 cm, 5.5 cm and 53 mL, respectively, was welded to the bottom portion of the manifold. The center arm of the manifold was welded into the center of two 0.64 cm O.D. SS tubes, which had been welded together to form a "+" pattern. These tubes were in turn welded to the arms of the lower manifold, at a point just below the Swagelok fittings. The cylinder on the bottom portion of the manifold was designed as a "safety" dead volume for the sampler. As the the cartridges enclosed in the manifold were lowered to the desired sampling depth, the air volume in the cartridges and cylinder compressed and the bottom portion of the manifold filled with water to a point below the 0.64 cm O.D. cross-tubes. Therefore, the dead volume in the lower portion of the manifold prevented the water from passing through the cartridges as they were lowered to the sampling point. As the sampler was lowered the check valve on the center arm of the manifold remained closed. Prior to the initiation of sampling this check valve was opened and the water which had accumulated in the lower manifold was forced to the upper portion of the polyethylene tube, as the tube filled with water to the height of the water table. Thus fresh water from the desired sampling depth was flushed through the lower manifold and was waiting at the entrance of each Tenax cartridge.

This sampler was operated in the following manner. One end of each of the two polyethylene tubes were connected to a pressurization control unit at the surface, see Figure 3.2. As mentioned above, the

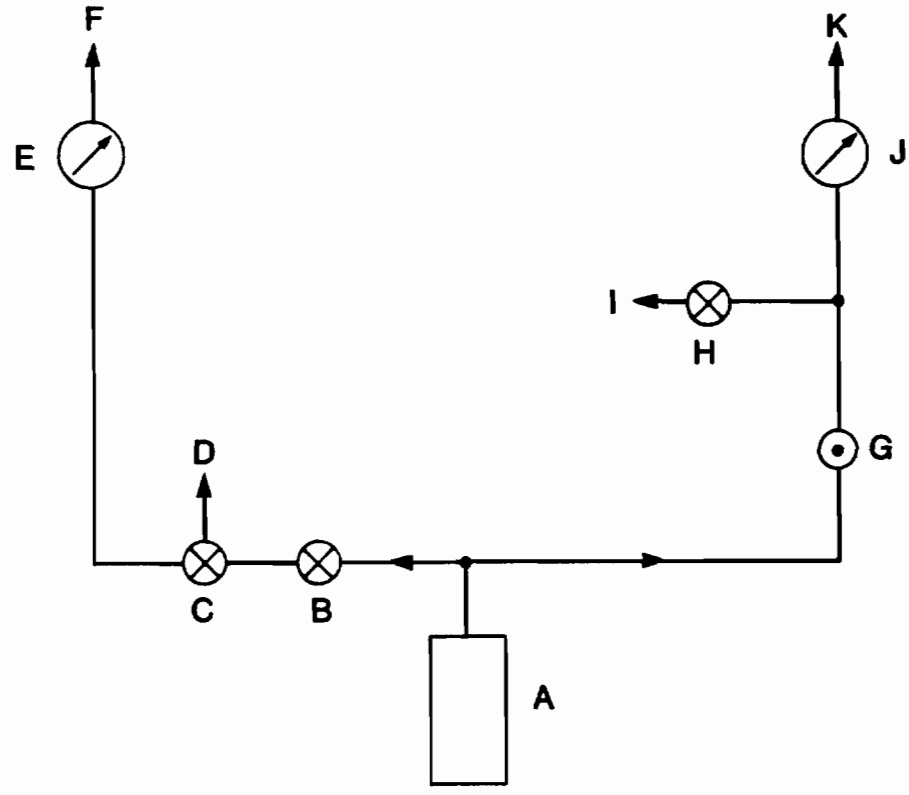

Figure 3.2. Diagram of the ATD sampler pressurization unit. **A** compressed gas supply (UP-He). **B** snap valve. **C** "2-way" snap valve, "open" position vents the line, "closed" position allows the transfer of gas. **D** vent. **E** 0 to 100 psi pressure gauge. **F** to 0.95 cm O.D. polyethylene tubing connected to the lower portion of the downhole-ATD syringe and cartridge sampling manifold. **G** pressure regulator. **H** snap valve. **I** vent. **J** 0 to 60 psi high accuracy pressure gauge. **K** to 0.95 cm O.D. polyethylene tubing connected to the upper portion of the downhole-ATD syringe and cartridge or tube and cartridge sampling manifold OR the surface-ATD sampling apparatus.

opposite ends of the tubes were connected to the upper and lower portions of the manifold. The pressurization control unit allowed the pressurization, venting and determination of the internal pressure of the sampler. A tank of UP-He, which was also connected to the unit, was used to supply gas for sampler pressurization. A 0 to 60 psi pressure gauge (3-D Instruments Inc., Huntington Beach, CA) accurate to $\pm$ 0.15 psi, was used to read the pressure in the polyethylene tubing connected to the upper portion of the manifold. The pressurization of this tubing controlled the opening and closing of the cartridge check valves. A second, lower accuracy, 0 to 100 psi pressure gauge was used to read the pressure in the polyethylene tubing connected to the check valve on the center arm of the lower portion of the manifold. The pressurization of this tubing controlled the opening and closing of the check valve on the center arm of the manifold. A 7 lb brass cylindrical weight (6.4 cm in diameter) with a 1.3 cm I.D. hole drilled through its center (not depicted in Figure 3.1), was inserted over the polyethylene tube connected to the top portion of the manifold. The weight rested on the manifold and assisted in the sinking of the sampler to the desired depth. A 7 lb weight was required to counteract the buoyant force of the > 60 m of tubing which were connected to the manifold and lowered down the well. In order to determine the depth the sampler was lowered to, each 3 m of the tubing connected to the upper portion of the manifold was marked.

Prior to the lowering of the sampler down the well both polyethylene tubes were pressurized to 10 psi. The sampler was lowered in increments of 3 m. At each increment the pressure in both tubes was increased in order to maintain a pressure against the check valves which was 10 psi greater than the pressure head inside the well, at that depth. This ensured that the check valves remained closed as the sampler was lowered. When the sampler had reached the desired sampling point, the tubing was secured at the surface to maintain the sampler at this depth. First, the pressure in the tubing connected to the lower portion of the manifold was relieved, at the surface, by opening a valve on the pressure control unit. This release of pressure opened the check valve (on the center arm of the lower portion of the manifold) and flushed the lower portion of the manifold with fresh water from the desired sampling depth, as described above.

The height of the water table was measured and the depth to the sampling point was known. Therefore, the pressure head in the well at the sampling depth could be calculated with reasonable accuracy. This allowed a pressure gradient of 5 psi to be set across each cartridge, and the the sampling flow rate to be controlled (see p.84). Sampling was initiated (the cartridge check valves were opened) by reducing the pressure in the tubing connected to the upper manifold to 5 psi below the pressure head in the well at the sampling point. The tubing was vented, at the surface, by opening another valve on the pressure control unit. Knowing the cartridge flow rates would be ~1.5 to

3.0 mL/min, the sampling step was timed to allow the desired volume of water to pass through each cartridge. The flow of water through the cartridges was stopped by increasing the pressure in the tubing by 15 psi, i.e., 10 psi in excess of the pressure head at that depth. Therefore the cartridge check valves were forced to close. As the sampler was raised to the surface the pressure was reduced in the tubing connected to the upper portion of the manifold at each 3 m increment. This reduced the pressure in the tubing to a reasonable level and also maintained a 10 psi pressure gradient in the upper portion of the manifold. Thus, the cartridge check valves remained closed as the sampler was raised through the well. The volume contained in each syringe, the sample volume which had passed through each cartridge, was measured at the surface.

3.4.2 Modified Tube and Cartridge Sampler

The second downhole sampler, depicted in Figure 3.3, was a modification of the tube and cartridge design of Pankow et al. (32) and was used to collect samples at the Syosset, NY and the Repauno, NJ sampling sites. The small bed ATD cartridges, described in Section 2.1.2, were used with this sampler. The sorbent bed volumes of these cartridges were 0.68 mL, and therefore the void volume of each cartridge was ~0.5 mL. The compound levels encountered at these sites were not expected to cause the Tenax bed to overload for sample volumes ranging from 20 to 30 mL. The use of the small bed ATD cartridges enabled the simplification of sampler design and sampling

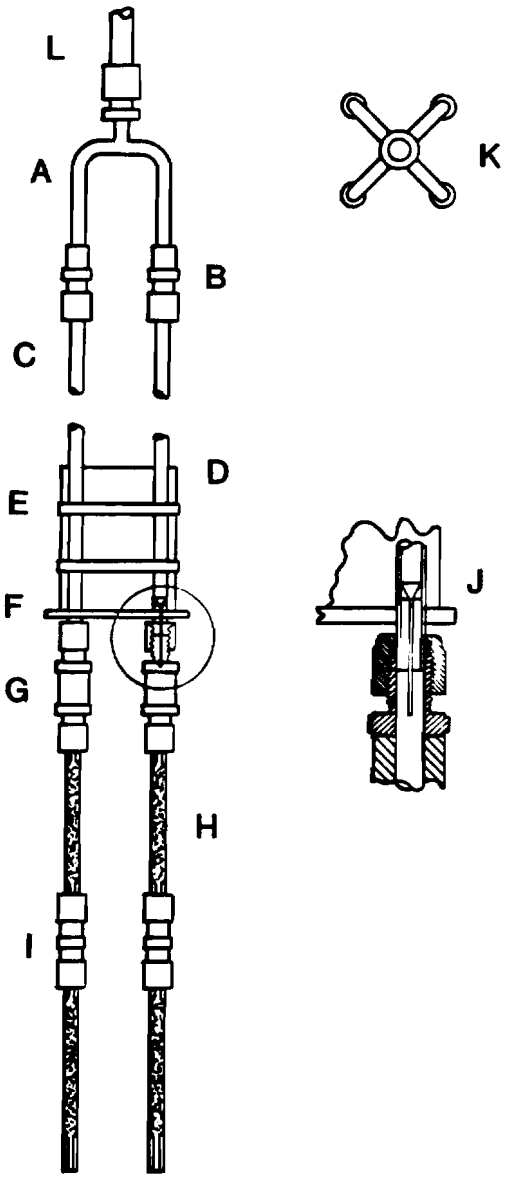

Figure 3.3 Diagram of the modified tube and cartridge downhole-ATD sampler. The diameter of the sampler at its widest point is ~7 cm. Its total length ranges from 1.6 to 2.1 m. **A** Manifold (two of four arms showing) constructed of 0.64 cm O.D. SS tubing. **B** Swagelok 0.64 cm SS fitting welded to the manifold and used with a PTFE ferrule. **C** 1.5-m length (25 mL internal volume) or 1.8-m length (35 mL internal volume) of 0.64 cm O.D., 0.47 cm I.D. PTFE tubing. **D** 5 lb brass weight; 13 cm in length and 7 cm in diameter. **E** locking nylon tie-band. **F** PTFE disk. **G** Nupro one-way SS check valve. **H** small bed Tenax cartridge, ~0.68 mL in volume. **I** Swagelok 0.64 cm SS union with PTFE ferrules. **J** enlarged view of 2.5 cm, 27 gauge syringe needle inserted within a PTFE support into the PTFE tubing. **K** overhead view of SS manifold. **L** Swagelok 0.95 cm SS fitting welded to the top of the manifold and connected to ~46 m of 0.95 cm O.D. polyethylene tubing.

procedure, with respect to the Camden samples. The samples from Syosset and Repauno were still collected under significant depths of water (13 to 16 m) and therefore, the air trapped in each cartridge would compress as it was lowered to the sampling point. Thus if simply lowered down a well, these cartridges would fill with ~0.3 mL of water. However, the acquisition of such a small fraction of the total volume of water to be sampled from a location above the designated sampling point was considered to be reasonable. Therefore, this sampler was not modified to prevent small ATD cartridges from filling with a small amount of water, prior to the initiation of sampling at the desired depth.

For this sampler the lower portion of the SS sampler manifold (see Figure 3.1) was not utilized, and a 1.5- or 2-m length of 0.64 cm O.D., 0.47 cm I.D. PTFE tubing replaced the syringe as a sample volume reservoir. A check valve was attached to the cartridge outlet, as described in the previous section, and a 2.5 cm, 27 gauge SS syringe needle was still used as a flow restrictor for each cartridge. In this case, the needle was inserted through a 2-cm length of 0.45 cm O.D. PTFE, with an I.D. equal to the O.D. of the syringe needle. The PTFE support, with syringe needle, was then inserted into the inlet end of the PTFE tubing reservoir. This portion of the tubing was then connected to the outlet end of a check valve with a 0.64 cm SS Swagelok nut and brass ferrule. When this Swagelok connection was tightened, the brass ferrule sealed the PTFE tubing to the check valve and also sealed the PTFE support to the syringe needle. Once

connected, the syringe needle extended ~0.64 cm into the check valve. The opposite end of the PTFE tubing was connected to one of the four fittings on the top portion of the SS sampler manifold. For the Syosset sampling trip, the lengths of PTFE tubing were ~1.5 m, and each had an internal volume of ~25 mL. For the Repauno trip, the lengths of tubing were ~1.8 m, and each had an internal volume of ~35 mL. Once the four tubes were connected to the top portion of the sampling manifold they were strapped to the outside of a 5 lb brass weight, which was utilized to help submerge the sampler.

Four 0.64 cm O.D. grooves were drilled along the outside of the 13 cm long, 7 cm in diameter weight. The grooves were set at 90^{o} angles from one another and were designed such that when the tubes were strapped to the weight, they were recessed. Therefore, the diameter of the sampler was no greater than ~7 cm at any point. Three nylon locking tie-bands were used to strap the tubes into the weight. A PTFE disk, slightly larger in diameter than the weight and 0.25 cm thick, was used to support the weight. The four PTFE tubes were inserted through holes in the disk and then connected to the syringe needles, check valves and cartridges. Therefore the weight rested on the PTFE disk, which rested on the four cartridge check valves. This kept the individual check valves and cartridges from spreading apart under the force of the weight. The sampling procedure for this sampler was identical to the one described in the previous section, except for the steps involving the pressurization of the lower portion

of the SS sampling manifold, which was not used in this design. See Section 3.3 for a discussion of the number of replicate downhole-ATD samples collected at each site.

3.5 Surface Samples - Collection Procedures

3.5.1 Surface-Adsorption/Thermal Desorption Samples

Surface-ATD samples were collected utilizing a submersible sampling pump and the surface sampling apparatus depicted in Figure 3.4. A 4.4 cm O.D. Johnson-Keck (St. Paul, MI) model SP-81 submersible sampling pump was used to pump groundwater at ~1 L/min from the desired depth in the well to the surface. In a previous study performed by Imbrigiotta et al. (54) of USGS-NJ, it was determined that gear-submersible pumps of this type achieve high percent recoveries with good precision for the collection of groundwater samples containing PPPs. The output of the pump was brought to the surface with 1.3 cm O.D. PTFE tubing. The tubing was connected to the surface sampling apparatus with a 1.3 to 0.64 cm SS Swagelok reducing union. Once at the sampling apparatus the water first passed through a short segment of 0.64 cm O.D. PTFE tubing and into a three-way glass and PTFE stopcock. In its fully open position the stopcock diverted a portion of the sampling stream to a 0.64 cm O.D. PTFE tube. This tube was used for the collection of the surface-P&T samples (see Section 3.5.2). The remaining portion of the sampling stream was passed through another section of PTFE tubing also connected to the second three-way stopcock. Each stopcock arm was

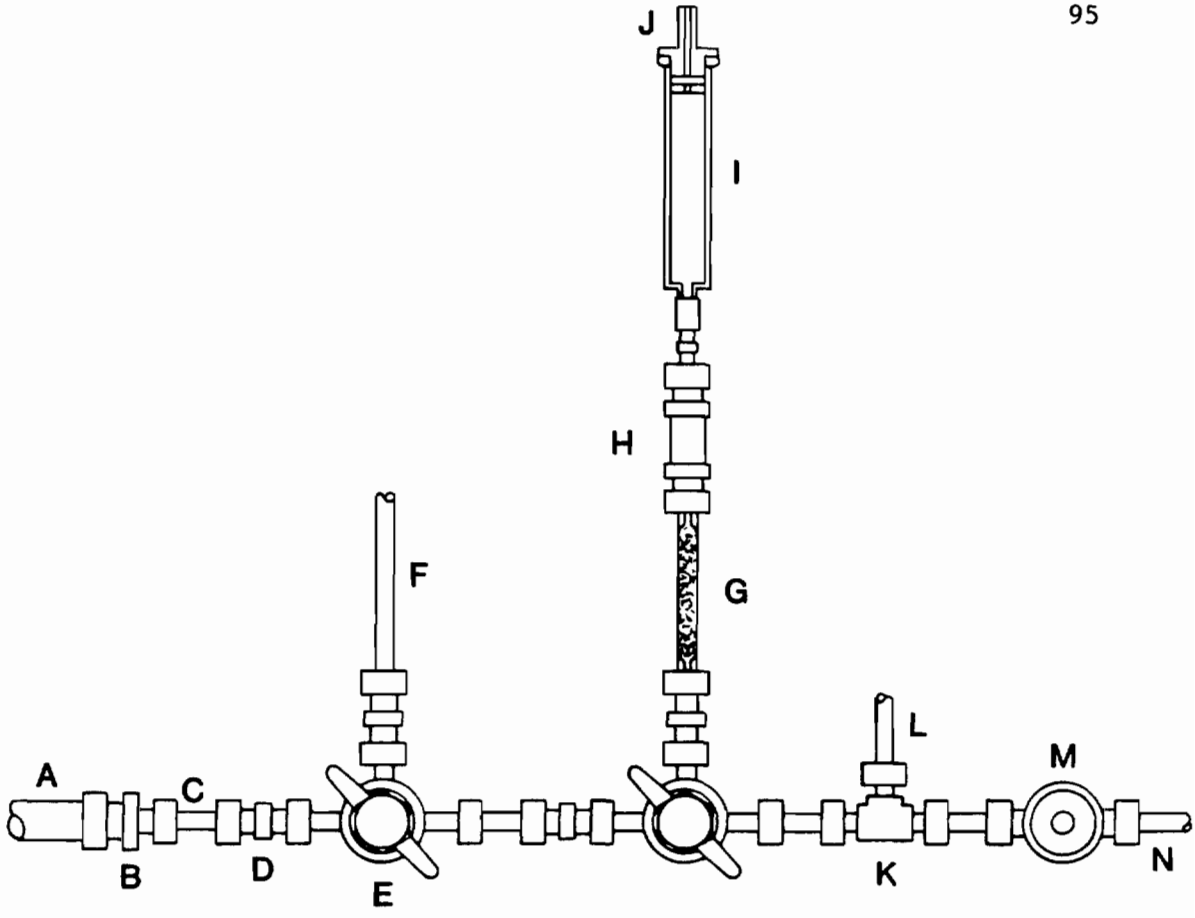

Figure 3.4. Diagram of the surface-ATD sampling apparatus. **A** 1.3 cm O.D. PTFE tubing (output line of the submersible sampling pump). **B** Swagelok 1.3 to 0.64 cm SS reducing union with a PTFE ferrule on the 0.64 cm end. **C** short segment of 0.64 cm O.D. PTFE tubing. **D** Swagelok 0.64 cm SS union with PTFE ferrules. **E** three-way glass and PTFE stopcock with arms constructed of 0.64 cm O.D. borosilicate tubing. **F** 0.64 cm O.D. PTFE tubing used for the collection of surface-P&T samples. **G** small bed Tenax cartridge, ~0.68 mL in volume. **H** Nupro one-way SS check valve, with same syringe needle flow restictor depicted in Figure 3.2. **I** 10 or 50 mL glass syringe barrel with luer-lok hub. **J** PTFE syringe barrel insert. **K** Swagelok 0.64 cm SS three-way union tee with PTFE ferrules. **L** 0.64 cm O.D. PTFE tube connected to 0 to 60 psi high accuracy pressure gauge (on ATD sampler pressurization control unit, see Figure 3.2). **M** PTFE fine metering valve. **N** 0.64 cm O.D. PTFE tubing, to waste.

constructed of 0.64 cm O.D. precision borosilicate glass tubing. This enabled 0.64 cm SS Swagelok fittings to be used for all tubing to stopcock connections. All tubing connections utilized PTFE ferrules.

The second stopcock was used to divert a portion of the sampling stream through a Tenax cartridge. As with the syringe and cartridge sampler described in Section 3.4.1, the outlet of each cartridge was connected to a one-way check valve and syringe barrel assembly. The check valve again contained a 2.5 cm, 27 gauge syringe needle, which acted as a flow restrictor. The inlet end of the cartidge was connected to an arm of the stopcock with a 0.64 cm SS Swagelok union. With the second stopcock fully open a portion of the sample stream was passed through the Tenax cartidge and the check valve/syringe barrel assembly.

The third arm of the second stopcock was connected to a short segment of PTFE tubing which in turn connected to a 0.64 cm three-way SS Swagelock union-tee. The center arm of the union-tee was connected to a length of PTFE tubing. The outlet of the tubing was connected to the inlet of the high accuracy pressure gauge used for the downhole sampler (see Section 3.4.1). The downhole sampler pressure control unit was easily converted and connected to the ATD-surface sampling apparatus. The third arm of the union-tee was connected to a short length of PTFE tubing which in turn connected to the inlet of a flow metering valve constructed of PTFE. The outlet of the metering valve was also connected to tubing which transferred the remaining portion of the sample stream to waste. The aperture of the metering valve was

used to adjust the pressure in the upstream sampling line to 5 psig, as read by the high accuracy pressure gauge. This set a pressure gradient of 5 psi across the Tenax cartridge. Thus, this downhole sampling condition was reproduced at the surface and comparable flow rates were obtained.

The ATD surface sampling apparatus was operated in the following manner. With the output of the submersible pump connected to the surface sampling apparatus, the first stopcock was positioned to be completely open. This enabled flow through and downstream of the P&T sampling tube. The second stopcock was positioned to direct all flow downstream of itself. The aperture in the PTFE metering valve was then adjusted to set the pressure in the upstream sampling line to 5 psig. A Tenax cartridge, check valve and syringe barrel were then connected to the middle arm of the second stopcock. The stopcock was then turned to its fully open position and a portion of the sample stream was diverted through the Tenax cartridge. Occasionally adjustments were made in the aperture of the PTFE metering valve to maintain the sampling pressure gradient at 5 psi. Fluctuations in the water pressure occurred due to occasional fluctuations in the pumping capacity. The elapsed time during sample acquisition was recorded in order to determine sampling flow rates. When the desired sample volume was collected in the syringe barrel the second stopcock was turned to direct all flow downstream of the Tenax cartridge. The sample volume retained by the syringe was measured and the Tenax

cartridge was removed from the stopcock, sealed and stored on ice. See Section 3.3 for a discussion of the number of replicate surface-ATD samples collected at each sampling site.

3.5.2 Surface-Purge and Trap Samples

All surface samples analyzed by P&T were collected using the submersible pump and the surface sampling apparatus described in the previous section. As was mentioned, a portion of the sampling stream was always diverted through a 0.64 cm O.D. PTFE tube by way of a three-way glass and PTFE stopcock. This tube was used to fill standard 40 mL P&T sample vials (10). Each P&T sample was collected while a corresponding surface-ATD sample was collected. USGS-NJ personnel collected the surface-P&T samples. The PTFE tubing was inserted into the bottom of the sample vial and the vial was first rinsed with sample water. It was filled to overflowing, then capped. If a vial contained headspace, it was opened and refilled. Each sample was stored on ice during transport to the laboratories. See Section 3.3 for a discussion of the number of replicate surface-P&T samples collected at each sampling site.

3.6 Sample Analysis

All OGC samples were analyzed according to the internal standard calibration, GC/MS/DS procedure described in Section 2.1.4. For the Camden and Syosset ATD samples the two step centrifugation/vacuum desiccation cartridge drying method was employed, see also Sections

2.1.3 and 2.2.2. For the Repauno samples only the centrifugation drying step was utilized and samples were analyzed using the glass bead drier system, according to the procedures outlined in Section 2.4.2. All P&T samples were analyzed by the P&T with whole column cryotrapping (P&T/WCC) analysis methodology developed by Pankow and Rosen (57). This methodology combines the standard P&T sample concentration method (10) with capillary column GC analysis. A Chrompack (Bridgewater, NJ) 25 m x 0.32 mm I.D. CP Sil 8 CB (0.25 μm film thickness) capillary column was used for the Camden ATD analyses, and the Camden and Syosset P&T/WCC analyses. A J&W Scientific 30 m x 0.32 mm I.D. DB-5 (1 μm film thickness) capillary column was used for the Syosset ATD, and the Repauno P&T/WCC analyses. Finally, a J&W Scientific 30 m x 0.53 mm I.D. DB-624 (~3 μm film thickness) capillary column was used for the Repauno ATD analyses.

For both the ATD and P&T/WCC analyses, a portion of the capillary column effluent stream was diverted to a flame ionization detector (FID) by use of a fused silica open-split GC/MS interface (column exit at 1 atm) developed by Pankow and Isabelle (58). The detector output was collected and stored by a personal computer which operated Nelson Analytical (Cuppertino, CA) 3000 Series Chromatographic Data System software. Use of the FID detector was necessary because in some samples some compounds occurred at concentrations as high as 130 to 400 ppb. For the PPPs, an FID detector has a much broader linear

response range per analyte mass than an MS detector. Therefore, the use of the FID detector provided a more accurate method of quantitation for some of these compounds.

3.7 Results and Discussion

3.7.1 Overview of Results

Appendix 1 contains the results of each ATD and P&T sample analyzed. The information is separated first by sampling trip and then by sampling and analysis method. Each table indicates the volume of sample analyzed. In the case of the ATD samples, the sample flow rate during collection is also given. Tables 3.2-3.10 are summaries of this data. These tables present the arithmetic mean analyte concentration, $\bar{C}$, standard deviation, s, and coefficient of variation, CV (s expressed as a percentage of the mean) for each compound detected in each sample.

The reproducibility of the results from the analysis of the surface-P&T samples was very good. For most compounds detected at each sampling site the coefficient of variation was < 5.0%. Therefore, with respect to this criterion, the surface-P&T sampling and analysis method performed very well for the determination of PPPs in groundwater.

All the ATD results from the first two sampling trips indicated that, for most compounds detected, there were serious problems with either the sampling or analysis portion of the methodology. The reproducibility was poor and the relative accuracy was questionable.

Table 3.2. Downhole-ATD[a] Camden, NJ Sampling Site - Data Summary.

Compound	$\bar{C}$[b] (μg/L)	s (μg/L)	CV[c] (%)	n[d]
1,1-Dichloroethene	.25	.13	52	7
1,1-Dichloroethane	1.9	.68	36	7
cis-1,2-Dichloroethene	7.2	2.5	35	7
Trichloromethane	.24	.090	38	7
1,1,1-Trichloroethane	.51	.12	24	7
1,2-Dichloroethane	1.7	.62	36	7
Benzene	.59	.26	44	7
Trichloroethene	86	28	33	7
1,1,2-Trichloroethane	.11	.027	25	7
Tetrachloroethene	7.1	2.1	30	7
Chlorobenzene	.20	.044	22	7
Ethylbenzene	.028	.010	36	7
m+p-Xylene	.084	.023	27	7
o-Xylene	.041	.015	37	7

[a]Average sample volume = 11 ± 2.6 mL, average sample flow rate = 1.8 ± .72 mL/min.
[b]Arithmetic mean concentration based on n sample analyses.
[c]Coefficient of variation, s expressed as a percentage of the mean.
[d]Samples in which the compound was detected at a quantifiable level.

Table 3.3. Surface-ATD[a] Camden, NJ Sampling Site - Data Summary.

Compound	$\bar{C}$[b] (μg/L)	s (μg/L)	CV[c] (%)	n[d]
1,1-Dichloroethene	.46	.52	110	8
1,1-Dichloroethane	1.4	.54	39	8
cis-1,2-Dichloroethene	4.6	1.8	39	8
Trichloromethane	.20	.13	65	8
1,1,1-Trichloroethane	.73	.15	21	8
1,2-Dichloroethane	1.2	.38	32	8
Benzene	.31	.094	30	7
Trichloroethene	60	16	27	8
1,1,2-Trichloroethane	.095	.010	11	8
Tetrachloroethene	6.1	.84	14	8
Chlorobenzene	.16	.0089	5.6	8
Ethylbenzene	.024	.0039	16	6
m+p-Xylene	.084	.0010	1.2	6
o-Xylene	.037	.0056	15	6

[a]Average sample volume = 12 $\pm$ .80 mL, average sample flow rate = 2.9 $\pm$ .40 mL/min.
[b]Arithmetic mean concentration based on n sample analyses.
[c]Coefficient of variation, s expressed as a percentage of the mean.
[d]Samples in which the compound was detected at a quantifiable level.

Table 3.4. Surface-P&T[a] Camden, NJ Sampling Site - Data Summary.

Compound	$\bar{C}$[b] (μg/L)	s (μg/L)	CV[c] (%)	n[d]
1,1-Dichloroethene	8.5	.49	5.8	8
1,1-Dichloroethane	6.2	.32	5.2	8
cis-1,2-Dichloroethene	23	.76	3.3	8
Trichloromethane	.79	.052	6.6	8
1,1,1-Trichloroethane	ND[e]	–	–	–
1,2-Dichloroethane	4.0	.20	5.0	8
Benzene	ND	–	–	–
Trichloroethene	170	9.9	5.8	8
1,1,2-Trichloroethane	ND	–	–	–
Tetrachloroethene	7.5	.24	3.2	8
Chlorobenzene	ND	–	–	–
Ethylbenzene	ND	–	–	–
m+p-Xylene	ND	–	–	–
o-Xylene	ND	–	–	–

[a]Analysis volume = 5.0 mL
[b]Arithmetic mean concentration based on n sample analyses.
[c]Coefficient of variation, s expressed as a percentage of the mean.
[d]Samples in which the compound was detected at a quantifiable level.
[e]Not Detected.

Table 3.5. Downhole-ATD[a] Syosset, NY Sampling Site - Data Summary.

Compound	$\bar{C}$[b] (μg/L)	s (μg/L)	CV[c] (%)	n[d]
1,1-Dichloroethene	5.3	6.0	110	8
TCTF-ethane*	24	1.5	6.3	8
1,1-Dichloroethane	.68	.32	47	8
cis-1,2-Dichloroethene	.23	.11	48	8
Trichloromethane	.12	.058	48	8
1,1,1-Trichloroethane	110	9.9	9.0	8
1,2-Dichloroethane	.26	.073	28	8
Tetrachloromethane	.81	.065	8.0	8
Benzene	.19	.055	29	8
Trichloroethene	3.5	1.3	37	8
1,1,2-Trichloroethane	.080	.0090	11	8
Tetrachloroethene	29	4.7	16	8
Chlorobenzene	.057	.0055	9.6	8

[a]Average sample volume = 11 ± 1.6 mL, average sample flow rate = 2.2 ± .23 mL/min.
[b]Arithmetic mean concentration based on n sample analyses.
[c]Coefficient of variation, s expressed as a percentage of the mean.
[d]Samples in which the compound was detected at a quantifiable level.
*1,1,2-Trichloro-1,2,2-trifluoroethane.

Table 3.6. Surface-ATD[a] Syosset, NY Sampling Site - Data Summary.

Compound	$\bar{C}$[b] (μg/L)	s (μg/L)	CV[c] (%)	n[d]
1,1-Dichloroethene	5.6	5.4	96	8
TCTF-ethane*	24	1.5	6.3	8
1,1-Dichloroethane	.57	.31	54	8
cis-1,2-Dichloroethene	.18	.097	54	8
Trichloromethane	.11	.048	44	8
1,1,1-Trichloroethane	100	6.6	6.6	7
1,2-Dichloroethane	.25	.069	28	8
Tetrachloromethane	.96	.051	5.3	8
Benzene	.20	.074	37	8
Trichloroethene	2.9	1.0	34	8
1,1,2-Trichloroethane	.076	.0068	8.9	8
Tetrachloroethene	27	3.0	11	7
Chlorobenzene	.069	.0078	11	8

[a]Average sample volume = 15 ± .40 mL, average sample flow rate = 2.3 ± .40 mL/min.
[b]Arithmetic mean concentration based on n sample analyses.
[c]Coefficient of variation, s expressed as a percentage of the mean.
[d]Samples in which the compound was detected at a quantifiable level.
*1,1,2-Trichloro-1,2,2-trifluoroethane.

Table 3.7. Surface-P&T[a] Syosset, NY Sampling Site - Data Summary.

Compound	$\bar{C}$[b] (μg/L)	s (μg/L)	CV[c] (%)	n[d]
1,1-Dichloroethene	120	5.3	4.4	7
TCTF-ethane*	NQ[e]	–	–	–
1,1-Dichloroethane	4.0	.098	2.5	7
cis-1,2-Dichloroethene	1.9	.13	6.8	7
Trichloromethane	.73	.017	2.3	7
1,1,1-Trichloroethane	120	5.3	4.4	7
1,2-Dichloroethane	.77	.039	5.1	7
Tetrachloromethane	.88	.054	6.1	7
Benzene	NQ	–	–	–
Trichloroethene	10	.51	5.1	7
1,1,2-Trichloroethane	NQ	–	–	–
Tetrachloroethene	37	1.2	3.2	7
Chlorobenzene	NQ	–	–	–

[a]Analysis volume = 5.0 mL.
[b]Arithmetic mean concentration based on n sample analyses.
[c]Coefficient of variation, s expressed as a percentage of the mean.
[d]Samples in which the compound was detected at a quantifiable level.
[e]Detected at a non-quantifiable level.
*1,1,2-Trichloro-1,2,2-trifluoroethane.

Table 3.8. Downhole-ATD[a] Repauno, NJ Sampling Site - Data Summary.

Compound	$\bar{C}$[b] (μg/L)	s (μg/L)	CV[c] (%)	n[d]
Dichloromethane	.25	.012	4.8	6
cis-1,2-Dichloroethene	1.9	.052	2.7	8
Trichloromethane	28	.74	2.6	8
1,2-Dichloroethane	1.4	.035	2.5	8
Tetrachloromethane	1.7	.046	2.7	8
Benzene	17	.53	3.1	8
Trichloroethene	35	.93	2.7	8
Toluene	.11	.013	12	8
Tetrachloroethene	360	36	10	8
Chlorobenzene	34	1.1	3.2	8
o-Xylene	.32	.023	7.2	8
Nitrobenzene	240	16	6.7	8

[a]Average sample volume = 22 ± 1.3 mL, average sample flow rate = 1.4 ± .094 mL/min.
[b]Arithmetic mean concentration based on n sample analyses.
[c]Coefficient of variation, s expressed as a percentage of the mean.
[d]Samples in which the compound was detected at a quantifiable level.

Table 3.9. Surface-ATD[a] Repauno, NJ Sampling Site - Data Summary.

Compound	$\bar{C}$[b] (μg/L)	s (μg/L)	CV[c] (%)	n[d]
Dichloromethane	.24	.037	15	6
cis-1,2-Dichloroethene	1.9	.035	1.8	8
Trichloromethane	29	.53	1.8	8
1,2-Dichloroethane	1.4	.083	5.9	8
Tetrachloromethane	1.8	.12	6.7	8
Benzene	18	.53	2.9	8
Trichloroethene	35	.52	1.5	8
Toluene	.15	.010	6.7	8
Tetrachloroethene	340	20	5.9	8
Chlorobenzene	36	2.6	7.2	8
o-Xylene	.34	.012	3.5	8
Nitrobenzene	210	15	7.1	8

[a]Average sample volume = 29 ± 2.3 mL, average sample flow rate = 5.4 ± 2.6 mL/min.
[b]Arithmetic mean concentration based on n sample analyses.
[c]Coefficient of variation, s expressed as a percentage of the mean.
[d]Samples in which the compound was detected at a quantifiable level.

Table 3.10. Surface-P&T[a] Repauno, NJ Sampling Site - Data Summary.

Compound	$\bar{C}$[b] (μg/L)	s (μg/L)	CV[c] (%)	n[d]
Dichloromethane	ND[e]	–	–	–
cis-1,2-Dichloroethene	2.7	.37	14	8
Trichloromethane	32	.64	2.0	8
1,2-Dichloroethane	1.1	.095	8.6	8
Tetrachloromethane	1.4	.035	2.5	8
Benzene	20	.83	4.2	8
Trichloroethene	35	1.3	3.7	8
Toluene	NQ[f]	–	–	–
Tetrachloroethene	370	17	4.6	8
Chlorobenzene	48	1.8	3.8	8
o-Xylene	NQ	–	–	–
Nitrobenzene	250	14	5.6	8

[a]Analysis volume = 5.00 mL.
[b]Arithmetic mean concentration based on n sample analyses.
[c]Coefficient of variation, s expressed as a percentage of the mean.
[d]Samples in which the compound was detected at a quantifiable level.
[e]Not detected.
[f]Detected at a non-quantifiable level.

For most compounds detected, the analyte concentrations determined by both ATD methods were found to be significantly lower than those determined by surface-P&T. Based on the cartridge drying information discussed in Section 2.2.2, it appeared that the poor ATD results were due to losses occurring during the cartridge vacuum-desiccation step used prior to the analysis of each Camden and Syosset sample. The vacuum-desiccation percent recovery study performed by Pankow et al. (41) indicated that this cartridge drying procedure may be used "safely" only for compounds with Henry's law constants which are less than ~2 x 10^{-3} atm-m^3/mole (see also Section 2.2.2, Table 2.1). As might be expected from those results, a few compounds with low Henry's law constants in the Camden and Syosset samples were determined with a fair amount of precision and relative accuracy (see Tables 3.2-3.7). However, the majority of compounds appeared to suffer significant losses during the vacuum-desiccation procedure.

Due to the systematic error caused by losses occurring during the vacuum-desiccation step, the ATD results from the first two sampling trips have been discounted concerning conclusions about the relative accuracy and precision of the methodology. However, some information from the Camden and Syosset ATD samples regarding the relative sensitivity of the methodology will be presented in Section 3.7.5. In addition, all of the results of the surface-P&T sample analyses have been retained for discussion.

The results of the ATD analyses from the third sampling trip were greatly improved. Each of the Repauno ATD samples was analyzed with

the glass bead drier system, after only the cartridge centrifugation-desiccation step. This sample analysis procedure was discussed in Section 2.4. In general, the CV for each compound detected was ~5.0%. The relative accuracy was also significantly improved. For most compounds detected at the Repauno site, there was little difference in the concentrations determined by either the ATD or surface-P&T methodologies. Finally, for each sampling trip several compounds were detected at ppt levels, exclusively, by the ATD sampling and analysis methodologies.

3.7.2 Statistical Comparison of Two Sample Sets

In order to determine whether there was a significant difference between the results of two sample sets (i.e., are they from two different populations), the following question was posed. Were the mean results of two sample sets significantly different? For example, was the mean concentration of trichloromethane determined by downhole-ATD, significantly different from its mean concentration determined by surface-P&T? In other words, did the two sampling and analysis methods provide significantly different results for the determination of the same compound? In order to answer this type of question, the arithmetic mean results of two sample sets were statistically compared using the two-sample t-test (59).

The two-sample t-test was used to test the null hypothesis, H_o, that the mean results, μ_n, of the two sample sets are equal ($H_o: \mu_1 = \mu_2$ vs. $H_1: \mu_1 \neq \mu_2$). A level of significance, $\alpha = 0.01$, was

set for the test and the probability, P, was calculated. If $P \leq 0.01$ the test was considered to be significant and H_o was rejected. When H_o was rejected, the two-sample t-test determined that there was a 1% chance, or less, that the values in the sample sets would occur if their arithmetic means were equal. Therefore, when $P \leq 0.01$ it was determined that the means of the two sample sets were significantly different and represented two different sample populations. In the sections to follow, this test was used to determine whether each mean analyte concentration of a sample set varied significantly as a function of downhole- vs. surface-ATD sampling, or ATD vs. surface-P&T sampling and analysis methodologies.

3.7.3 Performance of Purge and Trap with Whole Column Cryotrapping for the Analysis of the Surface-Purge and Trap Samples

As discussed in Sections 3.3 and 3.6, eight surface-P&T samples were collected from each of the three sampling sites for analysis at OGC. These samples were obtained to provide reference concentrations in order to determine the relative precision and accuracy of the ATD sampling and analysis methods. Each surface-P&T sample was analyzed using P&T/WCC. At the three sampling sites a total of 10 of the 31 PPPs were detected and quantified using P&T/WCC. In addition, concentrations for cis-1,2-dichloroethene and nitrobenzene were also detected. The latter compound is a base-neutral-extractable priority pollutant. A summary of these results are presented in Tables 3.4, 3.7 and 3.10. The sampling and analysis precision was generally very

good for each compound detected at each sampling site. The CV values for the method ranged from 3.2 to 6.6%, 2.3 to 6.8% and 2.0 to 14% for the Camden, Syosset and Repauno sampling trips, respectively. The overall precision (average CV) is 5.0, 4.4 and 5.4% for the Camden, Syosset and Repauno analyses, respectively. Therefore P&T/WCC was shown to be a consistently precise analysis methodology for the determination of PPPs in water. Further, these results enhance the credibility of using the surface-P&T samples as a reference for the determination of the relative precision and accuracy of the ATD sampling and analysis methodologies tested.

3.7.4 Downhole- and Surface-Adsorption/Thermal Desorption

As discussed in Section 3.7.1, most of the results of the Camden and Syosset ATD analyses were biased due to the analysis artifact caused by the cartridge vacuum-desiccation step. Therefore, the majority of conclusions concerning the performance of the ATD methodologies were based on results obtained from the analysis of the Repauno samples. The mean analyte concentrations for each compound detected in the eight downhole- and eight surface-ATD samples obtained at the Repauno site, were compared using the two-sample t-test. The test results are displayed in Table 3.11 along with each mean analyte concentration $\bar{C}$, and its corresponding s and CV values. The precision obtained for the downhole- and surface-ATD methodologies was generally good. The CV values for the downhole- and surface-ATD methods ranged from 2.5 to 12% and 1.5 to 15%, respectively. The overall precision,

Table 3.11. Comparison of Downhole- and Surface-ATD Results, Repauno Sampling Site.

Compound	Sampler	$\bar{C}$[a] (μg/L)	s (μg/L)	CV[b] (%)	P[c]
Dichloromethane	DH[d]	0.25	0.012	4.8	.40
	S[e]	0.24	0.037	15	
cis-1,2-Dichloroethene	DH	1.9	0.052	2.7	.06
	S	1.9	0.035	1.8	
Trichloromethane	DH	28	0.74	2.6	.01*
	S	29	0.53	1.8	
1,2-Dichloroethane	DH	1.4	0.035	2.5	.55
	S	1.4	0.083	5.9	
Tetrachloromethane	DH	1.7	0.046	2.7	.14
	S	1.8	0.12	6.7	
Benzene	DH	17	0.53	3.1	.00*
	S	18	0.53	2.9	
Trichloroethene	DH	35	0.93	2.7	.12
	S	35	0.52	1.5	
Toluene	DH	0.11	0.013	12	.00*
	S	0.15	0.010	6.7	
Tetrachloroethene	DH	360	36	10	.22
	S	340	20	5.9	
Chlorobenzene	DH	34	1.1	3.2	.04
	S	36	2.6	7.2	
o-Xylene	DH	0.32	0.023	7.2	.13
	S	0.34	0.012	3.5	

Table 3.11 (cont'd). Comparison of Downhole- and Surface-ATD Results, Repauno Sampling Site.

Compound	Sampler	$\bar{C}$[a] (μg/L)	s (μg/L)	CV[b] (%)	P[c]
Nitrobenzene	DH	240	16	6.7	.01*
	S	210	15	7.1	

[a]Arithmetic mean concentration based on eight replicate samples.
[b]Coefficient of variation, s expressed as a percentage of the mean.
[c]Probability, determined from the two-sample t-test (59), that the values in the two sample sets would occur if their arithmetic means were equal.
[d]Downhole-ATD sampler.
[e]Surface-ATD sampler.
*$P \leq 0.01$, therefore a significant difference exists between the arithmetic means of the two sample sets.

as expressed by the arithmetic mean CV, was 5.0% for downhole-ATD and 5.5% for surface-ATD. Thus, the overall precision of the two methodologies is equivalent. For eight of the 12 compounds detected there was no significant difference between the mean analyte concentrations determined using ATD with either downhole or surface sampling (see Table 3.11). Therefore, for the majority of compounds detected there was no statistically significant difference in the concentrations determined using downhole- or surface-ATD methodologies.

For trichloromethane, benzene, and toluene, the mean analyte concentrations determined using surface-ATD were significantly higher than those determined using downhole-ATD. The opposite was true for nitrobenzene. Therefore, for these four compounds there were statistically significant differences in the concentrations determined using the downhole- and surface-ATD methodologies. Thus, for some analytes, different concentrations will be determined if either downhole- or surface-ATD is used for the sampling and analysis of groundwater. However, some perspective may be gained on this issue by determining the actual differences in the concentrations determined by both methods for the analytes mentioned above.

The percent difference, PD, between two mean concentrations may be determined by the formula:

$$PD = 100\ \left[\frac{|X_1 - X_2|}{(X_1 + X_2)/2}\right] \qquad 3.1$$

where $X_{1,2}$ = the values for which the percent difference is to be determined. In this case, the mean analyte concentration determined by downhole- or surface-ATD. Therefore, the PD value is the absolute value of the difference in the two mean concentrations expressed as a percentage of their arithmetic mean. The PD values were determined to be 3.5, 5.7, 13 and 31% for trichloromethane, benzene, nitrobenzene and toluene, respectively. The high PD value for toluene may be attributed to its low concentration and the occurrence of a relatively significant amount of background contamination for this compound, see Appendix 1.27. Therefore, the result may not be indicative of the overall differences that may be expected in analyte concentrations determined using both methods. Thus, for three of the four compounds only a small difference exists between the concentrations determined by downhole- and surface-ATD. And so, while these differences are statistically significant they are not large enough to change one's assessment of the groundwater quality. Based on this, essentially the same information was provided by the downhole- and surface-ATD samples.

Downhole- and surface-ATD also performed very well with regard to percent breakthrough (i.e., the estimated sampling efficiency). Appendices 1.23 and 1.26 present the percent breakthrough data obtained for the Repauno downhole- and surface-ATD samples collected with backup cartridges. For all compounds, no breakthrough was detected with any of the four downhole-ATD samples collected with backup cartridges. For four compounds there was a minimal amount of

breakthrough detected with the four surface-ATD samples collected with backup cartridges. The average breakthrough for these compounds was less than 4%. It is likely that most of this breakthrough occurred due to the higher sampling flow rates of the surface- vs. downhole-ATD samples.

Due to the outgassing of dissolved gas in the Repauno samples, it was very difficult to control the surface-ATD sampling flow rates. Unfortunately the ratio of the volume of gas to the volume of water and the composition of the gas could not be determined accurately. It could be estimated however that ~100 to 300 μL of gas formed per 44 mL of water. In any event, as water was pumped to the surface outgassing occurred in the tubing of the surface sampling apparatus and caused the sample flow rate to fluctuate. For the Repauno surface-ATD samples, the average flow rate was 5.4 $\pm$ 2.6 mL/min. The average downhole-ATD flow rate at Repauno was 1.4 $\pm$ 0.094 mL/min. However, the higher than usual and erratic flow rates for the Repauno surface-ATD samples did not appear to cause any significant artifacts relative to the downhole-ATD samples collected there. As mentioned above, only a small amount of breakthrough was detected for some compounds in the surface samples collected with backup cartridges. Because sampling efficiency may be a function of sample flow rate, as discussed in Section 3.4.1, it appears reasonable to associate the analyte breakthrough observed in the surface samples with the relatively high sample flow rates. However, as discussed earlier in this section

there were no other significant differences in the relative performance of either the surface- or downhole-ATD methodologies for the Repauno samples.

3.7.5 Comparison of Adsorption/Thermal Desorption and Surface-Purge and Trap

As shown in the previous section the results of the Repauno downhole- and surface-ATD analyses were very similar. Therefore, these results may be combined for comparison with the Repauno surface-P&T results. ATD will now be used to refer collectively to downhole- and surface-ATD. This has been done in Table 3.12, and for the remainder of this section the term ATD will be used to refer collectively to those pooled data.

In terms of sampling and analysis precision there appears to be no difference between the ATD or surface-P&T methodologies. The average CV for the compounds detected at the Repauno site was 5.3 and 5.4% for the ATD and surface-P&T samples, respectively. Table 3.12 presents the results of the two-sample t-tests performed in order to compare the mean concentration of each compound detected using both methods.

For six of the nine compounds detected by both methods, there was a statistically significant difference between the mean concentrations determined using each method. For four of these compounds the mean concentrations determined from the surface-P&T samples were significantly higher than those determined from the ATD samples.

Table 3.12. Comparison of ATD (Downhole + Surface)[a] and Surface-P&T Results, Repauno Sampling Site.

Compound	Sampler	$\bar{C}$[b] (μg/L)	s (μg/L)	CV[c] (%)	P[d]
cis-1,2-Dichloroethene	ATD[e]	1.9	0.045	2.4	.00*
	PT[f]	2.7	0.37	14	
Trichloromethane	ATD	28	0.77	2.8	.00*
	PT	32	0.64	2.0	
1,2-Dichloroethane	ATD	1.4	0.063	4.5	.00*
	PT	1.1	0.095	8.6	
Tetrachloromethane	ATD	1.7	0.010	5.9	.00*
	PT	1.4	0.035	2.5	
Benzene	ATD	17	0.73	4.3	.00*
	PT	20	0.83	4.2	
Trichloroethene	ATD	35	0.75	2.1	.86
	PT	35	1.3	3.7	
Tetrachloroethene	ATD	350	30	8.5	.02
	PT	370	17	4.6	
Chlorobenzene	ATD	35	2.3	6.6	.00*
	PT	48	1.8	3.8	
Nitrobenzene	ATD	220	23	10	.02
	PT	250	14	5.6	

[a]Combined downhole- and surface-ATD sample sets.
[b]Arithmetic mean concentration based on eight replicate samples, a total of 16 for combined ATD data sets.
[c]Coefficient of variation, s expressed as a percentage of the mean.
[d]Probability, determined from the two-sample t-test (59), that the values in the two sample sets would occur if their arithmetic means were equal.
[e]ATD samples.
[f]Surface-P&T sampler.
*$P \leq 0.01$, therefore a significant difference exists between the arithmetic means of the two sample sets.

Therefore, in general, it can be said that the two sampling and analysis methods produced different results when they were directly compared. However, these differences do not appear to be large enough to change ones assessment of the groundwater quality. The PD values (see previous section, eqn. 3.1) for the six compounds ranged from 14 to 34%, or 24% on the average. And so, for the compounds detected at the Repauno site it may be said that on the average, the use of either method can be expected to predict an analyte concentration that is within 24% of the other. Therefore, essentially the same information concerning the concentrations of these compounds was provided by both methodologies. Since there appears to be no systematic error which can explain the different analyte concentrations determined by the two methods, it would be premature to conclude that either method is inherently more accurate than the other. However, it would be reasonable to conclude that the relative accuracy of both methods is generally equivalent.

One difference in the two sampling and analysis methodologies is their relative sensitivity. Each P&T/WCC analysis utilized 5 mL of sample, while the average ATD sample size was 26 mL. Therefore, as applied here ATD was a factor of five more sensitive than the surface-P&T methodology. As a result, at the Repauno site, ATD was able to detect and quantify dichloromethane, toluene, and o-xylene; these compounds were not found in the surface-P&T samples. Even though these compounds were at low concentrations (~200 ppt) the ATD method precision was very good (see Tables 3.8 and 3.9). In addition,

the ATD analyses from the other two sampling sites also showed that ATD was more sensitive than the surface-P&T method. Six compounds whose concentrations ranged from 24 to 700 ppt, were detected at the Camden site exclusively by ATD. Three compounds whose concentrations ranged from 54 to 200 ppt, were detected at the Syosset site, again, exclusively by ATD (see Tables 3.2, 3.3, 3.5 and 3.6).

3.6 Potential Artifacts Associated with Surface Sampling Procedures

Because ATD samples were acquired by both downhole and surface sampling procedures, it may be possible to come to some preliminary conclusions concerning potential artifacts believed to be caused by surface sampling. As discussed previously, prior to the adsorption step surface-ATD samples first passed through the submersible sampling pump and all the associated sampling materials. This included ~20 m of PTFE pump tubing. For the downhole-ATD procedure the sample contacted only the glass cartridge and Tenax, and therefore, would not be subject to any possible surface sampling related artifacts. Numerous researchers (14,15,21-24,60,61) have discussed the possibility of errors occuring during sampling due to volatilization losses caused by specific pumping mechanisms and analyte partitioning onto and from pumping surfaces and associated tubing. The possible systematic losses of analytes, in addition to sample cross-contamination (due to leaching of analytes which may have adsorbed onto sampling materials) has the potential to decrease the precision and accuracy of a sampling method which utilizes a pumping procedure.

Several researchers have also attempted to quantify these errors, and in some cases have found them to be significant for the sampling of PPPs in groundwater (24,54,60). However, as discussed in Section 3.7.4, there was no significant difference in the precision or relative accuracy of the results obtained from the Repauno, downhole- and surface-ATD samples. Therefore, it appears that the surface sampling procedure utilized at the Repauno site did not cause any significant artifacts.

3.8 Conclusions

The downhole- and surface-ATD and surface-P&T data sets have provided a considerable amount of information which has enabled some important conclusions concerning the sampling and analysis of PPPs in groundwater to be made.

(1) Surface-P&T was shown to be a consistently precise methodology for the determination of PPPs in groundwater.

(2) Both downhole- and surface-ATD have been shown to be precise and relatively accurate methodologies for the determination of PPPs in groundwater.

(3) There were no significant differences in the relative precision or accuracies among surface-P&T, surface-ATD, and downhole-ATD.

(4) Both downhole- and surface-ATD were consistently shown to be more sensitive sampling and analysis methodologies than surface-P&T.

CHAPTER 4 MEASURING ADSORBENT CARTRIDGE BREAKTHROUGH

4.1 Introduction

Adsorbent cartridge breakthrough (ACB) experiments were conducted to investigate: 1) the practical limitations of ATD with Tenax for the analysis of water contaminated with PPPs; and 2) the practicality of using experimentally determined parameters for the modeling of ACB with Tenax under a variety of sampling conditions.

The PPPs are a group of low molecular weight, nonpolar, organic compounds. They are also characterized by generally low solubilities in water and high vapor pressures. Their solubilities span over two orders of magnitude, from 79 ppm (parts per million = mg/L) for p-dichlorobenzene to 20,000 ppm for dichloromethane. Tenax is a nonpolar porous polymer (62), and the PPPs should show a reasonable affinity for this sorbent relative to polar water. However, among the PPPs, the specific analyte affinities should be distinct. It is reasonable to expect that there might be some usable empirical relationship between the solubility of individual PPPs in water and their affinity for the sorbent. The more hydrophobic molecules should be more strongly attracted to the hydrophobic surface of the sorbent. Therefore the capacity of Tenax should be highest for those PPPs with the lowest solubilities in water. This type of analyte/sorbent relationship has been discussed by Dressler (34). ACB experiments were conducted with a group of PPPs covering a range of solubilities, in order to determine whether a relationship of this type existed for

this system. In addition, these experiments were also used to determine key modeling parameters. The use of these parameters with appropriate chromatographic bed models allowed ACB predictions to be made for a variety of PPPs. Nine ACB experiments were performed. The first two experiments tested the feasibility and efficiency of the experimental design. The remaining seven experiments determined ACB for 13 of the PPPs under different sampling conditions. Table 1 (Section 2.1) lists the PPPs and indicates which compounds were tested. The average experiment required 16 to 40 continuous hours to complete and the analysis of over 100 samples. It was therefore impractical and uneconomical to work with every PPP. The challenge was to generate a body of data which would enable a complete understanding of ACB for the PPPs, and to do so economically. Therefore, in order to avoid the need for analyzing all the PPPs, the 13 compounds were selected in order to represent distinct solublity regions of the PPPs. Much information was obtained by studying this limited group.

4.2 Experimental Procedure

4.2.1 Adsorbent Cartridge Breakthrough Curves

The focus of each ACB experiment was the determination of analyte ACB curves. ACB curves were determined by passing a solution containing one or more PPPs in water through a small volume (0.68 mL) ATD bed. The solution contained a constant concentration of each analyte and was passed through the bed at a controlled flow rate. The

cartridge effluent concentration C_e (ng/g), of each analyte was measured at specific sample volume intervals. This allowed the percent ratio of each C_e to its corresponding influent concentration C_i (ng/g), to be determined as a function of the sample volume. When this ratio is plotted vs. sample volume an ACB curve is generated. Therefore, the ACB curve is simply a representation of the instantaneous percent breakthrough vs. sample volume for a cartridge. Each experiment was carried out until each C_e and C_i were equal (the 100% breakthrough point). At the 100% breakthrough point the total sorbent bed had reached mass transfer equilibrium with each analyte in water, in the bed. By determining the mass of each analyte retained by the bed at this point, the sorbent/water equilibrium partition coefficients of each analyte, K_w, could be calculated. $K_w = C_s/C_i$, where C_s = the analyte concentration in the sorbent bed (ng/g) at the 100% breakthrough point. C_s was calculated from the ACB curve. Also, it should be noted that for analyte concentrations in water, a ppb is equivalently expressed as either a ng/g or a μg/L.

ACB curves were measured for analyte concentrations which ranged from 20 to 150 ppb. This enabled the nature of the adsorption isotherm of the system to be established over a practical sampling concentration range. The adsorption isotherm is produced by plotting C_s vs. C_i. A curve with a constant slope (equal to K_w) is produced if the adsorption system operates in a linear manner for the analyte concentration range tested. This indicates that the capacity of the sorbent bed remains constant over the tested concentration range of

the analyte. In the design of this work it was felt to be important to establish what the nature of the adsorption isotherm was, and to what extent, and over what concentration range the system behaves linearly.

4.2.2 Determination of Adsorbent Cartridge Breakthrough Curves

All water used in the ACB experiments was of reagent grade quality, termed reagent water (RW). Distilled, deionized water was first passed through a Millipore Super-Q water purification system (Bedford, MA) and then further purified according to the procedure outlined in EPA Test Method 624, Section 6 (10). All RW was stored in 1 L amber bottles and sealed with a PTFE lined caps. The water was stored without headspace at $4^{o}C$ until used. The RW was always used as soon after preparation as possible. Maintenance and production of high quality RW was essential for the successful completion of these experiments. There was no detectable background level for most analytes tested.

Each experiment required that 2 to 20 L of water spiked at the desired C_i be pumped through the adsorption system for a period of 4 to 36 hours. Since each experiment required a large volume of spiked water that had to be maintained at the desired C_i for long periods, it was decided not to prepare a large batch of spiked water in advance. First, it would be difficult to thoroughly mix a large volume of solution, while minimizing analyte-volatilization losses. Indeed, the stability of a spiked solution over time would be in question because

it would be subject to analyte-volatilization losses both prior to and during its use. Finally, the impracticality of handling such large volumes of solution and the improbability of doing so without inducing volatilization losses (i.e., as a solution was transferred from storage to the pumping system) would also be a major concern. For these reasons, a mixing vessel system was used to produce a solution at the desired C_i.

The mixing vessel system used is depicted in Figure 4.1. RW was pumped into the bottom of one side of a small vessel. A concentrated analyte solution (CAS) in RW was pumped into the bottom of the opposite side of the vessel. The contents of the vessel were stirred using a mini-stir-bar and a magnetic stirrer. A solution of the desired concentration exited the top of the vessel. The mixing vessel was constructed of borosilicate glass and was composed of a top and bottom piece. The two pieces were connected with an O-ring joint and a PTFE coated Viton O-ring. The joint was held together using a clamp. The I.D. and length of the vessel were 1.5 and 5.8 cm, respectively, producing a volume of 10 mL. The RW and CAS inlet arms were set tangentially into the base of the vessel on opposite sides. The mini-stir-bar was ~1 cm in length. It was constructed by sealing a small piece of steel rod within a length of capillary glass tubing. RW was pumped into the mixing vessel at 8.0 mL/min, using a Spectra-Physics (San Diego, CA) 8100 high performance liquid chromatograph (HPLC) pump. The HPLC pump outlet was connected to the mixing vessel using 25 cm of 0.16 cm O.D. PTFE tubing. A Harvard Apparatus (Millis,

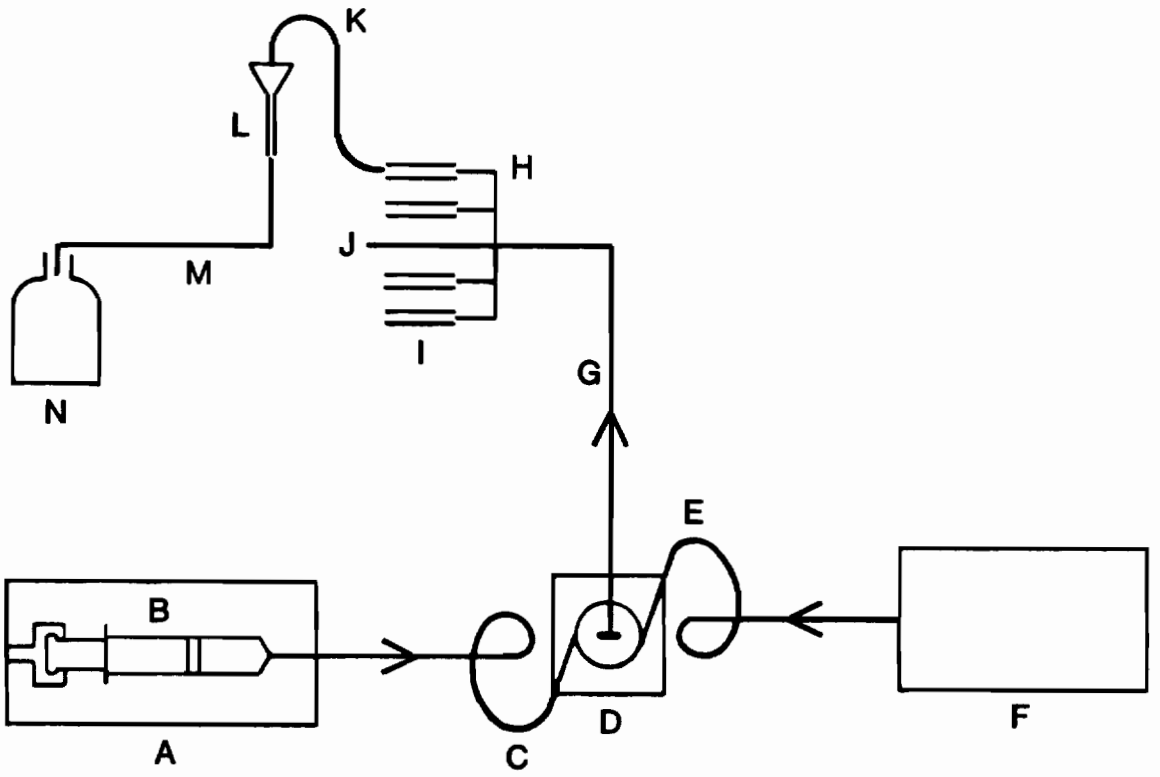

Figure 4.1. Schematic diagram of the mixing vessel system. This is an overhead view of the system and is not drawn to scale. **A** syringe pump. **B** Hamilton 50 mL gas tight syringe w/CAS. **C** 0.16 cm O.D. SS tubing. **D** Magnetic stirrer and 10 mL glass mixing vessel with mini-stir-bar. **E** 0.16 cm O.D. PTFE tubing. **F** HPLC pump used to pump RW. **G** orientation and distance from mixing vessel output to cartridge inlet is exaggerated for visual clarity. In reality, the inlet arm of the cartridge manifold (H) was "in line" with and not perpendicular to the outlet arm of the mixing vessel. They were connected with a Swagelok 0.64 cm SS union with PTFE ferrules. **H** cartridge manifold, constructed of 0.64 cm O.D. and 0.04 cm I.D. borosilicate glass tubing. The volume of the manifold was 1.6 mL. **I** small bed Tenax cartridge, ~0.68 mL in volume, connected to the manifold with a Swagelok 0.64 cm SS union with PTFE ferrules. **J** center arm of the cartridge manifold (mixing vessel port) used to collect samples from the mixing vessel. **K** 18-cm length of 0.16 cm O.D. SS tubing, connected to each cartridge outlet and used for the collection of effluent samples. **L** glass funnel (one per cartridge) used to direct cartridge effluent to collection container. **M** flexible tubing used to transfer cartridge effluent to collection container. **N** 4 L container used to collect cartridge effluent.

MA) infusion/withdrawal pump (Model 906) was used to pump the CAS into the mixing vessel. A flow rate of 0.0535 mL/min was used. A 50 mL Hamilton gas-tight syringe was used in the syringe pump.

The CAS was prepared in RW with neat standard compounds obtained from Chem Service Inc. The solution was prepared and stored in a 40 mL glass vial sealed with an open topped screw cap and PTFE faced septum. The CAS was transferred to the mixing vessel through a 17 gauge SS syringe needle connected to 35 cm of 0.16 cm O.D. SS tubing with a Swagelok 0.16 cm SS union. The luer hub of the needle was connected to the luer-lock fitting on the syringe barrel. The free end of the tubing was inserted through a Swagelok 0.16 to 0.64 cm SS reducing union. The 0.64 cm end of the union was attached with a PTFE ferrule to the CAS mixing vessel inlet arm. (All Swagelok metal to glass tubing connections utilized PTFE ferrules. Metal to metal tubing connections utilized brass ferrules.) The SS tubing extended ~1 mm beyond the arm and into the base of the vessel. Using a Swagelok 0.64 cm SS union, the mixing vessel outlet arm was connected to the inlet arm of a manifold constructed of 0.64 cm O.D. and 0.04 cm I.D. borosilicate glass tubing. The manifold had five outlet arms, each ~3.8 cm in length and separated by ~2.5 cm of tubing. The manifold was used to transfer the mixing vessel effluent to four ATD cartridges connected in parallel. The volume of the glass manifold was 1.6 mL. The ATD cartridge inlets were connected to the outlet arms of the manifold with Swagelok 0.64 cm SS unions. The outlet of each cartridge was connected to a Swagelok 0.16 to 0.64 cm brass

reducing union. Each of these unions were also connected to 18 cm of 0.16 cm O.D. SS tubing which rose above each cartridge in a question mark shape.

Cartridge effluent samples were collected in amber borosilicate vials whose volume was measured to be 5.00 $\pm$ 0.053 mL. Each vial was sealed with open-topped screw cap and a PTFE-faced silicon septum. Cartridge effluent not collected for analysis was transferred to 4 L containers by means of a tubing and funnel system. This enabled the measurement of the total volume passing through each cartridge as well as a calculation of the average volume flow rate for each cartridge. The center outlet arm on the cartridge manifold was connected directly to an 18-cm piece of SS tubing with a Swagelok 0.16 to 0.64 cm brass reducing union. This arm was used as a port for obtaining samples directly from the mixing vessel and allowed C_i to be monitored during the experiment. The mixing vessel port was kept closed during the experiment except when mixing vessel samples were collected.

The HPLC used had the capacity to store 3 L of water in three 1 L glass containers. Prior to starting each experiment, the 3 L of RW were transferred to the HPLC and vigorously sparged with UP-He for 1 hour. Aside from its excellent pumping precision and accuracy, use of the HPLC pump also enabled the continuous sparging of RW with UP-He (the HPLC solvent storage containers were provided with solvent degassing apparatus). This enabled all RW used to be air-free by saturating it with UP-He. The continuous sparging also allowed the high purity of the RW to be maintained. Most experiments required the

use of much more than 3 L of RW. Therefore, an additional 3 L RW reservoir was constructed. A 4 L amber bottle was stored on the shelf above the 3 L RW reservoir of the HPLC. The cap of the bottle was fitted with an UP-He sparging line, a vent line, and a 1.8 m, 0.64 cm O.D. PTFE tube to be used for siphoning. As the experiment consumed RW from the RW reservoir of the HPLC, an additional 3 L of RW was being saturated with UP-He in the backup reservoir. When the supply of RW in the HPLC reservoir was near depletion, RW was siphoned into it from the backup RW reservoir.

Prior to the start of each experiment, all the air contained in each dry sorbent bed was removed by dissolving it in RW. Based on an estimate of ~0.80 for the total bed porosity (interbead + intrabead porosity, see Section 5.3.2), it was calculated that 20 mL of RW degassed with UP-He was required to dissolve all of the air contained in each dry sorbent bed. To ensure that all of the air was removed, a total of 80 mL of RW degassed with UP-He was passed through each sorbent bed prior to the start of each experiment. It was necessary to remove the trapped air from each sorbent bed in order that a more accurate estimate of K_w could be obtained. Table 4.1 lists the masses of Tenax contained in each of the 32 cartridges used in the ACB experiments. The bed volume of each cartridge was 0.68 cm^3.

Before the effluent from the mixing vessel was allowed to pass through the cartridges, the syringe pump was started and the mixing vessel was run with the mixing vessel port open for at least 30 min. This allowed the mixing vessel output to reach its maximum

Table 4.1. Mass of Sorbent[a] (Tenax) in each Cartridge used in Adsorbent Cartridge Breakthrough Experiments 2 through 8.

Experiment	Cartridge No. and Letter[b]	Mass of Sorbent (g)
1	546 A	0.136
1	551 B	0.136
1	552 C	0.130
1	560 D	0.134
2	471 A	0.136
2	488 B	0.128
2	548 C	0.129
2	549 D	0.131
3	465 A	0.124
3	466 B	0.124
3	553 C	0.134
3	556 D	0.123
4	411 A	0.131
4	407 B	0.135
4	423 C	0.131
4	436 D	0.134
5	437 A	0.127
5	402 B	0.124
5	447 C	0.124

Table 4.1 (cont'd). Mass of Sorbent[a] (Tenax) in each Cartridge used in Adsorbent Cartridge Breakthrough Experiments 2 through 8.

Experiment	Cartridge No. and Letter[b]	Mass of Sorbent (g)
5	493 A	0.134
6	550 B	0.124
6	569 C	0.121
6	538 D	0.124
6	670 A	0.128
7	547 B	0.124
7	450 C	0.127
7	464 D	0.130
7	476 A	0.137
8	419 B	0.123
8	647 C	0.117
8	504 D	0.140
8	479 A	0.134

[a]Average mass = 0.129 ± 5.57 E-3 g, CV = 4.3%.
[b]Cartridge letter designation (see p.135).

concentration, C_i. C_i was calculated according to the equation derived in Section 4.3.1. With the syringe and HPLC pump on, all cartridges connected and the mixing vessel port open, all flow was passed through the mixing vessel port, traveling the path of least resistance. The experiment was started (t = 0) after the mixing vessel concentration had reached C_i and the mixing vessel port was closed.

Four cartridges were used in each experiment with one sample collected from a single cartridge at the end of each sampling interval. It was originally planned to collect four samples at once i.e., one sample from each cartridge. However, as explained in Section 4.3.2, this proved to be impractical. The sampling interval ranged from 4 to 45 min, with most samples collected every 10 to 20 min. The first four cartridge effluent samples were designated A1, B2, C3 and D4. The letters A through D corresponded to the four individual cartridges connected in parallel. If the sampling interval was every 5 min, the first sample collected was collected from cartridge A at the end of 5 min (i.e., 5 min from t = 0); and so was designated sample A1; sample B2 was collected from cartridge B at the end of 10 min; sample C3 was collected from cartridge C at the end of 15 min; and sample D4 was collected from cartridge D at the end of 20 min. Sample A5 was collected from cartridge A at the end of 25 min. This pattern continued until the end of the experiment.

In several experiments, ACB curves for several analytes were determined simultaneously. In such an instance, the sampling interval

varied throughout the experiment. Since it was desired to collect 30 to 40 sample points per ACB curve (i.e., seven to ten samples per cartridge for each analyte), an experiment including both weakly and strongly retained analytes was characterized by short sampling intervals at the beginning, and long sampling intervals during the middle and end of the experiment.

The sample volume (the total volume which had passed through the cartridge at the time of sample collection) was calculated to be the product of the elapsed sampling time and the cartridge flow rate + 2.5 mL. The total sample collected was 5.0 mL; therefore, the volume collected by the midpoint of the sample collection interval was added to each sample volume.

The HPLC pumped RW at 8.0 mL/min to the mixing vessel, ideally this would mean a flow rate of 2.0 mL/min (of solution) to each ATD cartridge. In reality, the individual cartridge flow rates ranged from 1.8 to 2.5 mL/min for most experiments, with this range never exceeding 1.5 to 3.0 mL/min. No attempts were made to reduce this range because the variation in flow rates among the cartridges (due to differences in the packing characteristics among the cartridges) were not expected to cause significant differences in individual bed performances. This assumption proved to be valid (see Section 4.3.7).

A sample was collected by inserting the 0.16 cm O.D. SS cartridge effluent tubing into the bottom of a sample vial. The end of the tubing was kept below the surface of the water. Each vial was filled until a convex meniscus, above the mouth of the vial, was

achieved. The vial was then sealed and refrigerated at 4°C until analysis. Since each cartridge flow rate was approximately 2.0 mL/min, a portion of the sample was exposed for approximately 2.5 min while the sample vial filled. This could have led to a systematic error due to analyte volatilization losses during sample collection. The magnitude of this error was examined using results obtained for samples collected at the 100% breakthrough point (see Section 4.3.4); the error was not significant.

Cartridge and mixing vessel effluent samples were analyzed (see Section 4.2.3) periodically during each experiment in order to monitor C_i and C_e. Five samples were collected from the mixing vessel port at several specified times during an experiment. One sample was analyzed immediately (to determine C_i) and the other four samples were stored under refrigeration. One of the remaining four mixing vessel samples from each of the collection periods was analyzed later (during the sample analysis period) to determine the average C_i of each analyte in each experiment. Single cartridge effluent samples were collected for immediate analysis following the collection of the mixing vessel samples. In most cases, when C_e was determined to equal C_i, the experiment was over, and the syringe and HPLC pumps were stopped.

4.2.3 Cartridge Influent and Effluent Analysis

All samples were analyzed within 48 to 72 hours of their collection. The method used was purging with whole column cryotrapping (P/WCC) a new state-of-the-art analytical methodology

developed by Pankow and Rosen (63). P/WCC possesses several practical advantages over P&T/WCC (57) that made it well suited for use within the context of these determinations. In particular, P/WCC allows rapid sample analysis and is simple to use. The apparatus required is simple, durable and easily maintained. Due to the very low background levels of analytes detected within the apparatus, the method proved to be very sensitive. On the average, P/WCC allowed the analysis of 3 to 4 samples per hour. By comparison, P&T/WCC may be used to analyze 1 to 2 samples per hour. The speed of P/WCC was very helpful since each experiment required the analysis of over 100 samples.

4.3 Results and Discussion

4.3.1 Predicting Mixing Vessel Output (C_i)

The following model of the mixing vessel system was used to predict the mixing vessel output, C_i. A first order differential equation was used to define the mass balance of the mixing vessel system. The total flow rate out of the mixing vessel was assumed to be equal to the HPLC pumping rate, 8.0 mL/min. The syringe pumping rate, 0.0535 mL/min, made an insignificant contribution to the total flow rate into or out of the vessel. The mixing vessel system is described by the following equations:

$$V_m(dC(t)/dt) = C_wR_m + C_{as}R_s - C(t)(R_m + R_s) \quad 4.1$$

therefore, for $C_w = 0$,

$$dC(t)/dt = (C_{as}R_s/V_m) - [C(t)(R_m + R_s)/V_m]$$

and for $R_m >> R_s$,

$$C(t) = (C_{as}R_s/R_m) + K[\exp((-R_m/V_m)t)] \qquad 4.2$$

where:

C_{as} = analyte solution concentration in the 50 mL syringe, (μg/L)

$C(t)$ = analyte concentration at time t, (μg/L)

C_w = analyte concentration in mixing vessel's influent RW, (μg/L)

K = constant of differentiation

R_m = flow rate into and out of mixing vessel, (mL/min)

R_s = syringe pump flow rate, (mL/min)

t = elapsed time, (s or min)

V_m = volume of mixing vessel, (mL).

At t = 0, C(0) = 0, therefore,

$$K = -C_{as}R_s/R_m$$

and so,

$$C(t) = (C_{as}R_s/R_m)[1 - \exp((-R_m/V_m)t)] \qquad 4.3$$

For R = 8.0 mL/min, R_s = 0.0535 mL/min and V = 10 mL,

$$C(t) = 6.688 \times 10^{-3}C_{as}[1 - \exp(-0.80t)] \qquad 4.4$$

and

$$C_{max} = 6.688 \times 10^{-3}C_{as} \qquad 4.5$$

Based on eqn. 4.5, C(t) reaches its maximum concentration, C_{max}, after approximately 8 min of CAS input into the mixing vessel. At t = 8 min, $\exp(-0.80t) = 0.002$ and $C_{max} = 6.688 \times 10^{-3}C_{as}$. In other

words, after 8 min., the concentration output of the mixing vessel is constant and equals C_i. Therefore, after 8 min $C_{max} = C_i$.

4.3.2 Preliminary Adsorbent Cartridge Breakthrough Experiments

Two preliminary experiments were performed to test the performance of the mixing vessel and the appropriateness of the experimental design. The first experiment was designed to test the precision of the mixing vessel system. The mixing vessel was set up as described previously (Section 4.2.2) and was run for 4 hours. For benzene and a desired C_i of 30.0 ppm, R_s = 0.0255 to 0.102 mL/min and R_m = 2.00 mL/min, 25 mixing vessel samples were collected, one every 10 min for 4 hours. The benzene concentrations of each sample were measured the next day with a UV-VIS spectrophotometer at a wavelength of 254 nm. It was desired to check the precision of the mixing vessel output at syringe flow rates of 0.0255, 0.0510 and 0.102 mL/min. This was the range of syringe flow rates most likely to be used during the ACB experiments. R_s was first set at 0.0510 mL/min and kept at this setting for 2 hours. It was predicted that a C_i of 30 ppm would result. The R_s was then reduced to 0.0255 mL/min for 1 hour, and then increased to 0.102 mL/min for the remaining hour. The following observations were made:

(1) The mixing vessel reached its maximum concentration within the approximate time predicted by eqn. 4.4.

(2) The mixing vessel concentrations ranged from 60 to 92% of their values predicted by eqn. 4.5.

(3) The mixing vessel delivered a constant C_i for 2 hours.

(4) As R_s was increased or decreased, C_i increased or decreased in the proportion predicted by eqn. 4.3.

(5) The mixing vessel produced a constant C_i at the three syringe pump flow rates tested.

The most important purpose of the mixing vessel procedure was to produce a constant C_i over the entire experiment. The ability of the mixing vessel procedure to accomplish this was documented by the first experiment. In addition, the ability to obtain C_i values within 60 to 92% of those predicted by eqn. 4.5 was also considered reasonable. Therefore, it appeared reasonable to proceed with the first ACB experiment, experiment 1, during which ACB curves would be generated. While the data generated from experiment 1 was not used quantitatively, the experiment was useful as a trial run. Experiment 1 revealed some of the problems in the planned execution and design of the ACB experiments. 1,2-Dichloroethane was tested in experiment 1 because, based on its high solubility in water, it was assumed that this compound would achieve 100% breakthrough relatively quickly. R and R_s were set at 8.0 and 0.103 mL/min, respectively. In all following experiments R_s was set at 0.0535 mL/min. Standards were prepared with C_{as} = 1600 ppb in order to produce C_i = 20 ppb.

Using a specially designed sample vial holder, four samples (one from each cartridge) were collected simultaneously every 4 min. This meant that 92 samples (23 from each of the four cartridges) were collected in 90 min. Unfortunately, the various flow rates among the

cartridges, ranging from 1.5 to 3.0 mL/min, made it difficult to collect four samples at once in a reproducible manner. This procedure caused excessive spilling which led to an inaccurate estimation of the total sample volume passing through each cartridge and therefore inaccurate ACB curves. The samples were also excessively exposed to air. Another problem encountered with this experiment was that it only proceeded to the 50% breakthrough point. This meant that the 100% breakthrough point could not be determined. Therefore, the ACB data from this experiment was discounted, and the experiment was viewed as a trial run for the remaining experiments. Further, due to the artifacts caused by attempting to collect four samples at once, it was decided to collect one sample from one cartridge at the end of each sampling interval (as was described in Section 4.2.2). It was felt that a total of 8 to 10 samples per cartridge (30 to 40 samples from all four cartridges) would be sufficient to provide a statistically well-defined ACB curve.

4.3.3 Mixing Vessel Performance

In ACB experiments 1 through 8 the mixing vessel performance proved to be excellent. On the average, C_i was within 20% of its value predicted using eqn. 4.5. The results of the analyses of the mixing vessel samples (analyzed during the cartridge effluent analysis period) are presented in Table 4.2. This table presents the average C_i, and its corresponding *s* and CV values for each of the 13 compounds analyzed in a total of eight experiments. The average CV (the

Table 4.2. Mixing Vessel Performance.

Compound	Exp't. No.	$\bar{C}_i$[a] (μg/L)	CV (%)	n[b]	Sampling/Total Time[c] (hr)
1,2-Dichloroethane	1	18 ± 1.9	11	4	0.5 / 1.5
1,1-Dichloroethane	2	26 ± 2.6	10	7	3.5 / 8.8
Trichloroethene	3	28 ± 2.7	9.8	8	3.0 / 24
1,1-Dichloroethane	4	26 ± 0.92	3.5	8	3.5 / 28
Trichloromethane		26 ± 0.87	3.3		
1,2-Dichloroethane		27 ± 1.7	6.1		
Trichloroethene		22 ± 0.75	3.3		
Bromodichloromethane		22 ± 1.0	4.5		
Tetrachloroethene		21 ± 0.96	4.6		
Chlorobenzene		21 ± 0.72	3.4		
1,1-Dichloroethane	5	140 ± 3.4	2.4	4	2.0 / 7.5
Trichloromethane		130 ± 3.9	3.1		
1,2-Dichloroethane		120 ± 3.7	3.0		
cis-1,2-Dichlorethene	6	25 ± 0.80	3.2	8	3.5 / 28
Benzene		1.3 ± 0.029	2.3		
1,2-Dichloropropane		24 ± 0.64	2.7		
Bromodichloromethane		25 ± 0.78	3.1		
1,1,2-Trichloroethane		20 ± 0.53	2.7		
Tribromomethane		21 ± 0.58	2.8		

Table 4.2 (cont'd.). Mixing Vessel Performance.

Compound	Exp't. No.	$\bar{C}_i$[a] (μg/L)	CV (%)	n[b]	Sampling/Total Time[c] (hr)
1,1,2,2-Tetrachloroethane	6	16 $\pm$ 0.45	2.8	8	3.5 / 28
cis-1,2-Dichloroethene	7	59 $\pm$ 2.3	3.9	4	3.0 / 13
Trichloromethane		61 $\pm$ 2.4	3.9		
Benzene		55 $\pm$ 2.1	3.9		
Trichloromethane	8	130 $\pm$ 4.5	3.3	6	1.5 / 7.5

[a]Arithmetic mean concentration of the mixing vessel output (C_i), $\pm$ 1 *s* based on n sample analyses.
[b]Total number of times samples were collected from the mixing vessel port. One of the five samples collected at each sampling interval was used for the determination of $\bar{C}_i$.
[c]Mixing vessel sampling interval (hr) / total time of experiment (hr).

arithmetic mean of the CV values obtained for each compound in the eight experiments) was ~4%. The excellent reproducibility of the mixing vessel system is further demonstrated by Figure 4.2. In this figure, C_i is plotted vs. time, for trichloromethane at three different concentrations (26, 61 and 130 ppb) in three separate experiments. In all three experiments the trichloromethane concentration produced by the mixing vessel system remained very constant (for up to 26 hours in one case).

4.3.4 Analyte Volatilization Losses During Sample Collection

As discussed in Section 4.2.2, a portion of each cartridge effluent sample was exposed for ~2.5 min, i.e., the time required to collect 5.0 mL of sample at a flow rate of 2.0 mL/min. There was concern that this sample exposure might cause significant analyte-volatilization losses. The magnitude of this error was estimated in the following manner. C_i was determined by collecting samples from the mixing vessel effluent port. The flow rate from this port was always 8.0 mL/min. Therefore, a 5.0 mL mixing vessel effluent sample was collected in 0.63 min, or four times faster than the cartridge effluent samples. With four times less exposure, analyte-volatilization losses from the mixing vessel samples would be expected to be significantly smaller than whatever volatilization losses were incurred during the collection of the cartridge effluent samples. If the latter error was significant, most compounds tested would never have reached 100% breakthrough. In other words, this systematic error

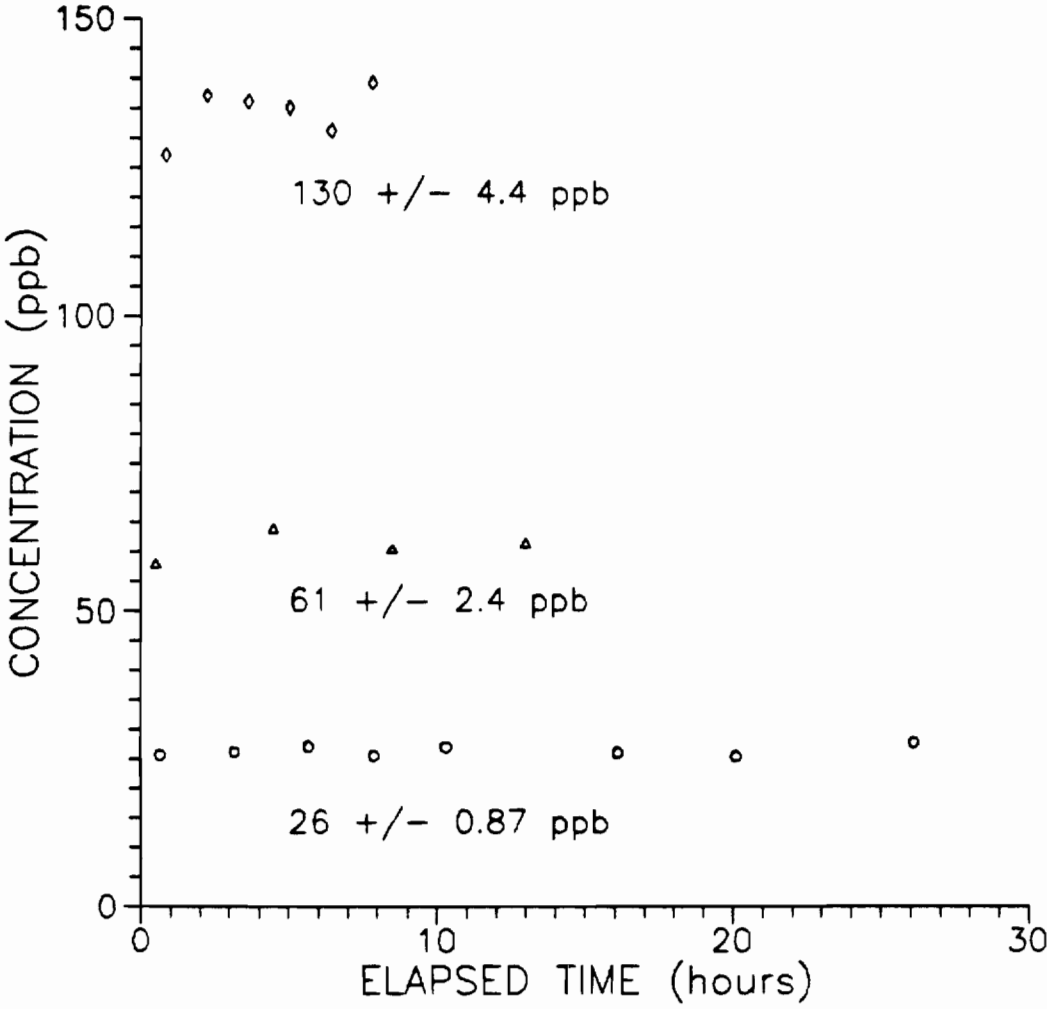

Figure 4.2. Plot of mixing vessel output, C_i (ppb), vs. elapsed time (hr) for trichloromethane, from ACB experiments 4, 7 and 8.

would alter the effluent concentration of a cartridge such that even at the 100% breakthrough point, C_e from a cartridge would be measured to be lower than the C_i produced by the mixing vessel. This systematic error would also be expected to be a function of the Henry's law constant, H of an analyte. The magnitude of the error would be expected to be greatest for the most volatile compounds, i.e., those with the highest values of H.

Table 4.3 presents the average equilibrium percent breakthrough and H values for several of the compounds tested. In the majority of cases the equilibrium percent breakthrough is not significantly different from 100%. Figure 4.3, a plot of the average percent breakthrough at equilibrium vs. H, shows there to be no correlation between these variables for this sampling system. A linear correlation coefficient, $r^2 = 0.0$ was calculated for the two variables (64). Therefore, there did not appear to be any losses correlated with the Henry's law constant. Further, a student's t-test (65) performed at $\alpha = 0.01$, determined that the average of all the equilibrium percent breakthrough values ($100 \pm 3.4\%$) was not significantly different from 100%. Therefore, on the average the error was not statistically significant.

4.3.5 Performance of Purging with Whole Column Cryotrapping for Sample Analysis

P/WCC operated well, with only minor problems, for the analysis of nearly 1000 samples. The P/WCC apparatus used consisted of only a

Table 4.3. Average Equilibrium Percent Breakthrough (BT) vs. Henry's Law Constant (H).

Compound	Exp't. No.	BT[a] (%)	n[b]	H[c] (atm·m^3/mole)
1,1,2,2-Tetrachloroethane	6	110 ± 18	3	3.8 E-4
Tribromomethane	6	98 ± 8.0	5	5.6 E-4
1,1,2-Trichloroethane	6	100 ± 3.9	13	7.4 E-4
1,2-Dichloroethane	4	98 ± 1.8	5	9.1 E-4
	5	100 ± 6.2	4	
1,2-Dichloropropane	6	100 ± 4.7	10	2.3 E-3
Bromodichloromethane	4	100 ± 2.3	14	2.4 E-3
	6	100 ± 5.2	9	
Trichloromethane	4	99 ± 8.5	7	2.9 E-3
	5	99 ± 3.2	11	
	7	100 ± 2.5	9	
	8	94 ± 2.3	6	
1,1-Dichloroethane	2	98 ± 1.3	11	4.3 E-3
	4	99 ± 1.4	11	
	5	100 ± 2.8	11	
Benzene	6	100 ± 5.4	8	5.5 E-3
	7	97 ± 2.2	4	
cis-1,2-Dichloroethene	6	100 ± 1.4	4	7.5 E-3
	7	100 ± 2.6	12	

Table 4.3 (cont'd.). Average Equilibrium Percent Breakthrough (BT) vs. Henry's Law Constant (H).

Compound	Exp't. No.	BT[a] (%)	n[b]	H[c] (atm·m^3/mole)
Trichloroethene	3	92 ± 0.67	3	9.1 E-3
	4	100 ± 6.6	6	

[a]BT = the arithmetic mean of (C_e/C_i) (%) ± 1 *s* based on n samples, for which C_e had reached a constant value (three consecutive measurements of $C_e \geq C_i$, or of C_e ± 5%).
[b]Number of samples at constant C_e.
[c]Ref. 11.

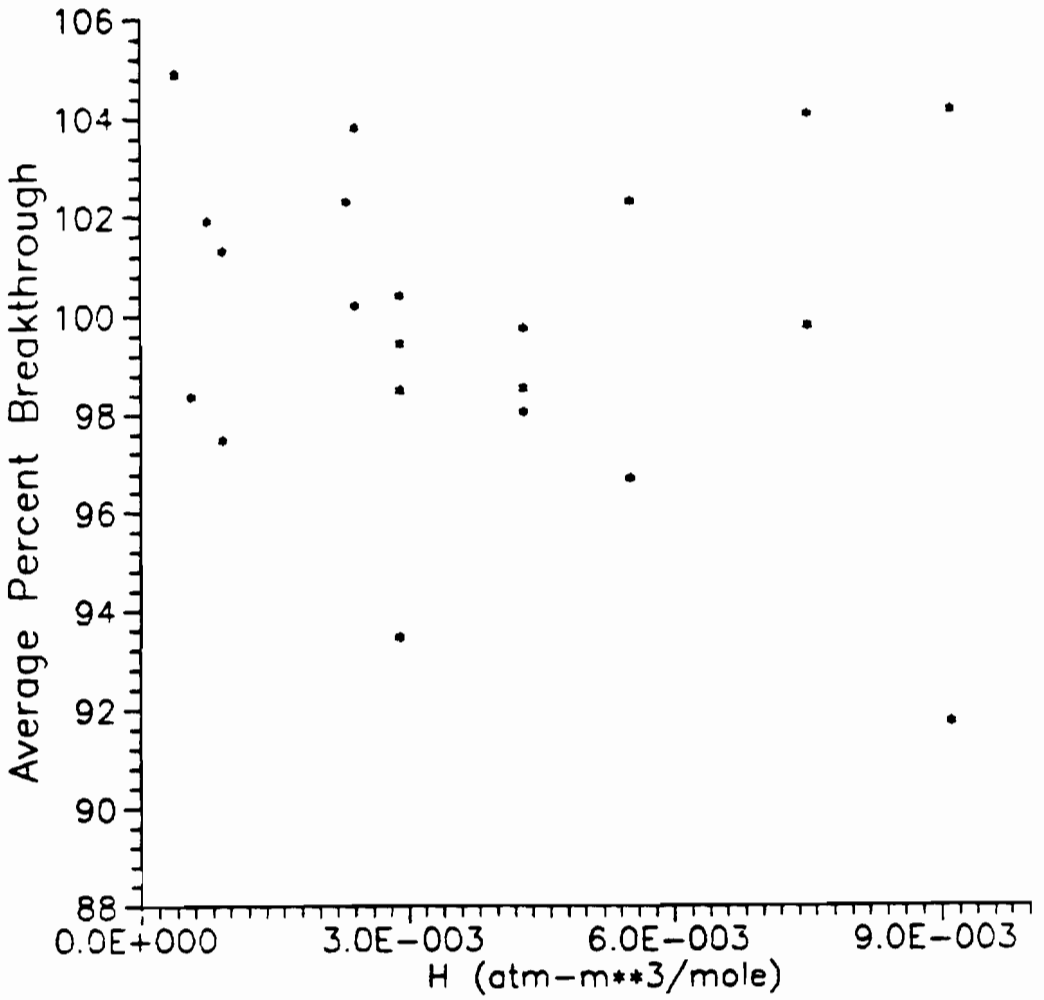

Figure 4.3. Plot of average percent breakthrough at equilibrium vs. Henry's law constant (H) (atm-m^3/mole); data from Table 4.3. A linear correlation coefficient, r^2 = 0.0 was calculated for the two variables.

purging vessel, a carrier gas flow control unit and associated plumbing. This contributed significantly to the lowering of background contamination in the analysis system, and therefore increased the method sensitivity relative to P&T/WCC. The concentration limit of detection, the lower limit of concentration which can be determined to be significantly different from zero, is often a function of the standard deviation of the mean blank level of an analyte (32,66-68). The blank level of most compounds tested was either insignificant or not detectable.

4.3.6 Equilibrium Partition Coefficient Determination

As discussed earlier K_w is defined as the ratio of the analyte concentration in the bed, C_s, to C_i at equilibrium. C_i was known by measuring the concentration of the mixing vessel effluent during each experiment. Knowledge of the amount sorbed at equilibrium on a cartridge as well as the mass of the sorbent bed will allow C_s to be determined. Each cartridge that had reached the 100% breakthrough point could have been thermally desorbed and the mass of each analyte retained by the cartridge could have been measured. However, the successful thermal desorption of very large quantities of material presents some problems. For the range of analyte K_w values expected (1000 to 20,000) the thermal desorption of the mass of each analyte retained by the sorbent (~5000 to 300,000 ng) would have overloaded the analysis system. Generally, the analysis system could be expected to respond linearly to ~500 ng of an analyte. Therefore, only a small

fraction of the mass of analyte retained by the cartridge could be allowed into the analysis system. While diversion of a fraction of the cartridge effluent stream during the thermal desorption step is possible, the diversion of a very large fraction would be difficult (69). Fortunately, a more manageable method for the determination of the mass sorbed by each cartridge exists.

Provided each ACB curve meets certain requirements, numerical methods may be utilized to determine the mass sorbed. As discussed previously, the ACB curve is simply a representation of the instantaneous percent breakthrough vs. sample volume for a cartridge. Therefore the ACB curve can be used to determine the mass of analyte retained by the sorbent up to any point in time during the sorption process (70). Figure 4.4 shows three hypothetical ACB curves for a constant analyte input, C_i, and a fixed flow rate into a sorbent cartridge. Curve A depicts a situation where virtually 100% of the analyte is retained by the sorbent from a 1000 mL sample volume. Curve B depicts a situation where virtually 0% of the analyte is retained from the sample volume. Curve C depicts a situation where 50% breakthrough occurs with a sample volume of 500 mL and virtually 100% breakthrough occurs with a sample volume of 1000 mL. Looking at curve A it is easy to visualize that the forward-slashed area, i.e., the area above the curve (A_{ac}), represents the mass of analyte retained by the sorbent. Therefore, the mass retained by the sorbent (M_s) equals the mass (M) in the 1000 mL sample (i.e., C_i x 1000 mL). For curve B, the mass that is not retained by the sorbent is

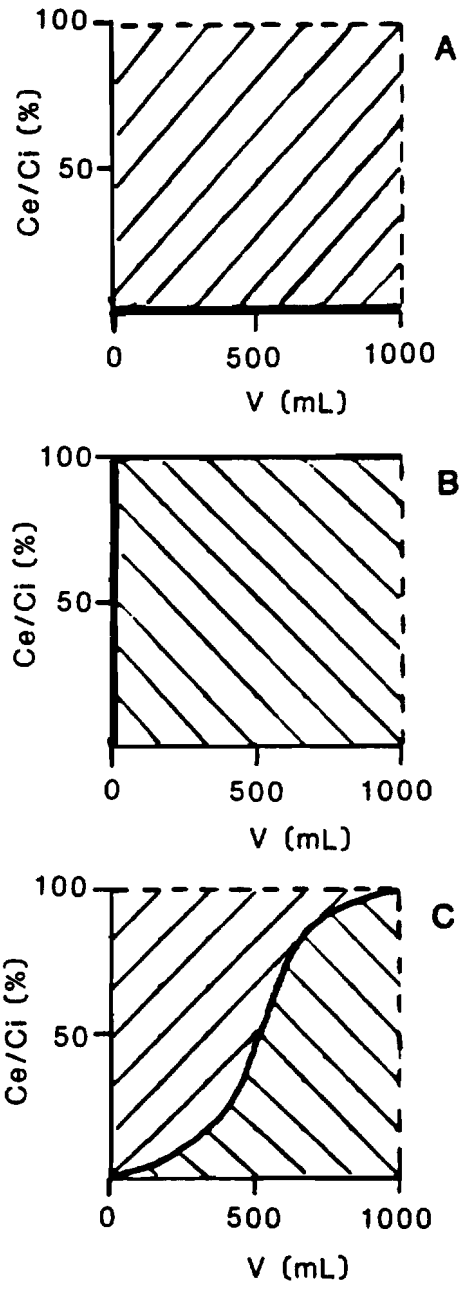

Figure 4.4. Three hypothetical ACB curves for a constant analyte input C_i, and a fixed flow rate into a sorbent cartridge. The forward-slashed area (the area above the curve) represents the mass that is retained by the bed. The backslashed area (the area below the curve) represents the mass that is not retained by the bed.

represented by the backslashed area, i.e., the area below the curve (A_{bc}). Therefore, in this case the mass not retained by the bed equals C_i x 1000 mL. Similar comments can be made for curve C, where the A_{bc} represents the mass which is not retained and the A_{ac} represents the mass that is retained by the sorbent bed, from the 1000 mL sample volume. For any given ACB curve, numerical integration may be used to determine A_{bc}. Therefore, the mass sorbed M_s, may be determined by the formula:

$$M_s = M\ (A_{ac} / A_t) \qquad 4.6$$

where:

V = sample volume (mL)

$M = C_i$ x V

A_t (Total area surrounding the curve) = V x 100%

$A_{ac} = A_t - A_{bc}$.

As explained above, K_w can be determined by knowing the mass of analyte retained by the sorbent bed, the mass of the individual sorbent bed, and C_i.

The ACB experiments were designed in order to obtain four separate ACB curves and K_w values per compound and experiment. However, due to the excessive length of each experiment and the variation in the individual cartridge flow rates, there were several cases where complete ACB curves were not obtained for each analyte on each cartridge. However, as long as it is reasonable to assume that

each ACB curve is symmetrical, and each curve extends to at least the 50% breakthrough point, a K_w value can be obtained for each analyte from each ACB curve.

If we examine an ACB curve which is symmetrical about the 50% breakthrough point (Figure 4.4, curve C) the following statements can be made. The sample volume at which 100% breakthrough occurs is twice the sample volume at which 50% breakthrough occurs. The sample volume at which 50% breakthrough occurs is defined as the retention volume V_R, of an analyte on the sorbent bed. Also, for an ACB curve carried to the 100% breakthrough point, the areas above and below the curve are equal.

Thus, for a curve which is symmetrical about the 50% breakthrough point, $A_{ac}/A_t = 0.50$ and $M = C_i \times 2V_R$. Therefore, eqn. 4.6 reduces to:

$$M_s = C_i \times V_R \qquad 4.7$$

Figures 4.5-4.8 display the combined ACB curves of four cartridges for 1,1-dichloroethane, experiments 2 and 4; trichloromethane, experiments 4 and 7; benzene, experiments 6 and 7; and trichloroethene, experiments 3 and 4. Based on their retention volumes, these compounds are representative, in a relative sense, of the weakly, moderately, and strongly retained compounds of the 13 PPPs tested. Figures 4.9-4.16 display the individual ACB curves obtained from each cartridge for the previously listed compounds and experiments. The curves are generally symmetrical and very well defined. Also, there is minimal scatter <u>within</u> each individual curve.

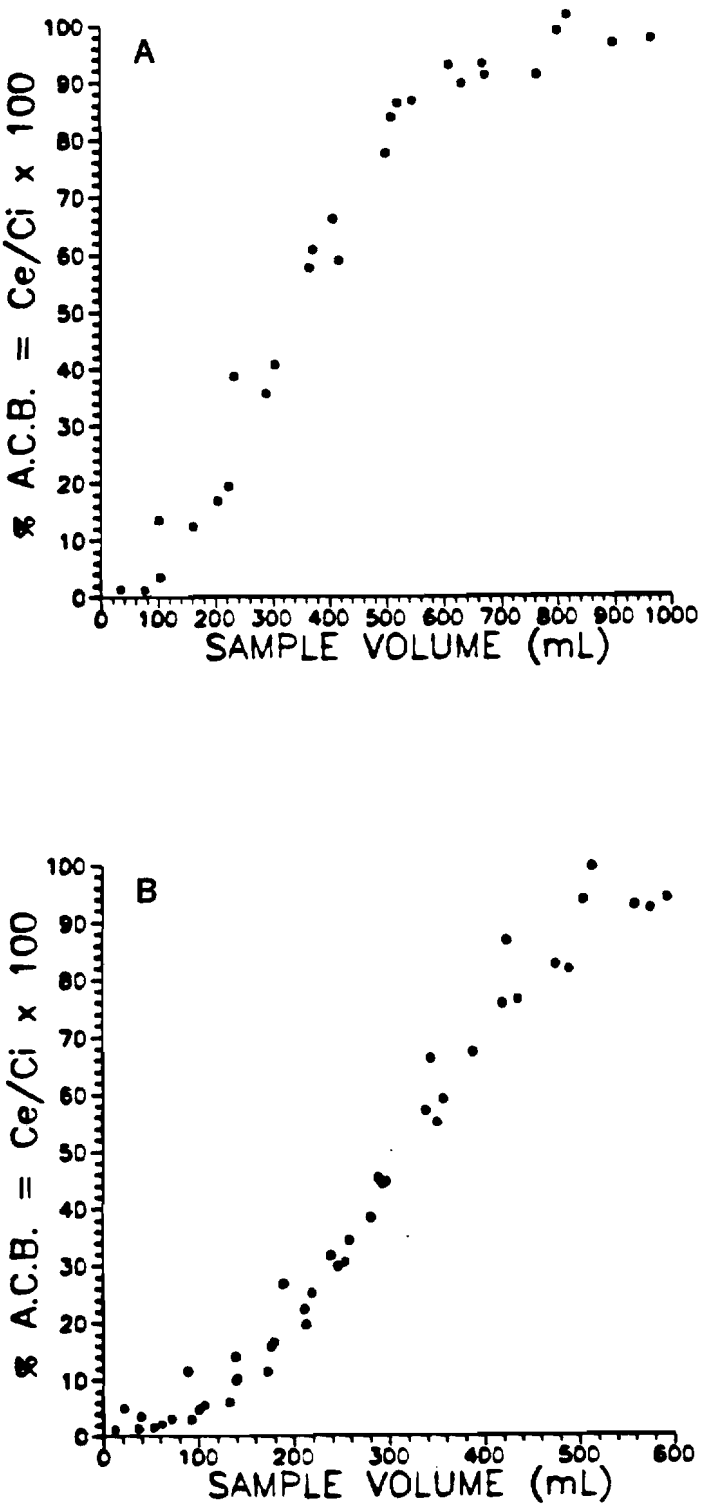

Figure 4.5. ACB curves obtained for 1,1-dichloroethane from experiments 2 and 4, A and B, respectively. Each curve represents the combined results of four cartridges. Each cartridge contained ~0.13 g of Tenax (see Table 4.1). C_i = 26 ppb for both experiments.

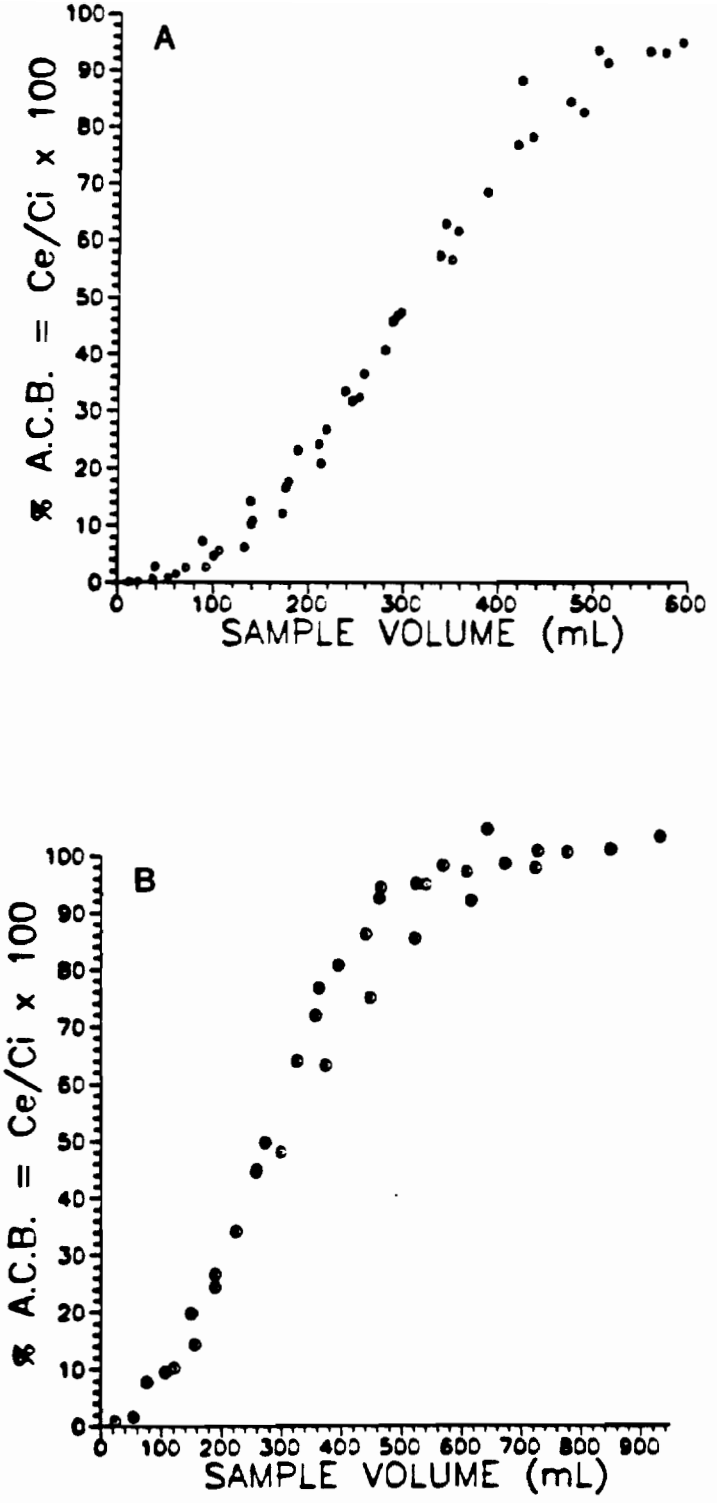

Figure 4.6. ACB curves obtained for trichloromethane from experiments 4 and 7, A and B, respectively. Each curve represents the combined results of four cartridges. Each cartridge contained ~0.13 g of Tenax (see Table 4.1). C_i = 26 and 61 ppb for experiments 4 and 7, respectively.

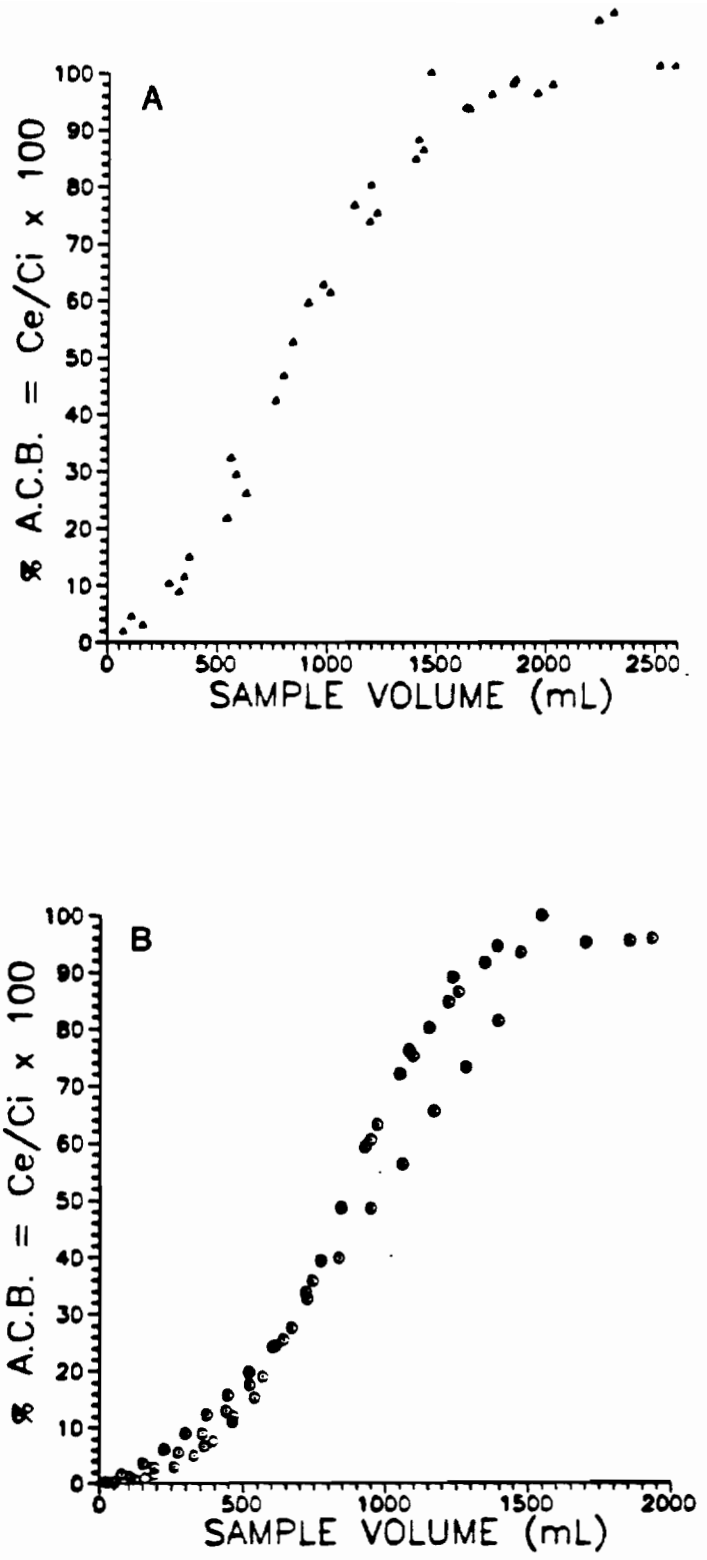

Figure 4.7. ACB curves obtained for benzene from experiments 6 and 7, A and B, respectively. Each curve represents the combined results of four cartridges. Each cartridge contained ~0.13 g of Tenax (see Table 4.1). C_i = 1.3 and 55 ppb for experiments 6 and 7, respectively.

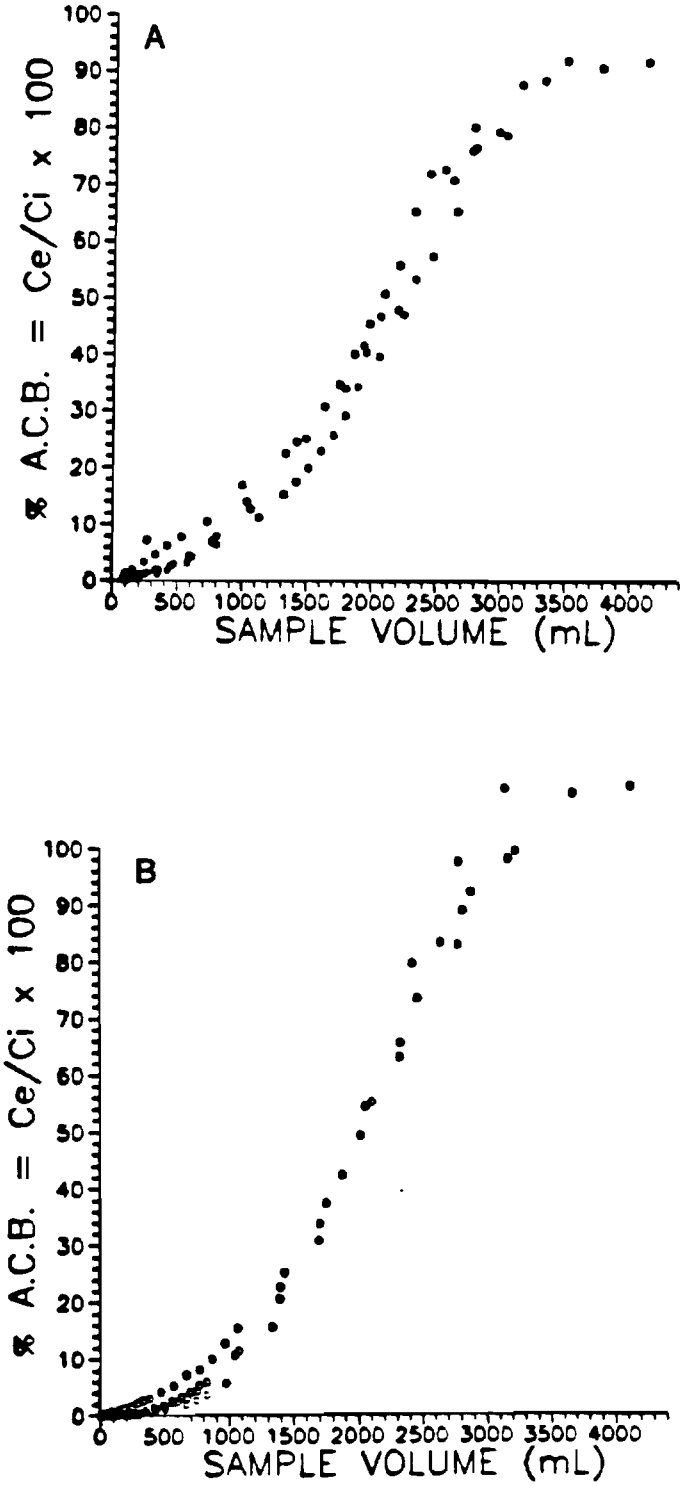

Figure 4.8. ACB curves obtained for trichloroethene from experiments 3 and 4, A and B, respectively. Each curve represents the combined results of four cartridges. Each cartridge contained ~0.13 g of Tenax (see Table 4.1). C_i = 28 and 22 ppb for experiments 3 and 4, respectively.

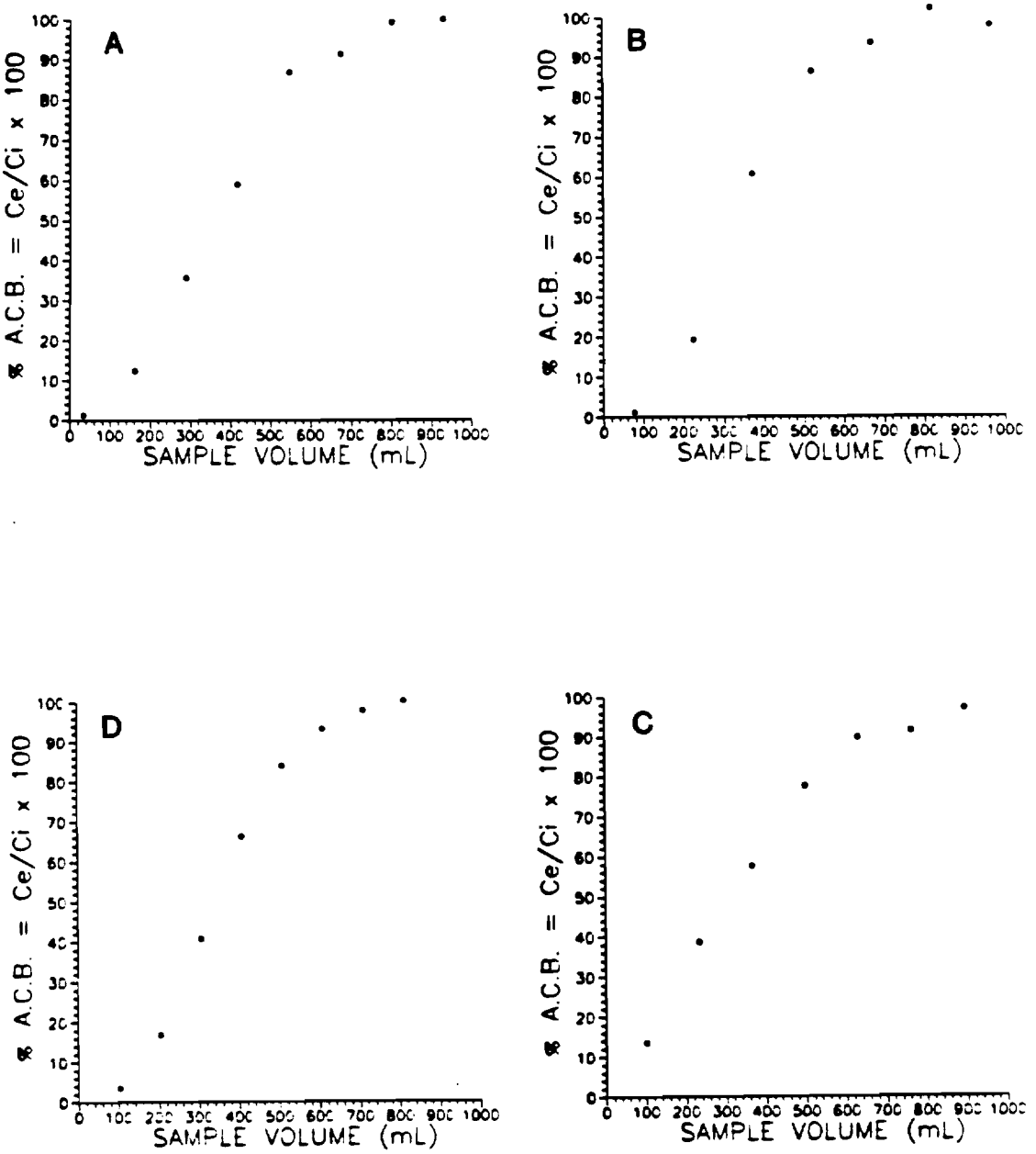

Figure 4.9. Individual ACB curves obtained for 1,1-dichloroethane (C_i = 26 ppb) from experiment 2. Each curve, A, B, C, and D, represents the results of the individual cartridge bearing the same letter. Each cartridge contained ~0.13 g of Tenax. For specific details concerning the mass of Tenax and the flow rate of each cartridge, see Tables 4.1 and 4.4.

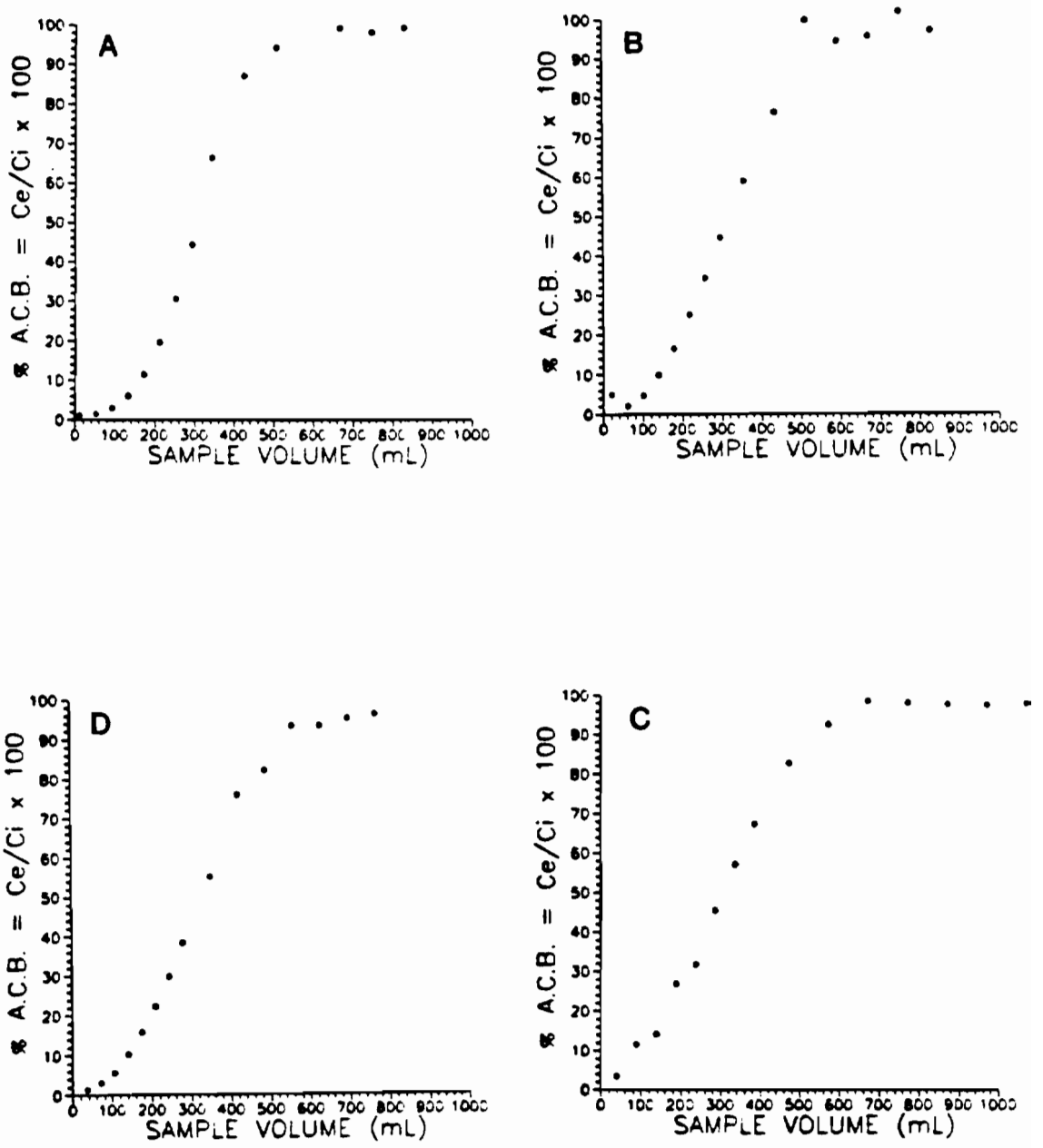

Figure 4.10. Individual ACB curves obtained for 1,1-dichloroethane (C_i = 26 ppb) from experiment 4. Each curve, A, B, C, and D, represents the results of the individual cartridge bearing the same letter. Each cartridge contained ~0.13 g of Tenax. For specific details concerning the mass of Tenax and the flow rate of each cartridge, see Tables 4.1 and 4.4.

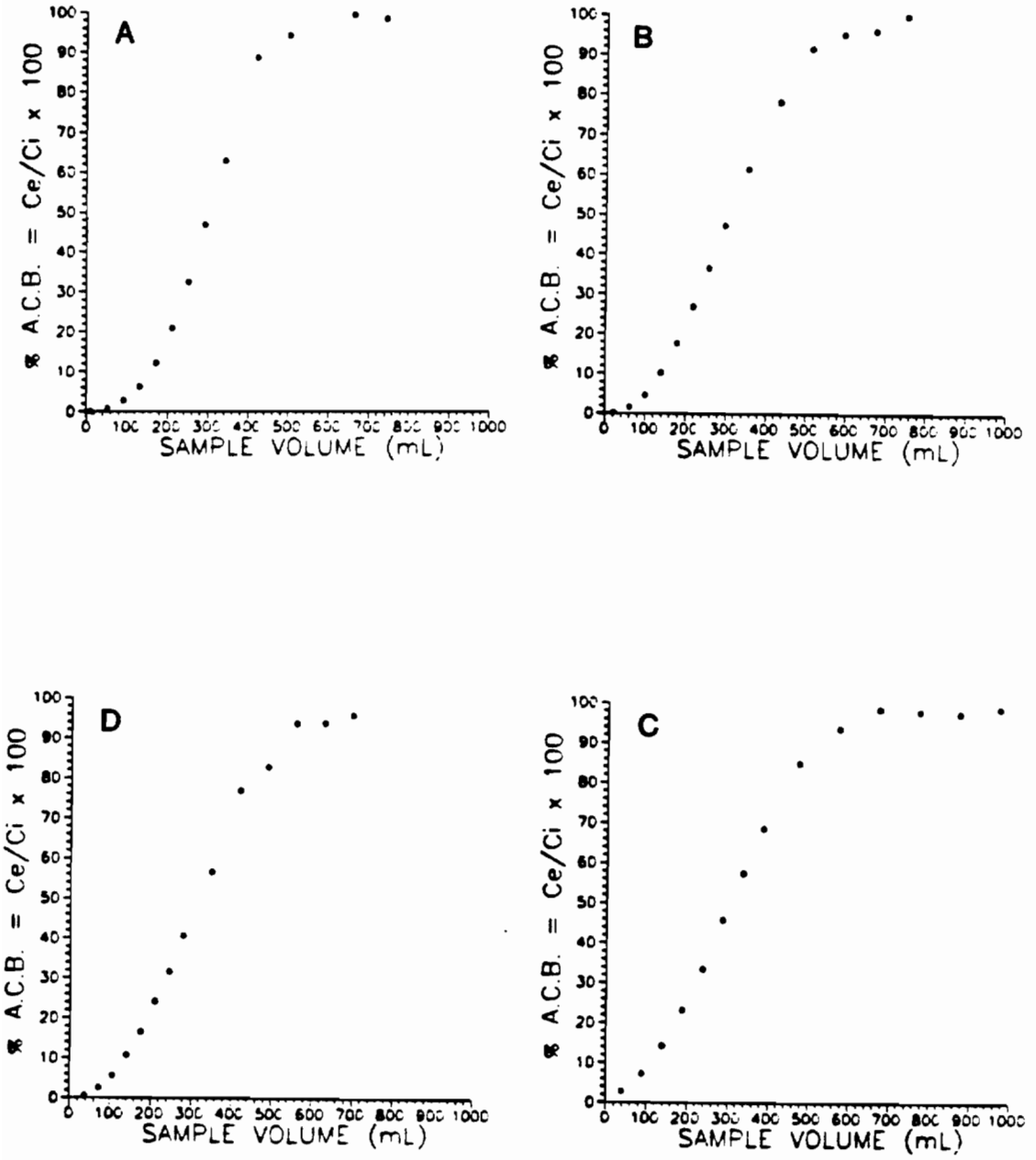

Figure 4.11. Individual ACB curves obtained for trichloromethane (C_i = 26 ppb) from experiment 4. Each curve, **A**, **B**, **C**, and **D**, represents the results of the individual cartridge bearing the same letter. Each cartridge contained ~0.13 g of Tenax. For specific details concerning the mass of Tenax and the flow rate of each cartridge, see Tables 4.1 and 4.4.

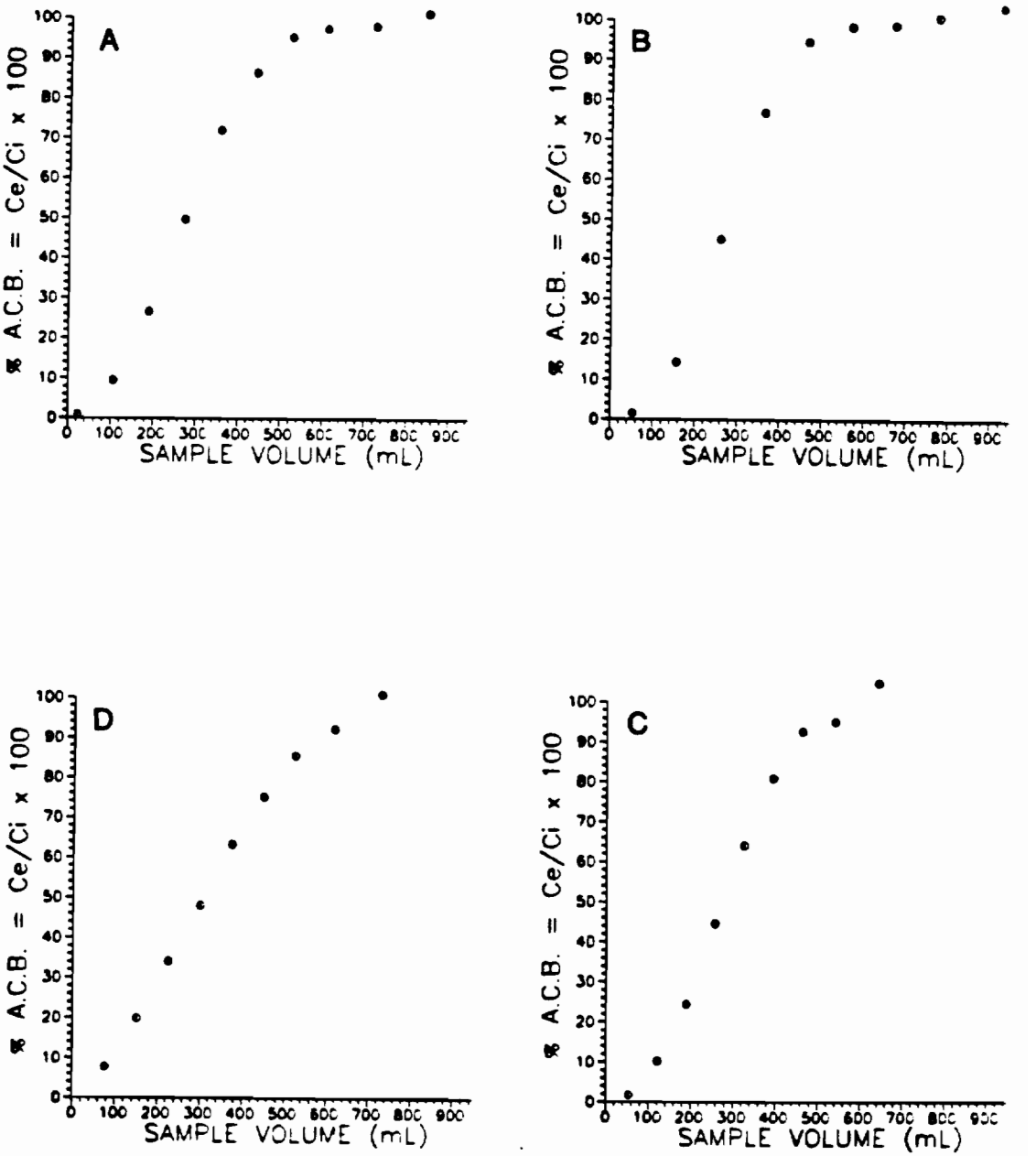

Figure 4.12 Individual ACB curves obtained for trichloromethane (C_i = 61 ppb) from experiment 7. Each curve, **A**, **B**, **C**, and **D**, represents the results of the individual cartridge bearing the same letter. Each cartridge contained ~0.13 g of Tenax. For specific details concerning the mass of Tenax and the flow rate of each cartridge, see Tables 4.1 and 4.4.

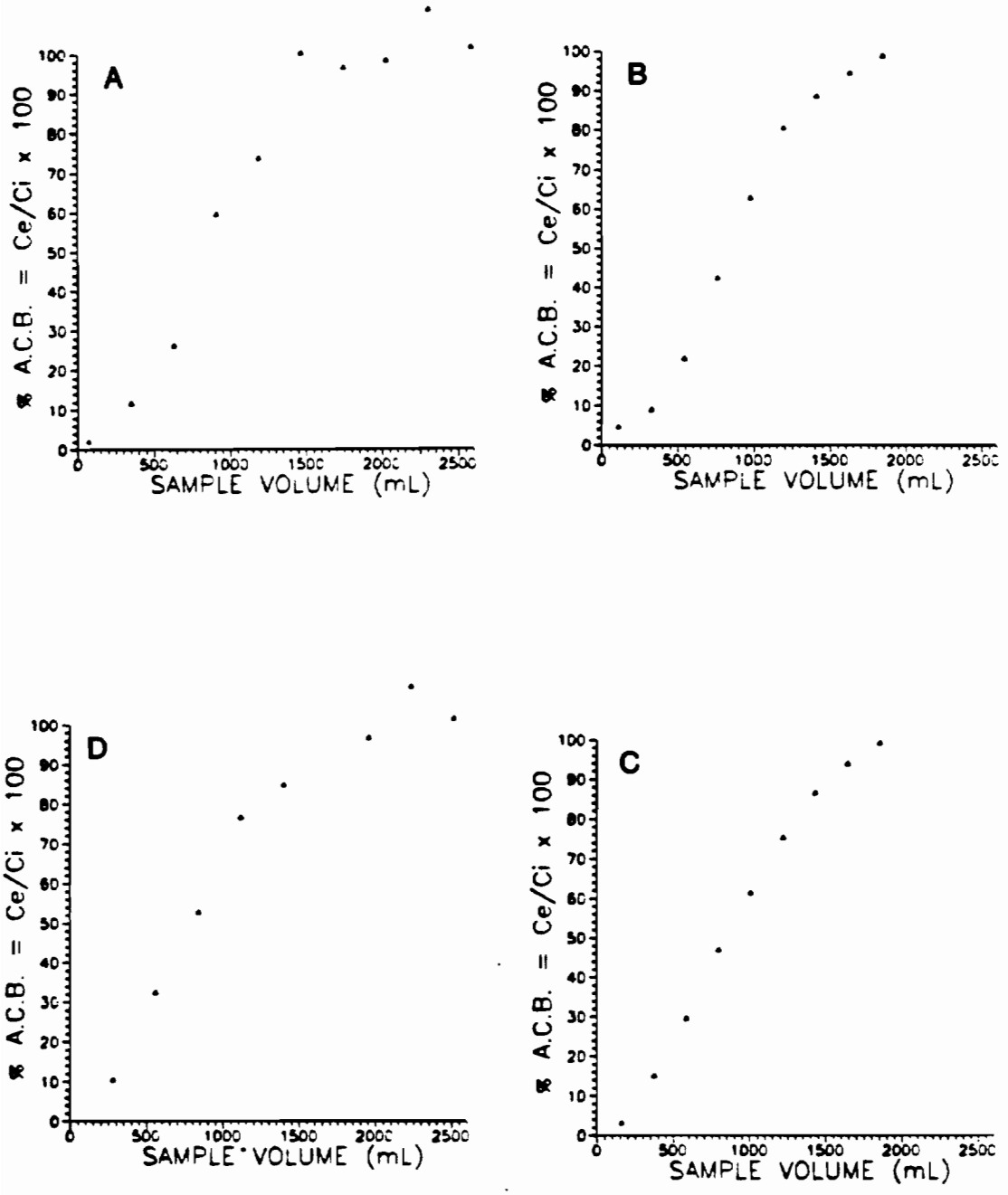

Figure 4.13. Individual ACB curves obtained for benzene (C_i = 1.3 ppb) from experiment 6. Each curve, A, B, C, and D, represents the results of the individual cartridge bearing the same letter. Each cartridge contained ~0.13 g of Tenax. For specific details concerning the mass of Tenax and the flow rate of each cartridge, see Tables 4.1 and 4.4.

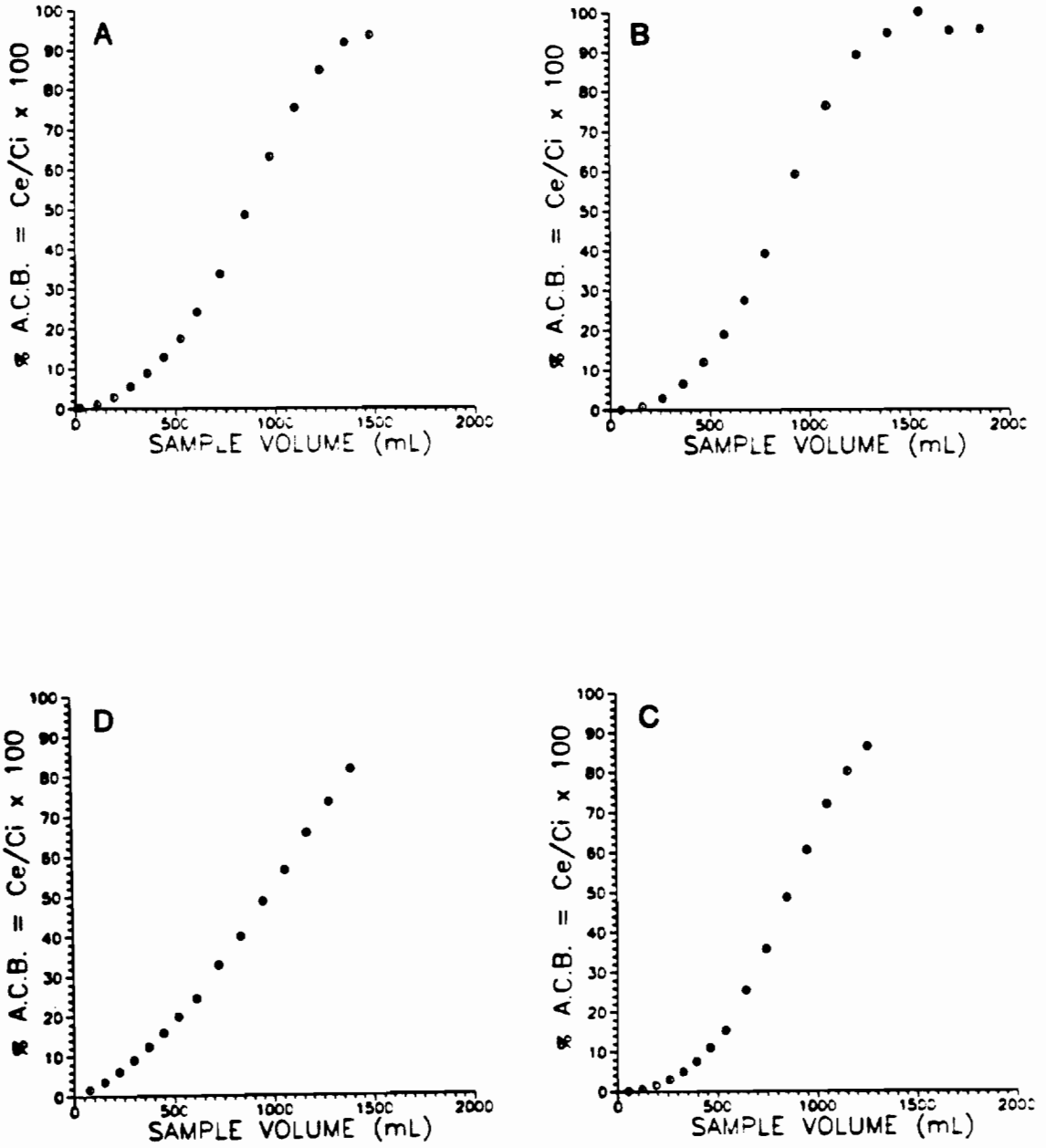

Figure 4.14. Individual ACB curves obtained for benzene (C_i = 55 ppb) from experiment 7. Each curve, **A**, **B**, **C**, and **D**, represents the results of the individual cartridge bearing the same letter. Each cartridge contained ~0.13 g of Tenax. For specific details concerning the mass of Tenax and the flow rate of each cartridge, see Tables 4.1 and 4.4.

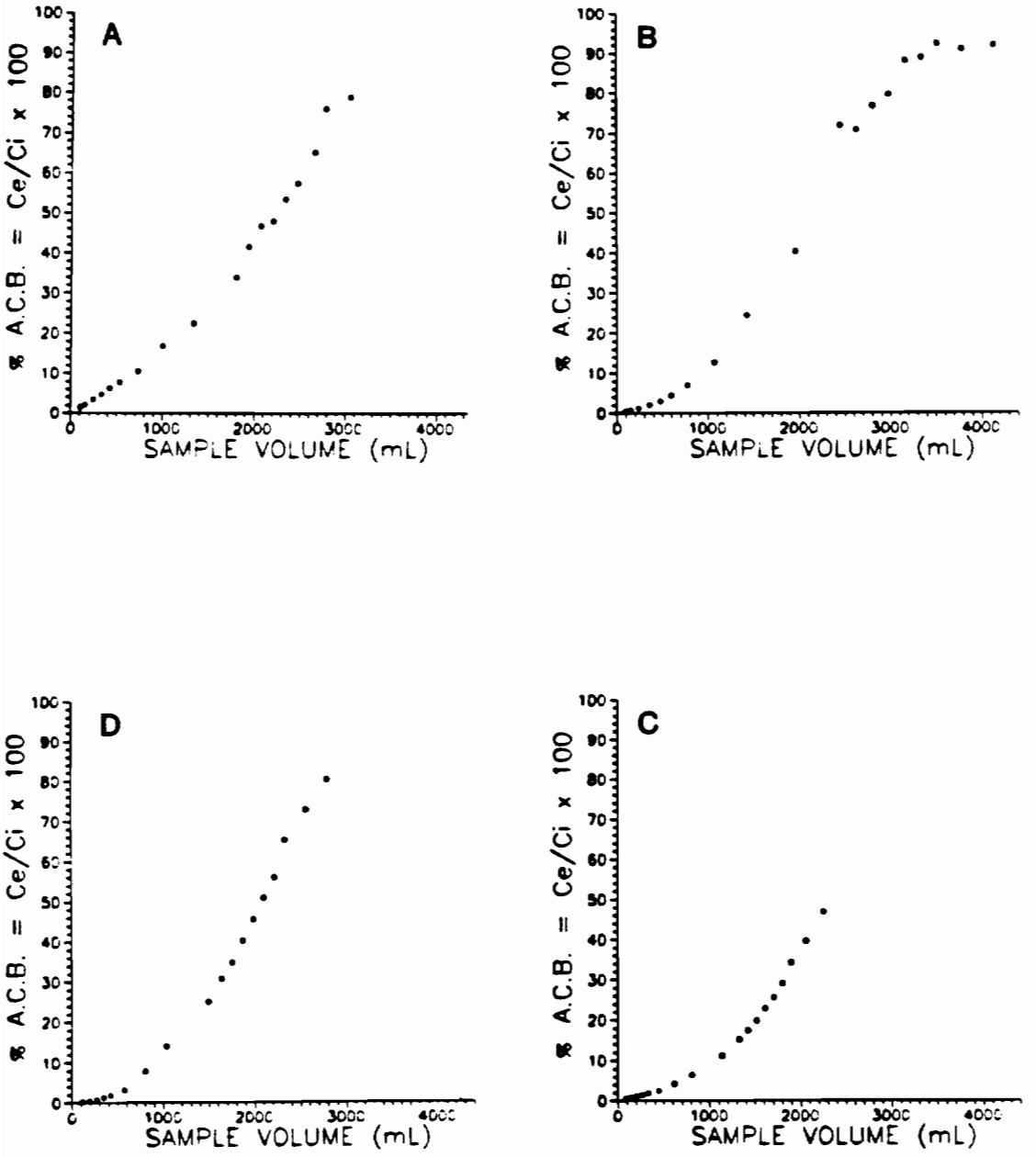

Figure 4.15. Individual ACB curves obtained for trichloroethene (C_i = 28 ppb) from experiment 3. Each curve, A, B, C, and D, represents the results of the individual cartridge bearing the same letter. Each cartridge contained ~0.13 g of Tenax. For specific details concerning the mass of Tenax and the flow rate of each cartridge, see Tables 4.1 and 4.4.

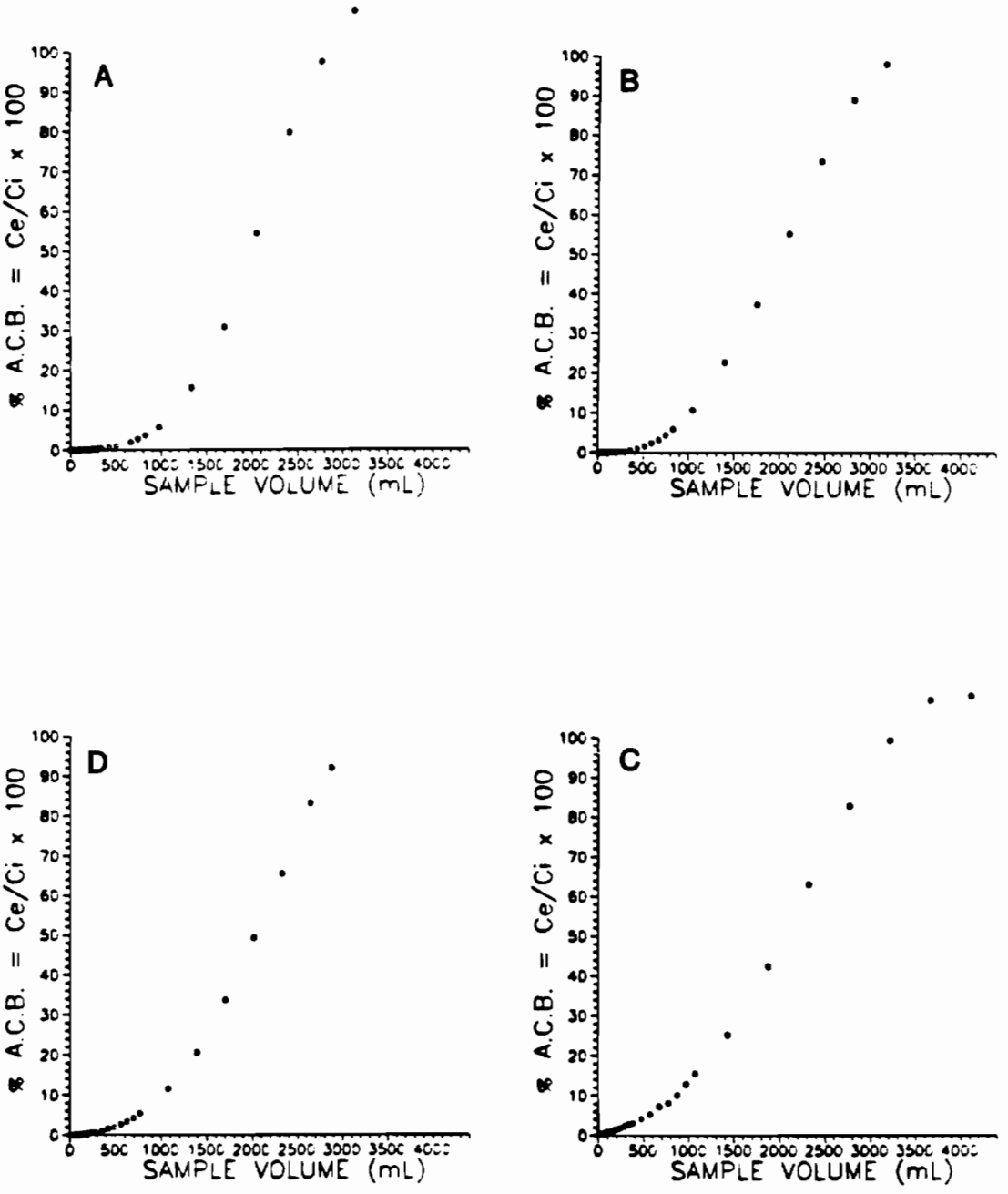

Figure 4.16. Individual ACB curves obtained for trichloroethene (C_i = 22 ppb) from experiment 4. Each curve, **A**, **B**, **C**, and **D**, represents the results of the individual cartridge bearing the same letter. Each cartridge contained ~0.13 g of Tenax. For specific details concerning the mass of Tenax and the flow rate of each cartridge, see Tables 4.1 and 4.4.

The variation between the individual curves is likely to be due to the varying flow rates among the cartridges and physical packing differences in the sorbent bed of each cartridge. The low scatter in the individual curves speaks well for the analytical and experimental methodology used to generate them. Due to the acceptable symmetry and and excellent definition of the individual cartridge ACB curves, it should be reasonable to approximate K_w using the individual cartridge retention volumes, V_R.

The retention volumes were determined from the individual ACB curves in the following manner. A third-order polynomial (with y-intercept = 0) was fit to the individual ACB curves, using a singular value decomposition curve fitting routine (71). The polynomial equation for the curve was then solved numerically using an iterative routine (72) to determine the sample volume at which 50% breakthrough occurs, i.e., V_R. The mass retained by the bed was then calculated using eqn. 4.7. K_w followed from a knowledge of C_i and the mass of the sorbent.

The advantage of having four independent measurements of K_w per compound and experiment is that there was a sound statistical basis for the direct comparison of the the arithmetic mean of the four measurements ($\bar{K}_w$), obtained for the same compounds under different sampling conditions.

4.3.7 Equilibrium Partition Coefficient as a Function of Cartridge Flow Rate

All inlet and outlet points of the mixing vessel were monitored for leaks and the system remained watertight throughout each experiment. In addition, the HPLC and syringe pumping rates were both observed to be consistent throughout each experiment. Cartridge flow rates were measured at the beginning of each experiment. These values compared well with those determined by measuring the total volume that passed through each cartridge over the total time of the experiment. As discussed in Section 4.2.2, within each experiment, cartridge-to-cartridge flow rates varied within the range of 1.5 to 3.0 mL/min. These variations in cartridge flow rates were due to differences in the packing characteristics among the cartridges. They did not cause significant differences in individual bed performances. Figure 4.17 is a plot of K_w vs. individual cartridge flow rate Q (ml/min), for trichloromethane. The plot is based on data from three separate ACB experiments. A linear regression analysis of K_w vs. Q shows no correlation ($r^2 = 0.0$) between these two variables.

4.3.8 Overview of Major Results Based on Equilibrium Partition Coefficient Determinations

Table 4.4 describes the individual ACB experiments from which $\bar{K}_w$ values were determined. As discussed previously, the compounds tested span a range of solubilities (S) and octanol water partition coefficients (K_{ow}). Appendix 2 contains the ACB curve (the combined

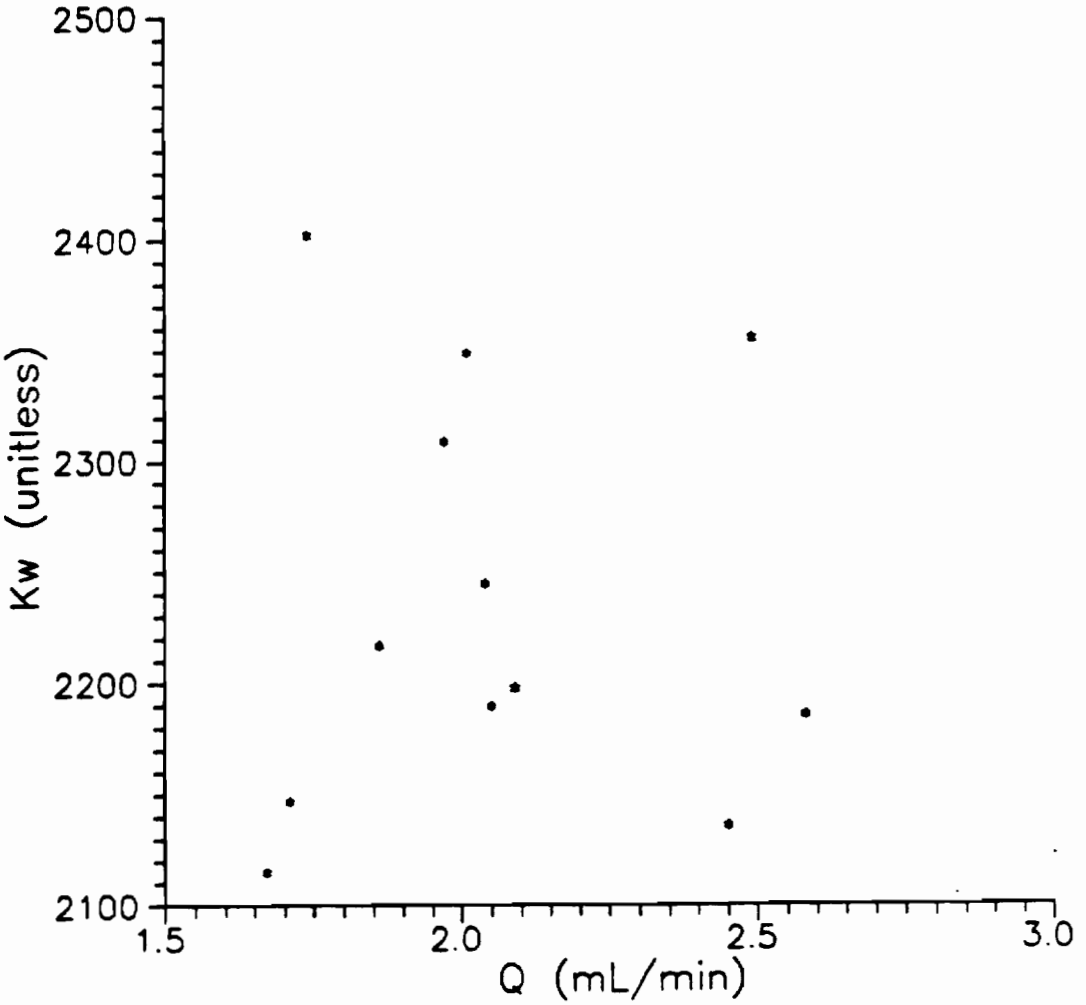

Figure 4.17. Plot of individual cartridge K_w values vs. individual cartridge flow rates (Q) for trichloromethane, from experiments 4, 7 and 8. A linear correlation coefficient, $r^2 = 0.0$ was calculated for the two variables.

Table 4.4. Description of Individual Adsorbent Cartridge Breakthrough Experiments.

Exp't No.	Compound(s) Analyzed	$\bar{C}_i$[a] (μg/L)	Cartridge Flow Rate (mL/min)			
			A[b]	B[b]	C[b]	D[b]
2	1,1-Dichloroethane	26	2.1	2.5	2.2	1.7
3	Trichloroethene	28	2.2	3.0	1.6	1.9
4	1,2-Dichloroethane	27	2.0	2.0	2.5	1.7
	Trichloromethane	26				
	1,1-Dichloroethane	26				
	Bromodichloromethane	22				
	Trichloroethene	22				
	Chlorobenzene	21				
	Tetrachloroethene	21				
5	1,2-Dichloroethane	120	1.7	2.5	2.5	1.6
	Trichloromethane	130				
	1,1-Dichloroethane	140				
6	Benzene	1.3	2.3	1.8	1.8	2.3
	1,2-Dichloropropane	24				
	1,1,2,2-Tetrachloroethane	16				
	Tribromomethane	21				
	cis-1,2-Dichloroethene	25				

Table 4.4 (cont'd.). Description of Individual Adsorbent Cartridge Breakthrough Experiments.

Exp't No.	Compound(s) Analyzed	$\bar{C}_i$[a] (μg/L)	Cartridge Flow Rate (mL/min)			
			A[b]	B[b]	C[b]	D[b]
6	1,1,2-Trichloroethane	20	2.3	1.8	1.8	2.3
	Bromodichloromethane	25				
7	Benzene	55	2.1	2.6	1.7	1.9
	cis-1,2-Dichloroethene	59				
	Trichloromethane	61				
8	Trichloromethane	130	2.1	1.7	2.0	2.5

[a]Average cartridge influent concentration.
[b]Cartridge letter designation (see Section 4.2.2).

curves of four cartridges) obtained for each compound analyzed in experiments 2 through 8. These experiments provided estimates of:

(1) The precision and accuracy of the ATD adsorption (sampling) step.

(2) The method sensitivity of ATD for the PPPs.

(3) The relationship between the water solubility of PPPs vs. their K_w for Tenax.

(4) The magnitude of the effect of single- vs. multiple-analyte solutions on ACB.

(5) The magnitude of the effect of analyte concentration on ACB.

4.3.8a Precision and Accuracy of the Adsorption Procedure

Table 4.5 presents each K_w determined from the four individual ACB curves generated for each compound analyzed in experiments 2 through 8. The corresponding *s* and CV values of each K_w are also presented. For all compounds and all experiments the mean CV is ~5.0%. Therefore, the reproducibility of the adsorption procedure is excellent.

The ACB curves can also be used to determine the accuracy of the adsorption procedure for specific instantaneous percent breakthrough values. The adsorption efficiency (or adsorbent cartridge sampling efficiency) (E), associated with the sample volume that corresponds to an instantaneous percent breakthrough value, is the percent fraction of the mass sampled (C_i x V) which was retained by the sorbent bed. Therefore E, a measure of the accuracy of the adsorption procedure,

Table 4.5. Average K_w Determined from Individual Adsorbent Cartridge Breakthrough Curves.

Compound	Exp't. No.	K_w[a]	*s*	CV[b] (%)
1,1-Dichloroethane	2	2600	200	7.7
Trichloroethene	3	17000	970	5.7
1,2-Dichloroethane	4	1400	19	1.4
Trichloromethane		2400	38	1.6
1,1-Dichloroethane		2400	52	2.2
Bromodichloromethane		4700	100	2.1
Trichloroethene		15000	340	2.3
1,2-Dichloroethane	5	1200	63	5.3
Trichloromethane		1900	58	3.1
1,1-Dichloroethane		1900	29	1.5
Benzene	6	6700	340	5.1
1,2-Dichloropropane		5900	480	8.1
1,1,2,2-Tetrachloroethane		16000	1600	10
Tribromomethane		12000	1100	9.2
1,1,2-Trichloroethane		4900	560	11
Bromodichloromethane		3800	210	5.5
Benzene	7	6900	180	2.6
cis-1,2-Dichloroethene		1800	38	2.1
Trichloromethane		2200	30	1.4

Table 4.5 (cont'd.). Average K_w Determined from Individual Adsorbent Cartridge Breakthrough Curves.

Compound	Exp't. No.	$\bar{K}_w$[a]	s	CV[b] (%)
Trichloromethane	8	2200	58	2.6

[a]Average K_w value determined from four individual ACB curves according to the procedure described in Section 4.3.6.
[b]Coefficient of variation, s expressed as a percentage of the mean.

can be determined for any instantaneous percent breakthrough value by determining the mass retained by the sorbent for the corresponding sample volume. The term percent breakthrough point is used synonymously with the term instantaneous percent breakthrough value. Thus, the 50% breakthrough point also indicates a value of C_e/C_i (%) which is equal to 50.

Selected ACB curves (the combined curves from the four cartridges used in each experiment) for several different compounds were used to estimate the accuracy of the adsorption step for the PPPs. The individual ACB curves were first normalized to the mass of their sorbent beds, by replotting instantaneous percent breakthrough (from each cartridge) vs. sample volume/g sorbent. This eliminated the variability between the combined ACB curves due to differences in the mass of the sorbent between individual cartridges. Using the same numerical routine discussed in Section 4.3.6, third order polynomials were then fit to the normalized versions of two ACB curves each for 1,1-dichloroethane, trichloromethane, benzene and trichloroethene. The compounds selected span the range of K_w values (2300 to 16,000) for all the compounds tested. The normalized curves and their polynomial fits are displayed in Figures 4.18-4.21. Using the method described in Section 4.3.6, these polynomials were then used to determine the mass retained by the sorbent at sample volumes corresponding to the 5, 10, 20 and 50% breakthrough points. Therefore, the E values corresponding to these instantaneous percent breakthrough values were determined.

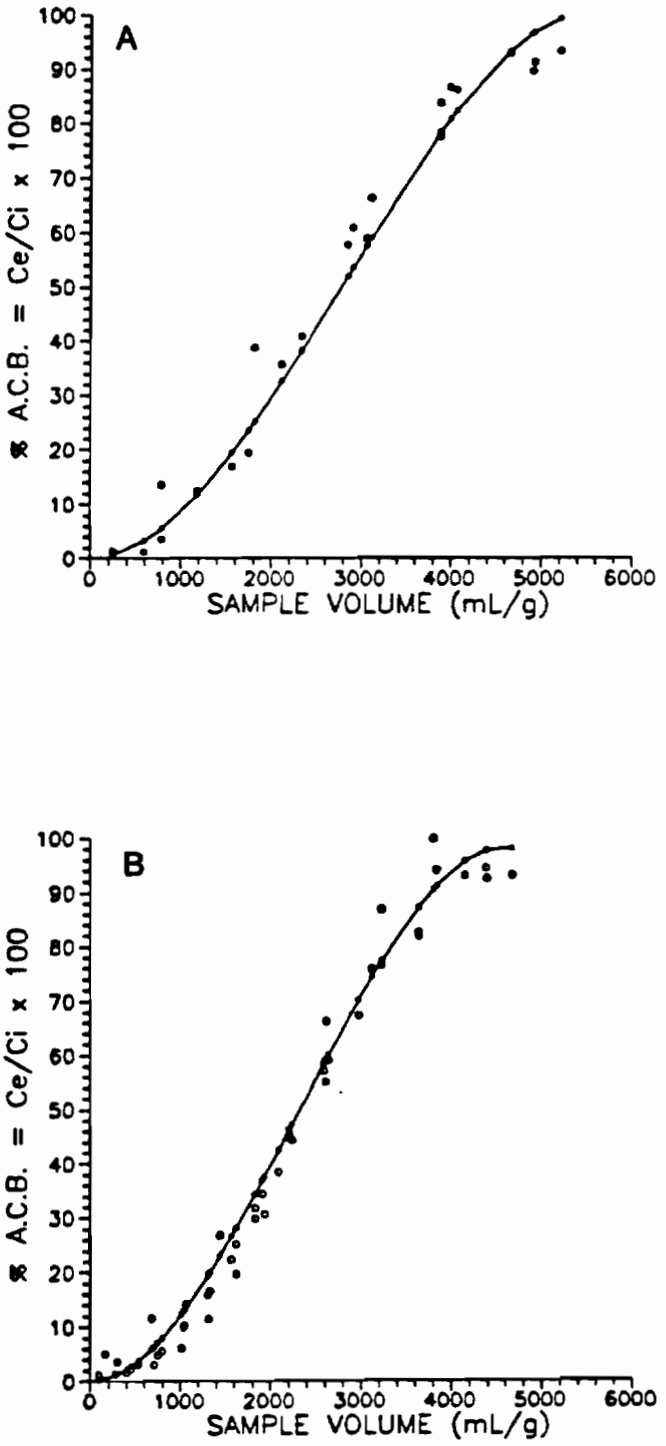

Figure 4.18. Polynomial curves fit to ACB results obtained for 1,1-dichloroethane from experiments 2 and 4, **A** and **B**, respectively. C_i = 26 ppb for both experiments. Each curve represents the combined results of four cartridges. Each C_e/C_i (%) value of a cartridge was plotted vs. sample volume (mL) ÷ the mass of Tenax (g) in the individual cartridge. A third order polynomial was fit to this data.

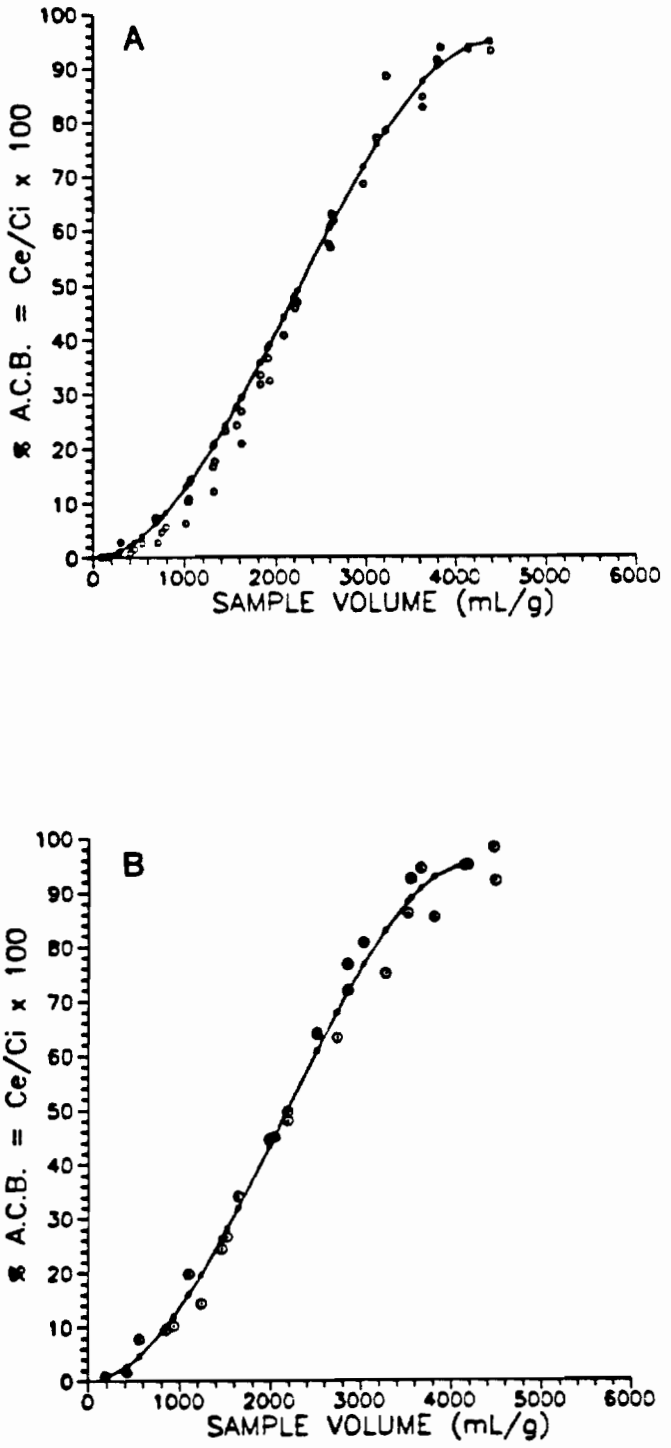

Figure 4.19. Polynomial curves fit to ACB results obtained for trichloromethane from experiments 4 and 7, A and B, respectively. C_i = 24 and 61 ppb for experiments 4 and 7, respectively. Each curve represents the combined results of four cartridges. Each C_e/C_i (%) value of a cartridge was plotted vs. sample volume (mL) ÷ the mass of Tenax (g) in the individual cartridge. A third order polynomial was fit to this data.

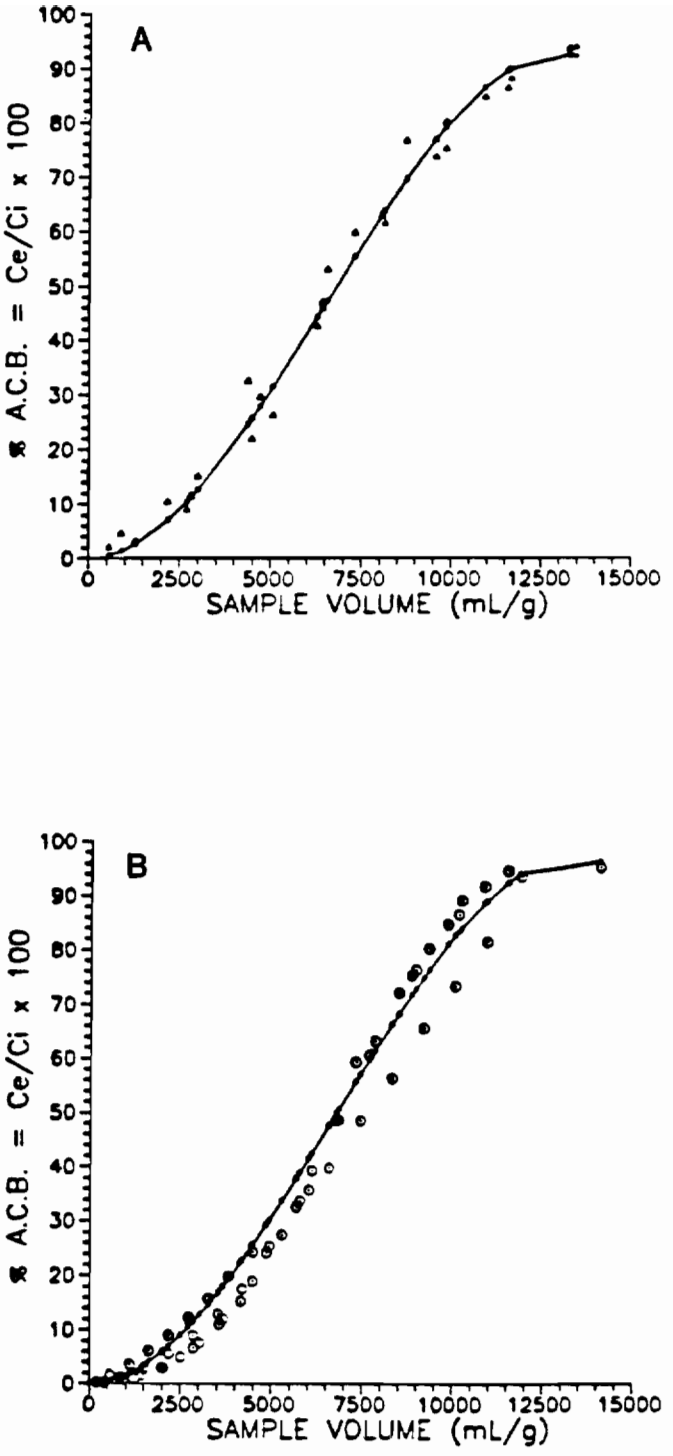

Figure 4.20. Polynomial curves fit to ACB results obtained for benzene from experiments 6 and 7, **A** and **B**, respectively. C_i = 1.3 and 55 ppb for experiments 6 and 7, respectively. Each curve represents the combined results of four cartridges. Each C_e/C_i (%) value of a cartridge was plotted vs. sample volume (mL) ÷ the mass of Tenax (g) in the individual cartridge. A third order polynomial was fit to this data.

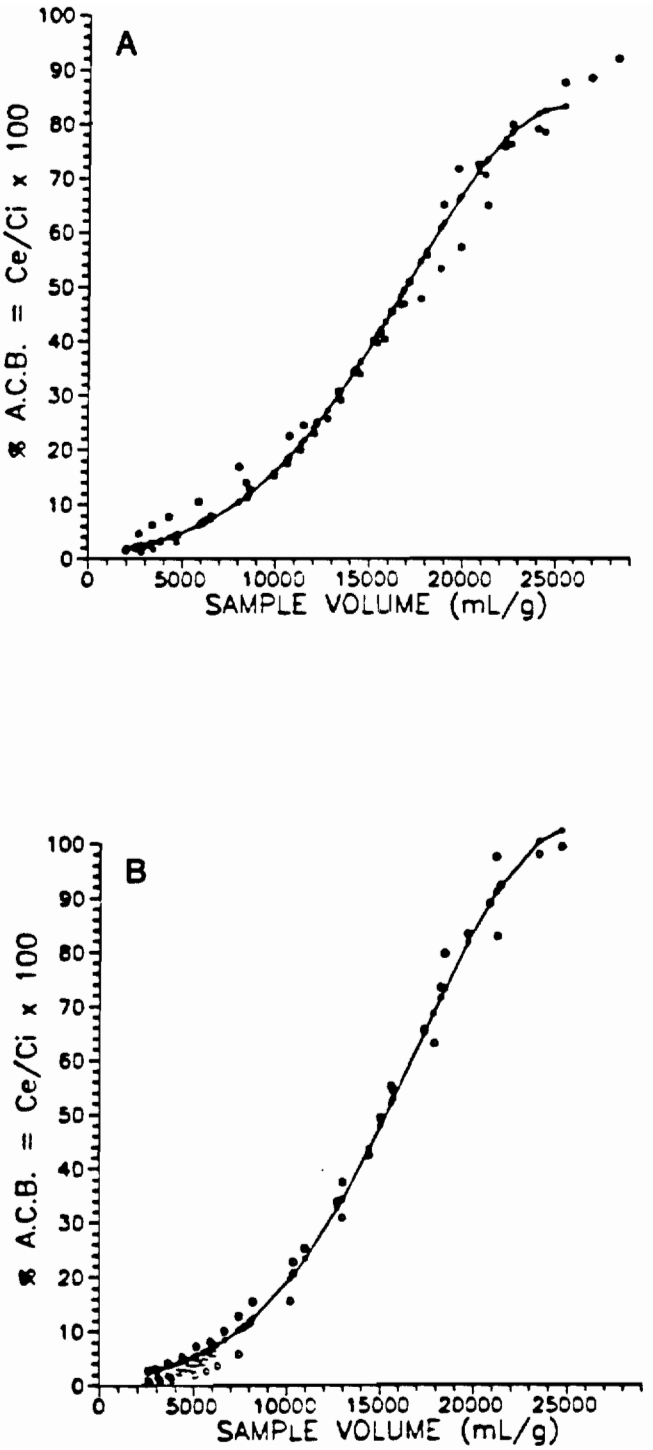

Figure 4.21. Polynomial curves fit to ACB results obtained for trichloroethene from experiments 3 and 4, A and B, respectively. C_i = 28 and 22 ppb for experiments 3 and 4, respectively. Each curve represents the combined results of four cartridges. Each C_e/C_i (%) value of a cartridge was plotted vs. sample volume (mL) ÷ the mass of Tenax (g) in the individual cartridge. A third order polynomial was fit to this data.

Figure 4.22 is a plot of E vs. instantaneous percent breakthrough. This plot shows that the E value at each of the four different instantaneous percent breakthrough values remains constant over the specified K_w range. This indicates that dispersion in the ACB curves increases proportionately with V_R, and that the behavior of even small bed adsorption systems is reproducible. One measure of the dispersion would be the distance in volume or time units between the 5 to 95% breakthrough points. Therefore, for the range of K_w values of the compounds selected, there is a strong linear correlation ($r^2 = 0.99$) between E and instantaneous percent breakthrough. As a result, the linear regression equation determined from a regression analysis performed on the data presented in Figure 4.22, may be used to predict the accuracy of the adsorption procedure. The linear regression equation is :

$$E = 100 - 0.36(IBT) \qquad 4.8$$

where IBT is the instantaneous percent breakthrough value. Thus, for a range of K_w values and therefore compounds, the E may be predicted for the sample volume corresponding to a specific instantaneous percent breakthrough value obtained from an analyte ACB curve. Therefore, the instantaneous percent breakthrough values per sample volume provided by the analyte ACB curves, may now be easily and accurately converted to a value for the adsorbent cartridge sampling efficiency.

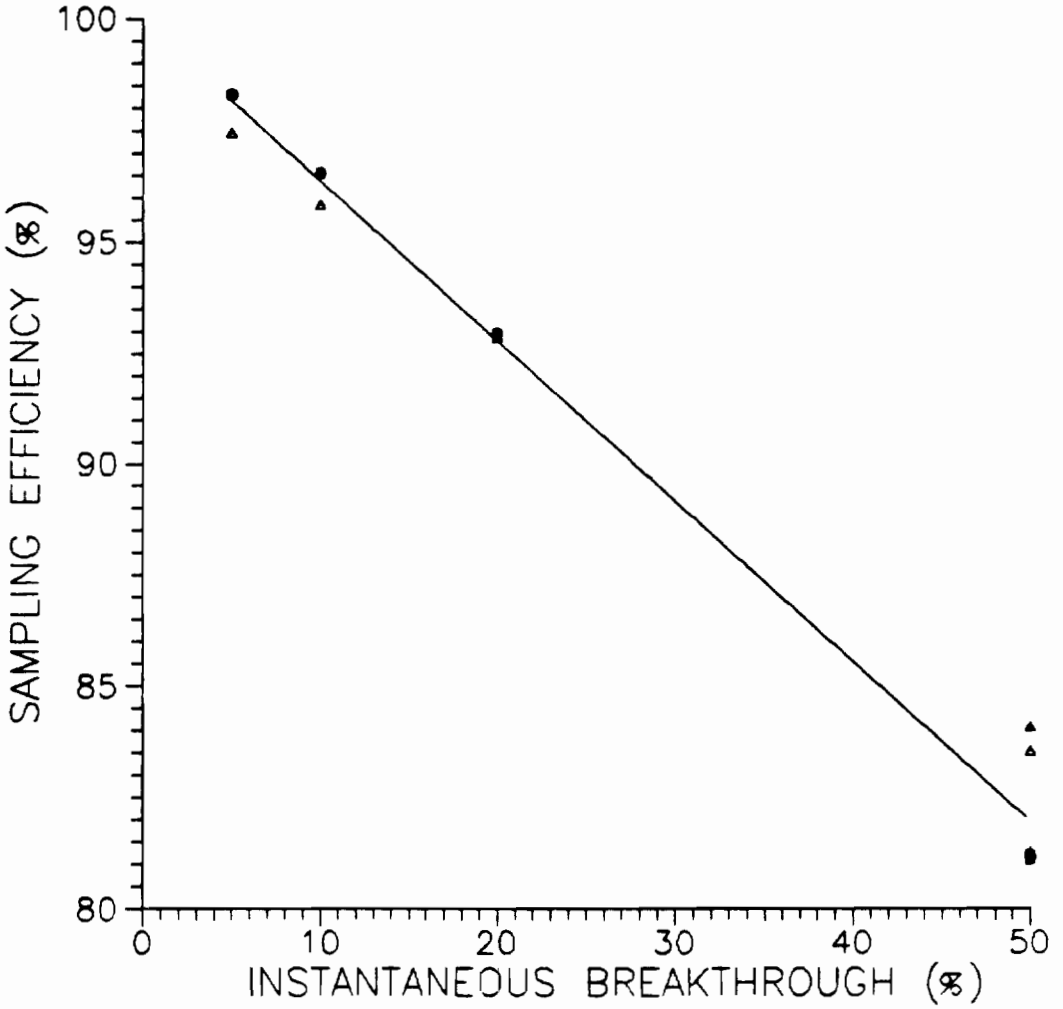

Figure 4.22. Plot of adsorbent cartridge sampling efficiency (E) vs. instantaneous percent breakthrough (IBT). E values were obtained from the polynomial curves fit to the normalized ACB data of 1,1-dichloroethane, trichloromethane, benzene and trichloroethene presented in Figures 4.18-4.21. Because two ACB curves were used for each of the four compounds, two E values are plotted for each compound at IBT values of 5, 10, 20, and 50%. The trichloromethane data (asterisks) correspond to an K_w of 2300. The 1,1-dichlorethane data (circles) correspond to an K_w of 2500. The benzene data (squares) corresponds to an K_w of 6800. The trichloroethene data (triangles) corresponds to an K_w of 16,000. The solid line represents the linear regression equation E = 100 - 0.36(IBT); r^2 = 0.99.

4.3.8b Adsorption/Thermal Desorption Method Sensitivity

The method sensitivity of an analysis procedure is defined here as the analyte mass (ng) required by a detector for analyte quantitation divided by the analysis volume (mL) of the sample. In the case of a mass spectrometer alone or a flame ionization detector, approximately 5 ng of analyte is required for the quantifiable detection of a PPP. Because the P&T/WCC method utilizes 5 mL of sample, P&T/WCC is at an immediate disadvantage relative to ATD. The sample volume for ATD is limited to the extent that E values for all analytes remain high. The ATD sample volume for many of the PPPs may therefore be much greater than 5 mL.

For this ATD system and most of the compounds tested, an E value of 93% should be achieved for each sample volume corresponding to the 20% breakthrough point (see Figure 4.22). Therefore, with these sample volumes, only 7% of the mass sampled will not be retained by the sorbent. A loss of this fraction of mass during sampling is justified by the enhanced sensitivity through increased sample volume. In addition, the excellent reproducibility of the sampling system may allow an accurate post-analysis concentration correction to be made. Therefore, the calculation of the method sensitivity for ATD will be based here on the sample volume of the analyte which corresponds to the 20% breakthrough point. Table 4.6 presents the estimated method sensitivity of ATD for a weakly, moderately and strongly retained compound relative to their estimated method sensitivity by analysis with P&T/WCC based on a sample volume of 5 mL. For the PPPs, the

range of method sensitivity using ATD is 3.3×10^{-3} to 3.8×10^{-2} ppb and is therefore significantly more sensitive than P&T/WCC, whose method sensitivity may be estimated as 5 ng/5 mL, or 1.0 ppb. Thus, ATD has the ability to concentrate from 26 to 300 times more analyte mass than P&T/WCC. For compounds like chlorobenzene which have very low water solubilities, (see Appendices 2.8 and 2.9), the achievable concentration factors of ATD relative to P&T/WCC will be significantly greater than 300.

4.3.8c Equilibrium Partition Coefficient as a Function of Analyte Solubility

In order to make approximations concerning the utility of ATD for the sampling and analysis of the PPPs that were not studied directly here, a reasonable relationship between $\bar{K}_w$ and S is needed. All S values were obtained from Mabey et al. (11). As discussed previously (Section 4.1), it is reasonable to expect that as S increases K_w will decrease. Figure 4.23, a plot of log $\bar{K}_w$ vs. log S for the 11 compounds whose complete ACB curves were determined, indicates that this is generally true. However, the linear correlation coefficient $r^2 = 0.56$, is poor. The regression equation is:

$$\log \bar{K}_w = 7.5 - 1.1 \log S \qquad 4.9$$

A better linear correlation exists for log $\bar{K}_w$ and log K_{ow}, where K_{ow} is the ratio of the equilibrium concentrations of an analyte in the octanol and aqueous phases of the two-phase octanol/water system.

Table 4.6. Calculation of Estimated Method Sensitivity[a] (S_m) of ATD and P&T/WCC for Three PPPs.

Compound --	1,2-Dichloroethane[b]	Benzene[c]	Trichloroethene[d]
ATD Sample Volume[e] (mL) --	130	500	1500
P&T/WCC Sample Volume (mL) --	5.0	5.0	5.0
Conc'n. Factor ATD vs. P&T/WCC --	26	100	300
ATD-S_m (μg/L) --	3.8 E-2	9.8 E-3	3.3 E-3
P&T/WCC-S_m (μg/L) --	1.0	1.0	1.0

[a]The approximate mass of a PPP (5 ng) required by a mass spectrometer alone or a flame ionization detector for quantifiable detection divided by the sample volume (mL).
[b]K_w = 1400 (experiment 4) therefore, 1,2-dichloroethane is considered to be relatively weakly retained by this adsorption system.
[c]K_w = 6800 (experiments 6 and 7) therefore, benzene is considered to be relatively moderately retained by this adsorption system.
[d]K_w = 16000 (experiments 3 and 4) therefore, trichloroethene is considered to be relatively strongly retained by this adsorption system.
[e]Sample volume corresponding to the 20% breakthrough point.

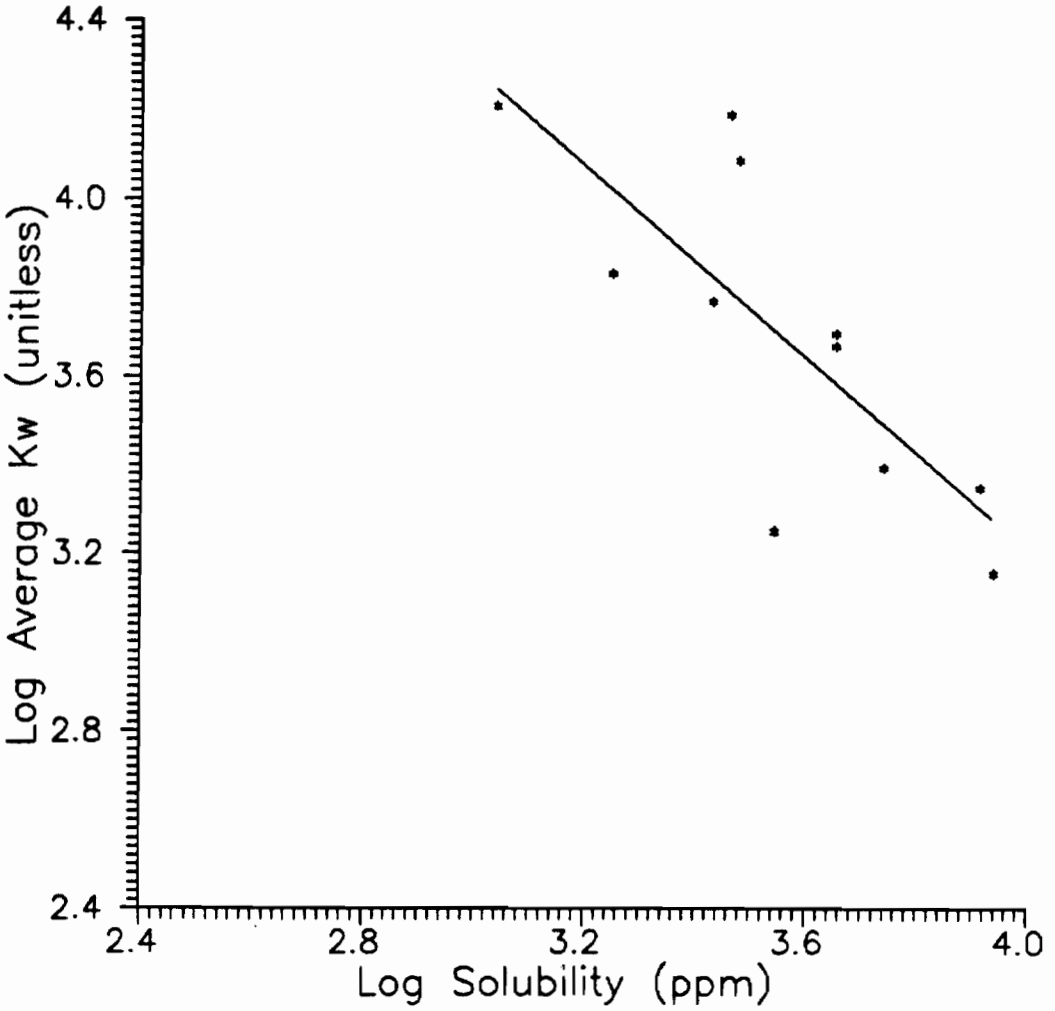

Figure 4.23. Plot of log $\bar{K}_w$ vs. log S. The linear regression equation is log $\bar{K}_w$ = 7.5 - 1.1 log S; r^2 = 0.56.

All K_{ow} values were obtained from Mabey et al. (11). Figure 4.24 presents the plot of log $\bar{K}_w$ vs. log K_{ow}. As would be expected, log $\bar{K}_w$ tends to increase with increasing log K_{ow}. Relative to water the PPPs will tend to favor octanol, the less polar of the two solvents, when partitioning between the two phases. Therefore, the least water-soluble analytes exhibit the highest K_{ow} and $\bar{K}_w$ values. The regression analysis of log $\bar{K}_w$ vs. log K_{ow} produces a much higher correlation coefficient $r^2 = 0.89$, than that of log$\bar{K}_w$ vs. log S. The regression equation is:

$$\log \bar{K}_w = 1.3 + 1.2 \log K_{ow} \qquad 4.10$$

This implies that $\bar{K}_w$ will be more accurately predicted by K_{ow} than S.

By using equations 4.9 and 4.10, predicted K_w values can be compared with those determined experimentally ($\bar{K}_w$). Table 4.7 compares $\bar{K}_w$, with the value of K_w predicted using S. That value will be given the symbol K_{w-s}. Table 4.7 also compares $\bar{K}_w$ with the K_w value predicted using K_{ow}. That value will be given the symbol K_{w-ow}. In most cases the K_{w-ow} and K_{w-s} values differ by less than a factor of two. Table 4.8 contains the K_{w-ow} and K_{w-s} values for the remaining PPPs (i.e., the PPPs not tested in experiments 2 through 8). The achievable method sensitivities with ATD for compounds with predicted K_w values falling within the range of 1500 to 16,000, may be similar to the ATD method sensitivities presented in Table 4.6.

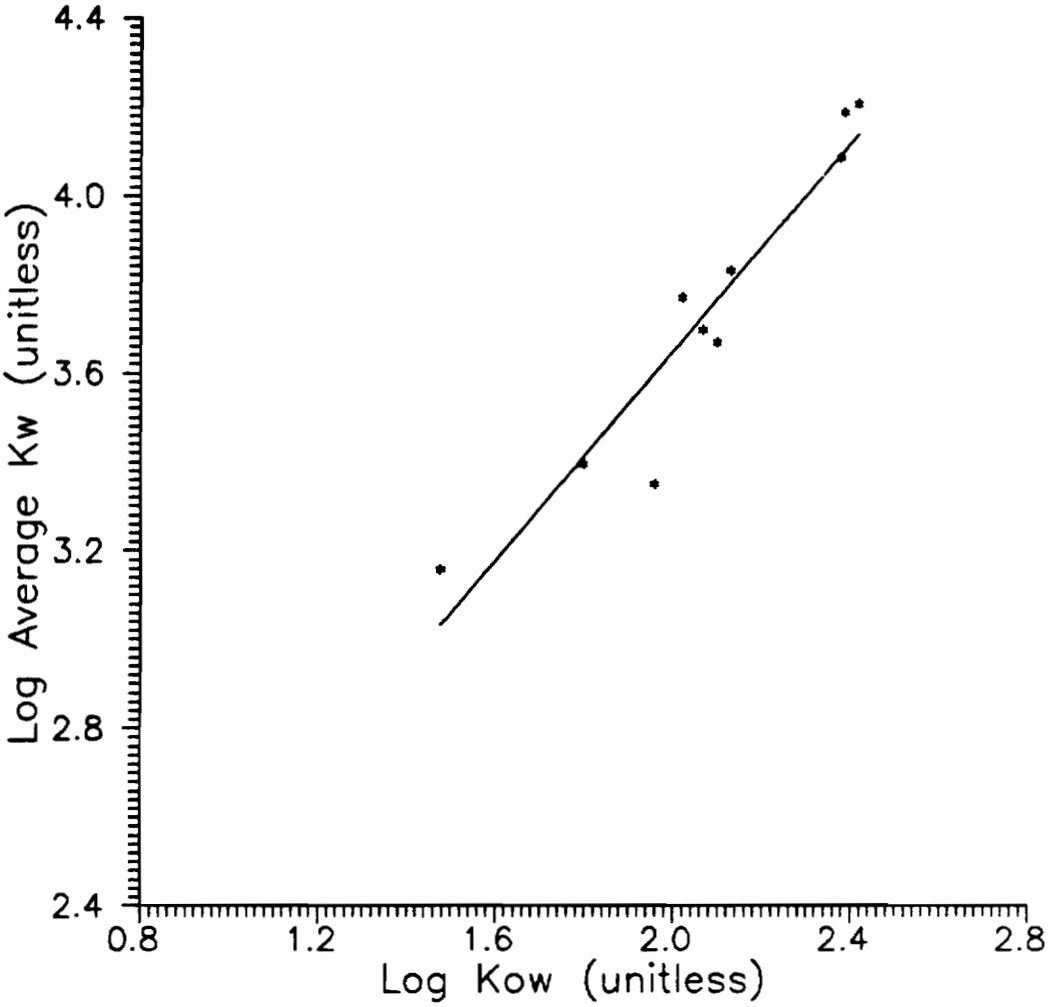

Figure 4.24. Plot of log $\bar{K}_w$ vs. log K_{ow}. The linear regression equation is log $\bar{K}_w$ = 1.3 + 1.2 log K_{ow}; r^2 = 0.89.

Table 4.7. Experimental vs. Predicted K_w.

Compound	K_w[a]	K_{w-s}[b]	K_{w-ow}[c]
1,2-Dichloroethane	1400	1900	1100
cis-1,2-Dichloroethene	1800	5000	NA[d]
Trichloromethane	2200	2000	4100
1,1-Dichloroethane	2500	3100	2600
Bromodichloromethane	4700	3800	6000
1,1,2-Trichloroethane	5000	3800	5500
1,2-Dichloropropane	5900	6700	4800
Benzene	6800	10000	6500
Tribromomethane	12000	5900	13000
1,1,2,2-Tetrachloroethane	16000	6200	13000
Trichloroethene	16000	18000	14000

[a] K_w determined from appropriate breakthrough experiments.
[b] Value predicted using K_w vs. S relationship, see Figure 4.23.
[c] Value predicted using K_w vs. K_{ow} relationship, see Figure 4.24.

Table 4.8. Predicted K_w using S and K_{ow} for the PPPs not Tested in Adsorbent Cartridge Breakthrough Experiments 2 through 8.

Compound	S[a] (μg/L)	K_{ow}[a]	K_{w-s}[b]	K_{w-ow}[c]
Dichloromethane	20000	18.2	770	610
2-Chloroethylvinylether	15000	13.8	1000	440
Chloromethane	6450	8.9	2600	260
Chloroethane	5740	30.9	3000	1100
Dibromochloromethane	4000	174	4400	8800
Chloroethene	2700	17	6700	560
trans-1,3-Dichloropropene	2700	100	6700	4600
Trichloroflouromethane	1100	331	18000	19000
Bromomethane	900	12.3	22000	390
Tetrachloromethane	785	912	25000	62000
1,1,1-Trichloroethane	720	320	28000	18000
trans-1,2-Dichloroethene	600	123	34000	5800
Toluene	535	620	38000	39000
Chlorobenzene*	488	690	42000	45000
1,1-Dichloroethene	400	135	52000	6500
Tetrachloroethene*	200	759	110000	50000
Ethylbenzene	152	2200	150000	180000
m-Dichlorobenzene	123	3600	190000	310000
o-Dichlorobenzene	100	3600	230000	310000

Table 4.8 (cont'd.). Predicted K_w using S and K_{ow} for the PPPs not Tested in Adsorbent Cartridge Breakthrough Experiments 2 through 8.

Compound	S^a (μg/L)	$K_{ow}{}^a$	$K_{w-s}{}^b$	$K_{w-ow}{}^c$
p-Dichlorobenzene	79	3600	300000	310000

[a]Ref. 11, value for each constant measured at 25°C.
[b]Value predicted using K_w vs. S relationship, see Figure 4.23.
[c]Value predicted using K_w vs. K_{ow} relationship, see Figure 4.24.
*Compound was tested in experiment 4, however, a complete breakthrough curve was not obtained.

4.3.8d Adsorbent Cartridge Breakthrough and Single- vs. Multiple-Analyte Solutions

The effects of single- vs. multiple-analyte solutions and analyte concentration on ACB were tested in experiments 2 through 8. In some cases the different experiments utilized solutions which contained different additional analytes, and in other cases the analytes were simply present at different concentrations (see Table 4.4). Table 4.9 presents the results of the two-sample t-tests performed on each compound whose K_w was determined in more than one experiment.

Experiments 2 through 4 were designed to ascertain whether K_w values determined from single-analyte experiments differed significantly from K_w values determined in the presence of other analytes. If analyte/analyte interactions in multiple-analyte solutions are determined to significantly effect ACB, a great number of possible analyte/analyte interactions would have to be considered in order to accurately predict the sampling efficiency of ATD for the PPPs in water. Indeed, groundwater systems are contaminated by more than one compound. It was also intended to ascertain whether multiple-analyte systems are equivalent in ACB response to single-analyte systems for the purposes of modeling (discussed in Section 5.3.1).

Dressler (34) has noted that compounds with approximately the same V_R tended to behave as one compound and not react competitively towards one another in a multiple-analyte adsorption situation. Dissimilar compounds however tended to react separately and affected

Table 4.9. Comparison of $\bar{K}_w$ Values Determined Under Different Sampling Conditions.

Compound	Exp't. No.	$\bar{C}_i$[a] (μg/L)	Solution Type S[b] or M[c]	$\bar{K}_w$[d]	p[e]
1,2-Dichloroethane	4	26	M	1400	.00*
	5	120	M	1200	
Trichloromethane	4	26	M	2400	.00*
	5	130	M	1900	
	4	26	M	2400	.00*
	7	61	M	2200	
	4	26	M	2400	.00*
	8	130	S	2200	
	7	61	M	2200	.66
	8	130	S	2200	
	5	130	M	1900	.00*
	8	130	S	2200	
1,1-Dichloroethane	2	26	S	2600	.17
	4	27	M	2400	
	2	26	S	2600	.00*
	5	140	M	1900	
	4	27	M	2400	.00*
	5	140	S	1900	
Bromodichloromethane	4	22	M	4700	.00*
	6	25	M	3800	
Benzene	6	1.3	M	6700	.37
	7	55	M	6900	

Table 4.9 (cont'd.). Comparison of $\bar{K}_w$ Values Determined Under Different Sampling Conditions.

Compound	Exp't. No.	$\bar{C}_i$[a] (μg/L)	Solution Type S[b] or M[c]	$\bar{K}_w$[d]	P[e]
Trichloroethene	3	28	S	17000	.05
	4	22	M	15000	

[a]Average cartridge influent concentration.
[b]Single-analyte solution, test solution contained only one compound.
[c]Multiple-analyte solution, test solution contained additional compounds.
[d]Average K_w value determined from four individual breakthrough curves.
[e]Probability, determined from the two-sample t-test (59), that the values in the two sample sets would occur if their arithmetic means were equal.
*$P \leq 0.01$, therefore a significant difference exists between the arithmetic means of the two sample sets.

the K_w values of one another. Bertoni et al. (73) have observed that in a multiple-analyte system of three compounds, one with a weak, one with a moderate and one with a strong affinity for the sorbent, the moderately retained compound was most adversely effected by competition for available adsorption sites, and the V_R of that compound was thereby decreased significantly.

The data that was obtained in this study did not exhibit the effects observed by Bertoni et al. (73). Two single-analyte ACB experiments were performed; experiment 2 for 1,1-dichloroethane, and experiment 3 for trichloroethene (see Appendices 2.1 and 2.2). 1,1-Dichloroethane was found to exhibit a V_R of approximately 2600 mL/g and so may be considered to be weakly to moderately retained by Tenax. Trichloroethene was found to exhibit a V_R of approximately 16,000 mL/g and therefore may be considered to be strongly retained. In experiment 4, ACB curves were obtained for both compounds in addition to 1,2-dichloroethane, trichloromethane and bromodichloromethane (see also Table 4.5). The $\bar{K}_w$ values obtained for 1,1-dichloroethane and trichloroethene with single- and multiple-analyte experiments were not found to be statistically significantly different (see Table 4.9). Figure 4.25 directly compares the ACB curves obtained for 1,1-dichloroethane in experiment 2 and experiment 4. Figure 4.26 directly compares the ACB curves obtained for trichloroethene in experiment 3 and experiment 4. For both compounds there was little difference in the ACB curves obtained in the single- and multiple-analyte experiments. Thus, it appears that

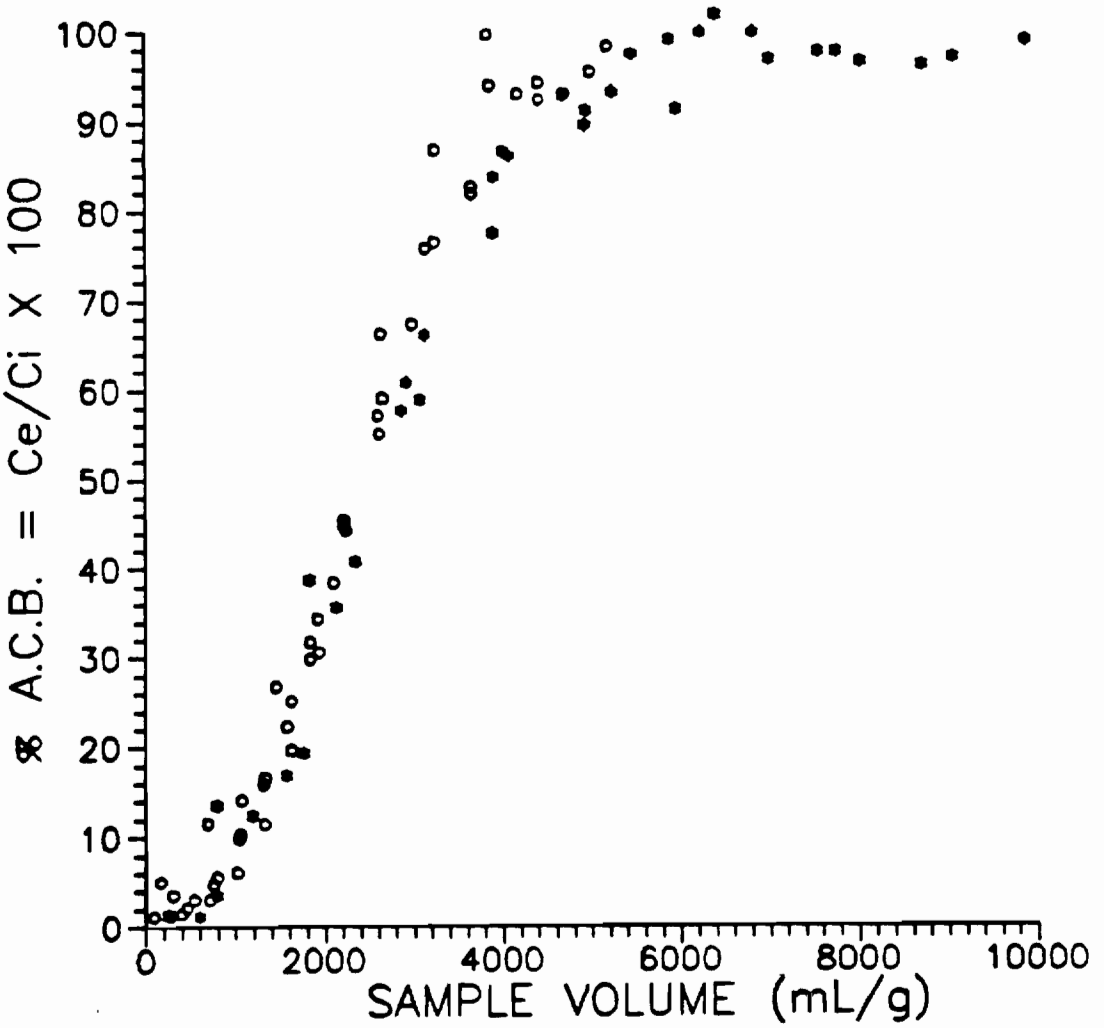

Figure 4.25. Direct comparison of ACB curves obtained for 1,1-dichloroethane from single- and multiple-analyte solutions. Each curve represents the combined results of four cartridges, and is normalized to individual sorbent bed weights. Therefore, sample volumes are expressed in terms of mL/g of sorbent. The results from the single-analyte solution (experiment 2) are plotted with stars and those of the multiple analyte solution (experiment 4) are plotted with circles. C_i = 26 ppb for both experiments.

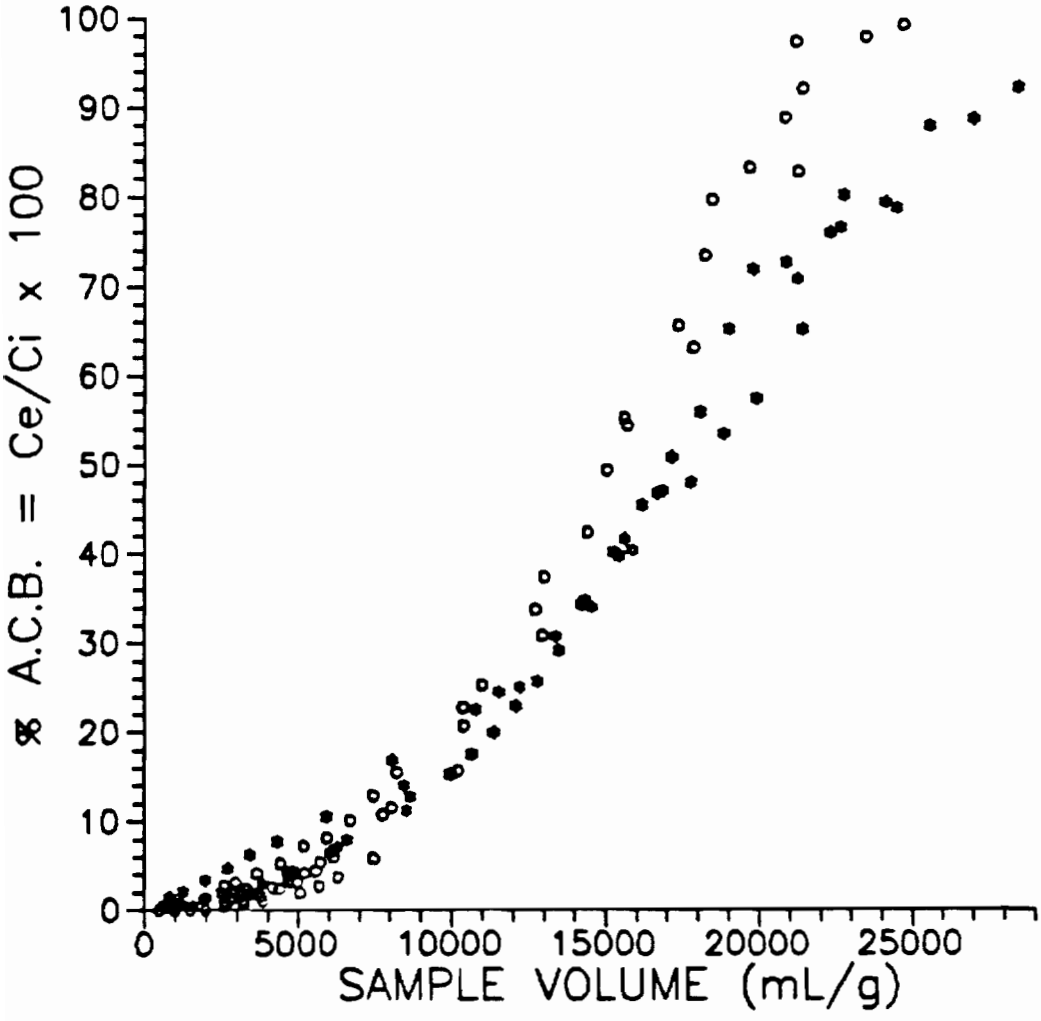

Figure 4.26. Direct comparison of ACB curves obtained for trichlorethene from single- and multiple-analyte solutions. Each curve represents the combined results of four cartridges, and is normalized to individual sorbent bed weights. Therefore, sample volumes are expressed in terms of mL/g of sorbent. The results from the single-analyte solution (experiment 3) are plotted with stars and those of the multiple analyte solution (experiment 4) are plotted with circles. C_i = 28 and 22 ppb for experiments 3 and 4, respectively.

there is no significant difference in the information provided by these single- and multiple-analyte ACB experiments. Based on this result, several compounds with varying retention affinities for Tenax were studied in single experiments. It may also be true, in addition to the two cases discussed, that other multiple-analyte systems are equivalent in ACB response to single-analyte systems.

4.3.8e Adsorbent Cartridge Breakthrough as a Function of Analyte Concentration

In order to determine whether the sampling efficiency of ATD for the PPPs is independent of concentration, it must be determined whether the K_w values of the compounds of interest remain constant over the sampling concentration range for which ATD is best suited (0 to 150 ppb). In addition, the concentration range over which the adsorption isotherm of the system is linear must also be determined so as to allow the proper use of models based on linear sorption (see Section 5.3).

As discussed previously, if the adsorption isotherm is linear, the slope of a plot of C_s (ng/g) vs. C_i (ng/g) will be constant and equal to the value of K_w. $K_w = C_s/C_i$, when the adsorption system has reached equilibrium. It is possible that at higher concentrations of analyte solutions, the sorbent bed will become overloaded. The overloading of the sorbent will be caused by a decrease in K_w and the system will be operating in a non-linear region of the adsorption isotherm. As such, premature analyte breakthrough will occur relative

to what occurs at lower concentration solutions, and shift the ACB curve to the left. Therefore, higher instantaneous percent breakthrough values per sample volume will result.

In experiment 5 the compounds examined were 1,1-dichloroethane, trichloromethane and 1,2-dichloroethane each at a C_i of ~130 ppb. Each compound had been examined previously in experiment 4 at a C_i of ~30 ppb. It was intended to determine whether there was a significant difference between ACB curves obtained at 30 and 130 ppb. A direct comparison of the ACB curves obtained for each compound in both experiments is presented in Figures 4.27-4.29. For each compound, the ACB curve determined at 130 ppb is shifted to the left of the curve determined at 30 ppb. For each of the three compounds, the K_w CV values remained below ~5.0% for both experiments (see Table 4.5). This indicated that at both concentrations the adsorption system operated reproducibly. However, according to the two-sample t-test results presented in Table 4.9, the K_w value determined for each compound at 130 ppb was significantly lower by 20% than those determined at 30 ppb. This implied that between 30 and 130 ppb, the adsorption isotherm is non-linear for 1,2-dichloroethane, 1,1-dichloroethane and trichloromethane. This was an unexpected result.

The total analyte concentration (the sum of the individual concentrations of the three compounds tested) was 400 ppb for experiment 5. The total analyte concentration for experiment 4 was 170 ppb, almost 2.5 times lower. This led to the hypothesis that the

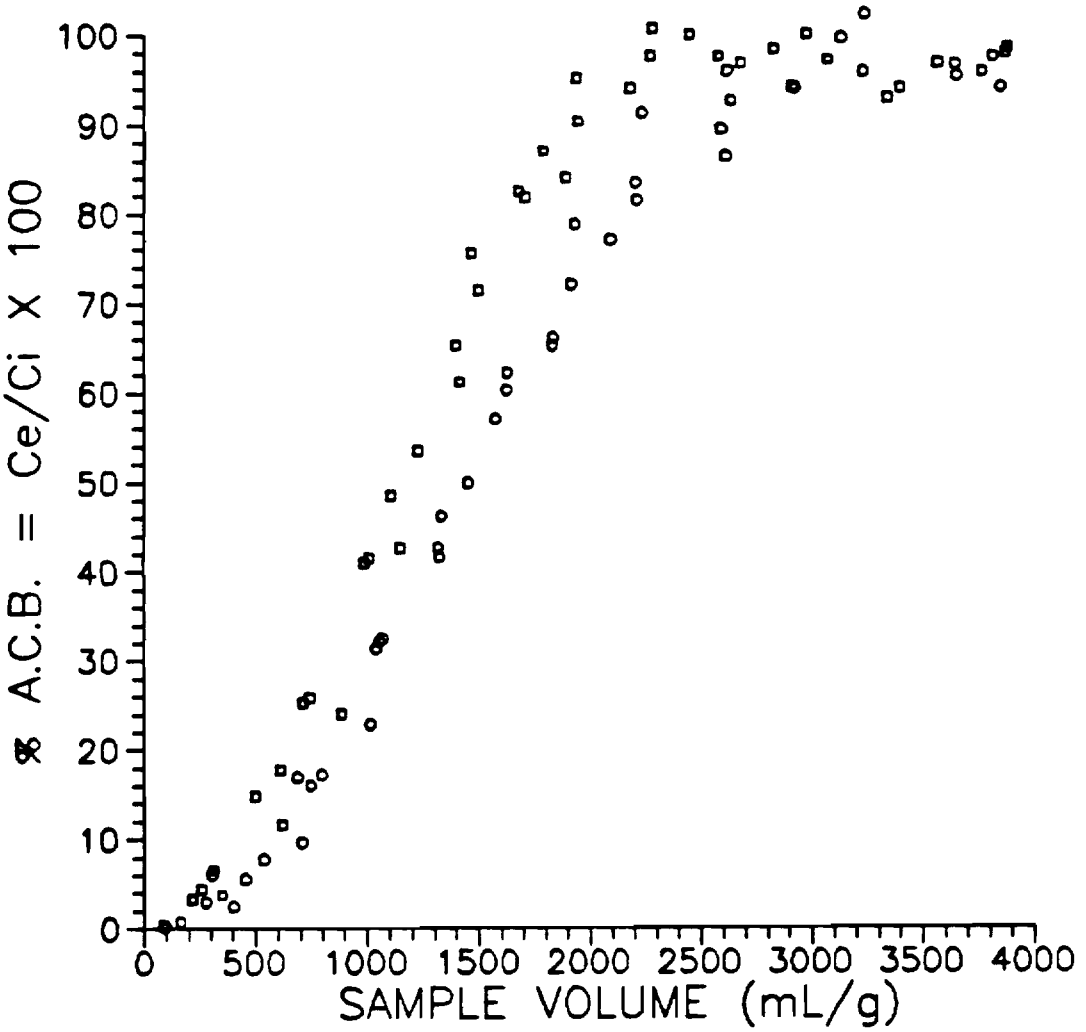

Figure 4.27. Direct comparison of ACB curves obtained for 1,2-dichloroethane at 27 and 120 ppb. Each curve represents the combined results of four cartridges, and is normalized to individual sorbent bed weights. Therefore, sample volumes are expressed in terms of mL/g of sorbent. The results obtained at 27 ppb (experiment 4) are plotted with circles. The results obtained at 120 ppb (experiment 5) are plotted with squares.

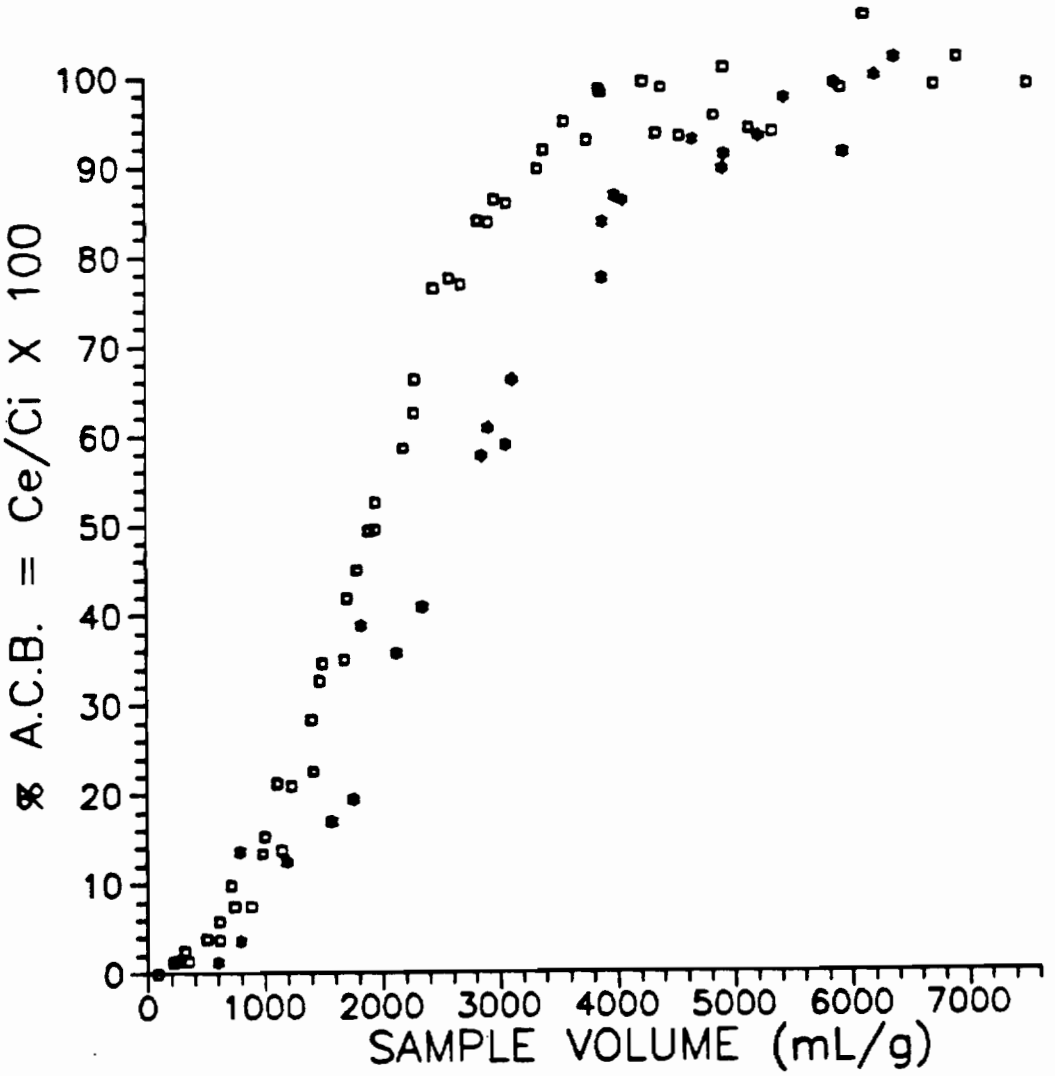

Figure 4.28. Direct comparison of ACB curves obtained for 1,1-dichloroethane at 26 and 140 ppb. Each curve represents the combined results of four cartridges, and is normalized to individual sorbent bed weights. Therefore, sample volumes are expressed in terms of mL/g of sorbent. The results obtained at 26 ppb (experiment 2) are plotted with stars. The results obtained at 140 ppb (experiment 5) are plotted with squares.

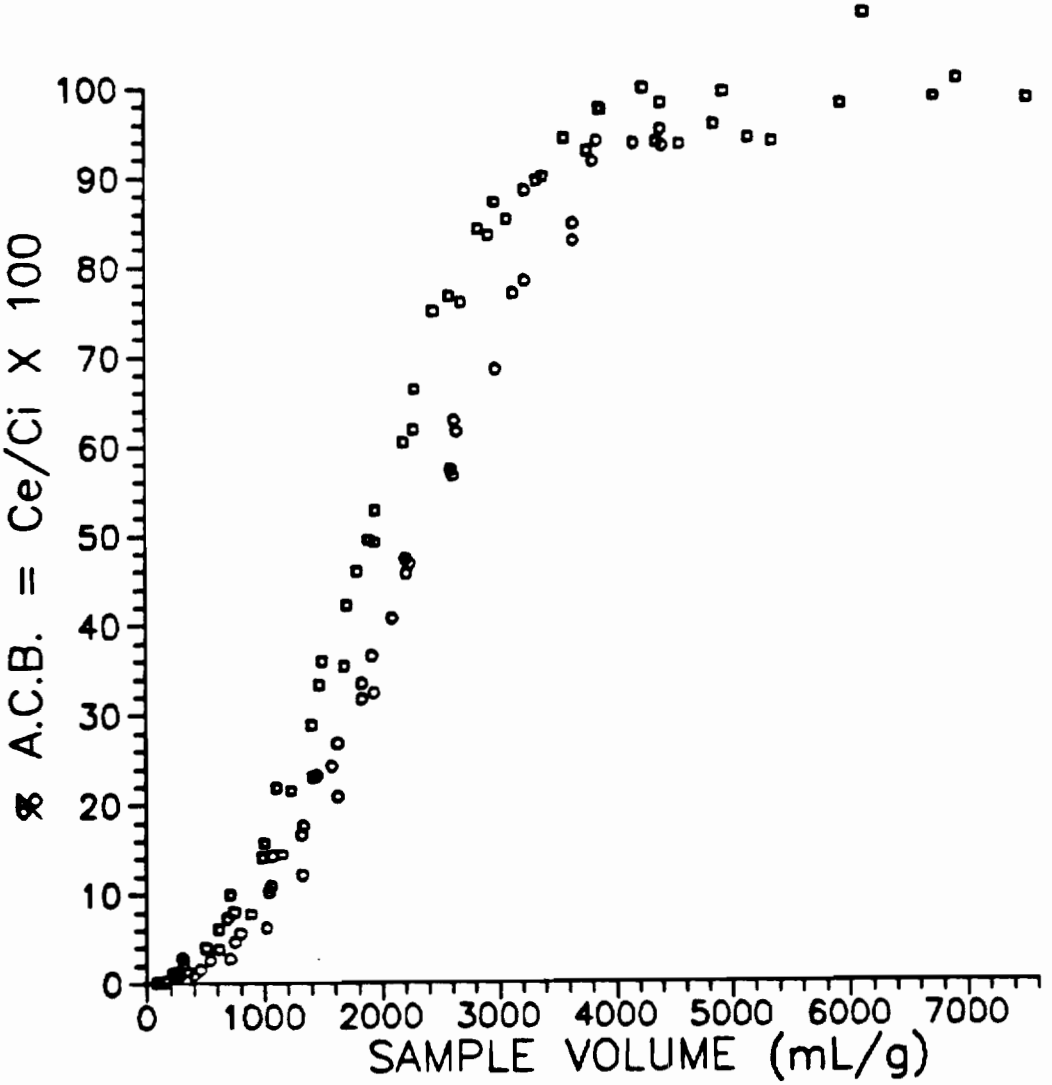

Figure 4.29. Direct comparison of ACB curves obtained for trichloromethane at 26 and 130 ppb. Each curve represents the combined results of four cartridges, and is normalized to individual sorbent bed weights. Therefore, sample volumes are expressed in terms of mL/g of sorbent. The results obtained at 26 ppb (experiment 4) are plotted with circles. The results obtained at 130 ppb (experiment 5) are plotted with squares.

adsorption isotherm between 30 and 130 ppb may be linear; however, the total analyte concentration in experiment 5 may have been too high and caused the sorbent bed to overload. This hypothesis was tested with experiments 7 and 8. It was first determined whether the adsorption isotherm was linear over a shorter concentration range, ~30 to 60 ppb. In experiment 7 ACB curves were obtained for three analytes each at a C_i of ~60 ppb. An ACB curve had previously been obtained in experiment 6 for each analyte at a lower concentration. In experiment 8 a single-analyte ACB curve was determined for trichloromethane at 130 ppb, in order to determine whether its $\bar{K}_w$ value at this concentration was significantly different from its value at 30 ppb (experiment 4).

For two of the three compounds tested in experiment 7, cis-1,2-dichloroethene and benzene, it was ascertained that there was no significant statistical difference between their $\bar{K}_w$ values determined at 60 ppb and at their lower concentrations in experiment 6, 25 and 1.3 ppb, respectively. The ACB curves obtained for each compound in both experiments are directly compared in Figures 4.30 and 4.31. For each compound, both curves appear to be almost identical.

It should be noted, however, that individual K_w values per cartridge were not determined for cis-1,2-dichloroethene in experiment 6 due to the collection of a limited number of data points per cartridge. A single K_w value of 1740, obtained from the curve as a whole, compared very well with the $\bar{K}_w$ value, 1800 $\pm$ 38, of experiment 7. Because $\bar{K}_w$ did not change significantly for

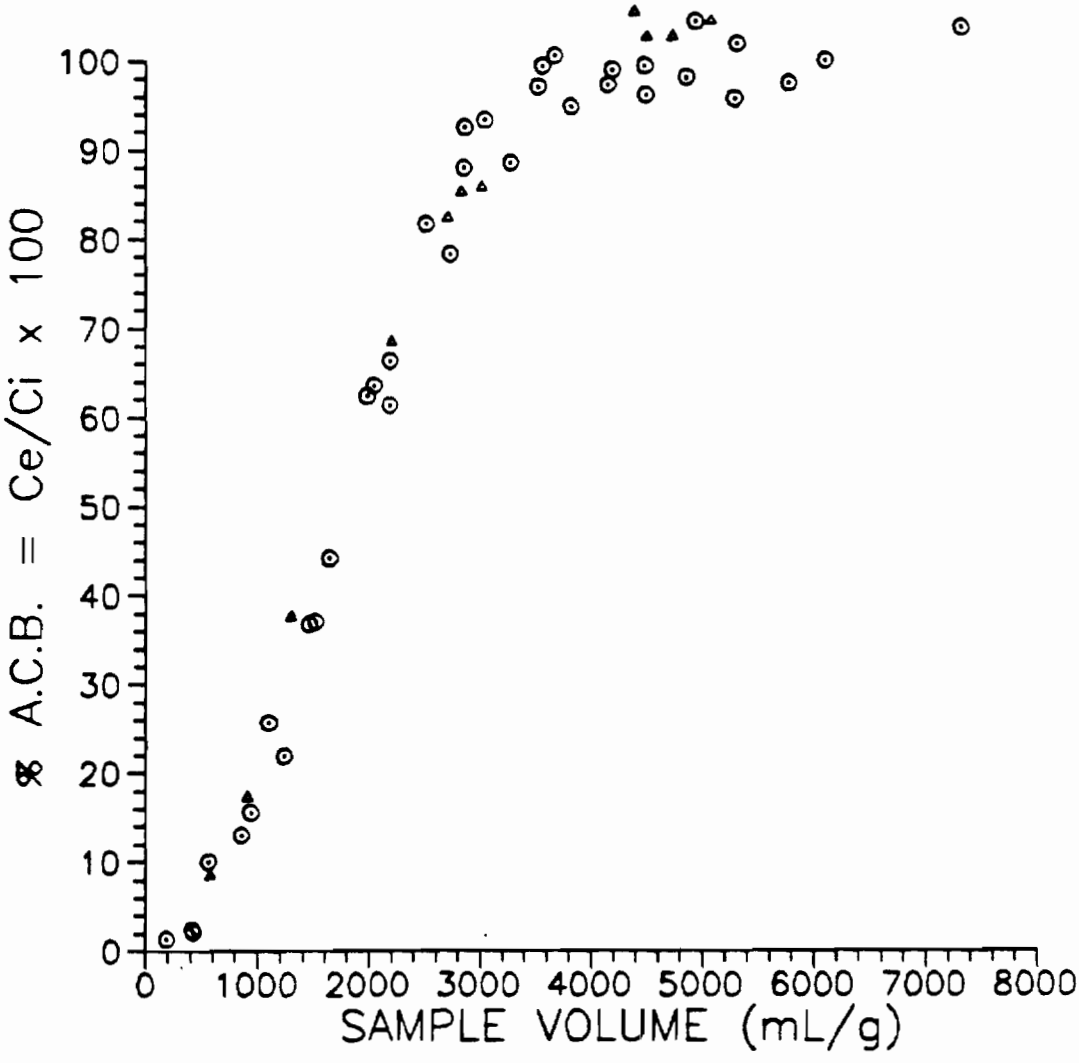

Figure 4.30. Direct comparison of ACB curves obtained for cis-1,2-dichloroethene at 25 and 59 ppb. Each curve represents the combined results of four cartridges, and is normalized to individual sorbent bed weights. Therefore, sample volumes are expressed in terms of mL/g of sorbent. The results obtained at 25 ppb (experiment 6) are plotted with triangles. The results obtained at 59 ppb (experiment 7) are plotted with dotted circles.

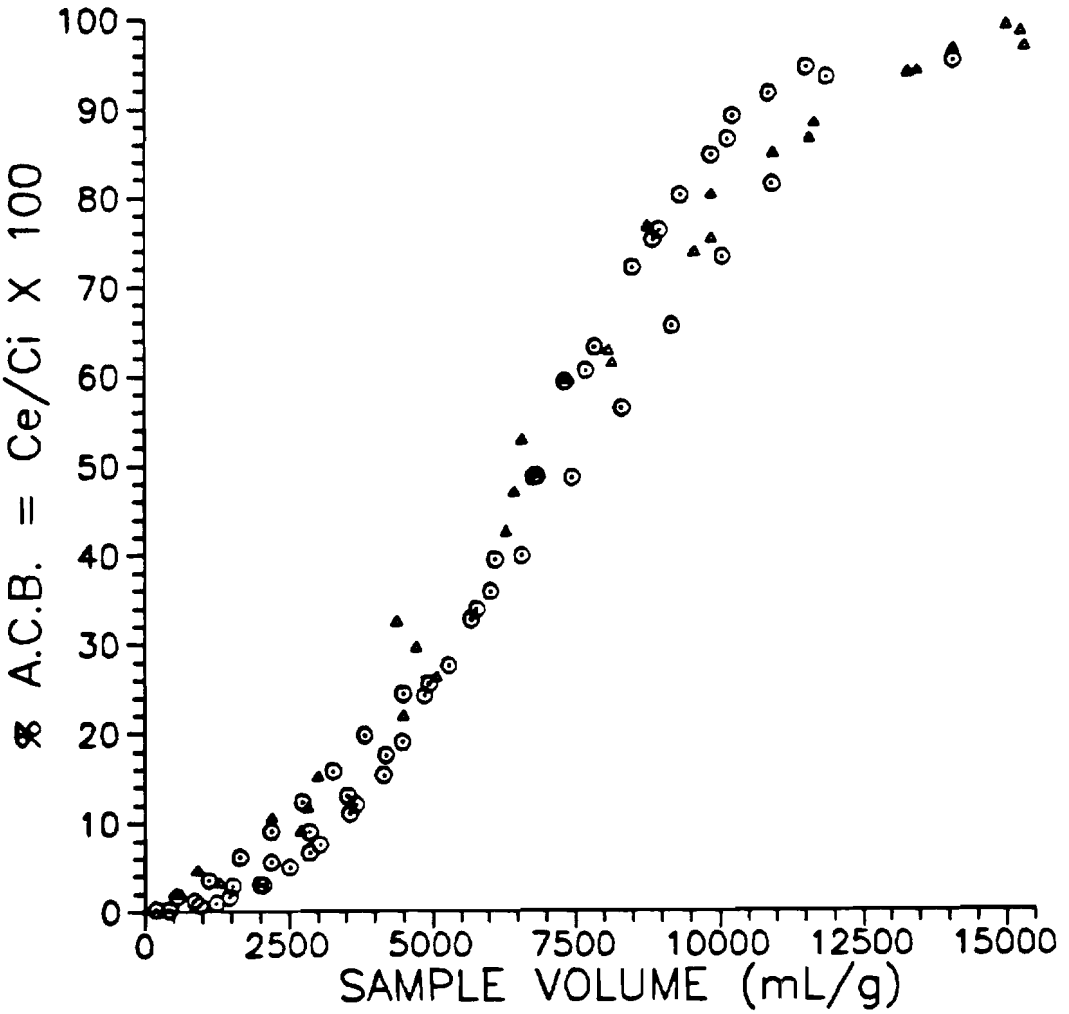

Figure 4.31. Direct comparison of ACB curves obtained for benzene at 1.3 and 55 ppb. Each curve represents the combined results of four cartridges, and is normalized to individual sorbent bed weights. Therefore, sample volumes are expressed in terms of mL/g of sorbent. The results obtained at 1.3 ppb (experiment 6) are plotted with triangles. The results obtained at 55 ppb (experiment 7) are plotted with dotted circles.

cis-1,2-dichloroethene from 30 to 60 ppb, or for benzene from 1 to 60 ppb, their adsorption isotherms are concluded to be linear for analyte concentrations up to 60 ppb.

According to the two-sample t-test results, the K_w value for trichloromethane at 60 ppb (experiment 7) was significantly lower by 7% than that value determined at 30 ppb (experiment 4). However, the K_w value of trichloromethane at 130 ppb (experiment 5) was 20% lower than its value at 30 ppb. Though a significant difference exists between the values of K_w for trichloromethane at 20 and 60 ppb, the absolute difference is relatively small. In addition, as discussed above, there was no significant difference between the values of K_w determined at 30 and 60 ppb for cis-1,2-dichloroethene or those determined at 1 and 60 ppb for benzene. The two ACB curves for trichloromethane at 30 and 60 ppb are directly compared in Figure 4.32. In addition to the other information, the fact that the two curves are almost identical leads to the conclusion that the adsorption isotherm is linear, from 30 to 60 ppb, for trichloromethane as well.

A single-analyte ACB curve was determined for trichloromethane at 130 ppb in experiment 8. The value of K_w for trichloromethane from that experiment was determined statistically (see Table 4.9) to be significantly lower by 8% than that determined at 30 ppb in experiment 4. However, in a manner similar to that discussed above, the following information should also be considered. The value of K_w for trichloromethane at 130 ppb in experiment 5 (the multiple-analyte

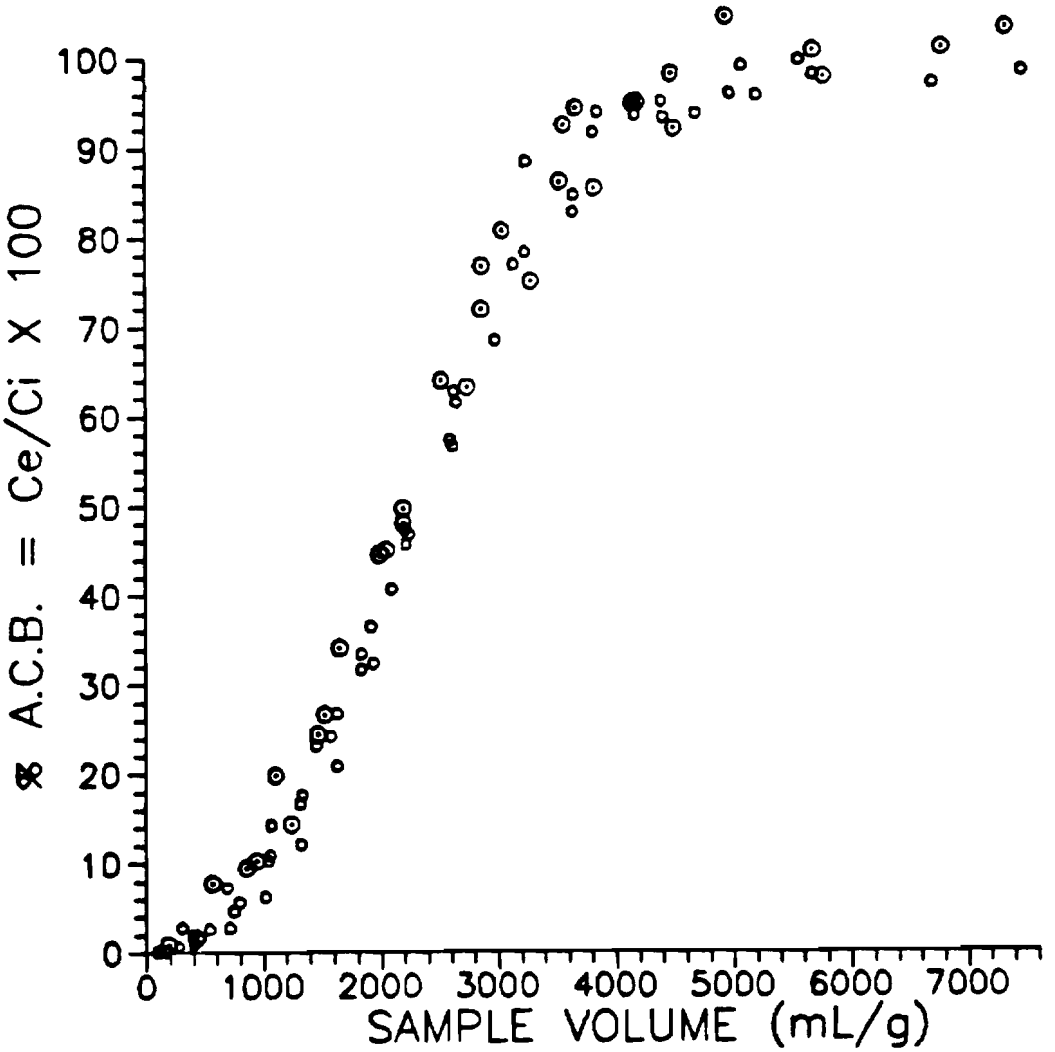

Figure 4.32. Direct comparison of ACB curves obtained for trichloromethane at 26 and 61 ppb. Each curve represents the combined results of four cartridges, and is normalized to individual sorbent bed weights. Therefore, sample volumes are expressed in terms of mL/g of sorbent. The results obtained at 26 ppb (experiment 4) are plotted with circles. The results obtained at 61 ppb (experiment 7) are plotted with dotted circles.

experiment with a total analyte concentration of 400 ppb) was 20% lower than that determined at 30 ppb. Also, there was no statistically significant difference between the $\bar{K}_w$ value of trichloromethane determined at 60 ppb in experiment 7 and that value determined at 130 ppb in experiment 8. The $\bar{K}_w$ at 130 ppb from experiment 5, however, was determined statistically to be significantly lower by 12% than the value determined at 130 ppb in experiment 8 (the single-analyte experiment). Figure 4.33 directly compares the ACB curves obtained for trichloromethane at 30 and 130 ppb (from experiments 4 and 8, respectively). In addition to the other information, the fact that the curves are almost identical leads to the conclusion that the adsorption isotherm for trichloromethane is also linear up to 130 ppb. Further, the results of experiment 5 could now possibly indicate that the sorbent capacity remains constant provided the total analyte concentration in solution remains below ~400 ppb.

Figure 4.34 presents a plot of C_s (ng/g) vs. C_i (ng/g) for trichloromethane with data obtained from experiments 4, 7 and 8. The trichloromethane C_i values range from ~30 to 130 ng/g. The slope of the line, determined from a linear regression analysis of the data, is 2100 (unitless). This value is within 7% of the $\bar{K}_w$ value for trichloromethane from the three experiments. The y-intercept of the line is relatively close to zero. The linear correlation coefficient $r^2 = 1.0$, is excellent and the regression equation is:

$$C_s = 4800 + 2100\ C_i \qquad 4.11$$

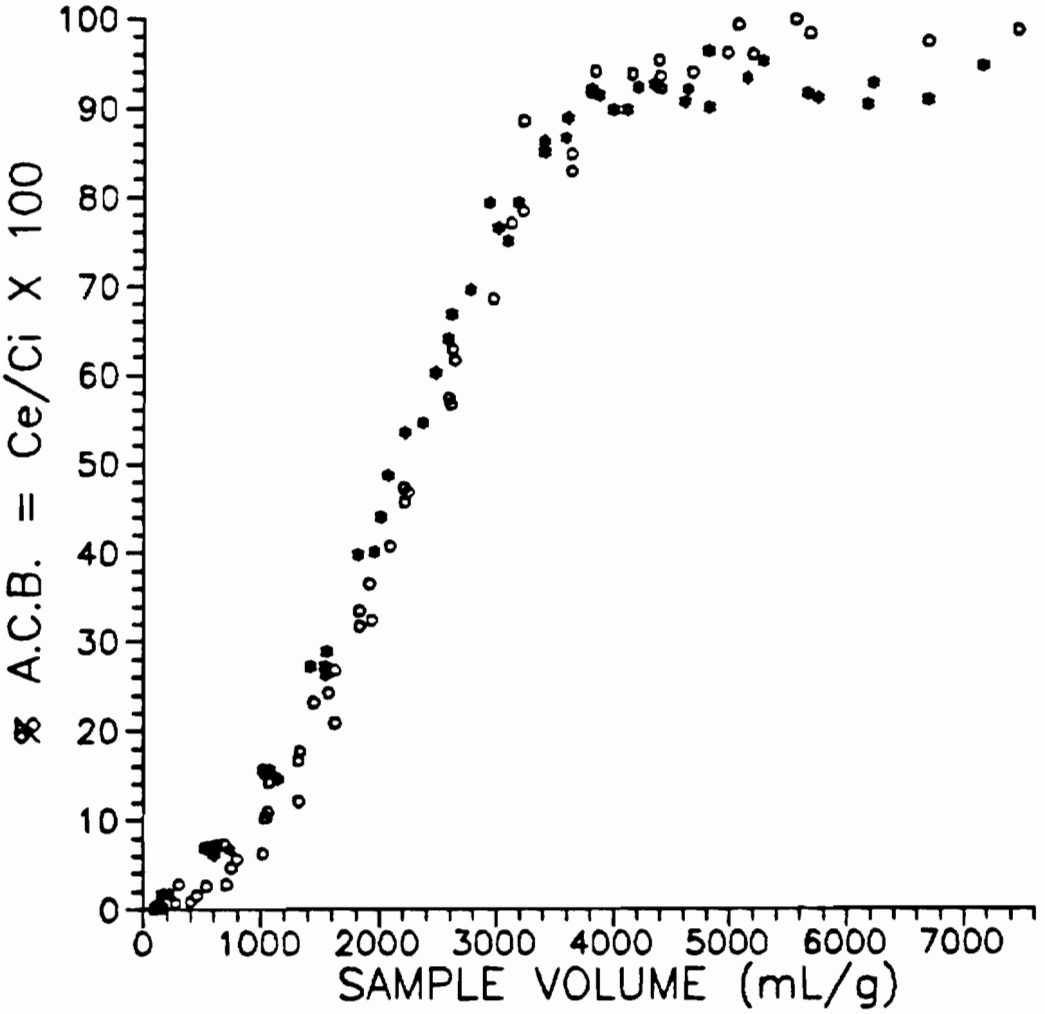

Figure 4.33. Direct comparison of ACB curves obtained for trichloromethane at 26 and 130 ppb (single analyte experiment). Each curve represents the combined results of four cartridges, and is normalized to individual sorbent bed weights. Therefore, sample volumes are expressed in terms of mL/g of sorbent. The results obtained at 26 ppb (experiment 4) are plotted with circles. The results obtained at 130 ppb (experiment 8, single-analyte experiment) are plotted with stars.

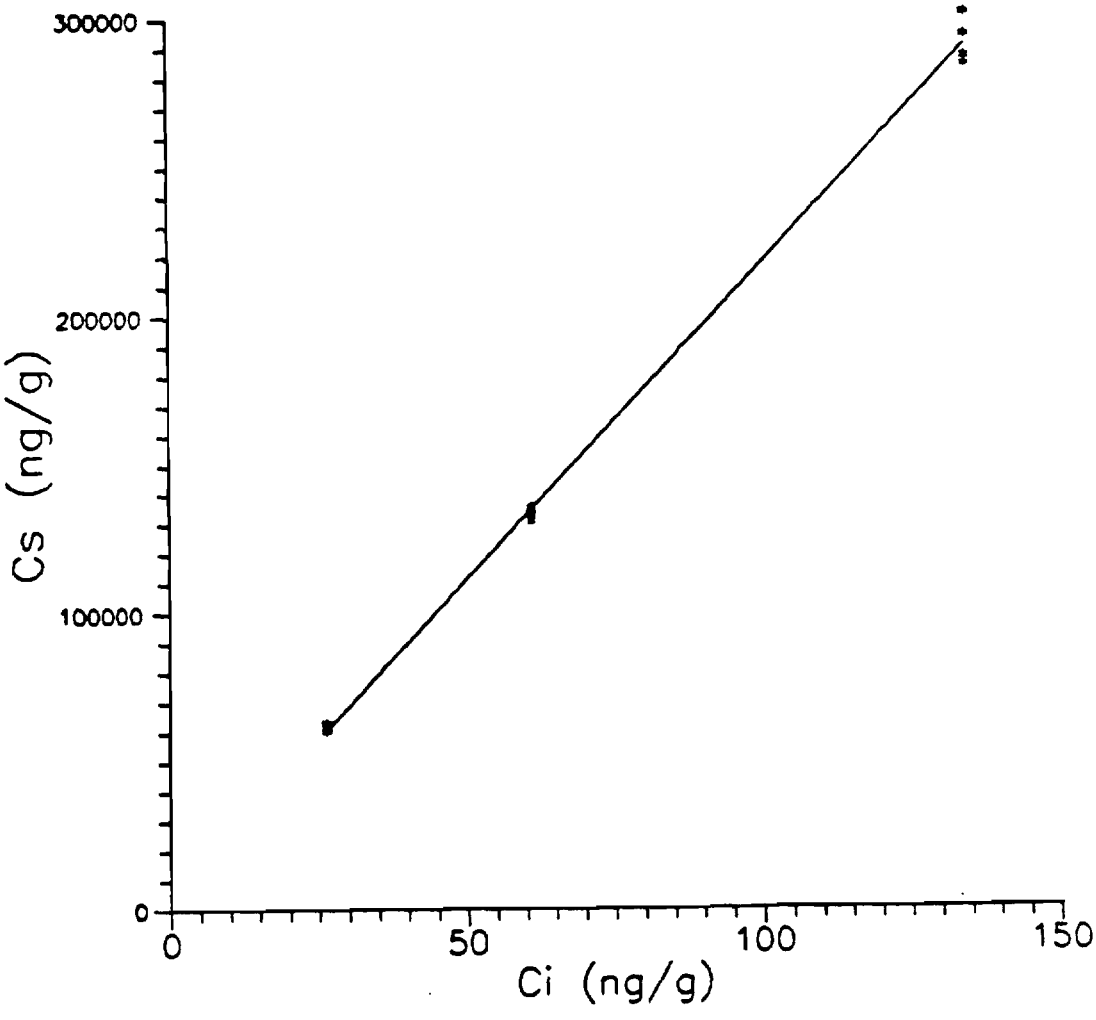

Figure 4.34. Plot of C_s vs. C_i for trichloromethane, from ACB experiments 4, 7, and 8. C_s represents the trichloromethane concentration in the Tenax bed at the 100% breakthrough point. C_i ranges from 30 to 130 ppb. Therefore, this plot represents the adsorption isotherm of trichloromethane for this concentration range. The solid line represents the linear regression equation $C_s = 4800 + 2100\ C_i$; $r^2 = 1.0$.

Considering that the adsorption isotherm for trichloromethane is linear over this range, in addition to the favorable results obtained for benzene and cis-1,2-dichloroethene for analyte concentrations up to 60 ppb, it is concluded that the adsorption isotherms of all the PPPs are likely to be linear for individual analyte concentrations of up to 150 ppb.

4.4 Conclusions

The 9 ACB experiments discussed have provided important information concerning the general performance and effective application of ATD for the sampling and analysis of trace quantities of the PPPs in water. Some important observations are listed:

(1) The adsorption isotherm of this system is linear for analyte concentrations of up to 150 ppb.

(2) When the total analyte concentration in water reaches ~400 ppb, the sorbent bed may become overloaded, causing a decrease in the sorbent bed capacity. However, the adsorption system still operates reproducibly.

(3) Provided the total analyte concentration in solution is below ~400 ppb, multiple-analyte solutions should not significantly affect individual analyte/sorbent interactions for most of the PPPs.

(4) The reproducibility of the adsorption system is excellent. On the average, the $\bar{K}_w$ CV, determined for each compound in seven ACB experiments, was ~5.0%.

(5) The adsorbent cartridge sampling efficiency was shown to be constant for a range of K_w values, for sample volumes corresponding to the 5, 10, 20 and 50% breakthrough points.

(6) ATD can be at least 26 to 300 times more sensitive (on an individual compound basis) than P&T/WCC for the analysis of most PPPs. The method sensitivity for these compounds is estimated to range from 3.3×10^{-3} to 3.8×10^{-2} ppb.

(7) A reasonable linear relationship has been shown to exist between log K_w and log K_{ow} for the PPPs. This relationship is defined by the following equation:

$$\log K_w = 1.3 + 1.2 \log K_{ow},\ r^2 = 0.89.$$

(8) A highly precise experimental system has been developed for the determination of ACB for varying concentrations of the PPPs in water.

CHAPTER 5 MODELING ADSORBENT CARTRIDGE BREAKTHROUGH

5.1 Introduction

The nine ACB experiments provided a great deal of information enabling the effective use of ATD for the sampling and analysis of PPPs in groundwater. Important additional information can be provided if it can be demonstrated that this fixed bed adsorption system (FBAS) can be modeled accurately. The ability to predict the response of such a system for a variety of compounds and sampling conditions (such as sampling flow rate and sorbent bed volume) will enhance the ability to effectively use ATD for the sampling and analysis of organic compounds in water.

The application of two different types of models to this system will be discussed. The first model is based on the principles of elution chromatography. The second model is much more rigorous in nature, and attempts to analytically describe the significant mass transfer phenomena which control an FBAS.

5.2 Application of the Principles of Linear-Elution Chromatography

5.2.1 Model Selection

Due to its simplicity, the following approach to the modeling of an FBAS has often been used. It is first noted that an adsorbent cartridge is simply a small chromatography column and therefore that the principles of liquid/solid linear-elution chromatography may be applied. In elution chromatography a narrow band of material is

placed at the head of a column. The material is usually composed of a mixture of unknown analytes. The intention is to separate and identify the components of the mixture. In this case, the material will be assumed to be composed of a single analyte. A mobile phase is passed through the column. The stationary phase in the column will be considered here to be a solid adsorbent material. As the band of analyte moves through the column, it partitions between the mobile and stationary phases. Both kinetic limitations in the bed and hydrodynamic dispersion act to cause the analyte band to spread out. As it finally elutes from the column, the width of the band of analyte material is measured in terms of a detector response over time.

If the resulting analyte peak may be approximated by a Gaussian curve, approximately 96% of its area falls within $\pm 2\sigma$ of the peak maxima. The peak width, W, is defined here as the elution volume required for 4σ of the peak zone to emerge from the column. The retention volume V_R, is the mobile phase volume (sample volume) V, required to elute the analyte peak maxima from the column. Therefore, when $V = V_R$, 50% of the analyte mass has eluted from the column. The column efficiency is defined in terms of W, by the following equation:

$$N = 16(V_R/W)^2 \qquad 5.1$$

N is the number of theoretical plates of the column. Thus, as N increases the efficiency of the column increases because the mass of analyte elutes from the column in a narrower band (W decreases).

The value of N for a given system has been found to depend on several physical/chemical parameters. Equations such as those derived by van Deemter (74) and Glueckauf (75) give N as a function of parameters such as K_w, mobile phase flow rate, and the physical characteristics of the stationary phase. Thus, these equations may be used to maximize N and therefore optimize the efficiency of a column. In a chromatographic elution analysis one is usually concerned with how peak width affects the ability to separate similar analytes i.e., analytes with similar values of V_R. However, in this study we are only concerned with how peak width contributes to the sampling efficiency of an adsorbent cartridge.

In adsorbent cartridge sampling a mobile phase with a constant concentration of analyte (the volume of water being sampled) is passed through a cartridge filled with an adsorbent material. The cartridge acts like a mini-chromatography column. A step input profile, which represents the concentration of analyte applied to the cartridge over volume, can be divided up into an infinite number of impulse peaks, each of which may be approximated by an ever broadening Gaussian curve as they elute through the cartridge. When the sample volume equals the retention volume, only 50% of the first impulse peak applied to the cartridge remains on the cartridge, see Figure 5.1. Therefore, if the analyte retention volume and the number of theoretical plates for the cartridge is known, one can predict the percent of the analyte mass retained on the cartridge at any point during sampling. Models of this type have been used periodically for the prediction of adsorbent

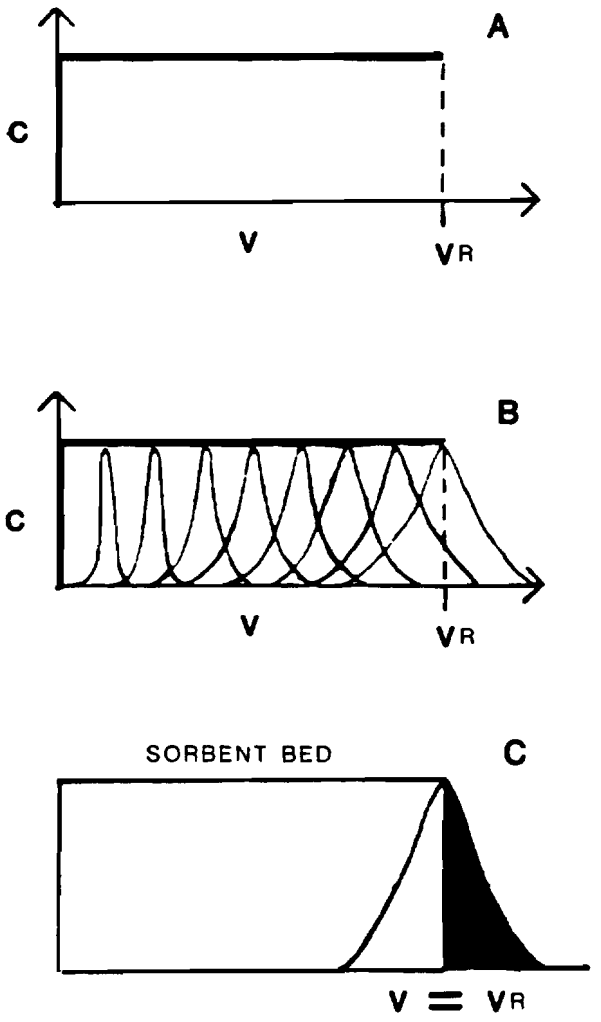

Figure 5.1. Adsorbent cartridge input profiles.
A A constant concentration (C) of analyte is applied to the cartridge per sample volume (V).
B The input profile can be approximated by the summation of an infinite number of impulse peaks, each of which may be approximated by an ever broadening Gaussian curve as they elute through the cartridge.
C When $V = V_R$, only 50% of the first impulse peak applied to the cartridge remains on the cartridge.

cartridge sampling efficiencies for a variety of adsorbents when sampling trace organic compounds in the atmosphere (76-81).

In 1963 Cropper and Kaminsky (76) developed a model which utilizes V_R and N and is capable of predicting adsorbent cartridge sampling efficiency for a specified sample volume. This model considers the case when $V = V_R$, and divides V into 100 arbitrary volume units. The cartridge is divided into 100 equal distance units. The model assumes that the sample loading is sufficiently low that the system is operating in the linear region of the adsorption isotherm. In this case each volume unit behaves independently of the others as it passes through the cartridge. Each of the peaks is assumed to be Gaussian in shape. Therefore when $V = V_R$, the first volume unit, i, added to the cartridge is centered exactly at the outlet of the cartridge (the 100^{th} distance unit) and is only 50% retained. The second volume unit added to the cartridge is greater than 50% retained and is centered on the 99^{th} distance unit of the cartridge, and so on.

Because each peak is considered to be Gaussian, the distribution of its area is determined by the Gaussian probability integral. The fraction of each of the 100 peaks which is not retained by the cartridge is given by the fraction of the area under the Gaussian probabilty integral for the portion of the peak which is outside the cartridge. Therefore the percent of the analyte which is not retained by the sorbent, Φ, in the 100 units sampled, is expressed by the following formula:

$$\Phi = \sum_{i=0}^{99} \{0.5 - \int_{0}^{i/\sigma} \exp\left(-\frac{u^2}{2}\right) du\} \qquad 5.2$$

where $\sigma = V_R/\sqrt{N}$.

For situations where only a fraction of the retention volume, f, is sampled; $V = fV_R$ and $0 < f \leq 1$, the following formula may be used to determine Φ:

$$\Phi = \frac{1}{f} \sum_{i=100(1-f)}^{99} \{0.5 - \int_{0}^{i/\sigma} \exp\left(-\frac{u^2}{2}\right) du\} \qquad 5.3$$

The adsorbent cartridge sampling efficiency E (%), is simply 100 - Φ.

Recently a correction in Cropper and Kaminsky's model has been made by Pankow and Rosen (82). V_R and N may be expected to vary linearly with column length and, therefore, it is incorrect to assume that σ is the same for each volume unit. As each unit i moves down the cartridge its peak sharpness degrades, and W increases. Therefore N and V_R are more accurately expressed in the following manner:

$$N_{i+1} = \left(\frac{100 - i}{100}\right) N \quad \text{and}$$

$$V_{R(i+1)} = \left(\frac{100 - i}{100}\right) V_R$$

Thus σ is now expressed as σ_{i+1}, and determined by the following equation:

$$\sigma_{i+1} = \left(\frac{100 - i}{100} \right)^{1/2} \cdot \left(\frac{V_R}{\sqrt{N}} \right) \qquad 5.4$$

The corrected version of the model simply substitutes σ_{i+1} into equations 5.2 and 5.3, where appropriate. On at least two occasions (79,80) Cropper and Kaminsky's model has been applied without this correction.

5.2.2 Calculation of Analyte Retention Volume and Analyte/Sorbent Theoretical Plates

If an ACB curve is symmetrical about the 50% breakthrough point, a symmetrical analyte peak would also be eluted from the adsorbent cartridge during a chromatographic elution analysis (78). Therefore ACB curves of this type may be used to accurately measure V_R values and also back out N values for an analyte-adsorbent system (77,78,83). The V_R for an analyte is given by the sample volume corresponding to the 50% breakthrough point. Analyte V_R values were determined from their ACB curves according to the procedure described in Section 4.3.6. The value of N is determined by the following formula (77):

$$N = 2\pi(V_R/\omega)^2 \qquad 5.5$$

where ω = the dispersion in the ACB curve; the distance in volume units between the sample volumes corresponding to the 5 and 95% breakthrough points.

5.2.3 Results and Discussion

Table 5.1 contains the V_R (mL/g), ω (mL/g) and N (unitless) values calculated for each compound for which at least one complete breakthrough curve was obtained (see Table 4.5). The values of N (calculated according to eqn. 5.5) range from 1.9 to 4.2, with an arithmetic mean, *s* and CV of 2.5, 0.71 and 28%, respectively. Thus the N values vary little, even for compounds with a large range of V_R values. Figure 5.2 is a plot of N vs. V_R. A linear regression analysis performed on the data shows there to be almost no correlation between the two variables, $r^2 = 0.0$.

The results of the Cropper and Kaminsky model as applied using Pankow and Rosen's corrections are displayed in Figure 5.3. The solid lines represent the model predictions for the adsorbent cartridge sampling efficiencies E (%), when the sample volume ranges from 5 to 100% of V_R, for N = 2, 3 and 4. Experimentally determined E values (see Section 4.3.8a) for six compounds with values of N ranging from 2 to 4 were also plotted, for sample volumes ranging from 0 to 100% of their V_R values. The model predictions agree very well with the experimental data, throughout the range of sampling volumes, and for compounds with a range of sorbent affinities. In general, the E values predicted by the model are within 5% of those values determined from the experimental data.

Recently, Lovkvist and Jonsson (84) have questioned the ability of models of the type developed by Cropper and Kaminsky to accurately relate the capacity of a sampling column to V_R and N, for systems

Table 5.1. Experimentally Determined V_R, ω and N Values.

Compound	V_R[a] (mL/g)	ω[b] (mL/g)	N[c]	Exp't(s).
1,2-Dichloroethane	1400	2300	2.4	4
cis-1,2-Dichloroethene	1800	3000	2.2	6,7
Trichloromethane	2200	3500	2.5	4,7,8
1,1-Dichloroethane	2500	4200	2.2	2,4
Bromodichloromethane	4700	7200	2.7	4
1,1,2-Trichloroethane	4900	8600	2.0	6
1,2-Dichloropropane	5900	10000	2.1	6
Benzene	6800	9200	3.4	6,7
Tribromomethane	12000	23000	1.9	6
1,1,2,2-Tetrachloroethane	16000	28000	2.0	6
Trichloroethene	16000	20000	4.2	3,4

[a]Sample volume which corresponds to the 50% breakthrough point, as determined from the combined breakthrough curves of the designated breakthrough experiments.
[b]Determined from the combined breakthrough curves of the designated breakthrough experiments.
[c]Calculated according to equation 5.5.

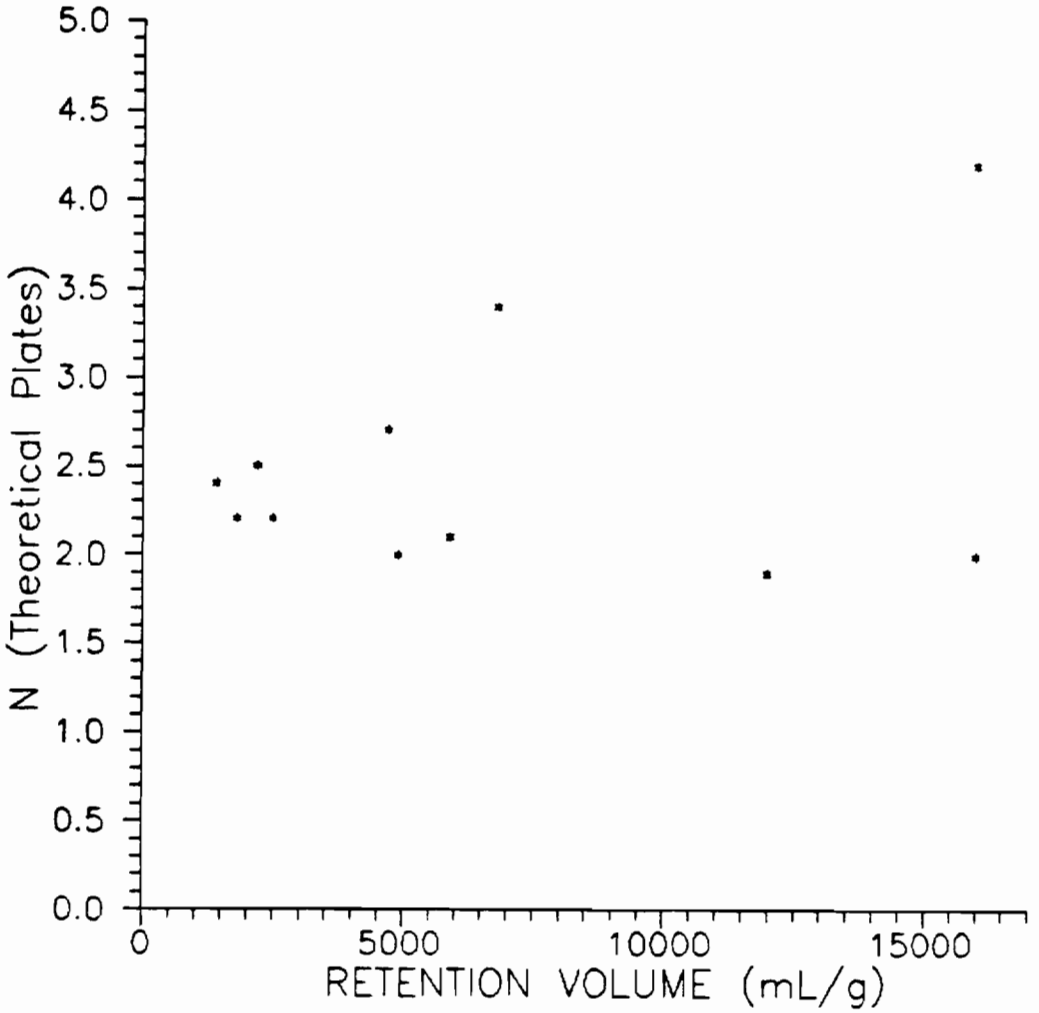

Figure 5.2. Plot of N vs. V_R. N (unitless) values were calculated according to eqn. 5.5 with information obtained from the ACB curves determined in experiments 2 through 8. All V_R and ω values used in eqn. 5.5 were expressed in units of mL/g of sorbent (see Table 5.1). A linear correlation coefficient $r^2 = 0.0$, was calculated for N and V_R.

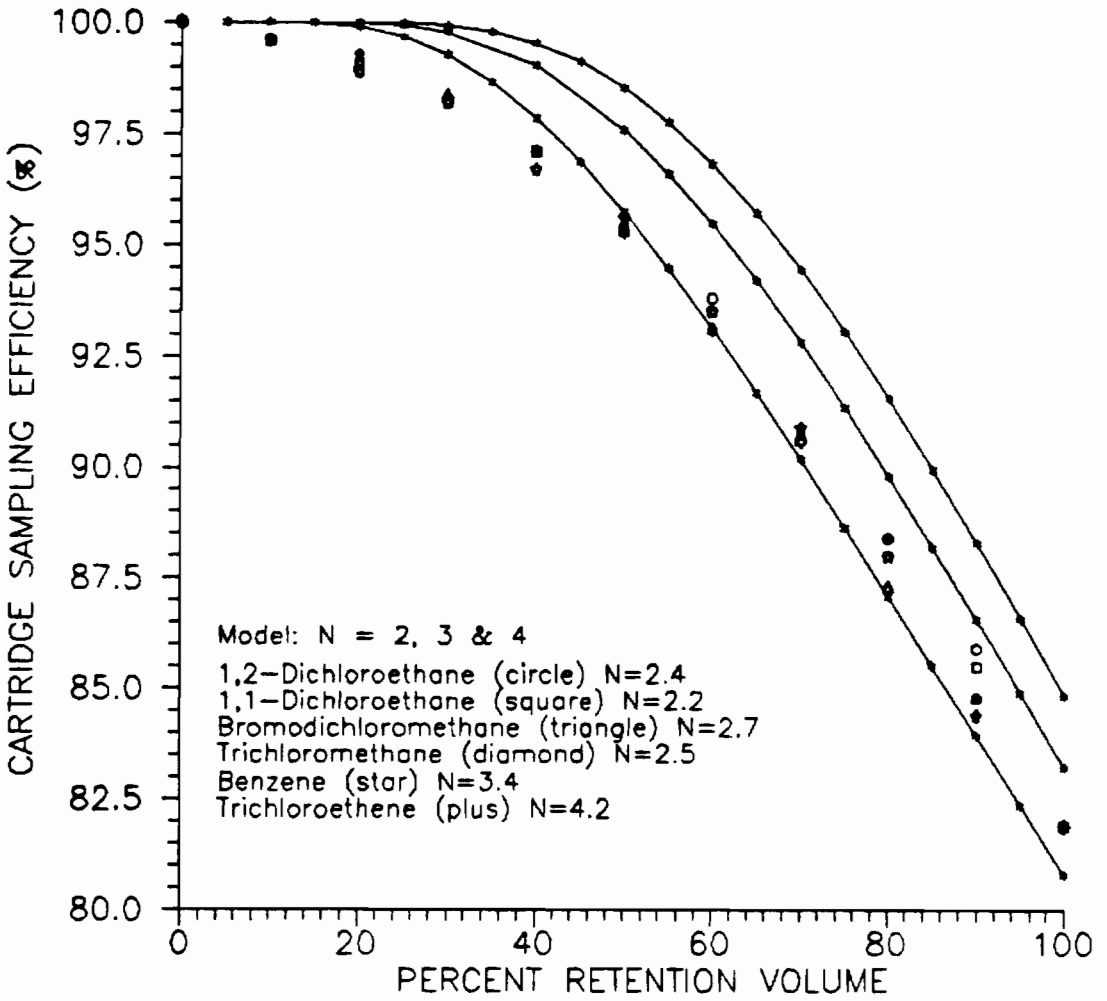

Figure 5.3. Plot of adsorbent cartridge sampling efficiency (E) vs. percent retention volume: a direct comparison of the Cropper and Kaminsky model results and experimental results. The solid lines represent values for E determined using the Cropper and Kaminsky model (with Pankow and Rosen's corrections), for N = 2 (lowest line), 3, and 4, and sample volumes ranging from 0 to 100% of V_R. Experimentally determined E values (see Section 4.3.8a) are also plotted for six compounds with values of N ranging from 2 to 4, and sample volumes ranging from 0 to 100% of their V_R values.

where N is less than 5. They believe that at low numbers of theoretical plates eluting fronts are not accurately described by the integral of a Gaussian curve. This however does not appear to be the case for the sampling system studied here. Thus, if the V_R and N values of this analyte-sorbent system are known, the corrected version of the Cropper and Kaminsky model may be used to accurately predict the adsorbent cartridge sampling efficiency over a range of sample volumes. It is important to note that for this FBAS, V_R and N will remain constant provided that individual analyte concentrations do not exceed 150 ppb and the total analyte concentration remains below ~400 ppb (see Sections 4.3.8d and 4.3.8e).

It should be possible to extend the use of this model by applying it to untested compounds. A relationship similar to the one between K_w and K_{ow}, discussed in Section 4.3.8c, should also exist between V_R and K_{ow} since K_w is proportional to V_R. As discussed in Section 4.3.6, K_w may be calculated from a knowledge of V_R, C_i and the mass of the sorbent bed. Therefore, it should be possible to predict the V_R values of untested PPPs, with reasonable accuracy. However, the <u>a priori</u> prediction of the corresponding N values does not appear to be possible. Nevertheless, the value of N varied little for the 11 PPPs studied. Therefore, it would seem reasonable to assume that N falls between 2 and 4, for most of the PPPs and this system. The use of this assumption together with a predicted V_R may be used with the modeling results presented in Figure 5.3 for the prediction of adsorbent cartridge sampling efficiencies for a range of sampling

volumes. In general, it appears that a sample volume which is equal to $0.5V_R$ will produce an E value of greater than 95% for most of the compounds tested.

As the physical characteristics of the sorbent bed and the sample flow rate change, the efficiency with which the analyte partitions to the sorbent will also change (75,85). Therefore the value of N may change under these new sampling conditions. Thus additional ACB experiments may be necessary to determine N, in order to accurately apply Cropper and Kaminsky's model. A more rigorous modeling approach however, such as the one discussed in the following sections, may be able to more easily account for such changes in the FBAS.

5.3 Application of the Principles of Mass Transfer Phenomena

5.3.1 Model Selection

In an FBAS a partitioning process occurs whereby the compound (adsorbate) is transferred from the solution (mobile) phase to the surface of the solid sorbent (stationary) phase. The adsorbate accumulates in the sorbent for subsequent extraction. In order to predict the concentration vs. volume relationship of the effluent stream (i.e., the ACB curve) the following mass transfer phenomena of this system must be considered: axial (longitudinal) dispersion, mass transfer to the particle surface, mass transfer within the particle, and sorption-desorption kinetics. In 1952, J. Rosen (86) developed a model which considered the sorption process to occur in three distinct stages:

(1) Diffusion of the adsorbate from the flowing water to the external surfaces of the sorbent particles (external or film diffusion).

(2) Diffusion through the porous network of sorbent particles (internal diffusion).

(3) The sorption process itself, when the adsorbate is bound on a sorption site of the sorbent (87).

J. Rosen used solute continuity equations to describe these phenomena for the mobile and stationary phase concentrations expressed as functions of time, and the axial and intraparticle radial positions in the sorbent bed (88). The exact solution to the system of differential equations corresponding to the diffusional resistances was facilitated by their transformation into the Laplace-domain and their subsequent inversion by a method of complex integration (86,89).

Eqn. 5.6 is a reduced version J. Rosen's exact solution (86,90). In eqn. 5.6 three dimensionless parameters χ, ϑ, and ξ, are used to calculate C_e/C_i as a function of sampling time or sample volume for an FBAS.

$$\frac{C_e}{C_i} = \frac{1}{2}\left[\, 1 + \operatorname{erf}\left(\frac{\frac{3\vartheta}{2\chi} - 1}{2\sqrt{\frac{1 + 5\xi}{5\chi}}} \right) \right] \qquad 5.6$$

where:

$$\chi = \text{bed length parameter} = \frac{3\bar{D}K_w z}{v_s r^2}\left(\frac{1 - p_t}{p_t}\right)$$

ϑ = contact time parameter = $\frac{2\bar{D}}{r^2}\left(t - \frac{z}{v_s}\right)$

ξ = film resistance parameter = $\frac{K_w \delta \bar{D}}{rD}$ and,

A_b = sorbent bed cross-sectional area (cm^2)

D = diffusion coefficient in the liquid phase (cm^2/s)

$\bar{D}$ = diffusion coefficient in the solid phase (cm^2/s)

p_e = interbead bed porosity (unitless)

p_a = intrabead bed porosity (unitless)

p_t = total bed porosity (= $p_e + p_a$) (unitless)

Q = sample volume flow rate (cm^3/s)

r = radius of sorbent particle (cm)

t = elapsed sampling time (s)

v_s = "superficial" linear velocity (= $Q/(p_e A_b)$) (cm/s)

z = length of sorbent bed (cm)

δ = thickness of stagnant liquid film surrounding a sorbent particle in a flowing system (= $0.2r/(1.0 + 70rv_s)$) (75,85) (cm).

According to the use of the model, the dimensionless bed length parameter χ has been calculated in slightly different ways in the literature (90-94). This parameter calculates the effective length of the sorbent bed. For this application, its most suitable form is as defined above (87-89).

The primary assumptions of J. Rosen's model are as follows:

(1) The mobile phase contains a single solute at a constant concentration.

(2) The diameter of each bed particle is small in comparison with overall bed dimensions and the porous medium is macroscopically uniform.

(3) The sorbent particles are considered to be spherical and monoporous (each sorbent particle is considered to have only one homogeneous porous structure (89)).

(4) The sorption equilibrium relationship, describing the intraparticle solute concentration as a function of external solute concentration, is linear.

(5) Local equilibrium is attained very rapidly, with the movement of solute within the particles described mathematically by Fick's First Law of Diffusion, where the effective particle diffusion coefficient is considered constant and independent of concentration.

(6) Axial/longitudinal dispersion within the bed is considered to be negligible (87,89).

Although J. Rosen's model was developed over three decades ago it has received considerable attention and use. J. Rosen has been credited with providing one of the first, as well as one of the best, models for an FBAS in which external and intraparticle diffusional resistances to mass transfer are dominant (87,88,92-108). J. Rosen's work has also been successfully used for several FBAS modeling applications (88,91,94,102). Additionally, J. Rosen's original work has been extended by others to provide solutions for systems with reactive solutes (109), bipore (each sorbent particle is considered to have a double porous structure: a macroporosity and a microporosity,

as with Zeolite sorbents (92)) systems (89), systems in which longitudinal dispersion may be significant (110,111), systems with generalized-linear, non-linear or Langmuir-type adsorption equilibrium relationships (98), and multiple-analyte systems (98).

Several points should now be addressed concerning the applicability of J. Rosen's model to an FBAS composed of a bed of Tenax used in a sampling stream of water. J. Rosen's model was intended for single-analyte adsorption systems operating within a concentration range for which the adsorption isotherm of the system is linear. For the PPPs, the ACB experiments conducted here have established that adsorption isotherms are likely to be linear for individual analyte concentrations of up to 150 ppb. Therefore J. Rosen's model in its original form as developed for linear sorption systems, should adequately define the response of this system for individual analyte concentrations below ~150 ppb. However, it would be unusual to encounter a single-analyte system in the environment. For the PPPs, the ACB experiments also showed that the capacity of the sorbent bed is likely to remain unchanged, whether analytes are sampled individually or in groups with analytes of varying sorbent affinities (provided that the total analyte concentration remains below ~400 ppb). Thus, it is reasonable to apply J. Rosen's model to a multiple-analyte system of this nature.

Finally, J. Rosen's model assumes that in a FBAS the resistance to mass transfer due to longitudinal dispersion is insignificant. Longitudinal dispersion is the tendency of analyte dispersion to occur

due to diffusion of the analyte while it is in the mobile phase. As a general rule, the effects of longitudinal dispersion are believed to be relatively insignificant in packed beds except where the sorbent bed length is less than 20 particle diameters (94). Assuming an average particle diameter of 1.1×10^{-2} cm for 60/80 mesh Tenax, the length of the sorbent bed of this system is 250 times that of the particle diameter. Therefore, the assumption that longitudinal dispersion is negligible may be reasonable.

5.3.2 Model Calibration

In situations where an experimental data set exists which defines an FBAS, the technique of model parameter estimation may be used in order to increase the accuracy of the model for the system to which it is being applied. This technique essentially "calibrates" the model by varying key modeling parameters until the ACB curve predicted by the model fits the experimentally determined ACB curve. This produces "effective" model parameters for the system in question (83,97,112). Using the results from ACB experiments 2 through 8, two model parameters (D, diffusion coefficient in the liquid phase and p_t, total bed porosity) were estimated. Starting with values that made physical sense with respect to this system, these parameters were adjusted individually until the closest fit of the ACB curve predicted by the model to the experimental ACB curve was obtained.

The total bed porosity, p_t, consists of the sum of the interbead and intrabead porosity, p_e and p_a, respectively. For the 32

cartridges used in the eight ACB experiments, the mean sorbent bed weight was 0.129 g $\pm$ 0.006 g (see Table 4.1). It may be assumed that Tenax, a porous polymer of poly-para-2,6-diphenylene oxide, has a density in the range of 0.85 to 1.0 g/mL. Tenax particles are roughly angular and therefore the interparticle porosity of the sorbent bed is approximately 0.40 (113). Thus, for a cartridge with a bed volume of 0.68 cm^3 the total volume of the interbead voids is calculated to be 0.27 cm^3. The total volume of intraparticle voids ranges from 0.26 to 0.28 cm^3. Therefore, the total bed porosity is estimated to range from 0.78 to 0.81.

Using eqn. 5.6, ACB curves were generated for K_w = 6800 (the K_w for benzene from experiments 6 and 7) and the range of p_t specified. The other model parameters were held constant. As p_t is varied, the dispersion of the ACB curve remained constant while the sorption capacity of the bed fluctuated. As p_t was increased, the percent breakthrough per sample volume increased. For p_t = 0.78 to 0.81 the model predicted premature breakthrough relative to the two experimental ACB curves obtained for benzene. For this reason, the total porosity was lowered to 0.70. At p_t = 0.70 the breakthrough curve of the model predicted the 50% breakthrough point to occur at a sample volume of ~850 mL. This closely agrees with the two experimental breakthrough curves obtained for benzene. An interbead bed porosity of p_e = 0.44 was used for the calculation

of the superficial flow velocity (v_s) through the bed. Values for p_e ranging from 0.35 to 0.45 have been used for other similar FBASs (92,97,112,114).

A liquid phase diffusion coefficient, $D = 8.0 \times 10^{-6}$ cm^2/s (115) was originally used for benzene. Although this value produced an ACB curve of the same general shape as those from experiments 6 and 7, the ACB curve predicted by the model had greater dispersion than the experimental ACB curves. This dispersion decreased when D was increased to 1.6×10^{-5} cm^2/s. For this value of D the model very closely approximated the dispersion in the experimental ACB curves obtained for benzene. Liquid/liquid diffusion is a slow process, and is also not expected to vary significantly for the range of organic compounds of interest here, because their D values should fall into a narrow range (1 to 2×10^{-5} cm^2/s) (116). Therefore $D = 1.6 \times 10^{-5}$ cm^2/s was used for all the PPPs modeled.

For the solid diffusion coefficient, $\bar{D}$, a value of 3.0×10^{-7} cm^2/s was selected. This value has been suggested by Helfferich (91). The model appears to be very insensitive to fluctuations in this parameter. There is no significant change in the dispersion of the ACB curve produced by the model for values of $\bar{D}$ ranging from 3.0×10^{-6} to 3.0×10^{-8} cm^2/s.

The particle radius, r, for the 60/80 mesh Tenax used in this system was set equal to 1.1×10^{-2} cm. This value equals the

arithmetic mean of the minimum and maximum particle radii in the 60/80 mesh range. This approximation for r has been used for the modeling of other FBASs (113,117,118).

To summarize, the following model parameters were used in eqn. 5.7 for the prediction of an ACB curve for benzene:

$A_b = 0.13\ cm^2$

$D = 1.6 \times 10^{-5}\ cm^2/s$

$\bar{D} = 3.0 \times 10^{-7}\ cm^2/s$

$K_w = 6800$ (the $\bar{K}_w$ for benzene from experiments 6 and 7)

$p_t = 0.70$

$p_e = 0.44$

$Q = 0.033\ cm^3/s$ (2.0 mL/min)

$r = 1.1 \times 10^{-2}\ cm$

$v_s = 0.38\ cm/s$

$z = 5.4\ cm.$

5.3.3 Results and Discussion

Figure 5.4 directly compares the ACB curve produced by the model with the experimental curves obtained for benzene from experiments 6 and 7. The ability of the calibrated model to accurately predict ACB can be judged by how well the model curve fits an experimental curve when they are plotted together (94,98,100,102,104,112,117,119-124). For benzene, the model very closely approximates the experimental results. Using the same modeling parameters listed in the previous section, ACB curves were generated for an additional 5 compounds

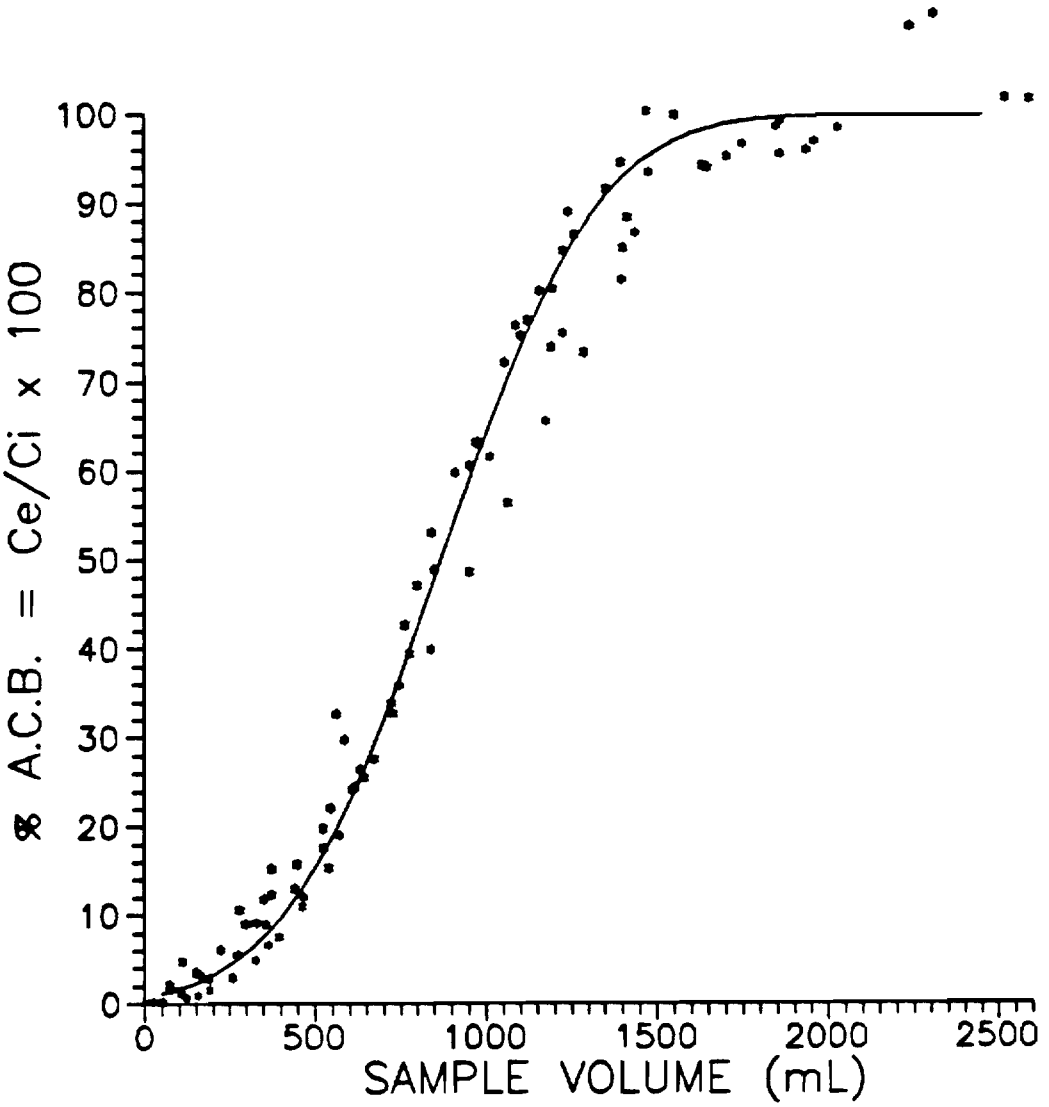

Figure 5.4. Direct comparison of experimental ACB results and the ACB results of the J. Rosen model for benzene. The solid line represents the ACB curve generated using an experimentally calibrated version of the J. Rosen model (eqn. 5.6, also see Section 5.3.2) and a K_w value of 6800 ($\overline{K}_w$ for benzene from experiments 6 and 7). The experimental data, plotted with stars, was obtained from experiments 6 and 7.

(using their experimentally determined K_w). In Figures 5.5-5.9 the model curves are directly compared with the appropriate experimental ACB curves of each compound. The six compounds represent a range of sorbent affinities from 1,2-dichloroethane (K_w = 1400) to trichloroethene (K_w = 16,000). In each case the model results accurately approximate the experimental results over the entire range of the adsorption process. A model which adequately predicts the entire range of the adsorption process for an FBAS with which it is calibrated, is likely to be as reliable when using system parameters which are outside the calibration range of the model (98). It is therefore likely that J. Rosen's model, calibrated in this manner, can adequately predict ACB for all the PPPs under a variety of sampling conditions.

5.4 Conclusions

The application of information provided by the nine ACB experiments discussed, has allowed the investigation of the use of two models designed for the prediction of ACB. Both models may be applied to a fixed bed adsorption system which is operating in the linear region of its adsorption isotherm. The FBAS in this study appears to operate linearly for the PPPs in water, provided that individual analyte concentrations are less than ~150 ppb and the total analyte concentration of the solution remains below ~400 ppb. Therefore, when these conditions are met, the following conclusions concerning the use of these models are valid.

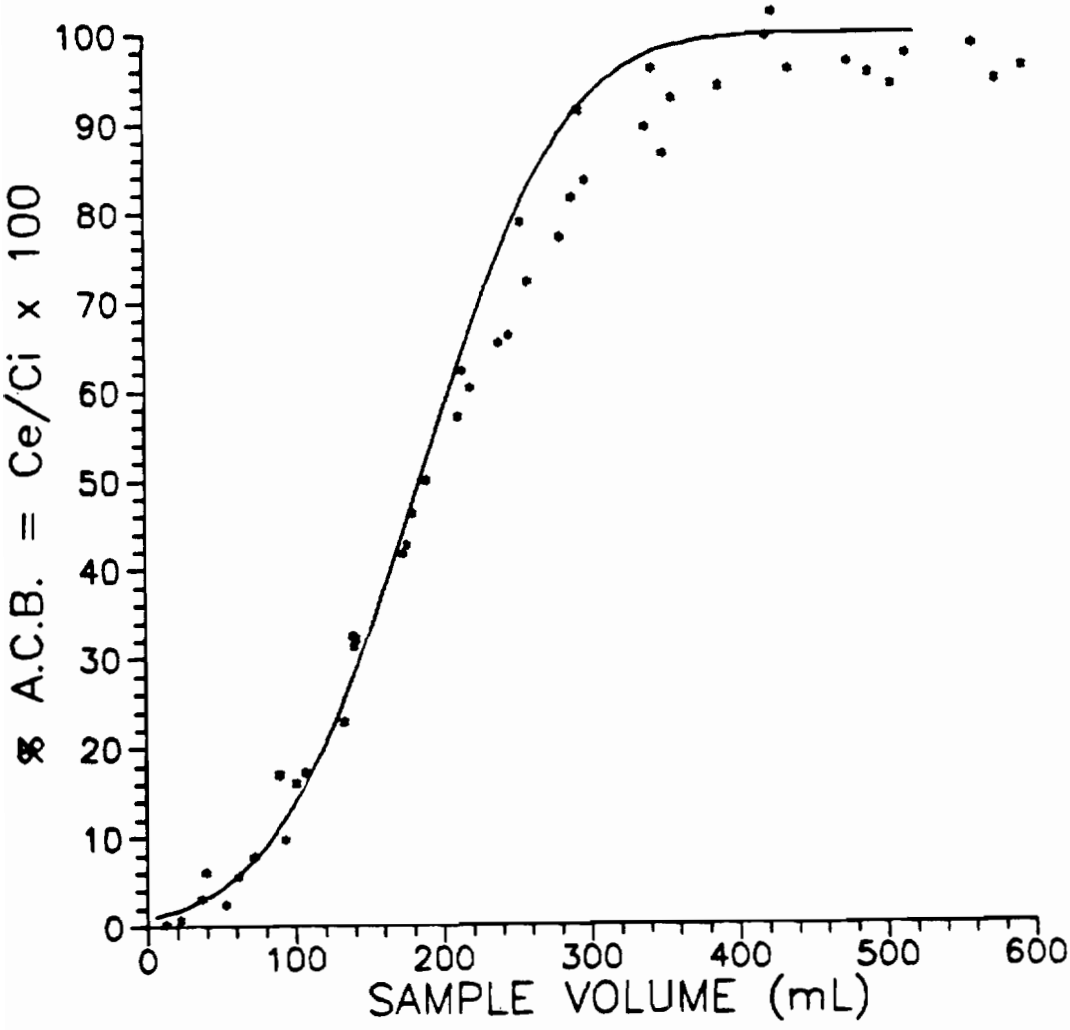

Figure 5.5. Direct comparison of experimental ACB results and the ACB results of the J. Rosen model for 1,2-dichloroethane. The solid line represents the ACB curve generated using an experimentally calibrated version of the J. Rosen model (eqn. 5.6, also see Section 5.3.2) and a K_w value of 1400 (K_w for 1,2-dichloroethane from experiment 4). The experimental data, plotted with stars, was obtained from experiment 4.

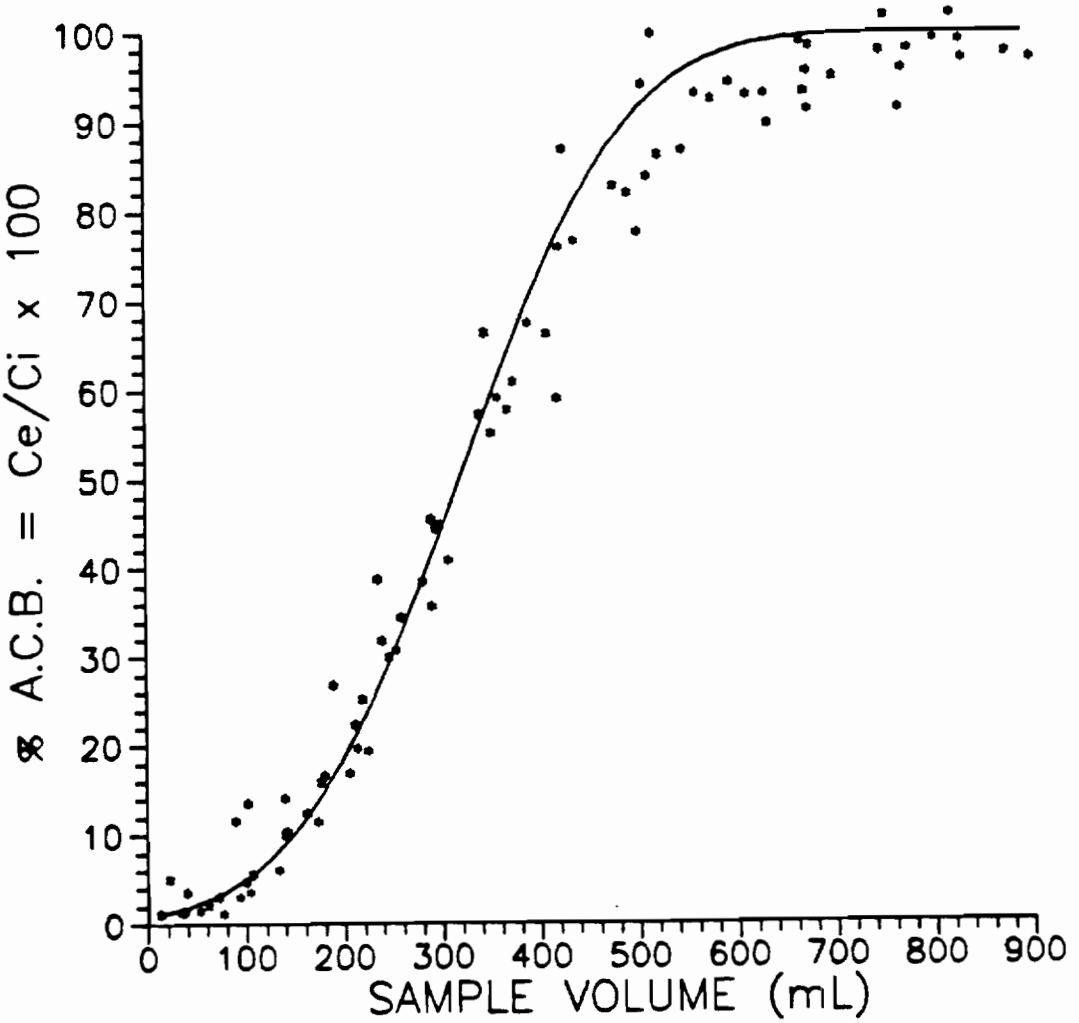

Figure 5.6. Direct comparison of experimental ACB results and the ACB results of the J. Rosen model for 1,1-dichloroethane. The solid line represents the ACB curve generated using an experimentally calibrated version of the J. Rosen model (eqn. 5.6, also see Section 5.3.2) and a K_w value of 2500 ($\bar{K}_w$ for 1,1-dichloroethane from experiments 2 and 4). The experimental data, plotted with stars, was obtained from experiments 2 and 4.

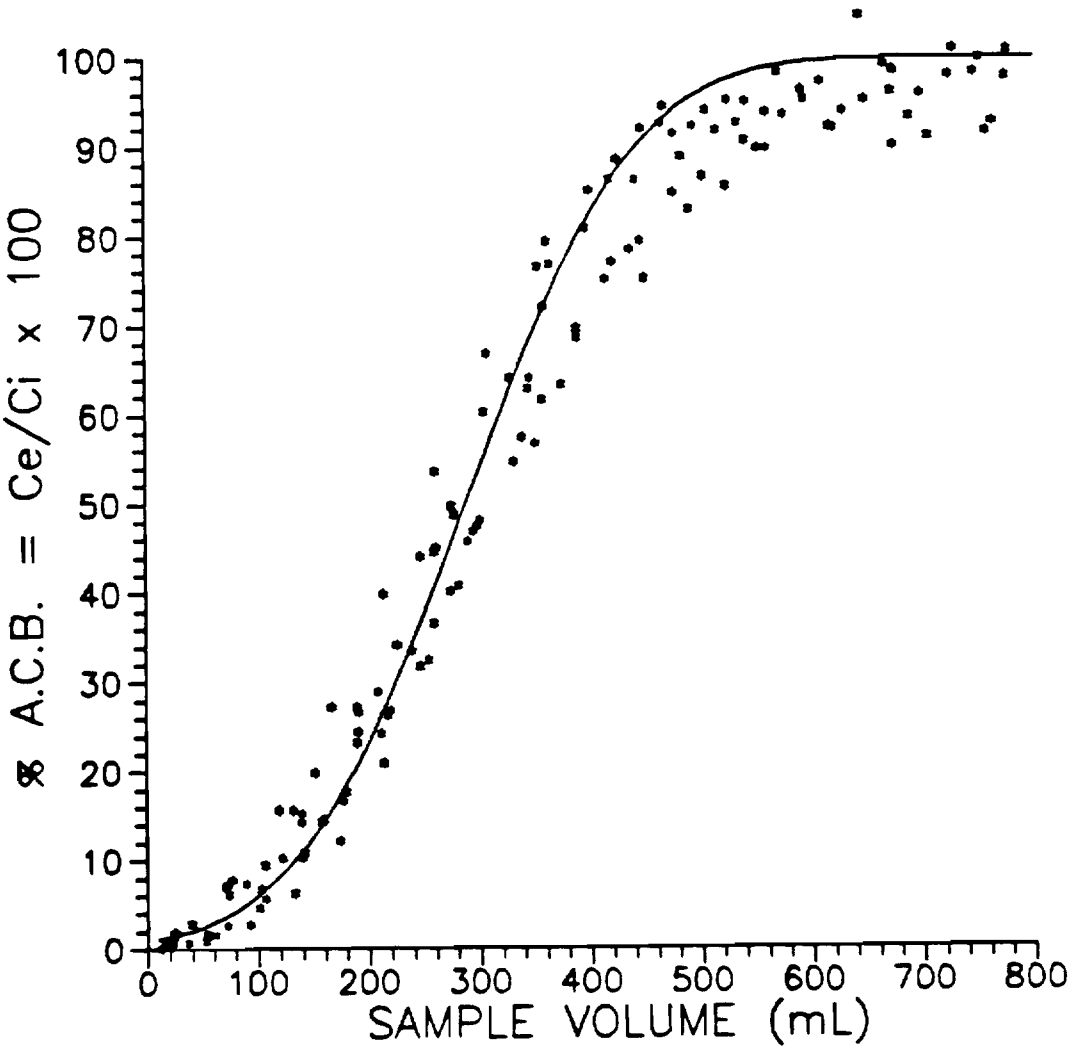

Figure 5.7. Direct comparison of experimental ACB results and the ACB results of the J. Rosen model for trichloromethane. The solid line represents the ACB curve generated using an experimentally calibrated version of the J. Rosen model (eqn. 5.6, also see Section 5.3.2) and a K_w value of 2300 ($\bar{K}_w$ for trichloromethane from experiments 4, 7 and 8). The experimental data, plotted with stars, was obtained from experiments 4, 7 and 8.

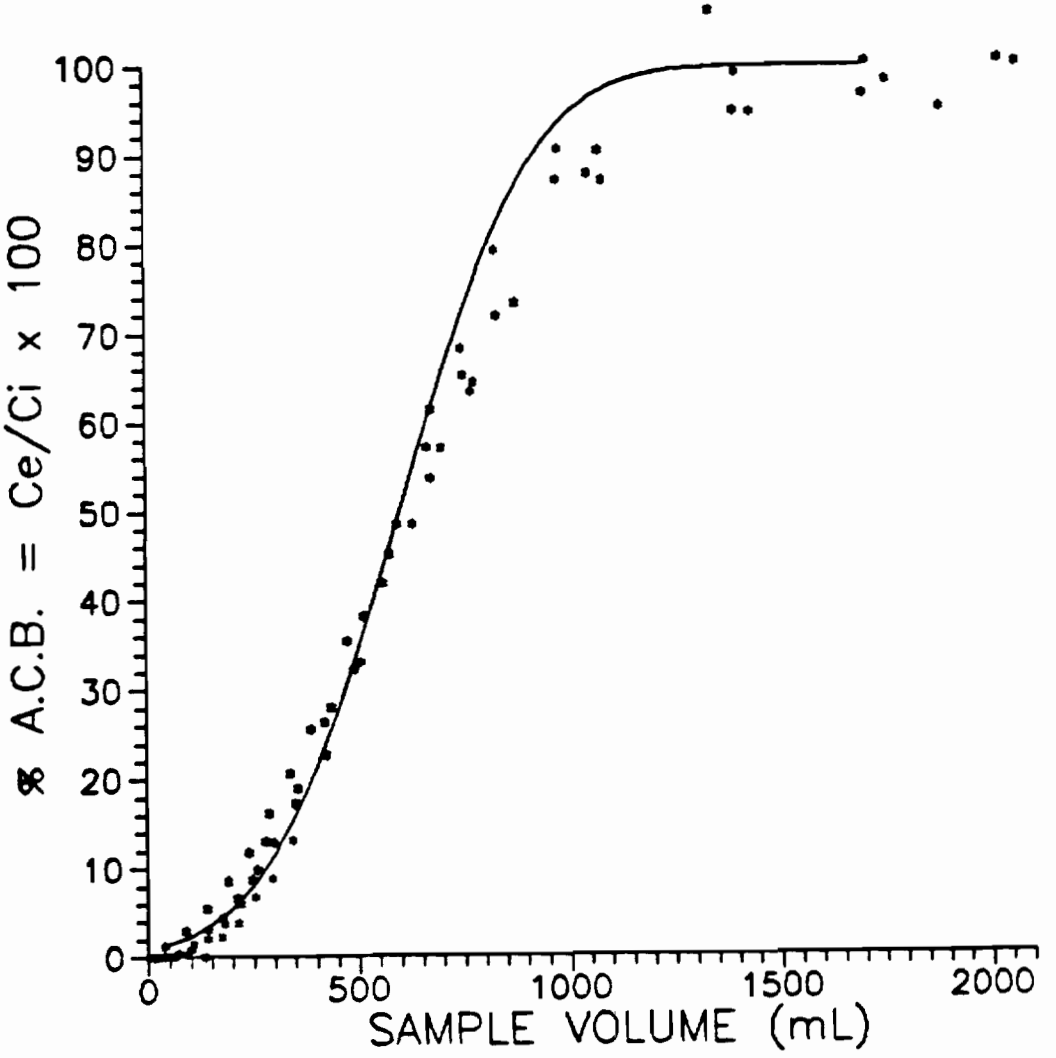

Figure 5.8. Direct comparison of experimental ACB results and the ACB results of the J. Rosen model for bromodichloromethane. The solid line represents the ACB curve generated using an experimentally calibrated version of the J. Rosen model (eqn. 5.6, also see Section 5.3.2) and a K_w value of 4700 (K_w for bromodichloromethane from experiment 4). The experimental data, plotted with stars, was obtained from experiment 4.

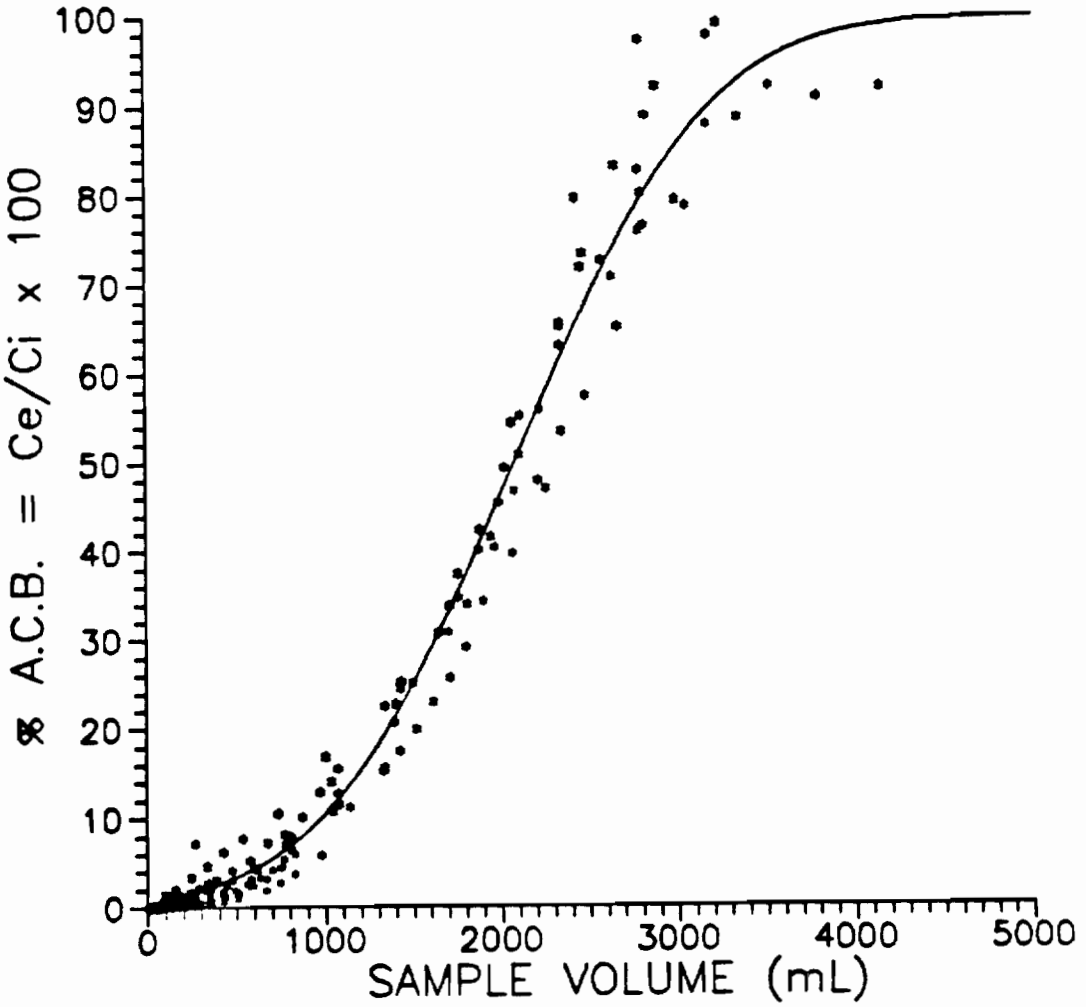

Figure 5.9. Direct comparison of experimental ACB results and the ACB results of the J. Rosen model for trichlorethene. The solid line represents the ACB curve generated using an experimentally calibrated version of the J. Rosen model (eqn. 5.6, also see Section 5.3.2) and a K_w value of 16,000 ($\bar{K}_w$ for benzene from experiments 3 and 4). The experimental data, plotted with stars, was obtained from experiments 3 and 4.

(1) The Cropper and Kaminsky model, with the correction by Pankow and Rosen, may be used to accurately predict adsorbent cartridge sampling efficiencies for sample volumes ranging from 0 to 100% of the V_R of an analyte.

(2) A calibrated version of J. Rosen's model may be used to accurately predict ACB, over the entire range of the adsorption process.

(3) Of the two models, only the one developed by J. Rosen has the ability to predict ACB under a variety of sampling flow rates and sorbent bed dimensions, without the acquisition of additional experimental data obtained under these new conditions.

CHAPTER 6 SUMMARY

The results of this study indicate that ATD is well suited for the determination of trace levels of volatile organic compounds in groundwater. As discussed previously, Tenax cartridges used for the concentration of organic compounds in water are subjected to a centrifugation/vacuum-desiccation procedure prior to their analysis. This procedure is used to remove residual water remaining in the cartridge (30). However, Pankow et al. (41) determined that the vacuum desiccation portion of the procedure was too strenuous for most of the PPPs, causing significant losses and thus analysis artifacts for these compounds. The development of the glass bead drier system enabled the analysis of wet ATD cartridges which had only been subjected to the centrifugation-desiccation step. The glass bead drier, which was connected between the thermal desorber and the capillary column GC/MS analysis system, successfully trapped residual water during the thermal desorption step and prevented the water from interfering with with compound separation and analysis. Compound transmission through the trap was found to be > 95% for all the PPPs. The glass bead drier was found to be easy to install, simple to operate, durable and reliable.

The results of a field evaluation conducted to compare the performance of downhole- and surface-ATD with surface-P&T were very positive. At the sampling site in Repauno, NJ each method was used for the sampling and analysis of groundwater contaminated with 12 PPPs

at levels ranging from 0.11 to 370 μg/L. The precision of each method was very good. For most compounds detected, the CV of eight replicate samples was ~5%. For the majority of compounds detected there were no statistically significant differences between the concentrations determined by downhole- and surface-ATD. For the majority of compounds detected there were statistically significant differences between the concentrations determined by ATD (results of both methods combined) and surface-P&T. However, these differences were not large and therefore the use of either method would likely lead one to the same general conclusions concerning groundwater quality. Therefore, it was concluded that there were no significant differences in the relative accuracies among downhole-ATD, surface-ATD, and surface-P&T. At levels ranging from 0.11 to 0.34 μg/L, three compounds were detected exclusively by ATD. Thus, in groundwater quality investigations where analytical sensitivity at the sub-μg/L level is required, ATD is the methodology of choice.

ACB experiments conducted with 13 PPPs spanning a range of physical properties affecting sampling efficiency, helped to determine the capacity of the sorption system under a variety of sampling conditions. The sorption isotherm of the system was determined to be linear for analyte concentrations of up to ~150 ppb. It is also likely that multiple-analyte solutions will not significantly affect individual analyte/sorbent interactions for most of the PPPs. However, it appears that as the total analyte concentration in solution reaches ~400 ppb the sorbent bed capacity may begin to

decrease. Through an analysis of selected ACB curves it was determined that for a group of compounds with a range of sorbent affinities, adsorbent cartridge sampling efficiency (E) varies linearly with instantaneous percent breakthrough (IBT). Therefore values of E may be easily computed for the PPPs by using eqn. 4.8 and the information provided by the ACB curve of the analyte. For a sample volume corresponding to the 20% breakthrough point a value of E equal to 93% should be obtained for each PPP. This information should allow an analyst to make an accurate a priori prediction of the sampling efficiency for an individual analyte. A reasonable linear relationship was also shown to exist between log K_w and log K_{ow}. For untested compounds, the ability to predict K_w values with a reasonable degree of accuracy will allow the use of models for the a priori prediction of E. The results of these experiments were also used to estimate the method sensitivity of ATD. It should be possible to detect the majority of PPPs at levels ranging from 3.3×10^{-3} to 3.8×10^{-2} μg/L. Therefore, on an individual compound basis, ATD can be at least 26 to 300 times more sensitive than P&T/WCC for the analysis of most PPPs.

Finally, data from the ACB experiments was also used to determine the accuracy of two models used for the prediction of ACB. The Cropper and Kaminsky model (76), with corrections by Pankow and Rosen (82), was used with V_R, N and ω values determined from analyte ACB curves. For sample volumes expressed as a fraction of the V_R of an analyte, E values may be predicted using this model. Model

predictions were found to agree within 5% of the experimentally determined values of E, over a range of sample volumes for compounds with a range of sorbent affinities. The J. Rosen model (88) was first calibrated with experimental ACB data. The calibrated model was then used with K_w values determined from analyte ACB curves to generate ACB curves. The model and experimental curves were then directly compared by plotting them together. For compounds with a range of sorbent affinities the model results closely approximated the experimental results over the entire range of the adsorption process. Therefore, it appears that either model may be used to accurately predict values of E for this adsorption system. Further, because V_R and K_w values can be predicted with a reasonable degree of accuracy, both these models may be used for the a priori prediction of E values for the untested PPPs.

The information provided by this study allows the effective and accurate use of ATD for the determination of PPPs in groundwater. The entire sampling and analysis procedure is sensitive, precise, and simple to execute. The method works well for a broad range of analyte concentrations. In addition, ACB information now exists for a representative group of PPPs. This information allows a priori predictions concerning adsorbent cartridge sampling efficiency to be made with a reasonable degree of accuracy for the entire group of PPPs.

REFERENCES

1. Pye, V. I.; Patrick, R. Science, **1983**, 221, 713-718.

2. Lehr, J.; Environ. Sci. Technol., **1983**, 17, 460A.

3. Newsbriefs, Groundwater Monit. Rev., **1984**, Winter, 14.

4. Pettyjohn, W.A.; Hounslaw, A.W. Groundwater Monit. Rev., **1983**, Fall, 41-47.

5. Newsbriefs, Groundwater Monit. Rev., **1984**, 12.

6. Fusillo, T.V.; Hochreiter, J.J; Lord, D.G. Ground Water, **1985**, 23, 354-360.

7. EPA Federal Register, **1985**, 219 (V.50), 46880-46932.

8. Government Concentrates, Chem. Eng. News, **1987**, 65, 15.

9. Neal, R.A. Envir. Sci. Technol., **1986**, 20, 1067.

10. U.S. EPA, "Method 624-Purgeables", in "Test Methods for the Organic Chemical Analysis of Municipal and Industrial Wastewater", Longbottom, J.E. and Lichtenberg, J.J. (Eds.), 1982, EPA-600/4-82-057.

11. Mabey, W.R.; Smith, J.H.; Podell, R.T.; Johnson, H.L.; Mill, T.; Chou, T.W.; Gates, J.; Waight Partridge, I.; Jaber, H.; Vandenberg, D. "Aquatic Fate Process Data for Priority Pollutants", 1982, EPA 440/4-81-014.

12. Nielson, D.M.; Yeates, G.L. Groundwater Monit. Rev., **1985**, Spring, 83-99.

13. Pankow, J.F. Anal. Chem., **1986**, 58, 1822-1826.

14. Pettyjohn, W.A.; Dunlap, W.J.; Cosby, R.; Keeley, J.W. Groundwater, **1981**, 19, 180-189.

15. Scalf, M.R.; McNabb, J.F.; Dunlap, W.J.; Cosby, R.L.; Fryberger, J. "Manual of Groundwater Sampling Procedures", Kerr Groundwater Research Laboratory, NWWA/EPA Joint Report, 1981.

16. Dressman, R.C.; McFarren, E.F. J. Chromatogr. Sci., **1977**, 15, 69-72.

17. Bellar, T.A.; Lichtenberg, J.J.; Eichelberger, J.W. Environ. Sci. Technol., **1976**, 10, 926-930.

18. Levine, S.P.; Puskar, M.A.; Dymerski, P.P; Warner, B.J.; Friedman, C.S. Environ. Sci. Technol., **1983**, 17, 125-127.

19. Hankin, G.G.; Reed, T.A.; Brand, G.N. Groundwater Monitor. Rev., **1984**, Winter, 43-45.

20. Miller, G.D. Second Nat. Sym. on Aquifer Restoration and Groundwater Monitoring, NWWA, 1981, 236-245.

21. Junk, G.A.; Svec, H.J.; Vick, R.D.; Avery, M.J. Environ. Sci. Technol., **1974**, 8, 1100-1106.

22. Curran, C.M.; Tomson, M.B. Groundwater Monit. Rev., **1983**, Summer, 68-71.

23. Fetter, C.W. Groundwater Monit. Rev., **1983**, Summer, 60-64.

24. Barcelona, M.J.; Helfrich, J.A.; Garske, E.E. Anal. Chem., **1985**, 57, 460-464.

25. Bertsch, W; Anderson, M.E.; Holzer, G. J. Chromatogr., **1975**, 112, 701-718.

26. Grob, K.; Zurcher, F. J. Chromatogr., **1976**, 117, 285-294.

27. Pankow, J.F.; Isabelle, L.M. J. Chromatogr., **1982**, 237, 25-39.

28. Pankow, J.F.; Kristensen, T.J. Anal. Chem., **1983**, 55, 2187-2192.

29. Pankow, J.F.; Isabelle, L.M. Anal. Chem., **1984**, 56, 2997-2999.

30. Pankow, J.F.; Ligocki, M.P.; Rosen, M.E.; Isabelle, L.M.; Hart, K.M. Anal. Chem., **1988**, 60, 40-47.

31. Pankow, J.F.; Isabelle, L.M.; Hewetson, J.P.; Cherry, J.A. Ground Water, **1984**, 22, 330-339.

32. Pankow, J.F.; Isabelle, L.M.; Hewetson, J.P.; Cherry, J.A. Ground Water, **1985**, 23, 775-782.

33. Pankow, J.F. J. High Resol. Chromatogr. Chromatogr. Commun., **1983**, 6, 292-299.

34. Dressler, M. J. Chromatogr., **1979**, 167, 165-206.

35. Ryan, J.P., "The Analysis of Organic Compounds in Water by Direct Adsorption and Thermal Desorption", University Microfilms Int'l., 1979.

36. May, W.E.; Chesler, S.N.; Cram, S.P.; Gump, B.H.; Hertz, H.S.; Enagonio, D.P.; Dyszel, S.M. J. Chromatogr. Sci., **1975**, 13, 535-540.

37. Leoni, V.; Puccetti, G.; Grella, A J. Chromatogr., **1975**, 106, 119-124.

38. Agostiano, A.M.; Caselli, M.; Provenzano, M.R. Water, Air, and Soil Poll.,**1983**, 19, 309-320.

39. Chladek, E.; Marano, R.S. J. Chromatogr. Sci., **1984**, 22, 313-320.

40. Versino, B.; Knoppel, H.; DeGroot, M.; Peil, A.; Poelman, J.; Schauenberg, H.; Vissens, H.; Geiss, F. J. Chromatogr., **1976**, 122, 373-388.

41. Pankow, J.F.; Ligocki, M.P.; Rosen, M.E.; Isabelle, L.M.; Hart, K.M. Unpublished work, 1987, Oregon Graduate Center.

42. Foulger, B.E.; Simmonds, P.G. Anal. Chem., **1979**, 51, 1089-1090.

43. Simmonds, P.G.; Kerns, E. J. Chromatogr., **1979**, 186, 785-794.

44. Simmonds, P.G. J. Chromatogr., **1984**, 289, 117-127.

45. Palmer, R.A.; Childers, J.W.; Smith, M.J. "Gas Chromatographic/Fourier Transform Infrared Analysis of Trace Organics", 1980, EPA/600/4-85/066.

46. Cox, R.D.; Earp, R.F. Anal. Chem., **1982**, 54, 2265-2270.

47. CHEMTECH, **1979**, February, 85.

48. Supelco Reporter, 1985 IV, 1.

49. Freeman, R.R.; Lautamo, R.M.A. Amer. Lab., **1986**, May, 60-68.

50. Pankow, J.F.; Isabelle, L.M. "The Development of Adorption/Thermal Desorption (ATD) with Tenax-GC as an Analytical Method for Trace Aqueous Organics in Field Well Water Samples", 1982, USGS/14-08-0001-A-0013.

51. Leuenbeger, C.; Ligocki, M.P.; Pankow, J.F. Environ. Sci. Technol., **1985**, 19, 1053-1058.

52. Pankow, J.F.; Rosen, M.E. "Evaluation of Water-Quality Sampling and Analysis Methods, 1984, USGS/14-08-0001G-719.

53. Ficken, J.H. "Field Methods for Groundwater Contamination Studies and Their Standardization", 1987, ASTM STP 963, In press.

54. Imbrigiotta, T.E.; Gibs, J.; Fusillo, T.V.; Kish, G.R.; Hochreiter, J.J. Proceedings ASTM Symposium "Field Methods for Groundwater Contamination Studies and Their Standardization", 1985, In press.

55. Schuller, R.M.; Gibb, J.P.; Griffin, R.A. Groundwater Monit. Rev., **1981**, Spring, 42-46.

56. Pankow, J.F.; Isabelle, L.M.; Kristensen, T.J. J. Chromatogr., **1982**, 245, 31-43.

57. Pankow, J.F.; Rosen, M.E. J. High Resol. Chromatogr. and Chromatogr. Commun., **1984**, 7, 504-508.

58. Pankow, J.F.; Isabelle, L.M. J. High Resol. Chromatogr. and Chromatogr. Commun., **1987**, 10, 617-619.

59. Ryan, T.A.; Joiner, B.L.; Ryan, B.F. "8. Comparing Two Means; Confidence Intervals and Tests", in "Minitab Student Handbook", Duxbury Press, MA, 1976.

60. Barcelona, M.J.; Helfrich, J.A.; Garske, E.E.; Gibb, J.P. Groundwater Monit. Rev., **1984**, Spring, 32-41.

61. Gibb, J.P.; Barcelona, M.J. Jour. AWWA, **1984**, May, 48-51.

62. Sakodynskii, K.; Panina, L.; Klinskaya, N. Chromatographia, **1974**, 7, 339-344.

63. Pankow, J.F.; Rosen, M.E. Environ. Sci. Technol., In press.

64. Ryan, T.A.; Joiner, B.L.; Ryan, B.F. "9. Correlation and Regression", in "Minitab Student Handbook", Duxbury Press, MA, 1976.

65. Ryan, T.A.; Joiner, B.L.; Ryan, B.F. "7. One Sample Confidence Intervals and Tests for Population Mean", in "Minitab Student Handbook", Duxbury Press, MA, 1976

66. Kirchmer, C.J. Environ. Sci. Technol., **1983**, 17, 174A-181A.

67. Long, G.L.; Winefordner, J.D. Anal. Chem., **1983**, 55, 712A-724A.

68. Glaser, J.A.; Foerst, D.L.; McKee, G.D.; Quave, S.A.; Budde, W.A. Environ. Sci. Technol., **1981**, 15, 1429-1435.

69. Rosen, M.E.; Pankow, J.F.; Schroeder, R.A. unpublished results, Oregon Graduate Center and U.S. Geological Survey, **1984**.

70. Harris, J.C.; Cohen, M.J.; Grosser, Z.A.; Hayes, M.J. "Evaluation of Solid Sorbents for Water Sampling", 1980, EPA-600/2-80-193.

71. Press, W.H.; Flannery, B.P.; Teukolsky, S.A.; Vetterling, W.T. "Numerical Recipes, the Art of Scientific Computing", Cambridge University Press, England, 1985.

72. Hewlett Packard, "HP-41C Math PAC", Hewlett Packard, Corvallis, 1982.

73. Bertoni, G.; Liberti, A.; Perrino, C. J. Chromatogr., **1981**, 203, 263-270.

74. Skoog, D.A.; West, D.M. "Principles of Instrumental Analysis", Saunders College, PA, 1980.

75. Glueckauf, E. in "Ion Exchange and its Aplications", Society of Chemical Industry, England, 1955.

76. Cropper, F.R.; Kaminsky, S. Anal. Chem., **1963**, 35, 735-743.

77. Reilly, C.N.; Hildebrand, G.P.; Ashley, J.W. Anal. Chem., **1962**, 34, 1198-1213.

78. Raymond, A.; Guichon, G. J. Chromatogr. Sci., **1975**, 13, 173-177.

79. Butler, L.D.; Burke, M.F. J. Chromatogr. Sci., **1976**, 14, 117-122.

80. Brown, R.H.; Purnell, C.J. J. Chromatogr., **1979**, 178, 79-90.

81. Sennum, G.I. Environ. Sci. Technol., **1981**, 15, 1073-1075.

82. Pankow, J.F.; Rosen, M.E. Unpublished work, 1983, Oregon Graduate Center.

83. Simon, G.P. American Laboratory, **1984**, August, 82-90.

84. Lovkvist, P.; Jonsson, J.A. Anal. Chem., **1987**, 59, 818-821.

85. Pankow, J.F.; Isabelle, L.M.; Kristensen, T.J. J. Chromatogr., **1982**, 245, 31.

86. Rosen, J.B. J. Chem. Phys., **1952**, 20, 387-394.

87. Rasmuson, A. Water Resour. Res., **1981**, 17, 321-328.

88. Lenhoff, A.M. J. Chromatogr., **1987**, 384, 285-299.

89. Drago, J.V. Warme und Stoffubertragung, **1986**, 20, 255-261.

90. Rosen, J.B. Ind. Eng. Chem., **1954**, 46, 1590-1600.

91. Helfferich, F. "Ion Exchange", McGraw-hill, NY, 1962.

92. Cen, P.L.; Yang, R.T. AIChE J., **1986**, 32, 1635-1641.

93. Liaw, C.H.; Wang, J.S.P.; Greenkorn, R.A.; Chao, K.C. AIChE J., **1979**, 25, 376-381.

94. Ruthven, D.M. AIChE J., **1978**, 24, 540-542.

95. Raghavan, N.S.; Ruthven, D.M. AIChE J., **1983**, 29, 922-925.

96. Bhairi, A.; Rothstein, D.; Madey, R.; Huang, J.; Lee, K.B. J. Chromatogr., **1986**, 361, 3-11.

97. DeLasa, H.; Hazlett, J.; Fuller, O.M. J. Chem. Eng. Sci., **1986**, 41, 1233-1242.

98. Weber, W.J.; Liang, S. Environ. Progress, **1983**, 2, 167-175.

99. Morbidelli, M.; Servida, A.; Storti, G.; Carra, S. Ind. Eng. Chem. Fundam., **1982**, 21, 123-131.

100. Rice, R.G. Chem. Eng. Sci., **1982**, 37, 83-91.

101. Rasmuson, A. AIChE J., **1981**, 27, 1032-1035.

102. Ghezelayagh, H.; Gidaspow, D. Chem. Eng. Sci., **1982**, 37, 1181-1197.

103. Mathews, A.P. Chem. Eng. Commun., **1982**, 15, 313-322.

104. Marcussen, L. Chem. Eng. Sci., **1982**, 37, 299-309.

105. Moharir, A.S.; Kunzru, D.; Saraf, D.N. Chem. Eng. Sci., **1980**, 35, 1795-1801.

106. Linek, F.; Dudukovic, M.P. Chem. Eng. J., **1982**, 23, 31-36.

107. Brunovska, A.; Hlavacek, V.; Ilavsky, J.; Valtyni, J. Chem. Eng. Sci., **1978**, 33, 1385-1391.

108. Omatete, O.O.; Clazie, R.N.; Vermeulen, T. Chem. Eng. J., **1980**, 19, 229-240.

109. Huang, J.C.; Rothstein, D.; Madey, R. AIChE J., **1984**, 30, 660-662.

110. Van Genuchten, M.T.; Tang, D.H.; Guennelon, R. Water Resour. Res., **1984**, 20, 335-346.

111. Rasmuson, A.; Neretnieks, I. AIChE J., **1980**, 26, 686-690.

112. Cowan, G.H.; Gosling, I.S.; Laws, J.F.; Sweetenham, W.P. J. Chromatogr., **1986**, 363, 37-56.

113. Fair, G.; Geyer, J.; Okun, D. "Water and Wastewater Engineering", Vol. 2, Wiley, NY, 1968.

114. Madey, R.; Photinos, P.J.; Rothstein, D.; Huang, J. Langmuir, **1986**, 2, 173-178.

115. Bonoli, L.; Witherspoon, P.A. J. Phys. Chem., **1969**, 72, 2532-2534.

116. Fish, W. "Transport Phenomena", Lecture Notes, Oregon Graduate Center, Spring 1986.

117. Goto, M.; Hayashi, N.; Goto, S. Environ. Sci. Technol., **1986**, 20, 463-467.

118. Omatete, O.; Clazie, R.N.; Vermeulen, T. Chem. Eng. J., **1980**, 19, 241-250.

119. Gibbs, S.J.; Lightfoot, E.N. Ind. Eng. Chem. Fundam., **1986**, 25, 490-496.

120. Weber, W.J.; Pirbazari, M. J. AWWA., **1982**, April, 203-209.

121. Weber, W.J.; Liu, K.T. Chem. Eng. Commun., **1980**, 6, 49-60.

122. Weber, W.J.; Crittenden, J.C. J. WPCF., **1975**, 47, 924-940.

123. Wiedemann, K.; Roethe, A.; Radeke, K.H.; Gelbin, D. Chem. Eng. J., **1978**, 16, 19-26.

124. Erickson, K.L.; Rase, H.F. Ind. Eng. Chem. Fundam., **1979**, 4, 312-317.

Appendix 1.1. Downhole-ATD Data Set[a] Camden, NJ Sampling Site - Sampling Round 1.

SAMPLE NUMBER	1	2	3	4
CARTRIDGE[b] NUMBER	68	70	71	73
SAMPLE VOLUME (mL)	11	16	9.0	9.3
SAMPLE FLOW RATE (mL/min)	1.9	2.7	1.5	1.6
COMPOUND	----------CONCENTRATION (μg/L)----------			
1,1-Dichloroethene	.40	.18	.33	.12
1,1-Dichloroethane	2.8	1.7	2.6	1.6
cis-1,2-Dichloroethene	11	6.2	9.7	6.6
Trichloromethane	.37	.19	.32	.26
1,1,1-Trichloroethane	.53	.43	.74	.56
1,2-Dichloroethane	2.5	1.5	2.5	1.6
Benzene	.87	.60	.88	.75
Trichloroethene	110	73	120	110
1,1,2-Trichloroethane	.13	.083	.14	.12
Tetrachloroethene	8.9	6.0	10	7.8
Chlorobenzene	.24	.18	.24	.24
Ethylbenzene	.026	.019	.040	.043
m+p-Xylene	.075	.060	.11	.12

Appendix 1.1 (cont'd.). Downhole-ATD Data Set[a] Camden, NJ Sampling Site - Sampling Round 1.

SAMPLE NUMBER	1	2	3	4
CARTRIDGE[b] NUMBER	68	70	71	73
SAMPLE VOLUME (mL)	11	16	9.0	9.3
SAMPLE FLOW RATE (mL/min)	1.9	2.7	1.5	1.6
COMPOUND	----------CONCENTRATION (μg/L)----------			
o-Xylene	.043	.029	.060	.059

[a]Samples 1-4 were collected Backup Cartridges, therefore concentrations listed are calculated as follows:

$$C = \frac{\text{(ng amt. on primary cartridge + ng amt. on backup cartridge)}}{\text{Sample Volume}}$$

[b]Cartridge Bed Volume (mL) = 5.7

Appendix 1.2. Downhole-ATD Data Set Camden, NJ Sampling Site - Sampling Round 2.

SAMPLE NUMBER	5	6	7	8
CARTRIDGE[a] NUMBER	10	25	26	28
SAMPLE VOLUME (mL)	9.6	9.8	11	15
SAMPLE FLOW RATE (mL/min)	2.1	2.2	2.4	3.2
COMPOUND	----------CONCENTRATION (μg/L)----------			
1,1-Dichloroethene	SL[b]	.30	.34	.056
1,1-Dichloroethane	SL	2.2	1.7	.81
cis-1,2-Dichloroethene	SL	7.6	6.3	3.2
Trichloromethane	SL	.23	.19	.099
1,1,1-Trichloroethane	SL	.43	.52	.36
1,2-Dichloroethane	SL	1.7	1.3	.81
Benzene	SL	.43	.33	.25
Trichloroethene	SL	79	64	43
1,1,2-Trichloroethane	SL	.13	.099	.070
Tetrachloroethene	SL	7.7	5.6	4.0
Chlorobenzene	SL	.23	.17	.13
Ethylbenzene	SL	.024	.026	.015
m+p-Xylene	SL	.086	.074	.065

Appendix 1.2 (cont'd). Downhole-ATD Data Set Camden, NJ Sampling Site - Sampling Round 2.

SAMPLE NUMBER	5	6	7	8
CARTRIDGE[a] NUMBER	10	25	26	28
SAMPLE VOLUME (mL)	9.6	9.8	11	15
SAMPLE FLOW RATE (mL/min)	2.1	2.2	2.4	3.2
COMPOUND	----------CONCENTRATION (μg/L)----------			
o-Xylene	SL	ND[c]	.030	.027

[a]Cartridge Bed Volume (mL) = 5.7
[b]SL = Sample lost during analysis.
[c]ND = Not Detected

Appendix 1.3. Downhole-ATD Camden, NJ Sampling Site - Breakthrough[a] Data.

SAMPLE NUMBER	1	2	3	4
CARTRIDGE[b] NUMBER	60	61	62	64
SAMPLE VOLUME (mL)	11	16	9.0	9.3
SAMPLE FLOW RATE (mL/min)	1.9	2.7	1.5	1.6
COMPOUND	----------BREAKTHROUGH (%)----------			
1,1-Dichloroethene	7.3	32	60	NB[c]
1,1-Dichloroethane	5.7	18	21	NB
cis-1,2-Dichloroethene	5.8	17	21	NB
Trichloromethane	NB	NB	NB	NB
1,1,1-Trichloroethane	6.4	25	9.2	NB
1,2-Dichloroethane	5.5	15	17	NB
Benzene	25	18	24	27
Trichloroethene	4.6	16	16	17
1,1,2-Trichloroethane	NB	NB	NB	NB
Tetrachloroethene	3.6	13	12	NB
Chlorobenzene	NB	16	16	NB
Ethylbenzene	NB	NB	NB	NB
m+p-Xylene	NB	NB	NB	NB

Appendix 1.3 (cont'd). Downhole-ATD Camden, NJ Sampling Site - Breakthrough[a] Data.

SAMPLE NUMBER	1	2	3	4
CARTRIDGE[b] NUMBER	60	61	62	64
SAMPLE VOLUME (mL)	11	16	9.0	9.3
SAMPLE FLOW RATE (mL/min)	1.9	2.7	1.5	1.6
COMPOUND	BREAKTHROUGH (%)			
o-Xylene	NB	NB	NB	NB

[a]Breakthrough (%) (BT) is calculated as follows:

$$BT = 100 \left[\frac{\text{(ng amt. on Backup Cartridge)}}{\text{(ng amt. on Primary Cartridge + ng amt. on Backup Cartridge)}} \right]$$

[b]Backup Cartridge Bed Volume (mL) = 5.7
[c]NB = No Breakthrough, compound not detected on backup cartridge.

Appendix 1.4. Surface-ATD Data Set[a] Camden, NJ Sampling Site - Sampling Round 1.

SAMPLE NUMBER	1	2	3	4
CARTRIDGE[b] NUMBER	21	37	52	56
SAMPLE VOLUME (mL)	13	13	12	13
SAMPLE FLOW RATE (mL/min)	2.1	2.9	2.7	3.0
COMPOUND	----------CONCENTRATION (μg/L)----------			
1,1-Dichloroethene	.29	.29	.55	.11
1,1-Dichloroethane	.73	1.4	2.2	.62
cis-1,2-Dichloroethene	2.2	4.4	6.1	1.7
Trichloromethane	.51	.16	.18	.065
1,1,1-Trichloroethane	.70	.54	.82	.47
1,2-Dichloroethane	.60	1.2	1.3	.65
Benzene	.92	.49	.38	.28
Trichloroethene	26	57	66	64
1,1,2-Trichloroethane	.077	.090	.10	.087
Tetrachloroethene	4.4	6.6	6.8	5.6
Chlorobenzene	.17	.16	.15	.14
Ethylbenzene	1.6 R98[c]	.072 R98	.024	.022
m+p-Xylene	1.9 R98	.162 R95[c]	.079	.081

Appendix 1.4 (cont'd.). Surface-ATD Data Set[a] Camden, NJ Sampling Site - Sampling Round 1.

SAMPLE NUMBER	1	2	3	4
CARTRIDGE[b] NUMBER	21	37	52	56
SAMPLE VOLUME (mL)	13	13	12	13
SAMPLE FLOW RATE (mL/min)	2.1	2.9	2.7	3.0
COMPOUND	CONCENTRATION (μg/L)			
o-Xylene	.51 R98	.064 R95	.033	.031

[a]Samples 1-4 were collected using Backup Cartridges, therefore concentrations listed are calculated as follows:

$$C = \frac{\text{(ng amt. on primary cartridge + ng amt. on backup cartridge)}}{\text{Sample Volume}}$$

[b]Cartridge Bed Volume (mL) = 5.7

[c]R98, R95 = Outlier, rejected at 98% or 95% confidence level, respectively.

Appendix 1.5. Surface-ATD Data Set Camden, NJ Sampling Site - Sampling Round 2.

SAMPLE NUMBER	5	6	7	8
CARTRIDGE[a] NUMBER	7	49	66	80
SAMPLE VOLUME (mL)	11	12	12	12
SAMPLE FLOW RATE (mL/min)	2.9	3.1	3.4	3.3
COMPOUND	----------CONCENTRATION (μg/L)----------			
1,1-Dichloroethene	.19	.30	.25	1.7
1,1-Dichloroethane	1.8	1.4	1.8	1.4
cis-1,2-Dichloroethene	5.9	4.4	6.4	5.9
Trichloromethane	.19	.15	.20	.18
1,1,1-Trichloroethane	.81	.87	.81	.81
1,2-Dichloroethane	1.4	1.2	1.7	1.4
Benzene	.24	.23	.26	.27
Trichloroethene	63	58	84	60
1,1,2-Trichloroethane	.10	.098	.11	.10
Tetrachloroethene	6.0	6.2	7.1	6.1
Chlorobenzene	.16	.16	.16	.16
Ethylbenzene	.028	.028	.022	.018
m+p-Xylene	.087	.10	.088	.071
o-Xylene	.041	.045	.038	.032

[a]Cartridge Bed Volume (mL) = 5.7

Appendix 1.6. Surface-ATD Camden, NJ Sampling Site - Breakthrough[a] Data.

SAMPLE NUMBER	1	2	3	4
CARTRIDGE[b] NUMBER	31	45	57	67
SAMPLE VOLUME (mL)	13	13	12	13
SAMPLE FLOW RATE (mL/min)	2.1	2.9	2.7	3.0
COMPOUND	----------BREAKTHROUGH (%)----------			
1,1-Dichloroethene	NB[c]	NB	6.5	12
1,1-Dichloroethane	NB	NB	NB	NB
cis-1,2-Dichloroethene	2.3	.62	8.6	2.0
Trichloromethane	NB	NB	NB	NB
1,1,1-Trichloroethane	NB	NB	NB	NB
1,2-Dichloroethane	NB	NB	NB	NB
Benzene	7.1	44	23	52
Trichloroethene	.38	.37	7.7	1.0
1,1,2-Trichloroethane	NB	NB	NB	NB
Tetrachloroethene	.53	.29	4.9	.44
Chlorobenzene	NB	NB	NB	NB
Ethylbenzene	NB	NB	NB	NB
m+p-Xylene	NB	NB	NB	NB

Appendix 1.6 (cont'd). Surface-ATD Camden, NJ Sampling Site - Breakthrough[a] Data.

SAMPLE NUMBER	1	2	3	4
CARTRIDGE[b] NUMBER	31	45	57	67
SAMPLE VOLUME (mL)	13	13	12	13
SAMPLE FLOW RATE (mL/min)	2.1	2.9	2.7	3.0
COMPOUND	BREAKTHROUGH (%)			
o-Xylene	NB	NB	NB	NB

[a]Breakthrough (%)(BT) is calculated as follows:

$$BT = 100\left[\frac{\text{(ng amt. on Backup Cartridge)}}{\text{(ng amt. on Primary Cartridge + ng amt. on Backup Cartridge)}}\right]$$

[b]Backup Cartridge Bed Volume (mL) = 5.7
[c]NB = No Breakthrough, compound not detected on backup cartridge.

Appendix 1.7. ATD Camden, NJ Sampling Site - Travel Blank Data.

Compound	$\bar{B}$[a] (ng)	s (ng)	L[b] (ng)
1,1-Dichloroethene	ND[c]	-	-
1,1-Dichloroethane	ND	-	-
cis-1,2-Dichloroethene	ND	-	-
Trichloromethane	ND	-	-
1,1,1-Trichloroethane	ND	-	-
1,2-Dichloroethane	ND	-	-
Benzene	.40	.31	.49[d]
Trichloroethene	ND	-	-
1,1,2-Trichloroethane	ND	-	-
Tetrachloroethene	ND	-	-
Chlorobenzene	ND	-	-
Ethylbenzene	ND	-	-
m+p-Xylene	ND	-	-
o-Xylene	ND	-	-

[a]Mean Blank determined from the analysis of 2 travel blanks and 4 system blanks.
[b]Calculated according to procedure outlined in Ref. 32.
[c]ND = Not Detected in the travel blanks or the system blanks.
[d]ϕ = 11, L = 1.6s.

Appendix 1.8. Surface-P&T Data Set Camden, NJ Sampling Site - Sampling Round 1.

SAMPLE NUMBER	1[a]	2[a]	3	4
ANALYSIS VOLUME (mL)	5.0	5.0	5.0	5.0
COMPOUND	----------CONCENTRATION (μg/L)----------			
1,1-Dichloroethene	9.1	8.5	8.9	8.7
1,1-Dichloroethane	6.5	6.4	6.2	6.3
cis-1,2-Dichloroethene	24	23	22	23
Trichloromethane	.66	.79	.80	.82
1,1,1-Trichloroethane	ND[b]	ND	ND	ND
1,2-Dichloroethane	3.7	3.8	4.0	4.0
Benzene	ND	ND	ND	ND
Trichloroethene	150	170	170	180
1,1,2-Trichloroethane	ND	ND	ND	ND
Tetrachloroethene	7.4	7.7	7.5	7.7
Chlorobenzene	ND	ND	ND	ND
Ethylbenzene	ND	ND	ND	ND
m+p-Xylene	ND	ND	ND	ND
o-Xylene	ND	ND	ND	ND

[a]Represents the average concentration of two replicate sample analyses.
[b]ND = Not Detected

Appendix 1.9. Surface-P&T Data Set Camden, NJ Sampling Site - Sampling Round 2.

SAMPLE NUMBER	5[a]	6	7	8
ANALYSIS VOLUME (mL)	5.0	5.0	5.0	5.0
COMPOUND	----------CONCENTRATION (μg/L)----------			
1,1-Dichloroethene	8.1	7.6	8.3	8.8
1,1-Dichloroethane	5.9	5.6	6.0	6.5
cis-1,2-Dichloroethene	23	22	23	24
Trichloromethane	.82	.78	.80	.81
1,1,1-Trichloroethane	ND[b]	ND	ND	ND
1,2-Dichloroethane	4.1	4.0	4.3	4.2
Benzene	ND	ND	ND	ND
Trichloroethene	170	170	180	180
1,1,2-Trichloroethane	ND	ND	ND	ND
Tetrachloroethene	7.5	7.0	7.7	7.4
Chlorobenzene	ND	ND	ND	ND
Ethylbenzene	ND	ND	ND	ND
m+p-Xylene	ND	ND	ND	ND
o-Xylene	ND	ND	ND	ND

[a]Represents the average concentration of 2 replicate sample analyses.
[b]ND = Not Detected

Appendix 1.10. P&T Camden, NJ Sampling Site - Travel Blank Data.

Compound	$\bar{C}$[a] (μg/L)	s (μg/L)	L[b] (μg/L)
1,1-Dichloroethene	ND[c]	-	-
1,1-Dichloroethane	ND	-	-
cis-1,2-Dichloroethene	ND	-	-
Trichloromethane	.073	.0044	.0069[d]
1,1,1-Trichloroethane	ND	-	-
1,2-Dichloroethane	ND	-	-
Benzene	NA[e]	-	-
Trichloroethene	ND	-	-
1,1,2-Trichloroethane	ND	-	-
Tetrachloroethene	.24	.032	.050[d]
Chlorobenzene	NA	-	-
Ethylbenzene	NA	-	-
m+p-Xylene	NA	-	-
o-Xylene	NA	-	-

[a]Mean Blank determined from the analysis of 5 travel blanks.
[b]Calculated according to procedure outlined in Ref. 32.
[c]ND = Not Detected in the travel blanks or the system blanks.
[d]ϕ = 11, L = 1.6s.
[e]NA = Not available, compound not detected in purge and trap samples.

Appendix 1.11. Downhole-ATD Data Set[a] Syosset, NY Sampling Site - Sampling Round 1.

SAMPLE NUMBER	1	2	3	4
CARTRIDGE[b] NUMBER	403	407	408	411
SAMPLE VOLUME (mL)	10	8.8	9.5	9.4
SAMPLE FLOW RATE (mL/min)	2.5	2.2	2.4	2.3
COMPOUND	----------CONCENTRATION (μg/L)----------			
1,1-Dichloroethene	2.0	2.7	16	14
TCTF-ethane*	26	24	25	25
1,1-Dichloroethane	.70	.56	.76	1.4
cis-1,2-Dichloroethene	.21	.17	.31	.45
Trichloromethane	.13	.10	.14	.25
1,1,1-Trichloroethane	120	110	100	120
1,2-Dichloroethane	.31	.21	.30	.37
Tetrachloromethane	.81	.87	.71	.90
Benzene	.23	.18	.22	.29
Trichloroethene	4.2	3.1	3.9	5.9
1,1,2-Trichloroethane	.089	.081	.082	.093
Tetrachloroethene	33	29	32	36
Chlorobenzene	.062	.053	.057	.064
Ethylbenzene	NQ[c]	NQ	NQ	NQ
m+p-Xylene	NQ	NQ	NQ	NQ

Appendix 1.11 (cont'd). Downhole-ATD Data Set[a] Syosset, NY Sampling Site - Sampling Round 1.

SAMPLE NUMBER	1	2	3	4
CARTRIDGE[b] NUMBER	403	407	408	411
SAMPLE VOLUME (mL)	10	8.8	9.5	9.4
SAMPLE FLOW RATE (mL/min)	2.5	2.2	2.4	2.3
COMPOUND	----------CONCENTRATION (μg/L)----------			
o-Xylene	NQ	NQ	NQ	NQ

[a]Samples 1-4 were collected Backup Cartridges, therefore concentrations listed are calculated as follows:

$$C = \frac{\text{(ng amt. on primary cartridge + ng amt. on backup cartridge)}}{\text{Sample Volume}}$$

[b]Cartridge Bed Volume (mL) = 0.68.
[c]Detected at a non-quantifiable level.
*1,1,2-Trichloro-1,2,2-trifluoroethane.

Appendix 1.12. Downhole-ATD Data Set Syosset, NY Sampling Site - Sampling Round 2.

SAMPLE NUMBER	5	6	7	8
CARTRIDGE[a] NUMBER	419	420	422	424
SAMPLE VOLUME (mL)	12	13	12	11
SAMPLE FLOW RATE (mL/min)	2.1	2.2	2.0	1.9
COMPOUND	----------CONCENTRATION (μg/L)----------			
1,1-Dichloroethene	2.1	1.2	1.4	3.2
TCTF-ethane	22	22	25	25
1,1-Dichloroethane	.66	.44	.34	.58
cis-1,2-Dichloroethene	.26	.12	.089	.23
Trichloromethane	.12	.083	.054	.104
1,1,1-Trichloroethane	97	99	99	98
1,2-Dichloroethane	.28	.18	.15	.25
Tetrachloromethane	.79	.80	.86	.74
Benzene	.16	.15	.12	.15
Trichloroethene	3.9	2.1	1.6	3.0
1,1,2-Trichloroethane	.082	.068	.067	.079
Tetrachloroethene	27	24	23	25
Chlorobenzene	.061	.051	.049	.055
Ethylbenzene	NQ[b]	NQ	NQ	NQ
m+p-Xylene	NQ	NQ	NQ	NQ

Appendix 1.12 (cont'd.). Downhole-ATD Data Set Syosset, NY Sampling Site - Sampling Round 2.

SAMPLE NUMBER	5	6	7	8
CARTRIDGE[a] NUMBER	419	420	422	424
SAMPLE VOLUME (mL)	12	13	12	11
SAMPLE FLOW RATE (mL/min)	2.1	2.2	2.0	1.9
COMPOUND	----------CONCENTRATION (μg/L)----------			
o-Xylene	NQ	NQ	NQ	NQ

[a]Cartridge Bed Volume (mL) = 0.68.
[b]Detected at a non-quantifiable level.
*1,1,2-Trichloro-1,2,2-trifluoroethane.

Appendix 1.13. Downhole-ATD Syosset, NY Sampling Site - Breakthrough[a] Data.

SAMPLE NUMBER	1	2	3	4
CARTRIDGE[b] NUMBER	466	475	476	477
SAMPLE VOLUME (mL)	10	8.8	9.5	9.4
SAMPLE FLOW RATE (mL/min)	2.5	2.2	2.4	2.3
COMPOUND	----------BREAKTHROUGH (%)----------			
1,1-Dichloroethene	8.1	18	14	.072
TCTF-ethane*	5.4	NB[c]	NB	NB
1,1-Dichloroethane	6.7	NB	NB	NB
cis-1,2-Dichloroethene	13	NB	6.6	NB
Trichloromethane	13	NB	NB	NB
1,1,1-Trichloroethane	6.0	.96	.045	.022
1,2-Dichloroethane	9.6	NB	5.3	NB
Tetrachloromethane	6.2	NB	NB	NB
Benzene	NB	NB	NB	NB
Trichloroethene	2.7	.76	1.7	NB
1,1,2-Trichloroethane	NB	NB	NB	NB
Tetrachloroethene	2.9	.54	1.6	NB
Chlorobenzene	8.2	NB	NB	NB
Ethylbenzene	NQ[d]	NQ	NQ	NQ
m+p-Xylene	NB	NB	NB	NB

Appendix 1.13 (cont'd.). Downhole-ATD Syosset, NY Sampling Site - Breakthrough[a] Data.

SAMPLE NUMBER	1	2	3	4
CARTRIDGE[b] NUMBER	466	475	476	477
SAMPLE VOLUME (mL)	10	8.8	9.5	9.4
SAMPLE FLOW RATE (mL/min)	2.5	2.2	2.4	2.3
COMPOUND	BREAKTHROUGH (%)			
o-Xylene	NQ	NB	NB	NB

[a]Breakthrough (%) (BT) is calculated as follows:

$$BT = 100\left[\frac{\text{(ng amt. on Backup Cartridge)}}{\text{(ng amt. on Primary Cartridge + ng amt. on Backup Cartridge)}}\right]$$

[b]Backup Cartridge Bed Volume (mL) = 0.68.
[c]NB = No Breakthrough, compound not detected on backup cartridge.
[d]Detected at a non-quantifiable level.
*1,1,2-Trichloro-1,2,2-trifluoroethane.

Appendix 1.14. Surface-ATD Data Set[a] Syosset, NY Sampling Site - Sampling Round 1.

SAMPLE NUMBER	1	2	3	4
CARTRIDGE[b] NUMBER	432	449	450	455
SAMPLE VOLUME (mL)	14	15	15	15
SAMPLE FLOW RATE (mL/min)	2.5	2.1	1.8	2.4
COMPOUND	----------CONCENTRATION (μg/L)----------			
1,1-Dichloroethene	18	2.0	1.1	2.9
TCTF-ethane*	26	24	24	24
1,1-Dichloroethane	.54	.52	.41	.45
cis-1,2-Dichloroethene	.16	.19	.12	.13
Trichloromethane	.11	.11	.083	.090
1,1,1-Trichloroethane	100	110	110	NA[c]
1,2-Dichloroethane	.28	.28	.23	.22
Tetrachloromethane	.97	1.0	.97	1.0
Benzene	.34	.22	.20	.21
Trichloroethene	2.8	3.1	2.5	2.3
1,1,2-Trichloroethane	.085	.083	.073	.077
Tetrachloroethene	29	27	26	NA
Chlorobenzene	.079	.070	.065	.075
Ethylbenzene	NQ[d]	NQ	NQ	NQ
m+p-Xylene	NQ	NQ	NQ	NQ

Appendix 1.14 (cont'd.). Surface-ATD Data Set[a] Syosset, NY Sampling Site - Sampling Round 1.

SAMPLE NUMBER	1	2	3	4
CARTRIDGE[b] NUMBER	432	449	450	455
SAMPLE VOLUME (mL)	14	15	15	15
SAMPLE FLOW RATE (mL/min)	2.5	2.1	1.8	2.4
COMPOUND	----------CONCENTRATION (μg/L)----------			
o-Xylene	NQ	NQ	NQ	NQ

[a]Samples 1-4 were collected Backup Cartridges, therefore concentrations listed are calculated as follows:

$$C = \frac{\text{(ng amt. on primary cartridge + ng amt. on backup cartridge)}}{\text{Sample Volume}}$$

[b]Cartridge Bed Volume (mL) = 0.68.
[c]Not available.
[d]Detected at a non-quantifiable level.
*1,1,2-Trichloro-1,2,2-trifluoroethane.

Appendix 1.15. Surface-ATD Data Set Syosset, NJ Sampling Site - Sampling Round 2.

SAMPLE NUMBER	5	6	7	8
CARTRIDGE[a] NUMBER	456	461	464	465
SAMPLE VOLUME (mL)	15	15	15	15
SAMPLE FLOW RATE (mL/min)	2.1	2.6	2.6	2.7
COMPOUND	----------CONCENTRATION (μg/L)----------			
1,1-Dichloroethene	4.5	3.7	6.8	5.4
TCTF-ethane*	21	23	24	22
1,1-Dichloroethane	.36	.55	1.3	.39
cis-1,2-Dichloroethene	.098	.19	.40	.12
Trichloromethane	.071	.11	.22	.074
1,1,1-Trichloroethane	96	100	110	96
1,2-Dichloroethane	.16	.24	.38	.18
Tetrachloromethane	.87	.89	1.0	.95
Benzene	.11	.14	.22	.12
Trichloroethene	2.0	3.3	5.2	2.2
1,1,2-Trichloroethane	.065	.074	.082	.071
Tetrachloroethene	23	27	32	24
Chlorobenzene	.059	.071	.076	.058
Ethylbenzene	NQ[b]	NQ	NQ	NQ
m+p-Xylene	NQ	NQ	NQ	NQ

Appendix 1.15. Surface-ATD Data Set Syosset, NJ Sampling Site - Sampling Round 2.

SAMPLE NUMBER	5	6	7	8
CARTRIDGE[a] NUMBER	456	461	464	465
SAMPLE VOLUME (mL)	15	15	15	15
SAMPLE FLOW RATE (mL/min)	2.1	2.6	2.6	2.7
COMPOUND	----------CONCENTRATION (μg/L)----------			
o-Xylene	NQ	NQ	NQ	NQ

[a]Cartridge Bed Volume (mL) = 0.68
[b]Detected at a non-quantifiable level.
*1,1,2-Trichloro-1,2,2-trifluoroethane.

Appendix 1.16. Surface-ATD Syosset, NY Sampling Site - Breakthrough[a] Data.

SAMPLE NUMBER	1	2	3	4
CARTRIDGE[b] NUMBER	479	481	483	488
SAMPLE VOLUME (mL)	14	15	15	15
SAMPLE FLOW RATE (mL/min)	2.5	2.1	1.8	2.4
COMPOUND	----------BREAKTHROUGH (%)----------			
1,1-Dichloroethene	.15	2.0	NB[c]	1.8
TCTF-ethane*	NB	NB	NB	NB
1,1-Dichloroethane	NB	NB	NB	NB
cis-1,2-Dichloroethene	NB	NB	NB	NB
Trichloromethane	NB	NB	NB	NB
1,1,1-Trichloroethane	.037	.19	NB	NB
1,2-Dichloroethane	NB	NB	NB	NB
Tetrachloromethane	NB	NB	NB	NB
Benzene	38	15	NB	NB
Trichloroethene	NB	.30	NB	NB
1,1,2-Trichloroethane	NB	NB	NB	NB
Tetrachloroethene	.098	.16	.13	NA[d]
Chlorobenzene	9.1	6.7	7.1	5.1
Ethylbenzene	NQ[e]	NQ	NQ	NQ
m+p-Xylene	NB	NB	NB	NB

Appendix 1.16 (cont'd.). Surface-ATD Syosset, NY Sampling Site - Breakthrough[a] Data.

SAMPLE NUMBER	1	2	3	4
CARTRIDGE[b] NUMBER	479	481	483	488
SAMPLE VOLUME (mL)	14	15	15	15
SAMPLE FLOW RATE (mL/min)	2.5	2.1	1.8	2.4
COMPOUND	BREAKTHROUGH (%)			
o-Xylene	NQ	NQ	NB	NB

[a]Breakthrough (%) (BT) is calculated as follows:

$$BT = 100\left[\frac{\text{(ng amt. on Backup Cartridge)}}{\text{(ng amt. on Primary Cartridge + ng amt. on Backup Cartridge)}}\right]$$

[b]Backup Cartridge Bed Volume (mL) = 0.68.
[c]NB = No Breakthrough, compound not detected on backup cartridge.
[d]Not available.
[e]Detected at a non-quantifiable level.
*1,1,2-Trichloro-1,2,2-trifluoroethane.

Appendix 1.17. ATD Syosset, NY Sampling Site - Travel Blank Data.

Compound	$\bar{B}$[a] (ng)	s (ng)	L[b] (ng)
1,1-Dichloroethene	ND[c]	-	-
TCTF-ethane*	ND	-	-
1,1-Dichloroethane	ND	-	-
cis-1,2-Dichloroethene	ND	-	-
Trichloromethane	ND	-	-
1,1,1-Trichloroethane	.26	.0035	.0066[d]
1,2-Dichloroethane	ND	-	-
Tetrachloromethane	ND	-	-
Benzene	.35	.21	.28[e]
Trichloroethene	ND	-	-
1,1,2-Trichloroethane	ND	-	-
Tetrachloroethene	ND	-	-
Chlorobenzene	ND	-	-
Ethylbenzene	.10	.019	.025[f]
m+p-Xylene	.14	.15	.21[e]

Appendix 1.17 (cont'd.). ATD Syosset, NY Sampling Site - Travel Blank Data.

Compound	$\bar{B}$[a] (ng)	s (ng)	L[b] (ng)
o-Xylene	ND	-	-

[a]Mean Blank determined from the analysis of 2 travel blanks and 4 system blanks.
[b]Calculated according to procedure outlined in Ref. 32.
[c]ND = Not Detected in the travel blanks or the system blanks.
[d]ϕ = 9, L = 1.9s.
[e]ϕ = 13, L = 1.4s.
[f]ϕ = 14, L = 1.3s.
*1,1,2-Trichloro-1,2,2-trifluoroethane.

Appendix 1.18. Surface-P&T Data Set Syosset, NY Sampling Site - Sampling Round 1.

SAMPLE NUMBER	1[a]	2[a]	3	4
ANALYSIS VOLUME (mL)	5.0	5.0	5.0	5.0
COMPOUND	----------CONCENTRATION (μg/L)----------			
1,1-Dichloroethene	120	120	110	120
TCTF-ethane*	NQ[b]	NQ	NQ	NQ
1,1-Dichloroethane	4.1	4.0	3.9	3.9
cis-1,2-Dichloroethene	1.7	1.8	1.9	2.0
Trichloromethane	.75	.74	.75	.73
1,1,1-Trichloroethane	120	130	120	120
1,2-Dichloroethane	.74	.77	.80	.75
Tetrachloromethane	.80	.88	.88	.83
Benzene	ND[c]	ND	ND	ND
Trichloroethene	9.8	10	11	11
1,1,2-Trichloroethane	ND	ND	ND	ND
Tetrachloroethene	36	38	38	38
Chlorobenzene	NQ	NQ	NQ	NQ
Ethylbenzene	ND	ND	ND	ND
m+p-Xylene	ND	ND	ND	ND

Appendix 1.18 (cont'd.). Surface-P&T Data Set Syosset, NY Sampling Site - Sampling Round 1.

SAMPLE NUMBER	1[a]	2[a]	3	4
ANALYSIS VOLUME (mL)	5.0	5.0	5.0	5.0
COMPOUND	----------CONCENTRATION (μg/L)----------			
o-Xylene	ND	ND	ND	ND

[a]Represents the average concentration of 2 replicate sample analyses.
[b]Detected at a non-quantifiable level.
[c]ND = Not Detected
*1,1,2-Trichloro-1,2,2-trifluoroethane.

Appendix 1.19. Surface-P&T Data Set Syosset, NY Sampling Site - Sampling Round 2.

SAMPLE NUMBER	5	6	7	8[a]
ANALYSIS VOLUME (mL)	5.0	5.0	5.0	5.0
COMPOUND	----------CONCENTRATION (μg/L)----------			
1,1-Dichloroethene	110	SL[b]	110	120
TCTF-ethane*	NQ[c]	SL	NQ	NQ
1,1-Dichloroethane	3.8	SL	4.0	4.0
cis-1,2-Dichloroethene	2.1	SL	2.0	1.9
Trichloromethane	.73	SL	.70	.73
1,1,1-Trichloroethane	120	SL	130	130
1,2-Dichloroethane	.85	SL	.75	.75
Tetrachloromethane	.96	SL	.90	.92
Benzene	ND[d]	ND	ND	ND
Trichloroethene	10	SL	10	10
1,1,2-Trichloroethane	ND	ND	ND	ND
Tetrachloroethene	35	SL	37	37
Chlorobenzene	NQ	SL	ND	NQ
Ethylbenzene	ND	SL	ND	ND
m+p-Xylene	ND	SL	ND	ND

Appendix 1.19 (cont'd.). Surface-P&T Data Set Syosset, NY Sampling Site - Sampling Round 2.

SAMPLE NUMBER	5	6	7	8[a]
ANALYSIS VOLUME (mL)	5.0	5.0	5.0	5.0
COMPOUND	----------CONCENTRATION (μg/L)----------			
o-Xylene	ND	SL	ND	ND

[a]Represents the average concentration of 2 replicate sample analyses.
[b]SL = Sample lost, sample froze and burst during storage.
[c]ND = Not detected.
[d]Detected at a non-quantifiable level.
*1,1,2-Trichloro-1,2,2-trifluoroethane.

Appendix 1.20. P&T Syosset, NY Sampling Site - Travel Blank Data.

Compound	$\bar{C}$[a] (μg/L)	s (μg/L)	L[b] (μg/L)
1,1-Dichloroethene	ND[c]	-	-
TCTF-ethane*	NA[d]	-	-
1,1-Dichloroethane	ND	-	-
cis-1,2-Dichloroethene	ND	-	-
Trichloromethane	ND	-	-
1,1,1-Trichloroethane	NA	-	-
1,2-Dichloroethane	ND	-	-
Tetrachloromethane	ND	-	-
Benzene	NA	-	-
Trichloroethene	ND	-	-
1,1,2-Trichloroethane	NA	-	-
Tetrachloroethene	ND	-	-
Chlorobenzene	NA	-	-
Ethylbenzene	NA	-	-
m+p-Xylene	NA	-	-

Appendix 1.20 (cont'd.). P&T Syosset, NY Sampling Site - Travel Blank Data.

Compound	$\bar{C}^a$ (μg/L)	s (μg/L)	L^b (μg/L)
o-Xylene	NA	-	-

[a]Mean Blank determined from the analysis of 5 travel blanks.
[b]Calculated according to procedure outlined in Ref. #.
[c]ND = Not Detected.
[d]NA = Not available, compound not detected in purge and trap samples.
*1,1,2-Trichloro-1,2,2-trifluoroethane.

Appendix 1.21. Downhole-ATD Data Set[a] Repauno, NJ Sampling Site - Sampling Round 1.

SAMPLE NUMBER	1	2	3	4
CARTRIDGE[b] NUMBER	402	403	407	411
SAMPLE VOLUME (mL)	20	22	21	22
SAMPLE FLOW RATE (mL/min)	1.4	1.5	1.5	1.6
COMPOUND	----------CONCENTRATION (μg/L)----------			
Dichloromethane	NS[c]	NS	.26	.26
cis-1,2-Dichloroethene	1.9	1.9	1.9	1.8
Trichloromethane	28	26	27	28
1,2-Dichloroethane	1.5	1.4	1.4	1.4
Tetrachloromethane	1.7	1.7	1.7	1.7
Benzene	17	17	17	17
Trichloroethene	37	35	35	35
Toluene	.11	.10	.14	.11
Tetrachloroethene	440	360	350	350
Chlorobenzene	34	32	34	32
m+p-Xylene	NQ[d]	NQ	NQ	NQ
o-Xylene	.37	.30	.30	.31

Appendix 1.21 (cont'd.). Downhole-ATD Data Set[a] Repauno, NJ Sampling Site - Sampling Round 1.

SAMPLE NUMBER	1	2	3	4
CARTRIDGE[b] NUMBER	402	403	407	411
SAMPLE VOLUME (mL)	20	22	21	22
SAMPLE FLOW RATE (mL/min)	1.4	1.5	1.5	1.6
COMPOUND	----------CONCENTRATION (μg/L)----------			
Nitrobenzene	250	270	220	240

[a]Samples 1-4 were collected Backup Cartridges, therefore concentrations listed are calculated as follows:

$$C = \frac{\text{(ng amt. on primary cartridge + ng amt. on backup cartridge)}}{\text{Sample Volume}}$$

[b]Cartridge Bed Volume (mL) = 0.68.
[c]NS = Not significant, with respect to the Limit of Detection.
[d]Detected at a non-quantifiable level.

Appendix 1.22. Downhole-ATD Data Set Repauno, NJ Sampling Site - Sampling Round 2.

SAMPLE NUMBER	5	6	7	8
CARTRIDGE[a] NUMBER	414	419	420	450
SAMPLE VOLUME (mL)	23	24	22	22
SAMPLE FLOW RATE (mL/min)	1.4	1.4	1.3	1.3
COMPOUND	----------CONCENTRATION (μg/L)----------			
Dichloromethane	.23	.25	.26	.25
cis-1,2-Dichloroethene	1.9	1.8	1.8	1.9
Trichloromethane	28	28	28	28
1,2-Dichloroethane	1.4	1.4	1.4	1.4
Tetrachloromethane	1.7	1.7	1.6	1.6
Benzene	16	16	16	16
Trichloroethene	35	35	34	34
Toluene	.10	.10	.11	.11
Tetrachloroethene	340	340	330	330
Chlorobenzene	34	35	34	33
m+p-Xylene	NQ[b]	NQ	NQ	NQ
o-Xylene	.32	.33	.33	.32
Nitrobenzene	240	220	230	240

[a]Cartridge Bed Volume (mL) = 0.68.
[b]Detected at a non-quantifiable level.

Appendix 1.23. Downhole-ATD Repauno, NJ Sampling Site - Breakthrough[a] Data.

SAMPLE NUMBER	1	2	3	4
CARTRIDGE[b] NUMBER	437	447	449	463
SAMPLE VOLUME (mL)	20	22	21	22
SAMPLE FLOW RATE (mL/min)	1.4	1.5	1.5	1.6
COMPOUND	----------BREAKTHROUGH (%)----------			
Dichloromethane	NB[c]	NB	NB	NB
cis-1,2-Dichloroethene	NB	NB	NB	NB
Trichloromethane	NB	NB	NB	NB
1,2-Dichloroethane	NB	NB	NB	NB
Tetrachloromethane	NB	NB	NB	NB
Benzene	NB	NB	NB	NB
Trichloroethene	NB	NB	NB	NB
Toluene	NB	NB	NB	NB
Tetrachloroethene	NB	NB	NB	NB
Chlorobenzene	NB	NB	NB	NB
m+p-Xylene	NA[d]	NA	NA	NA
o-Xylene	NB	NB	NB	NB

Appendix 1.23 (cont'd.). Downhole-ATD Repauno, NJ Sampling Site - Breakthrough[a] Data.

SAMPLE NUMBER	1	2	3	4
CARTRIDGE[b] NUMBER	437	447	449	463
SAMPLE VOLUME (mL)	20	22	21	22
SAMPLE FLOW RATE (mL/min)	1.4	1.5	1.5	1.6
COMPOUND	----------BREAKTHROUGH (%)----------			
Nitrobenzene	NB	NB	NB	NB

[a]Breakthrough (%) (BT) is calculated as follows:

$$BT = 100 \left[\frac{\text{(ng amt. on Backup Cartridge)}}{\text{(ng amt. on Primary Cartridge + ng amt. on Backup Cartridge)}} \right]$$

[b]Backup Cartridge Bed Volume (mL) = 0.68.
[c]NB = No Breakthrough, compound not detected on backup cartridge.
[d]NA = Not available, non-quantifiable amount detected on primary cartridge.

Appendix 1.24. Surface-ATD Data Set[a] Repauno, NJ Sampling Site - Sampling Round 1.

SAMPLE NUMBER	1	2	3	4
CARTRIDGE[b] NUMBER	423	424	432	436
SAMPLE VOLUME (mL)	30	32	29	33
SAMPLE FLOW RATE (mL/min)	4.3	8.7	3.6	8.8
COMPOUND	----------CONCENTRATION (μg/L)----------			
Dichloromethane	NS[c]	.21	.19	NS
cis-1,2-Dichloroethene	1.9	1.9	1.9	1.9
Trichloromethane	29	28	28	28
1,2-Dichloroethane	1.4	1.4	1.3	1.3
Tetrachloromethane	1.8	1.7	1.7	1.7
Benzene	17	17	18	18
Trichloroethene	36	35	35	35
Toluene	.16	.16	.15	.15
Tetrachloroethene	350	360	320	340
Chlorobenzene	36	31	36	37
m+p-Xylene	NQ[d]	NQ	NQ	NQ
o-Xylene	.35	.34	.34	.35

Appendix 1.24 (cont'd.). Surface-ATD Data Set[a] Repauno, NJ Sampling Site - Sampling Round 1.

SAMPLE NUMBER	1	2	3	4
CARTRIDGE[b] NUMBER	423	424	432	436
SAMPLE VOLUME (mL)	30	32	29	33
SAMPLE FLOW RATE (mL/min)	4.3	8.7	3.6	8.8
COMPOUND	CONCENTRATION (μg/L)			
Nitrobenzene	230	190	220	220

[a]Samples 1-4 were collected Backup Cartridges, therefore concentrations listed are calculated as follows:

$$C = \frac{\text{(ng amt. on primary cartridge + ng amt. on backup cartridge)}}{\text{Sample Volume}}$$

[b]Cartridge Bed Volume (mL) = 0.68.
[c]NS = Not significant, with respect to the Limit of Detection.
[d]NQ = Detected at a non-quantifiable level.

Appendix 1.25. Surface-ATD Data Set Repauno, NJ Sampling Site - Sampling Round 2.

SAMPLE NUMBER	5	6	7	8
CARTRIDGE[a] NUMBER	455	456	461	464
SAMPLE VOLUME (mL)	30	26	27	30
SAMPLE FLOW RATE (mL/min)	6.6	2.3	2.4	6.5
COMPOUND	----------CONCENTRATION (μg/L)----------			
Dichloromethane	.21	.27	.28	.25
cis-1,2-Dichloroethene	1.8	1.9	1.9	1.9
Trichloromethane	28	29	29	29
1,2-Dichloroethane	1.3	1.5	1.5	1.4
Tetrachloromethane	1.7	1.7	1.9	2.0
Benzene	17	17	18	18
Trichloroethene	35	35	36	36
Toluene	.15	.14	.13	.14
Tetrachloroethene	300	320	350	340
Chlorobenzene	35	39	39	34
m+p-Xylene	NQ[b]	NQ	NQ	NQ
o-Xylene	.32	.33	.36	.34
Nitrobenzene	220	200	210	190

[a]Cartridge Bed Volume (mL) = 0.68.
[b]Detected at a non-quantifiable level.

Appendix 1.26. Surface-ATD Repauno, NJ Sampling Site - Breakthrough[a] Data.

SAMPLE NUMBER	1	2	3	4
CARTRIDGE[b] NUMBER	493	504	647	683
SAMPLE VOLUME (mL)	30	32	29	33
SAMPLE FLOW RATE (mL/min)	4.3	8.7	3.6	8.8
COMPOUND	----------BREAKTHROUGH (%)----------			
Dichloromethane	NB[c]	NB	NB	NB
cis-1,2-Dichloroethene	2.5	NB	NB	2.0
Trichloromethane	3.0	NB[d]	NB[d]	1.7
1,2-Dichloroethane	3.5	NB	NB	1.8
Tetrachloromethane	NB	NB	NB	NB
Benzene	5.0	NB[e]	NB[e]	NB[e]
Trichloroethene	NB[e]	NB	NB[d]	NB[e]
Toluene	NB	NB	NB	NB
Tetrachloroethene	NB[e]	NB[d]	NB[d]	NB[e]
Chlorobenzene	NB[e]	NB[d]	NB[d]	NB[e]
m+p-Xylene	NA[f]	NA	NA	NA
o-Xylene	NB	NB	NB	NB

Appendix 1.26 (cont'd.). Surface-ATD Repauno, NJ Sampling Site - Breakthrough[a] Data.

SAMPLE NUMBER	1	2	3	4
CARTRIDGE[b] NUMBER	493	504	647	683
SAMPLE VOLUME (mL)	30	32	29	33
SAMPLE FLOW RATE (mL/min)	4.3	8.7	3.6	8.8
COMPOUND	----------BREAKTHROUGH (%)----------			
Nitrobenzene	6.7	1.6	NB*	4.4

[a]Breakthrough (%) (BT) is calculated as follows:

$$BT = 100\left[\frac{\text{(ng amt. on Backup Cartridge)}}{\text{(ng amt. on Primary Cartridge + ng amt. on Backup Cartridge)}}\right]$$

[b]Backup Cartridge Bed Volume (mL) = 0.68.
[c]NB = No Breakthrough, compound not detected on backup cartridge.
[d]NB = Breakthrough << 1%.
[e]NB = Breakthrough < 1%.
[f]NA = Not available, non-quantifiable amount detected on the primary cartridge.

Appendix 1.27. ATD Repauno, NJ Sampling Site - Travel Blank Data.

Compound	$\bar{B}$[a] (ng)	s (ng)	L[b] (ng)
Dichloromethane	4.3	.77	1.2[d]
cis-1,2-Dichloroethene	ND[c]	-	-
Trichloromethane	ND	-	-
1,2-Dichloroethane	ND	-	-
Tetrachloromethane	ND	-	-
Benzene	1.7	.78	1.2[d]
Trichloroethene	ND	-	-
Toluene	.36	.39	.69[e]
Tetrachloroethene	ND	-	-
Chlorobenzene	ND	-	-
m+p-Xylene	NA[f]	-	-
o-Xylene	ND	-	-
Nitrobenzene	ND	-	-

[a]Mean Blank determined from the analysis of 5 travel blanks.
[b]Calculated according to procedure outlined in Ref. 32.
[c]ND = Not Detected in the travel blanks.
[d]ϕ = 11, L = 1.6s.
[e]ϕ = 9, L = 1.9s.
[f]NA = Not available, compound not quantfiable in sample.

Appendix 1.28. Surface-P&T Data Set Repauno, NJ Sampling Site - Sampling Round 1.

SAMPLE NUMBER	1[a]	2[a]	3	4
ANALYSIS VOLUME (mL)	5.0	5.0	5.0	5.0
COMPOUND	----------CONCENTRATION (μg/L)----------			
Dichloromethane	ND[b]	ND	ND	ND
cis-1,2-Dichloroethene	2.5	2.4	2.9	3.0
Trichloromethane	32	31	33	32
1,2-Dichloroethane	1.2	1.1	1.0	.97
Tetrachloromethane	1.4	1.4	1.4	1.4
Benzene	20	19	21	20
Trichloroethene	34	34	37	35
Toluene	NQ[c]	NQ	NQ	NQ
Tetrachloroethene	360	360	390	380
Chlorobenzene	47	47	52	47
m+p-Xylene	ND	ND	ND	ND
o-Xylene	NQ	NQ	NQ	NQ
Nitrobenzene	220	250	270	240

[a]Represents the average concentration of 2 replicate sample analyses.
[b]ND = Not Detected
[c]Detected at a non-quantifiable level.

Appendix 1.29. Surface-P&T Data Set Repauno, NJ Sampling Site - Sampling Round 2.

SAMPLE NUMBER	5[a]	6	7	8
ANALYSIS VOLUME (mL)	5.0	5.0	5.0	5.0
COMPOUND	CONCENTRATION (μg/L)			
Dichloromethane	ND[b]	ND	ND	ND
cis-1,2-Dichloroethene	2.8	1.9	3.0	2.7
Trichloromethane	32	32	32	33
1,2-Dichloroethane	1.0	1.2	1.0	1.0
Tetrachloromethane	1.4	1.4	1.3	1.4
Benzene	20	19	21	21
Trichloroethene	35	34	37	36
Toluene	ND	ND	NQ[c]	NQ
Tetrachloroethene	340	370	390	370
Chlorobenzene	48	46	48	48
m+p-Xylene	ND	ND	ND	ND
o-Xylene	NQ	NQ	NQ	NQ
Nitrobenzene	240	250	240	250

[a]Represents the average concentration of 2 replicate sample analyses.
[b]ND = Not Detected
[c]Detected at a non-quantifiable level.

Appendix 1.30. P&T Syosset, NJ Sampling Site - Travel Blank Data.

Compound	$\bar{C}$[a] (μg/L)	s (μg/L)	L[b] (μg/L)
Dichloromethane	NA[c]	-	-
cis-1,2-Dichloroethene	ND[d]	-	-
Trichloromethane	ND	-	-
1,2-Dichloroethane	ND	-	-
Tetrachloromethane	ND	-	-
Benzene	.13	.092	.18[e]
Trichloroethene	ND	-	-
Toluene	NA	-	-
Tetrachloroethene	NA[f]	-	-
Chlorobenzene	ND	-	-
m+p-Xylene	NA	-	-
o-Xylene	NA	-	-
Nitrobenzene	ND	-	-

[a]Mean Blank determined from the analysis of 4 travel blanks.
[b]Calculated according to procedure outlined in Ref. #.
[c]NA = Not Available, compound not detected or not quantifiable in samples.
[d]ND = Not Detected in the travel blanks.
[e]ϕ = 9, L = 1.9s.
[f]NA = Not available, compound not detected at << 1% of sample amount.

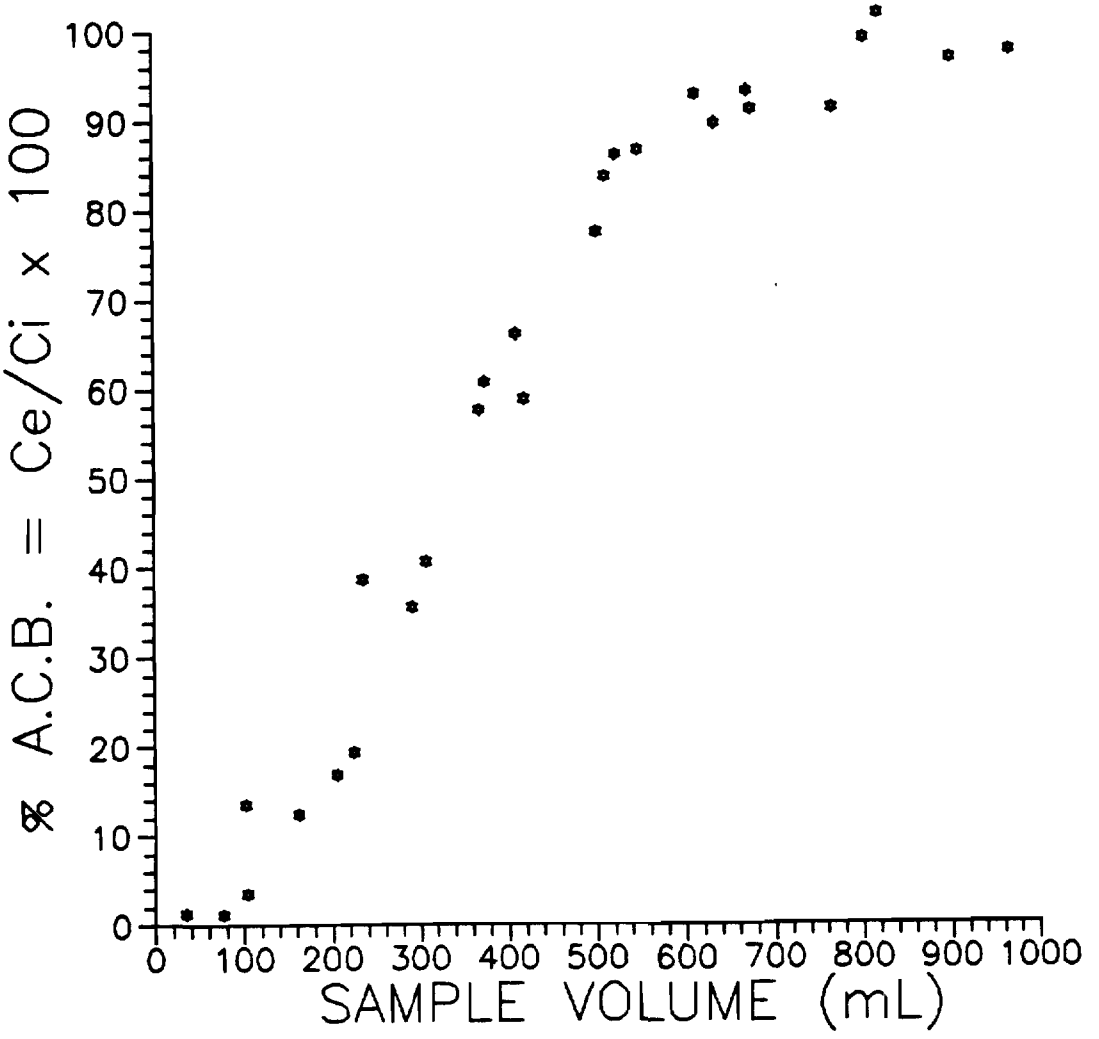

Appendix 2.1. ACB curve obtained for 1,1-dichloroethane from experiment 2, C_i = 26 ppb. This curve represents the combined results of four cartridges. Each cartridge contained ~0.13 g Tenax (see Table 4.1).

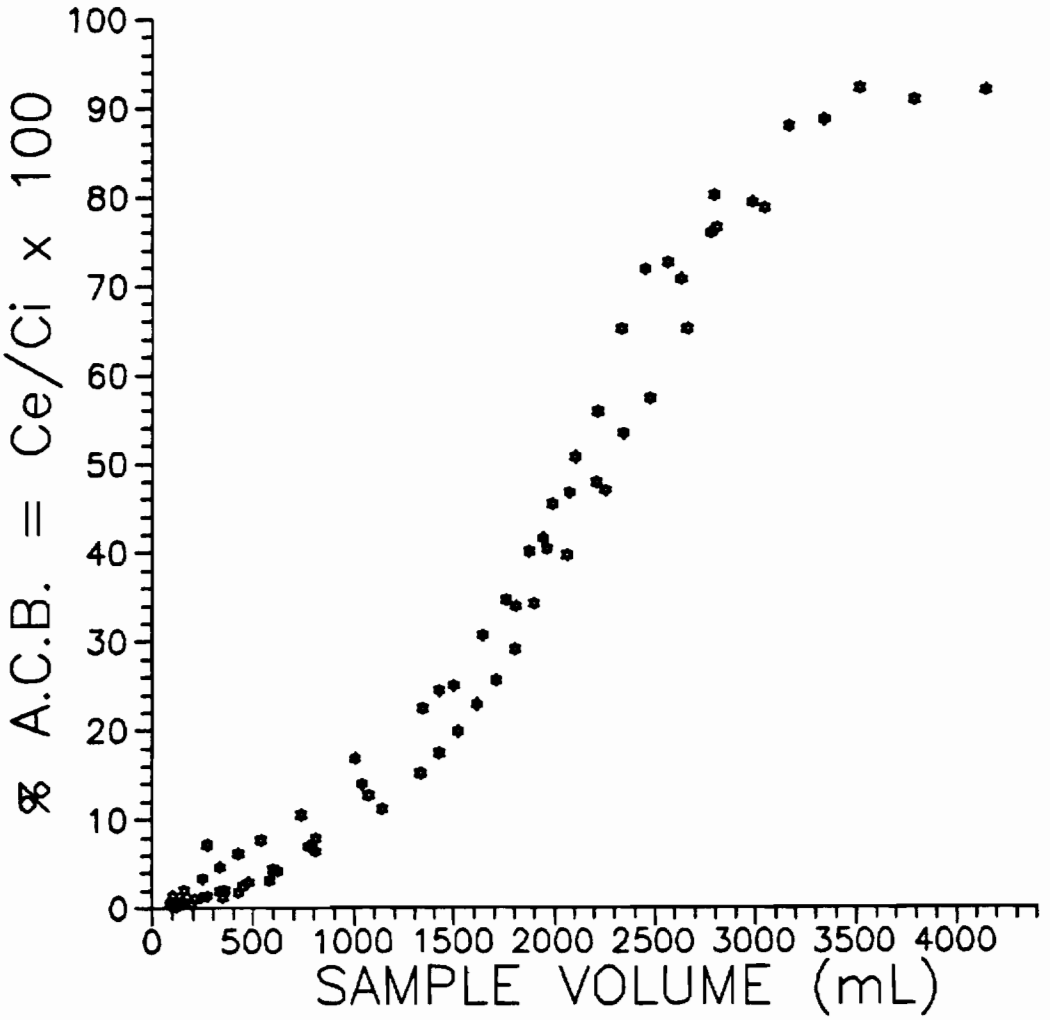

Appendix 2.2. ACB curve obtained for trichloroethene from experiment 3, C_i = 28 ppb. This curve represents the combined results of four cartridges. Each cartridge contained ~0.13 g Tenax (see Table 4.1).

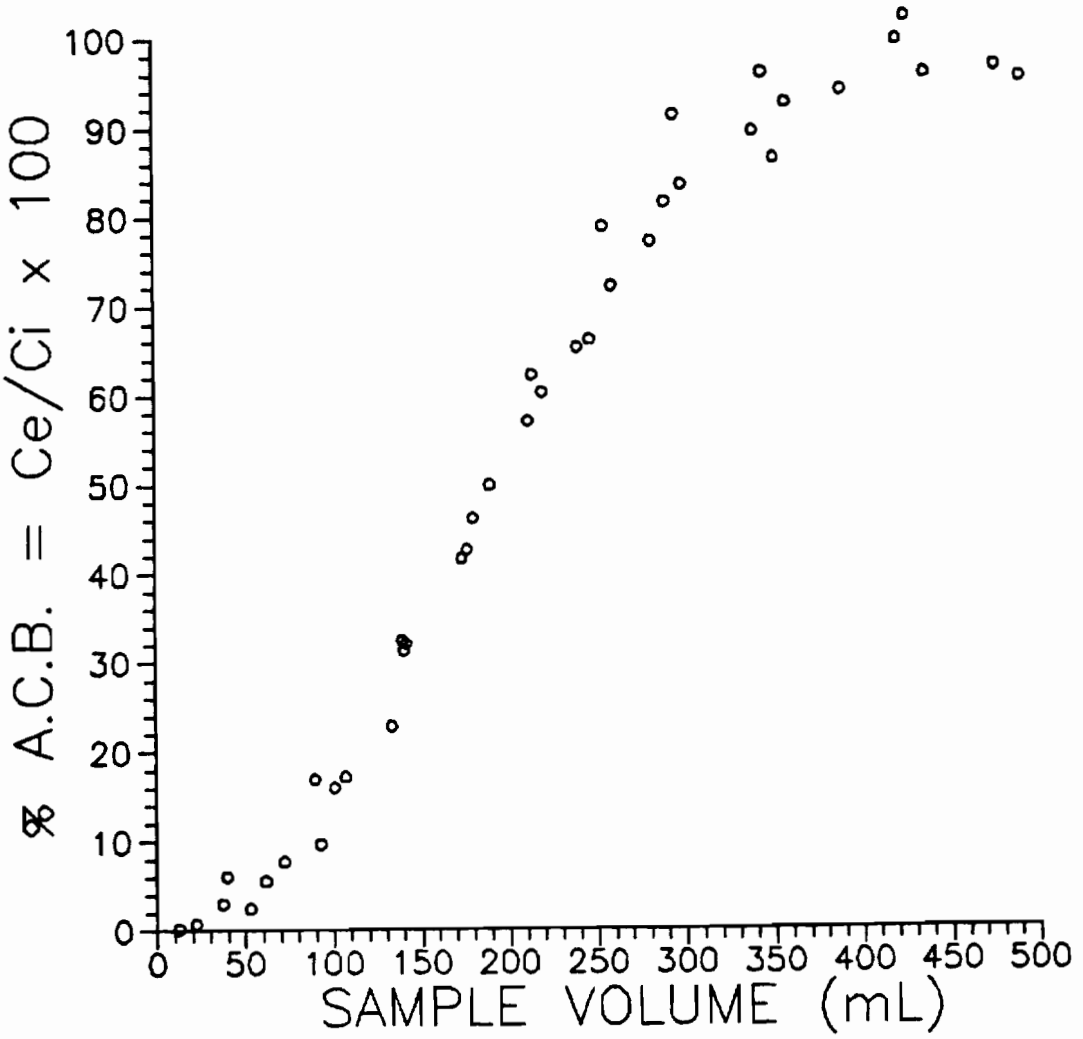

Appendix 2.3. ACB curve obtained for 1,2-dichloroethane from experiment 4, C_i = 27 ppb. This curve represents the combined results of four cartridges. Each cartridge contained ~0.13 g Tenax (see Table 4.1).

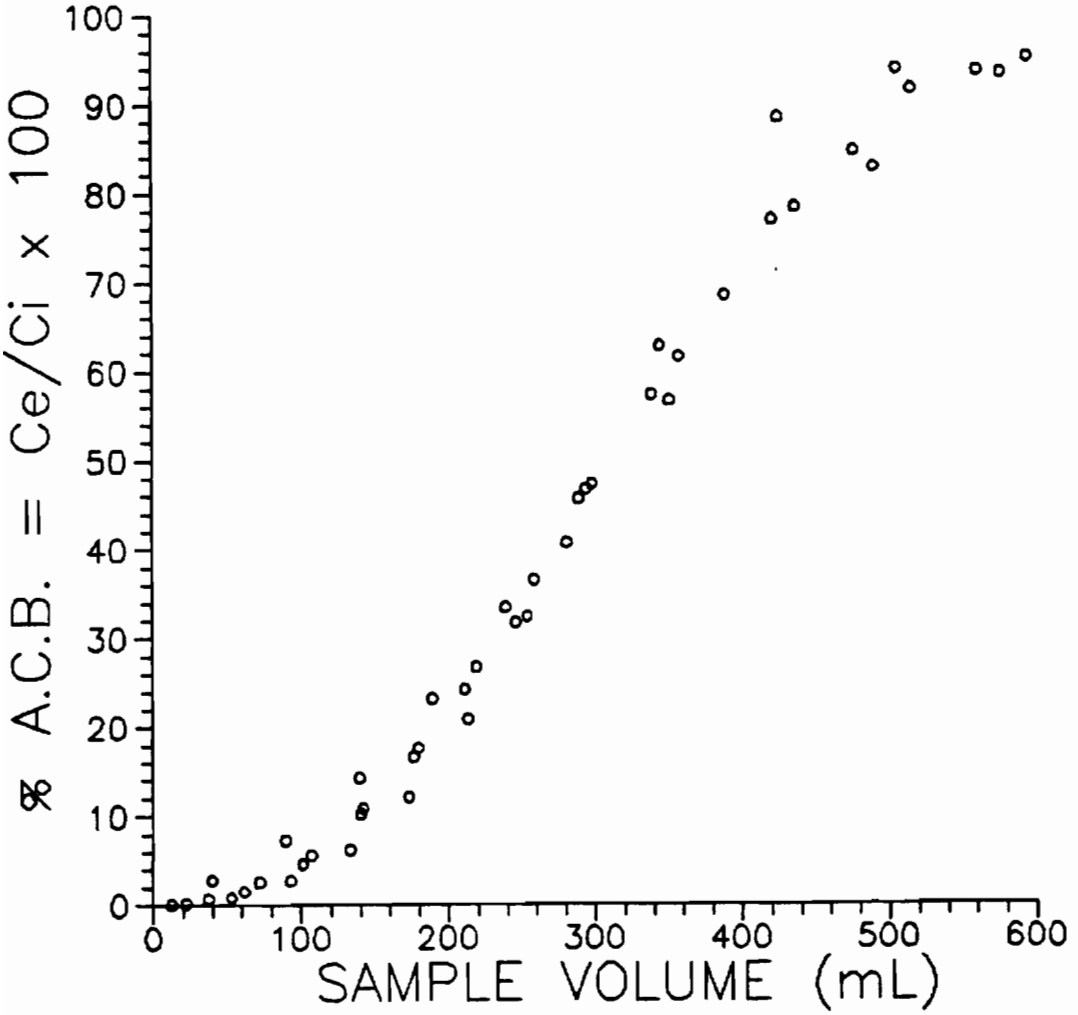

Appendix 2.4. ACB curve obtained for trichloromethane from experiment 4, C_i = 26 ppb. This curve represents the combined results of four cartridges. Each cartridge contained ~0.13 g Tenax (see Table 4.1).

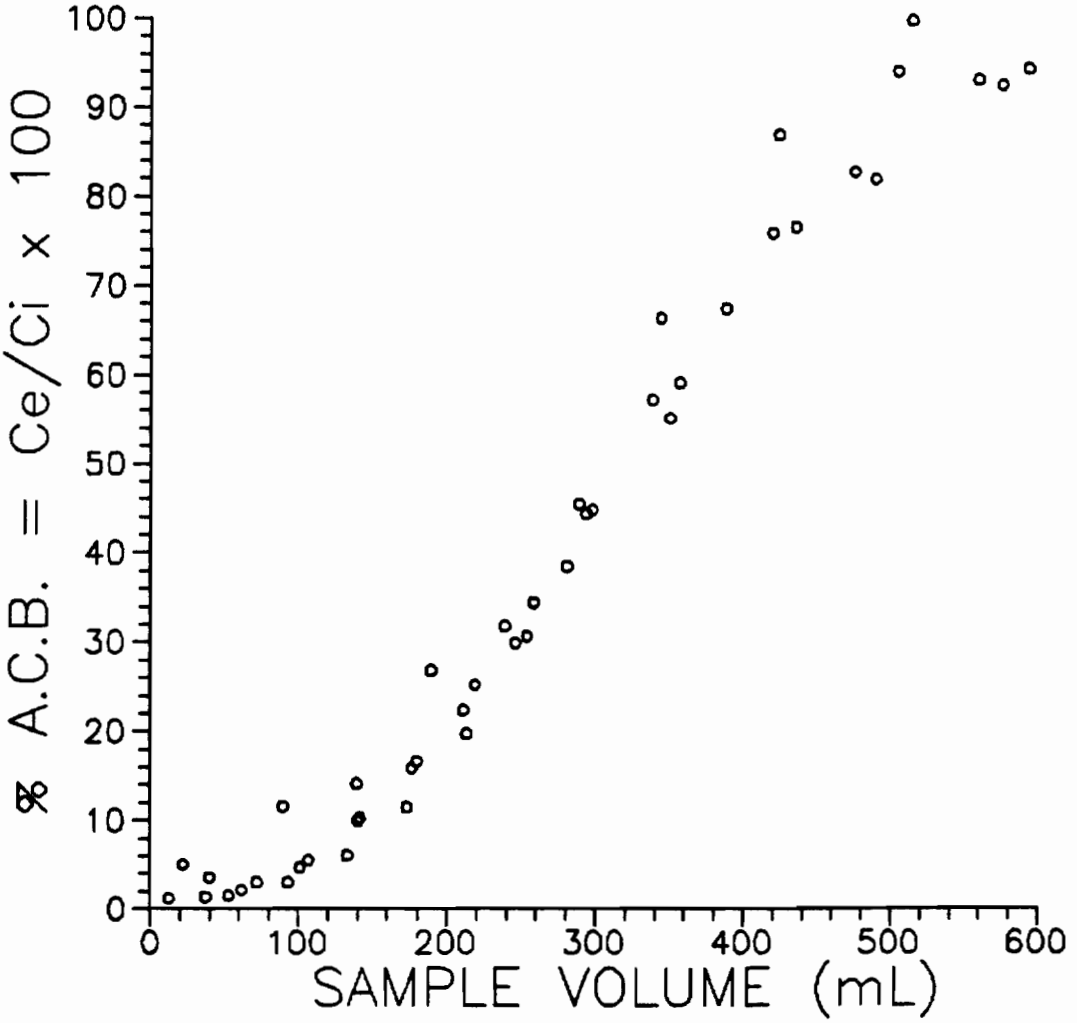

Appendix 2.5. ACB curve obtained for 1,1-dichloroethane from experiment 4, C_i = 26 ppb. This curve represents the combined results of four cartridges. Each cartridge contained ~0.13 g Tenax (see Table 4.1).

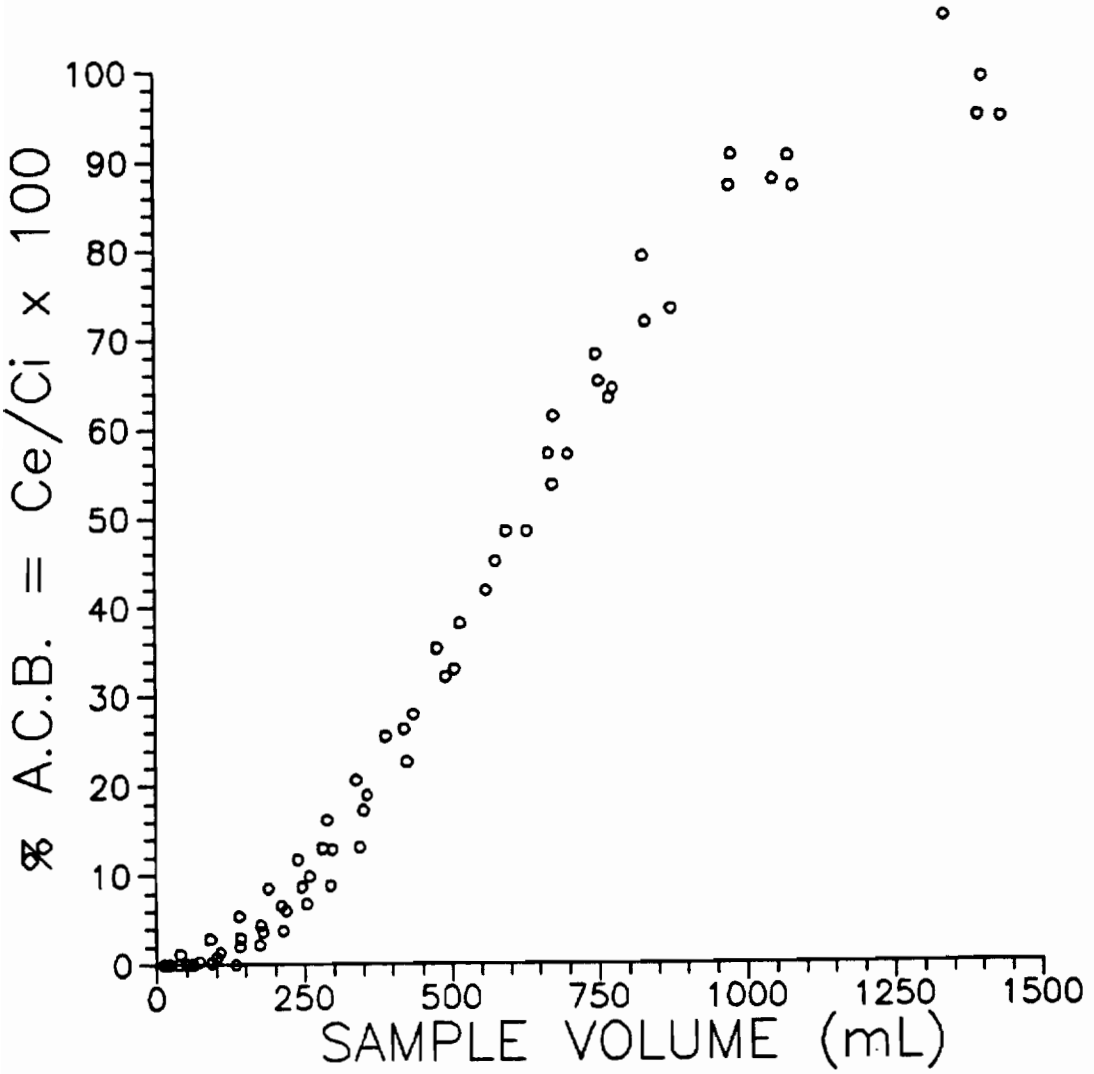

Appendix 2.6. ACB curve obtained for bromodichloromethane from experiment 4, C_i = 22 ppb. This curve represents the combined results of four cartridges. Each cartridge contained ~0.13 g Tenax (see Table 4.1).

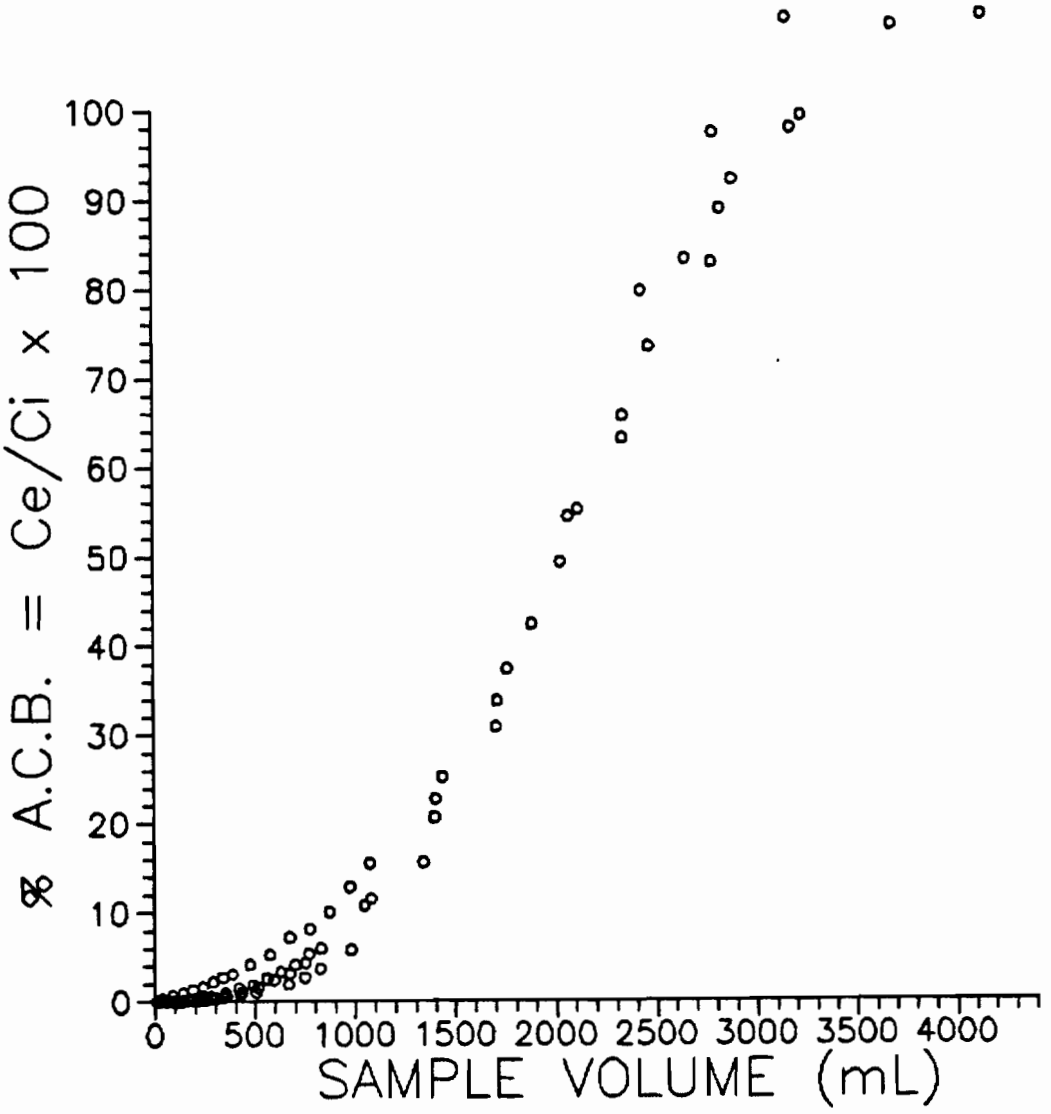

Appendix 2.7. ACB curve obtained for trichloroethene from experiment 4, C_i = 22 ppb. This curve represents the combined results of four cartridges. Each cartridge contained ~0.13 g Tenax (see Table 4.1).

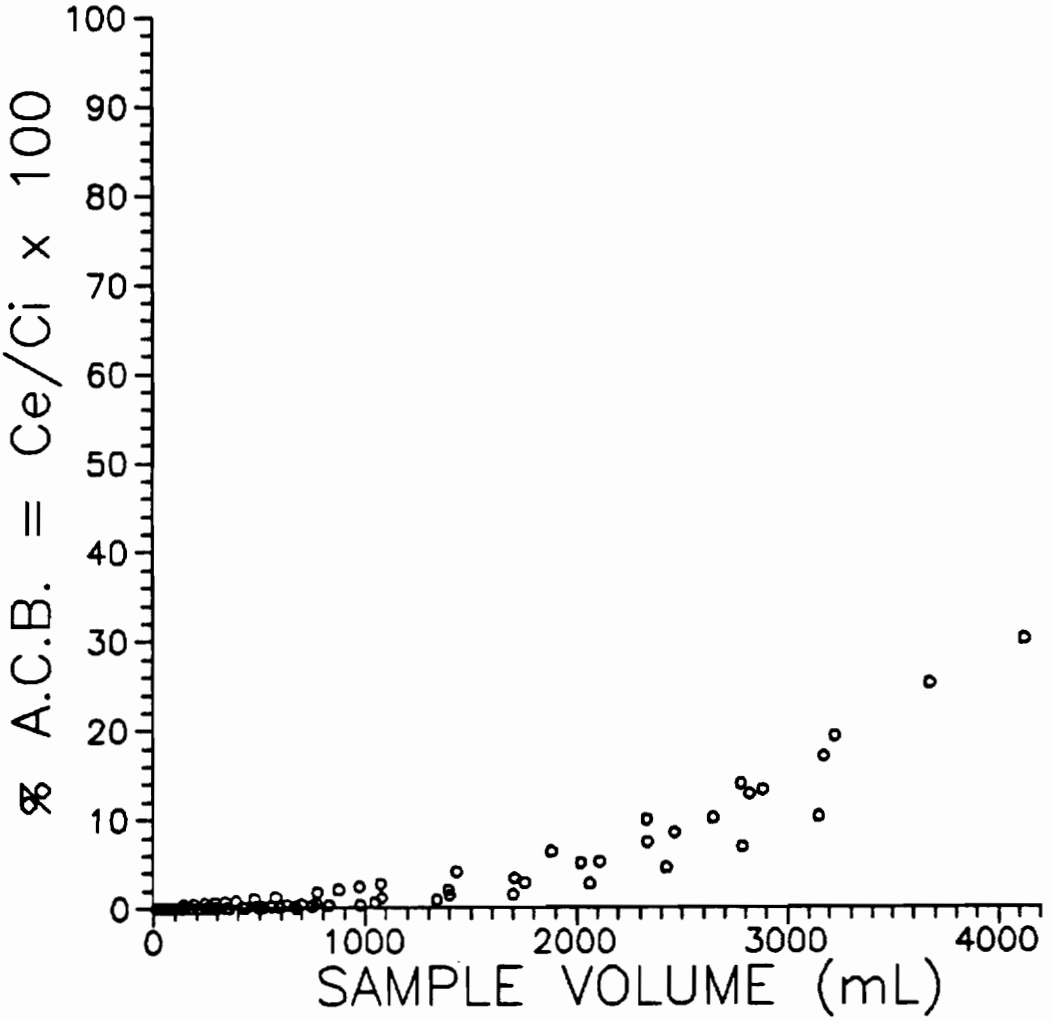

Appendix 2.8. ACB curve obtained for chlorobenzene from experiment 4, C_i = 21 ppb. This curve represents the combined results of four cartridges. Each cartridge contained ~0.13 g Tenax (see Table 4.1).

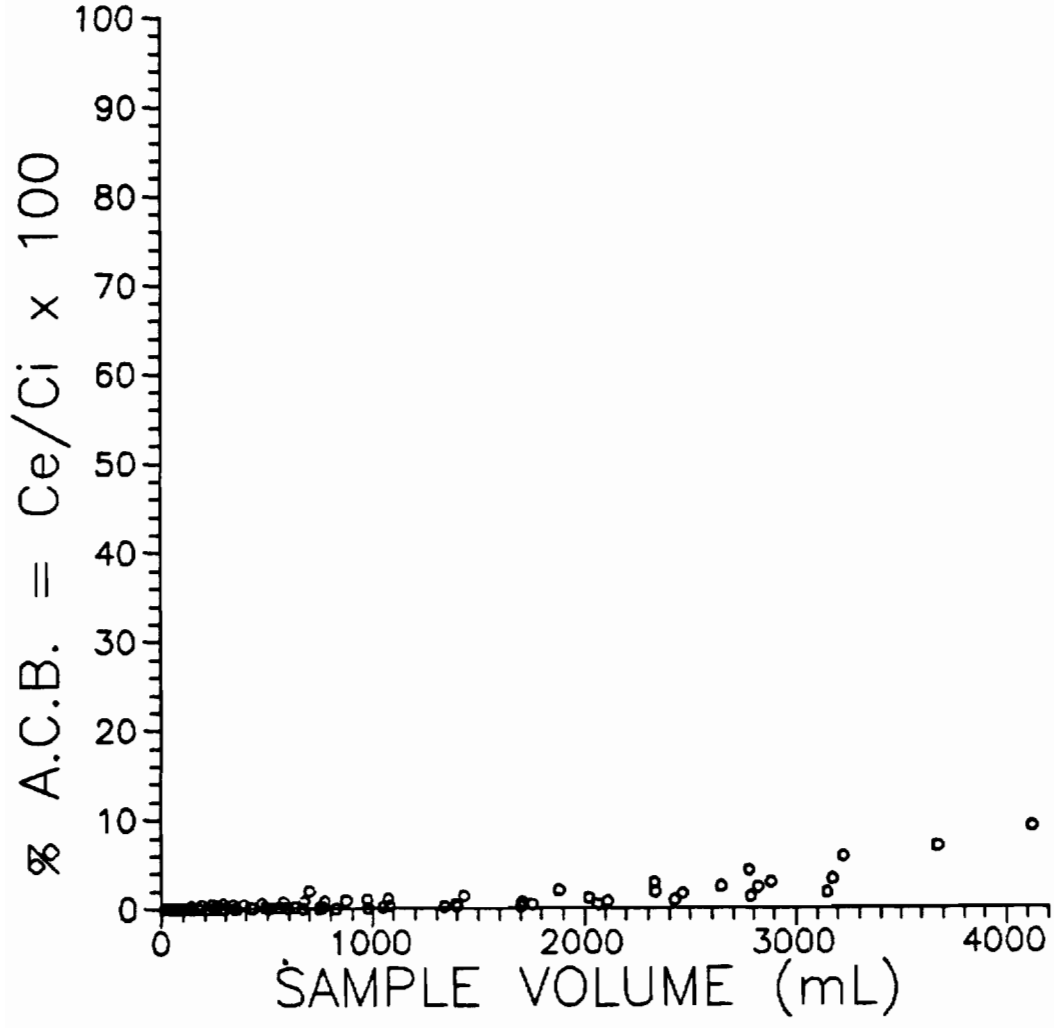

Appendix 2.9. ACB curve obtained for tetrachloroethene from experiment 4, C_i = 21 ppb. This curve represents the combined results of four cartridges. Each cartridge contained ~0.13 g Tenax (see Table 4.1).

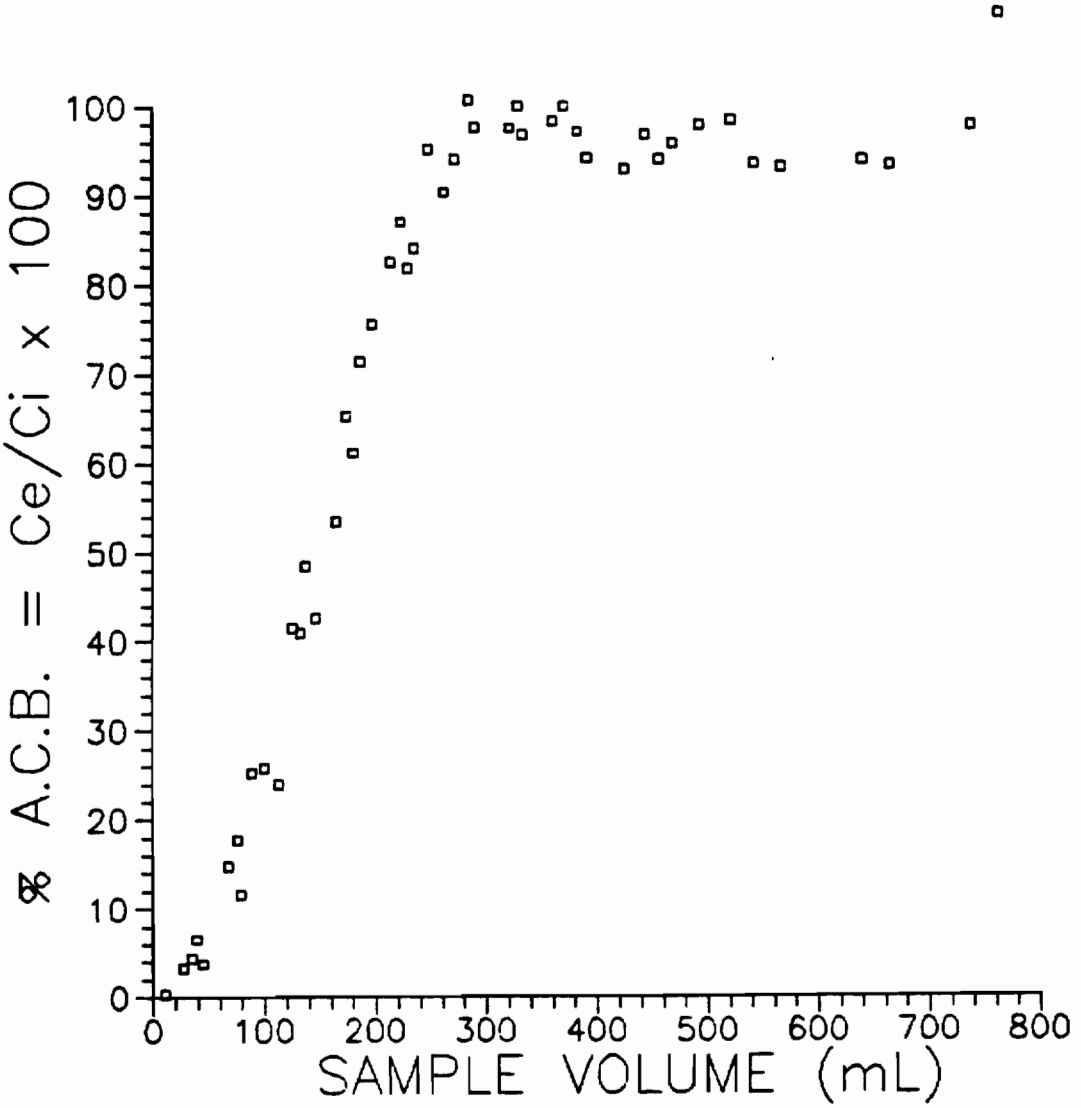

Appendix 2.10. ACB curve obtained for 1,2-dichloroethane from experiment 5, C_i = 120 ppb. This curve represents the combined results of four cartridges. Each cartridge contained ~0.13 g Tenax (see Table 4.1).

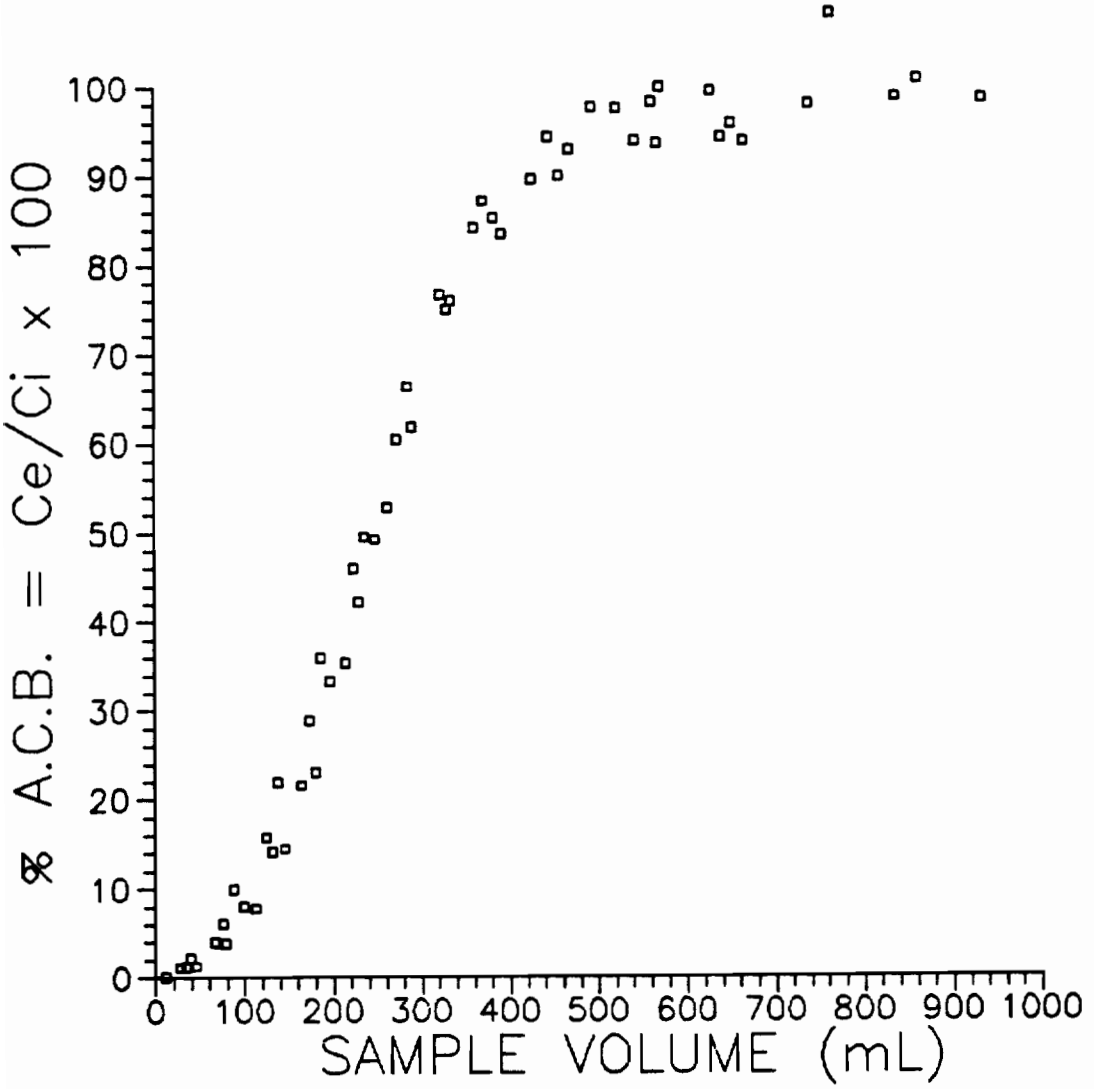

Appendix 2.11. ACB curve obtained for trichloromethane from experiment 5, C_i = 130 ppb. This curve represents the combined results of four cartridges. Each cartridge contained ~0.13 g Tenax (see Table 4.1).

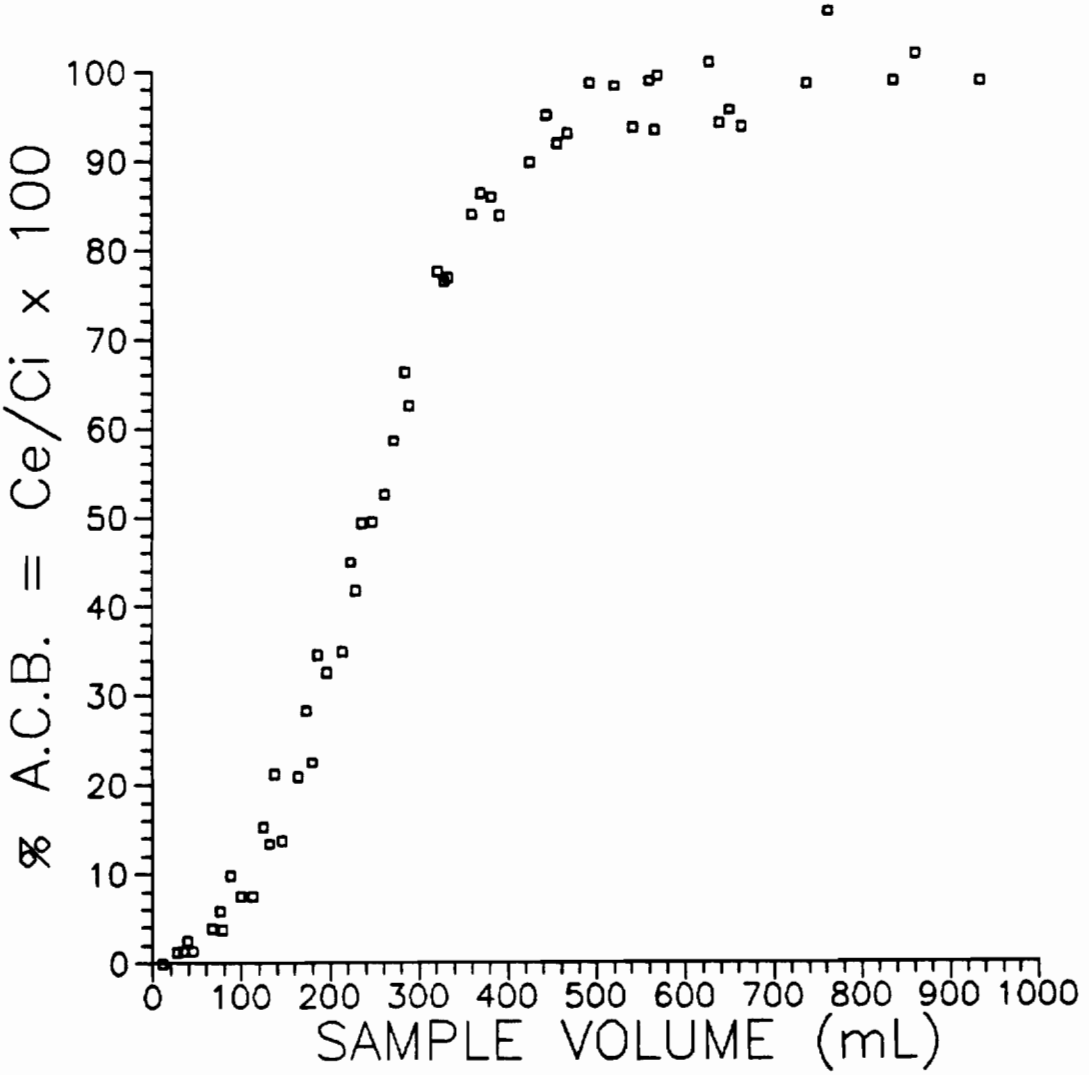

Appendix 2.12. ACB curve obtained for 1,1-dichloroethane from experiment 5, C_i = 140 ppb. This curve represents the combined results of four cartridges. Each cartridge contained ~0.13 g Tenax (see Table 4.1).

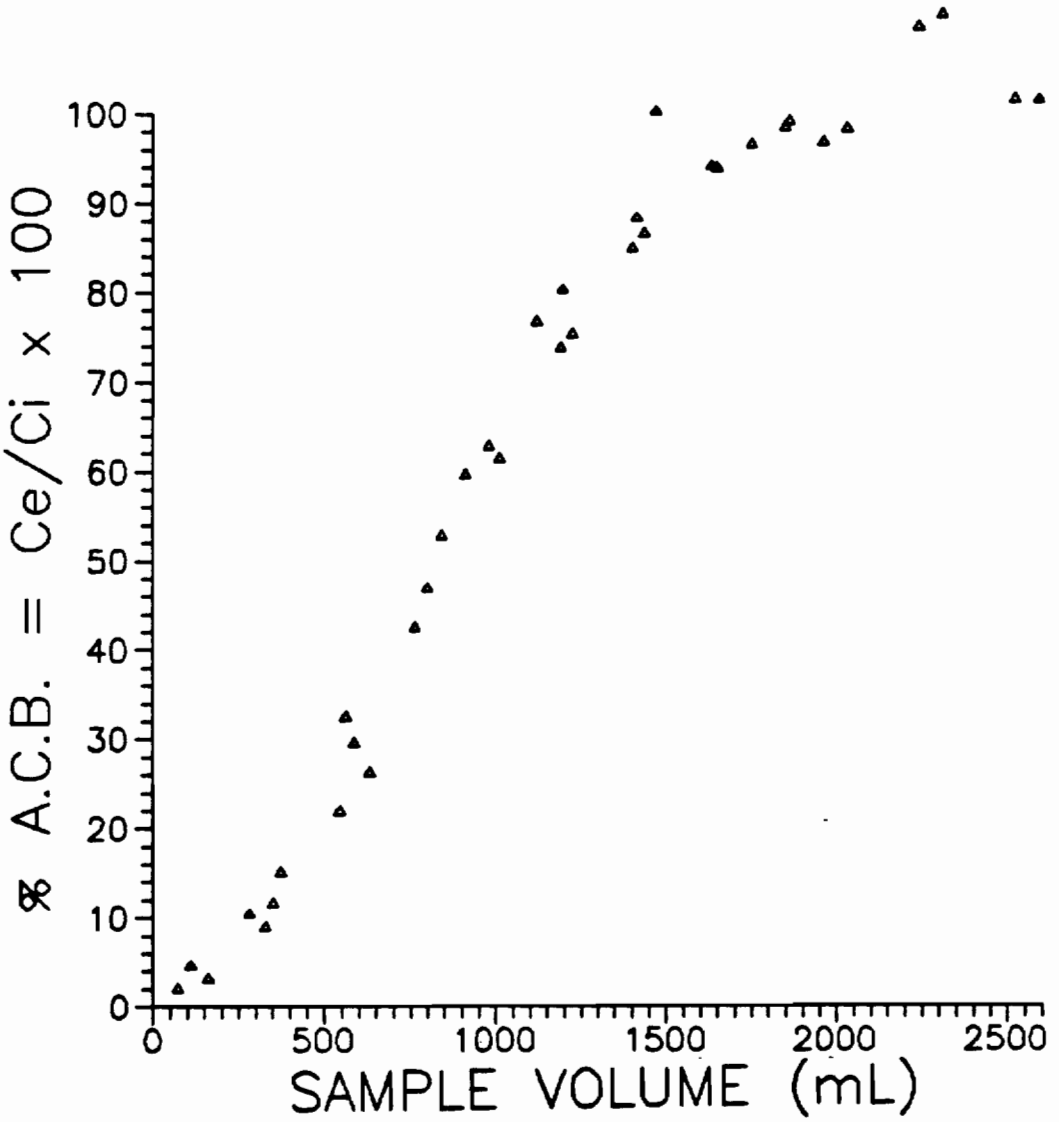

Appendix 2.13. ACB curve obtained for benzene from experiment 6, C_i = 1.3 ppb. This curve represents the combined results of four cartridges. Each cartridge contained ~0.13 g Tenax (see Table 4.1).

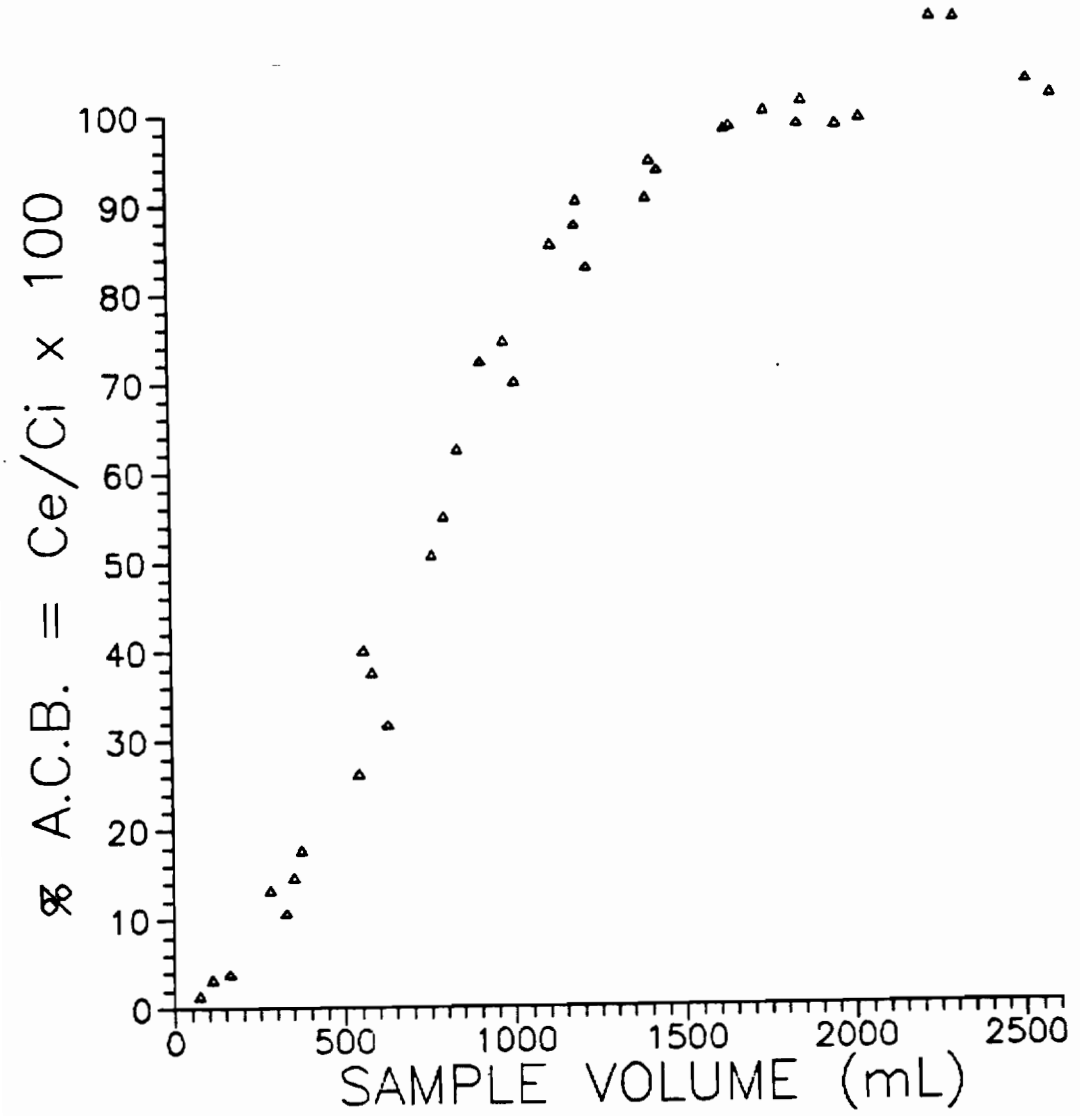

Appendix 2.14. ACB curve obtained for 1,2-dichloropropane from experiment 6, C_i = 24 ppb. This curve represents the combined results of four cartridges. Each cartridge contained ~0.13 g Tenax (see Table 4.1).

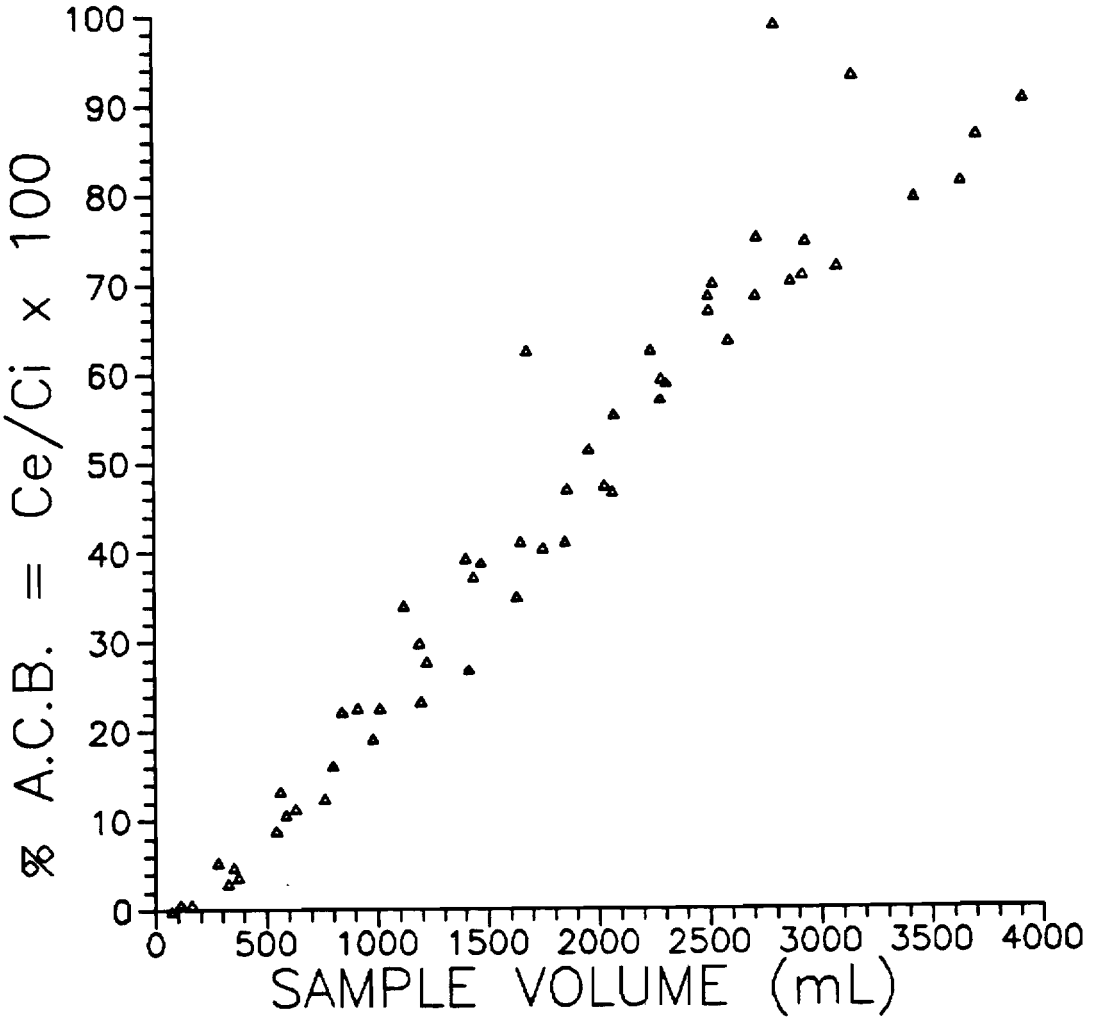

Appendix 2.15. ACB curve obtained for 1,1,2,2-tetrachloroethane from experiment 6, C_i = 16 ppb. This curve represents the combined results of four cartridges. Each cartridge contained ~0.13 g Tenax (see Table 4.1).

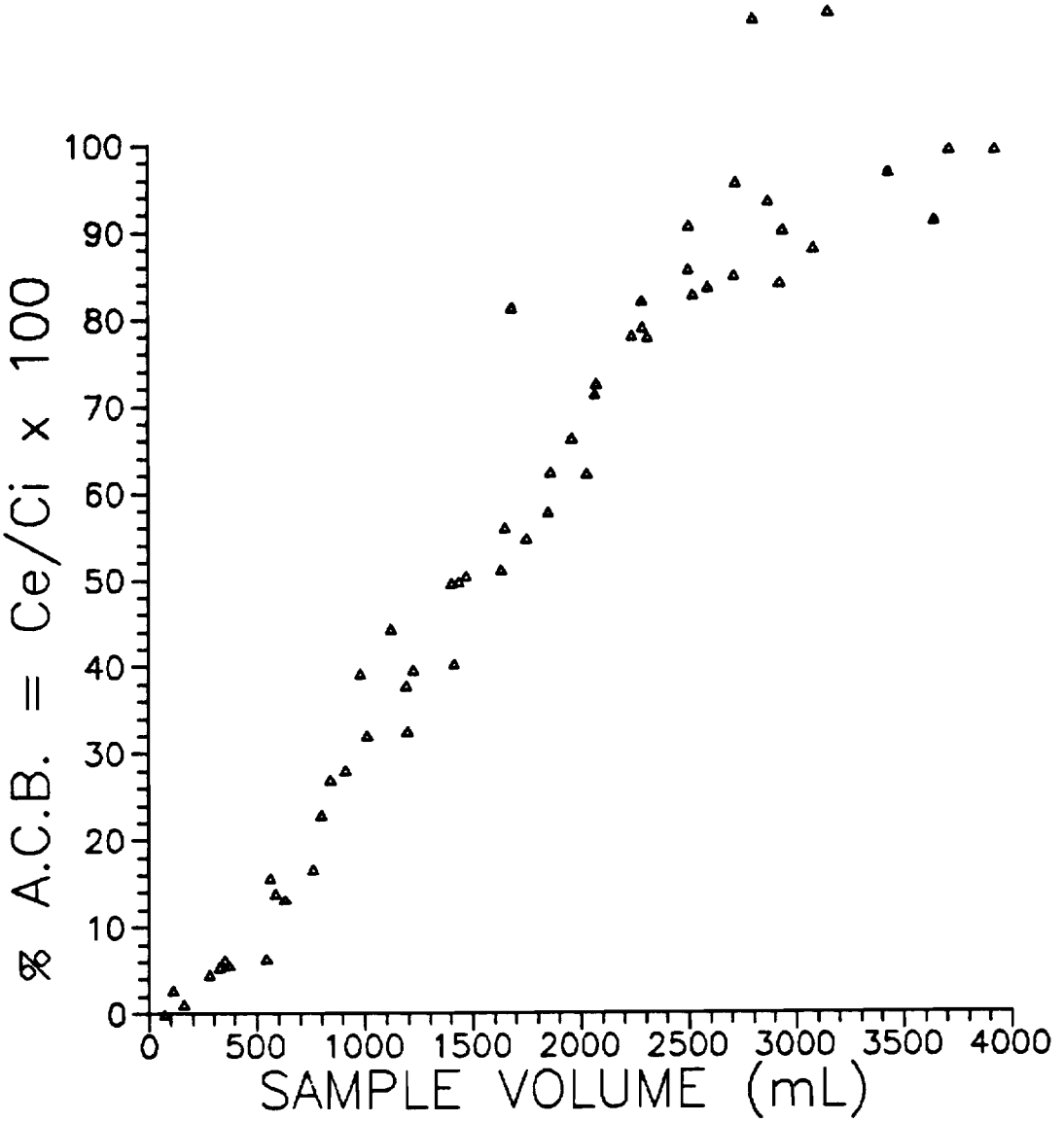

Appendix 2.16. ACB curve obtained for tribromomethane from experiment 6, C_i = 21 ppb. This curve represents the combined results of four cartridges. Each cartridge contained ~0.13 g Tenax (see Table 4.1).

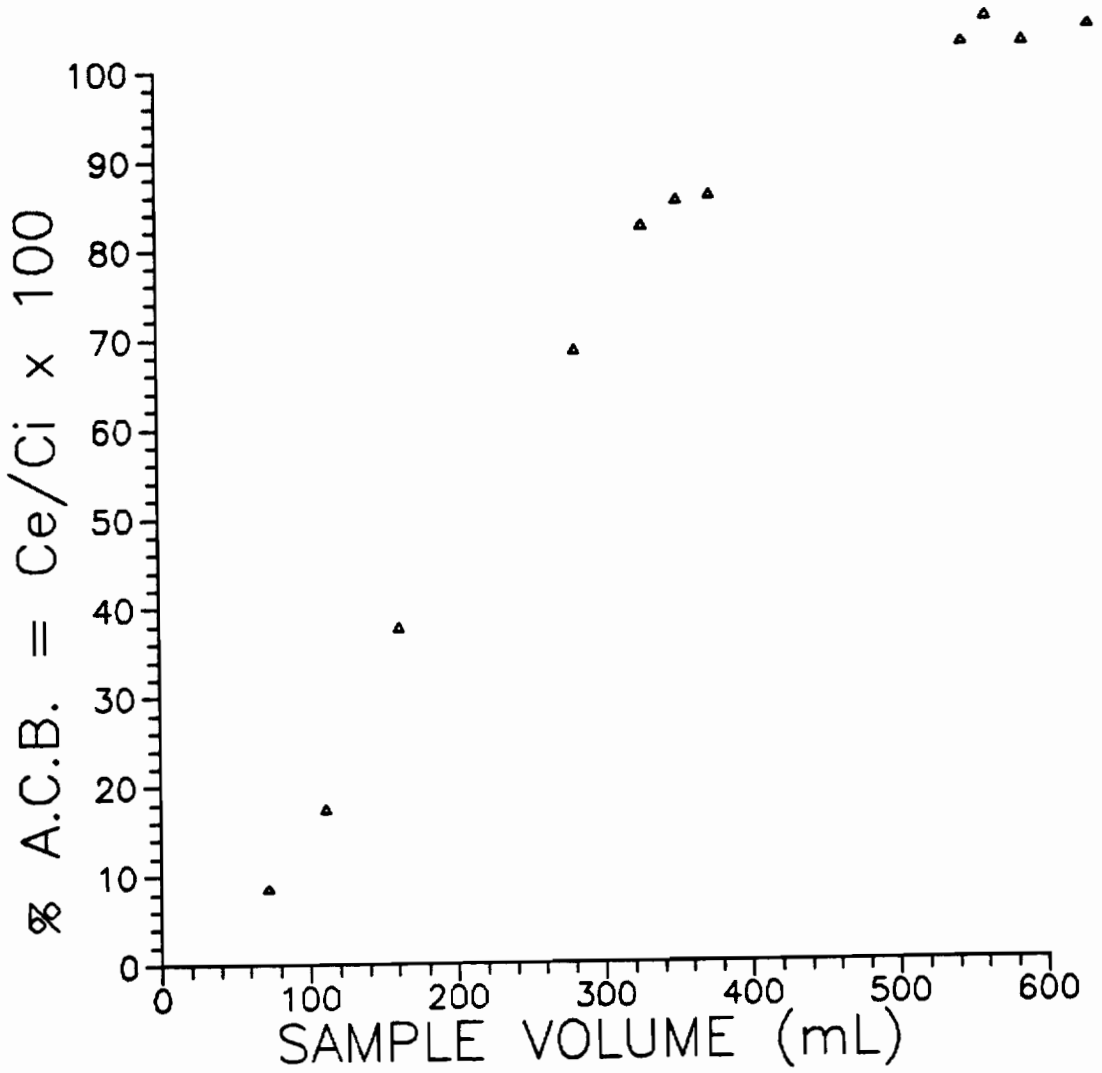

Appendix 2.17. ACB curve obtained for cis-1,2-dichloroethene from experiment 6, C_i = 25 ppb. This curve represents the combined results of four cartridges. Each cartridge contained ~0.13 g Tenax (see Table 4.1).

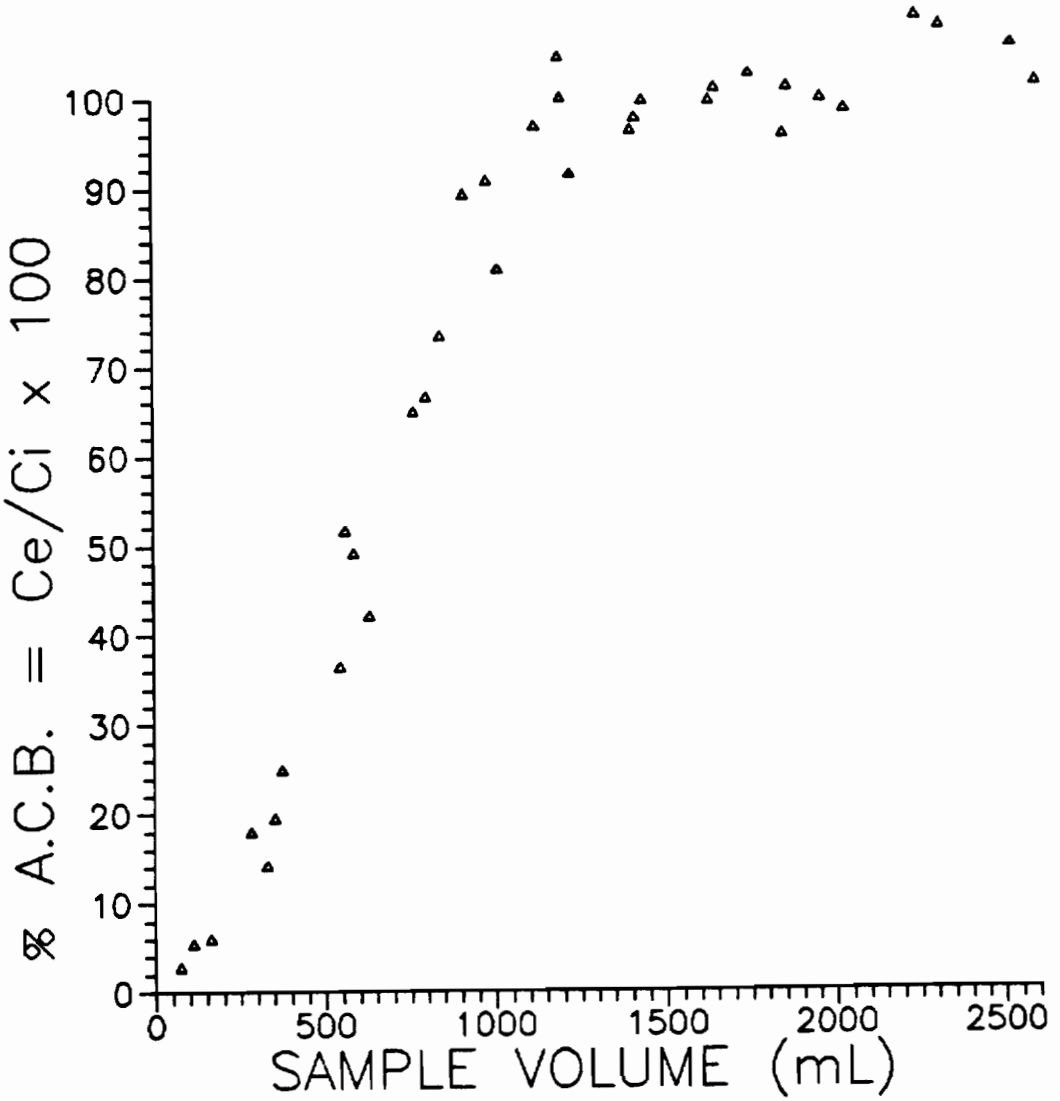

Appendix 2.18. ACB curve obtained for 1,1,2-trichloroethane from experiment 6, C_i = 20 ppb. This curve represents the combined results of four cartridges. Each cartridge contained ~0.13 g Tenax (see Table 4.1).

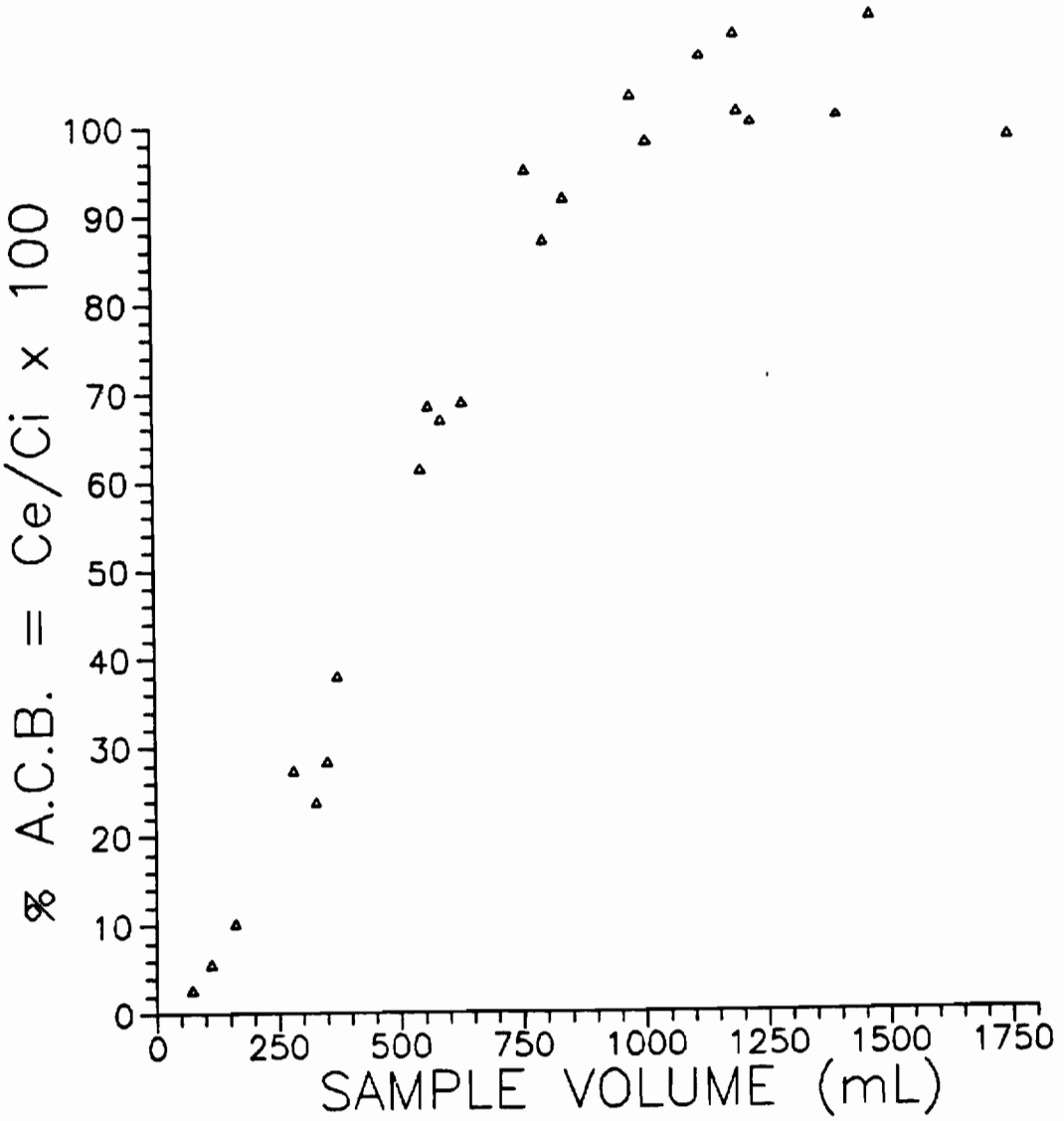

Appendix 2.19. ACB curve obtained for bromodichloromethane from experiment 6, C_i = 25 ppb. This curve represents the combined results of four cartridges. Each cartridge contained ~0.13 g Tenax (see Table 4.1).

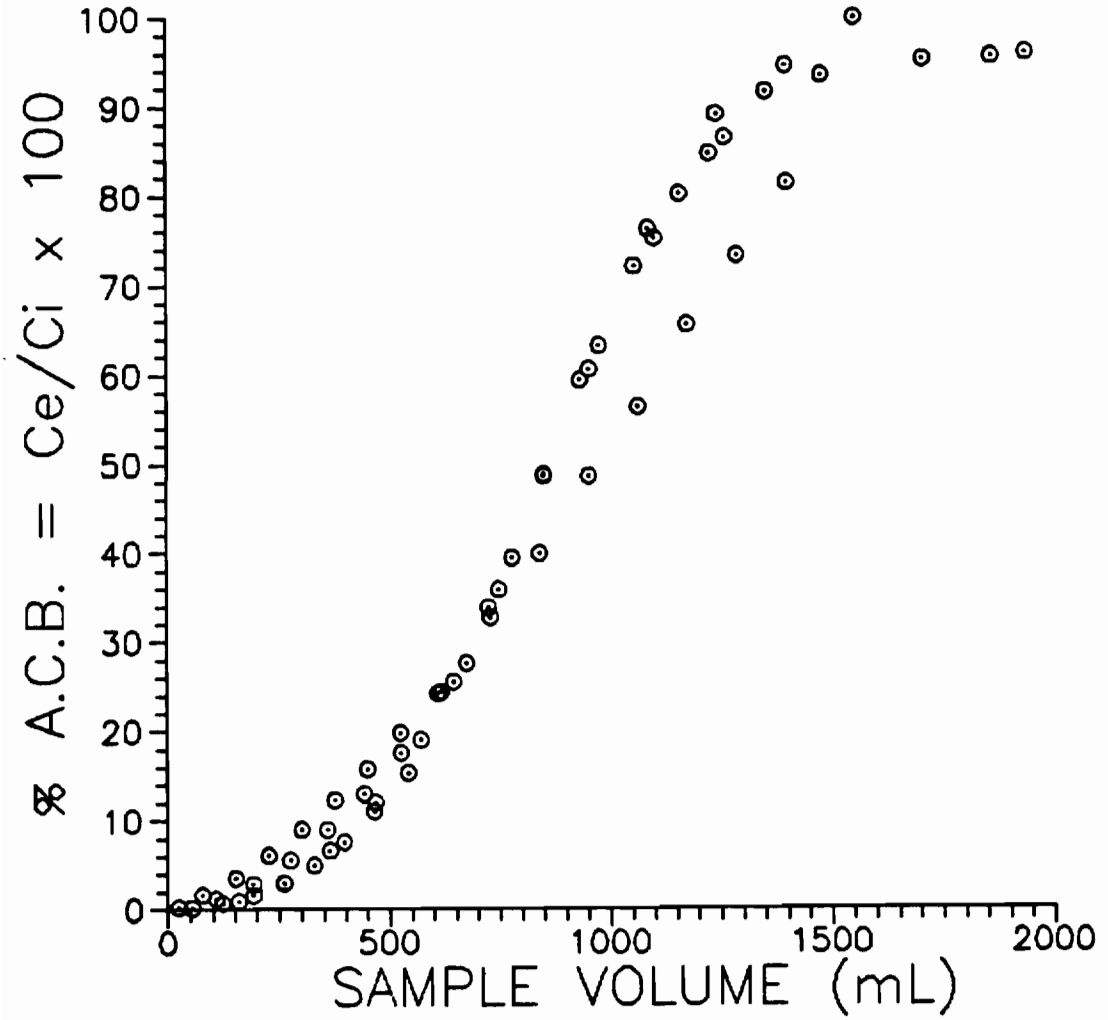

Appendix 2.20. ACB curve obtained for benzene from experiment 7, C_i = 55 ppb. This curve represents the combined results of four cartridges. Each cartridge contained ~0.13 g Tenax (see Table 4.1).

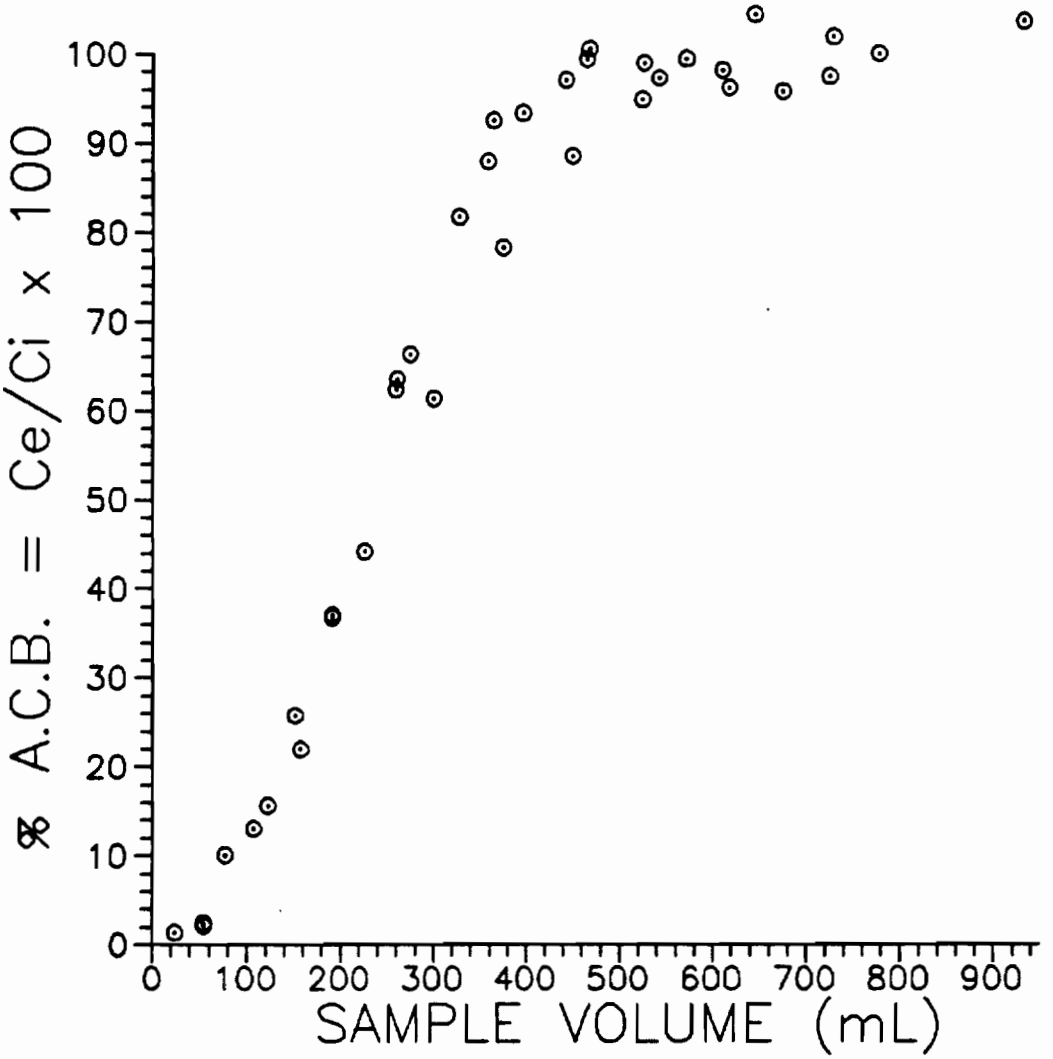

Appendix 2.21. ACB curve obtained for cis-1,2-dichloroethene from experiment 7, C_i = 60 ppb. This curve represents the combined results of four cartridges. Each cartridge contained ~0.13 g Tenax (see Table 4.1).

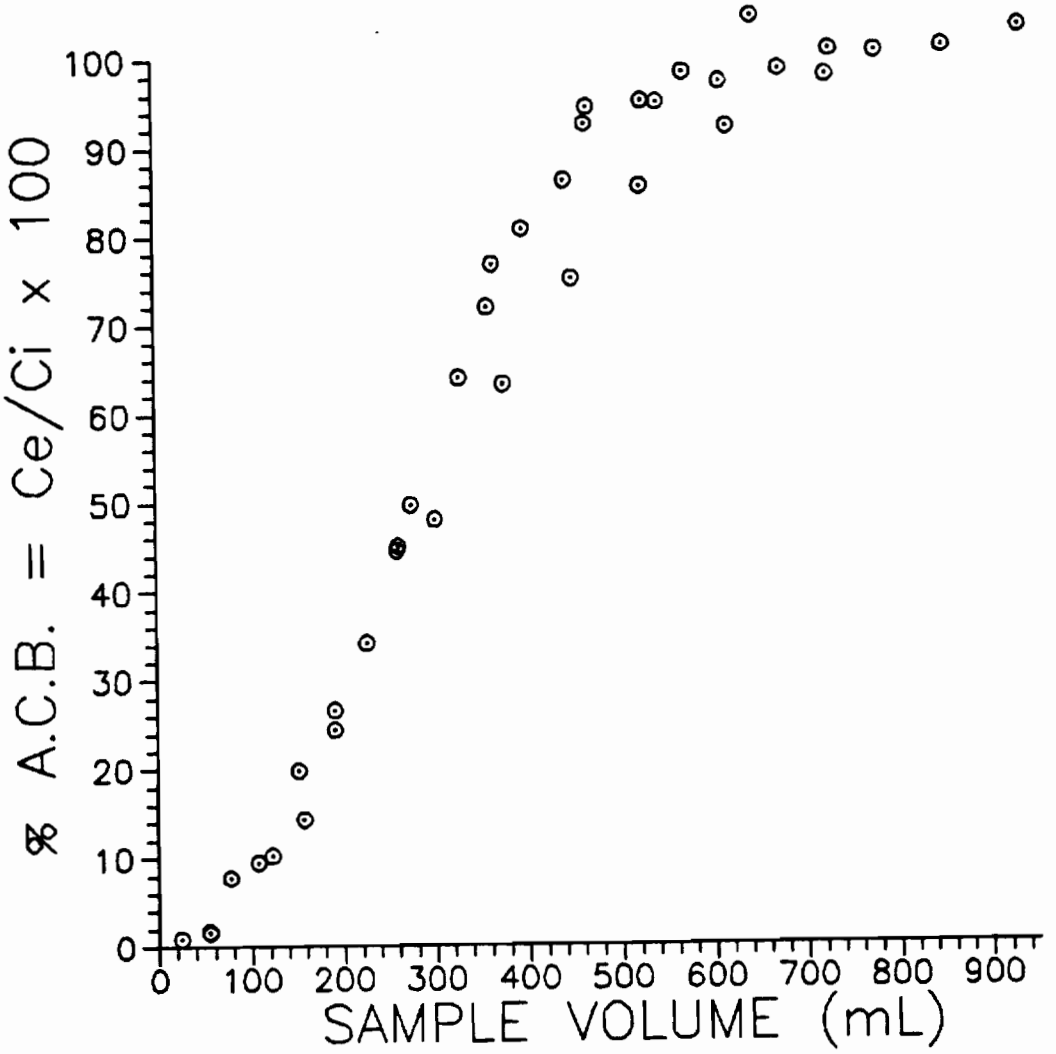

Appendix 2.22. ACB curve obtained for trichloromethane from experiment 7, C_i = 60 ppb. This curve represents the combined results of four cartridges. Each cartridge contained ~0.13 g Tenax (see Table 4.1).

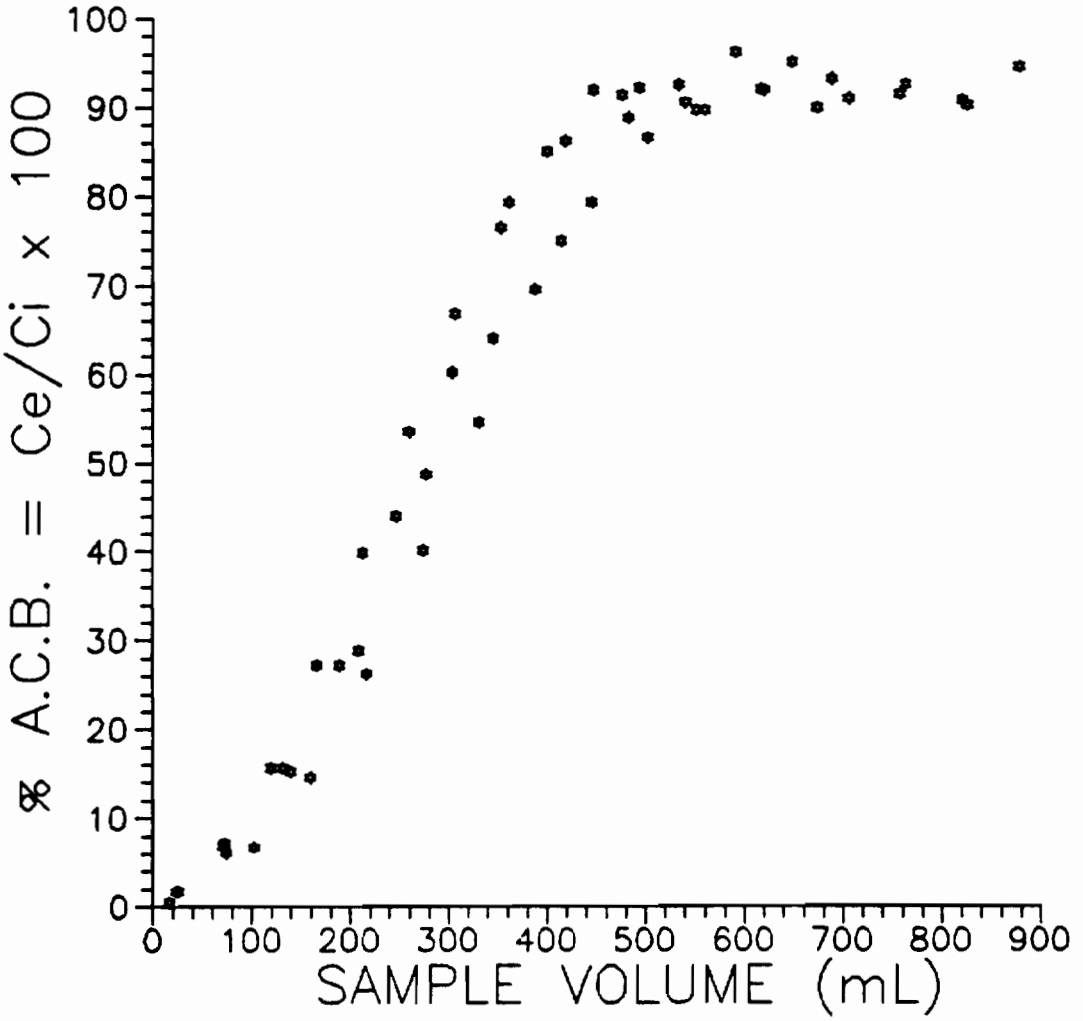

Appendix 2.23. ACB curve obtained for trichloromethane from experiment 8, C_i = 130 ppb. This curve represents the combined results of four cartridges. Each cartridge contained ~0.13 g Tenax (see Table 4.1).

Vitae

The author was born in 1960 in Detroit, Michigan. At some time prior to achieving consciousness, he was whisked away to Brooklyn, New York where he spent his formative years.

Of course, nothing of relevance occurred in the author's life until 1981 when he received a B.A. in Chemistry from the State University of New York at Binghamton. Almost immediately following this event, the author whisked himself away (in a semi-conscious state) to the Oregon Graduate Center to study Environmental Analytical Chemistry with Dr. James F. Pankow.

Over the past six years the author has enjoyed the company of many wonderful friends, has had many wonderful experiences, and has learned that there is no correlation between one's level of education and maturity.

Over the coming years, I look forward to using my skills in the service of the public, enjoying the company of many wonderful friends, and making some contribution to the world which will help me to feel less guilty about how lucky I am.